Many-Body Anderson Localization of Strongly Interacting Bosons in Random Lattices

Dissertation
zur
Erlangung des Doktorgrades (Dr. rer. nat.)
der
Mathematisch-Naturwissenschaftlichen Fakultät
der
Rheinischen Friedrich-Wilhelms-Universität Bonn

von
Roman Katzer
aus
Siegburg

Bonn, Januar 2015

Dieser Forschungsbericht wurde als Dissertation von der
Mathematisch-Naturwissenschaftlichen Fakultät der Universität Bonn angenommen und ist
auf dem Hochschulschriftenserver der ULB Bonn http://hss.ulb.uni-bonn.de/diss_online
elektronisch publiziert.

1. Gutachter:	Prof. Dr. Johann Kroha
2. Gutachterin:	Prof. Dr. Corinna Kollath
Tag der Promotion:	12.05.2015
Erscheinungsjahr:	2015

Abstract

In the present work, we investigate the problem of many-body localization of strongly interacting bosons in random lattices within the disordered Bose-Hubbard model. This involves treating both the local Mott-Hubbard physics as well as the non-local quantum interference processes, which give rise to the phenomenon of Anderson localization, within the same theory.

In order to determine the interaction induced transition to the Mott insulator phase, it is necessary to treat the local particle interaction exactly. Therefore, here we use a mean-field approach that approximates only the kinetic term of the Hamiltonian. This way, the full problem of interacting bosons on a random lattice is reduced to a local problem of a single site coupled to a particle bath, which has to be solved self-consistently. In accordance to previous works, we find that a finite disorder width leads to a reduced size of the Mott insulating regions.

The transition from the superfluid phase to the Bose glass phase is driven by the non-local effect of Anderson localization. In order to describe this transition, one needs to work within a theory that is non-local as well. Therefore, here we introduce a new approach to the problem. Based on the results for the local excitation spectrum obtained within the mean-field theory, we reduce the full, interacting model to an effective, non-interacting model by applying a truncation scheme to the Hilbert space. Evaluating the long-ranged current density within this approximation, we identify the transition from the Bose glass to the superfluid phase with the Anderson transition of the effective model. Resolving this transition using the self-consistent theory of localization, we obtain the full phase diagram of the disordered Bose-Hubbard model in the regime of strong interaction and larger disorder. In accordance to the theorem of inclusions, we find that the Mott insulator and the superfluid phase are always separated by the compressible, but insulating Bose glass phase.

Contents

1 Introduction **1**

2 Interacting Bosons in Disordered Lattice Systems **5**
2.1 The Bose-Hubbard Model . . . 5
2.1.1 The Hamiltonian . . . 5
2.1.2 The Strongly Correlated Regime: Mott Lobes . . . 7
2.1.3 The Weakly Correlated Regime: Bogoliubov Excitations . . . 12
2.1.4 Landau Criterion for Superfluidity . . . 15
2.1.5 Mean Field Amplitude and Superfluid Velocity . . . 16
2.2 Anderson Localization . . . 18
2.2.1 Absence of Diffusion . . . 18
2.2.2 The Localization Length . . . 20
2.2.3 Lifshitz Tails . . . 20
2.2.4 Mobility Edges . . . 22
2.2.5 Coherent Backscattering . . . 22
2.2.6 Scaling Theory of Localization . . . 26
2.2.7 Self-Consistent Theory of Localization . . . 28
2.3 The Disordered Bose-Hubbard Model . . . 30
2.3.1 Mott Lobes: Shifted Phase Boundaries . . . 31
2.3.2 Depletion of the Condensate and the Superfluid . . . 32
2.3.3 The Bose Glass Phase and the Theorem of Inclusions . . . 34

3 Mean-Field Theory for the Disordered Bose-Hubbard Model **39**
3.1 Mean-Field Theory for the Bose-Hubbard Model . . . 39
3.1.1 Direct Diagonalization . . . 40
3.1.2 Perturbation Theory . . . 46
3.2 Stochastic Mean-Field Theory for the Disordered Bose-Hubbard Model . . . 49
3.2.1 Decoupling Approximation . . . 49
3.2.2 Self-Consistent Integral Equation . . . 51
3.2.3 The Phase Boundary for the Disordered System . . . 53
3.2.4 Numerical Results for Three Dimensions . . . 56
3.2.5 Conclusions . . . 66

4 Transport Theory for the Disordered Bose-Hubbard Model **71**
4.1 The Superfluid Current . . . 71
4.1.1 The Current Density Operator . . . 71

4.1.2 Expectation Value of the Current Density Operator . . . 73
4.2 Effective Non-Interacting Model . . . 75
4.2.1 Locator Expansion of the Interacting Green's Function . . . 75
4.2.2 The Eigenbasis of the Mean-Field Hamiltonian . . . 77
4.2.3 Representing the Propagator Using the Mean-Field Eigenbasis . . . 80
4.2.4 Local Spectrum and Transition Amplitudes . . . 85
4.2.5 Defining the Effective Model . . . 88
4.2.6 Summary . . . 89
4.3 The Current Density Within the Single-Excitation Approximation . . . 91
4.3.1 Boundary Conditions for the Order Parameter . . . 94
4.3.2 Complex Transition Amplitudes . . . 96
4.3.3 Summary . . . 98
4.4 Numerical Evaluation and Results for Three Dimensions . . . 99
4.4.1 Parameters of the Effective Model . . . 99
4.4.2 Density of States within the Coherent Potential Approximation . . . 109
4.4.3 The Diffusion Coefficient and the Localization Length . . . 110
4.4.4 Density of States and Diffusion as Functions of the Hopping Amplitude . 113
4.4.5 Trajectory of the Anderson Transition . . . 116
4.4.6 Summary and Complete Phase Diagram . . . 119

5 Conclusion **123**

A Mean-Field Theory for the Bose-Hubbard Model **127**
A.1 Compressibility and the Mean-Field Parameter . . . 127
A.2 Perturbation Theory . . . 129

B Transport Theory for the Disordered Bose-Hubbard Model **133**
B.1 Relations for the Green's Functions . . . 133
B.2 Locator Expansion . . . 134
B.3 Coherent Potential Approximation . . . 136
B.4 Self-Consistent Theory of Anderson Localization . . . 139
B.4.1 Derivation of the Diffusion . . . 139
B.4.2 Evaluation of the Diffusion Integral for a Periodic Dispersion Relation . . 143

Bibliography **147**

Danksagung **155**

CHAPTER 1

Introduction

The interplay of Coulomb interaction and Anderson localization represents one of the fundamental problems in the field of many-body and condensed matter theory. Initially, research on this topic was motivated by the need to provide for a realistic description of transport in real materials, and therefore, focused on investigating the problem for fermionic particles. Theoretical research on bosonic particles in disordered environments was initiated by the fundamental work of Fischer et al. [1] and has gained more and more interest since, also triggered, of course, by the new possibilities for experimental testing of theoretical predictions that became available with the development of optical lattices.

What separates the bosonic from the fermionic case is the absence of a Pauli principle, giving rise to the phenomenon of Bose-Einstein condensation (BEC). Based on the work of Bose [2], in 1925 Einstein [3] introduced the concept of a macroscopic occupation of the single-particle ground state at low temperatures in an ideal Bose gas, i.e., the condensation of a macroscopic fraction of the particle density into one single quantum state. It then took seventy years until the first direct experimental observation of a BEC in ultracold gases of rubidium [4] and sodium atoms [5] in 1995. Still, the first manifestation of the effect of BEC was already observed in 1938 in the form of the superfluidity (SF) of liquid ^{4}He [6–8].

Due to the bosonic nature of ^{4}He, the vicinity of the measured and predicted transition temperatures to the SF and the BEC phase, respectively, as well as the absence of superfluidity in the fermionic ^{3}He in this temperature regime, this effect was immediately connected to the phenomenon of Bose-Einstein condensation by London [9]. However, the strongly interacting ^{4}He is far away from being an ideal gas and this hypothesis remained controversial. A phenomenological explanation for the effect of superfluidity based on the linear dispersion of the low-lying excitation spectrum of ^{4}He was given by Landau [10]. A microscopical theory providing for a connection between the excitation spectrum of a (weakly interacting) Bose gas and its Bose condensed nature at low temperatures was later presented by Bogoliubov [11], which, in fact, implied that the particle interaction plays an important role for the phenomenon of SF.

Interaction can also have quite the opposite effect in that it can give rise to an insulating phase. One of the first to point out the possibility of a metal-insulator transition (MIT) in crystalline structures driven by strong particle-particle interaction was Mott in 1961 [12]. This led to the formulation of the Hubbard model [13], which could describe the formation of the Mott-Hubbard gap and the incompressible Mott insulator (MI) phase. The bosonic version of this model, the Bose-Hubbard model, exhibits a direct transition from the localized MI phase

to the extended SF phase [1, 14], which was experimentally observed in 2002 [15] for a gas of ultracold rubidium atoms in a three-dimensional optical lattice.

However, the first experiments placing a SF inside structured systems were again performed for ^{4}He [16], which was subjected to various porous media. Depending on the properties of the medium, the SF behavior of the ^{4}He is changed, even with the possibility of a vanishing SF current [17]. Due to the irregular character of these media, these experiments naturally lead to the problem of disorder and the phenomenon of Anderson localization.

The theoretical research on disordered systems was initiated by the seminal work of Anderson [18] published in 1958, in which he introduced the concept of spatial localization of non-interacting particles in a disordered environment. He proposed that all particles would be localized above some critical strength of disorder, leading to an *absence of diffusion* and turning the system into an insulator. Later, the scaling theory of localization [19] shaped the modern picture of disordered systems with the observation that (non-interacting) one- and two-dimensional systems are always insulating in the thermodynamic limit, whereas a conducting phase only exists in three dimensions. The first direct experimental observation of Anderson localization was achieved in 2008, releasing an ultracold gas of (again) rubidium atoms into a one-dimensional disordered optical potential [20].

Since in real-world materials one always has to deal with both effects, i.e., disorder and interaction, it is of great interest to investigate the combined problem of interaction and localization. For fermions it is of special interest whether or not particle interaction can induce a metallic phase in two dimensions, especially with experiments suggesting the possibility of an interaction-driven MIT in quasi-two-dimensional systems [21].

In the bosonic case, the interesting question is, of course, what influence the disorder has on the SF nature of the conducting phase and how the transition to the MI phase is affected. Based on the work of Giamarchi and Schulz [22], in 1989 Fischer et al. [1] proposed the existence of an additional, insulating phase emerging from the localizing effect of the disorder, which they termed the Bose glass (BG) phase. They argued that this third phase always separates the incompressible MI and the conducting SF phase and a direct transition would only be possible in a pure system. Further works then established the quantitative shape of the MI phase [23] and also the possibility of a direct transition from the SF to the MI phase seems to be ruled out by the *theorem of inclusions* [24], fixing the qualitative shape of phase diagram of the disordered Bose-Hubbard model. Nevertheless, it is still of great interest to resolve the phase boundary between BG and SF also quantitatively.

In this thesis, we present an approximative method to describe the transition from the conducting SF to the insulating BG phase by observing the long-ranged SF current. Motivated by a previous work on the fermionic Anderson-Hubbard model [25, 26], we will first investigate the system using a local mean-field (MF) approximation [27, 28]. Based on the results for the local spectrum obtained thereby, we will introduce an approximative mapping of the interacting disordered Bose-Hubbard model onto a non-interacting effective model by applying a truncation scheme to the Hilbert space of the full problem. This allows us to calculate transport properties, such as, the diffusion and the localization length, within the well developed framework for the problem of Anderson localization of non-interacting particles. In particular, we are able to identify the Anderson transition of the effective model with the SF to BG transition of the underlying disordered Bose-Hubbard model.

The thesis is organized as follows. In chapter 2, we will give a brief introduction to the topic of bosons in disordered lattice systems in order to establish the basic concepts needed at the later stages of this work. We will first review the formation of the MI and the SF

phase in the pure Bose-Hubbard model. This is then followed by an introduction to the topic of Anderson localization. Finally, we will discuss the properties of the combined problem of interaction and disorder in the context of the disordered Bose-Hubbard model. In chapter 3, we will give a detailed description of the aforementioned local MF approximation, applied to both the pure and the disordered Bose-Hubbard model. We will present the numerical evaluation of the theory and will discuss its shortcomings in resolving the transition to the MI phase as well as its limitations with respect to the distinction between the SF and BG phase. In chapter 4, we will finally introduce our proposed method to determine the SF to BG phase transition. First, we will derive an expression for the long-ranged SF current in terms of single-particle Green's functions, which we will then expand using the local solutions of the MF approximation. This will lead us to the formulation of a selection criterion that defines the truncation scheme and determines the mapping of the full interacting problem onto the effective non-interacting one. Afterward, we will explain the link between the Anderson transition of the effective model and the SF to BG transition of the full problem. Finally, we will evaluate our effective theory using the self-consistent theory of localization [29] and will be able to resolve the transition line between SF and BG phase.

CHAPTER 2

Interacting Bosons in Disordered Lattice Systems

In this chapter, we want to introduce the basic properties of interacting bosons in disordered lattice systems, which we will describe using the most basic model that includes all these effects, i.e., the disordered Bose-Hubbard model. In order to properly establish all concepts needed in later chapters of this work, we will first consider the problem of interaction in a translational invariant lattice system (i.e., without disorder) by discussing the pure Bose-Hubbard model. Afterward, we will focus on Anderson localization of non-interacting particles in disordered systems in the context of the Anderson Hamiltonian. Finally, we will merge the two problems and give a brief introduction to the disordered Bose-Hubbard model.

2.1 The Bose-Hubbard Model

2.1.1 The Hamiltonian

The Bose-Hubbard model for spinless bosons in the grand canonical ensemble is defined by the following Hamiltonian,

$$\hat{H}_{BH} = \hat{H}_{loc} + \hat{H}_{kin} = \sum_i \left[(\varepsilon_0 - \mu)\hat{n}_i + \frac{U}{2}\hat{n}_i(\hat{n}_i - 1) \right] + \sum_{i \neq j} J_{ij} \hat{b}_i^\dagger \hat{b}_j \,, \tag{2.1}$$

where $\hat{b}_i^\dagger$ and $\hat{b}_i$ are the creation and annihilation operators for a boson on site i, $\hat{n}_i = \hat{b}_i^\dagger \hat{b}_i$ is the occupation number operator, and the summations are taken over all lattice sites. The local properties of the model are contained in the first part of the Hamiltonian, $\hat{H}_{loc}$, with ε_0 being the energy of the local single-particle states, μ is the chemical potential, and U the strength of the on-site repulsion. The second part of the Hamiltonian, $\hat{H}_{kin}$, is the kinetic part, which describes the tunneling (or *hopping*) processes from one site j to another site i with a corresponding *hopping amplitude* J_{ij}. For simplicity, we will restrict our analysis to the tight-binding version of this model,

$$J_{ij} = \begin{cases} -J & \text{if } i,j \text{ are nearest neighbors,} \\ 0 & \text{otherwise.} \end{cases} \tag{2.2}$$

Whenever a summation is restricted to only nearest neighbor sites i, j, this will be indicated by angle brackets, $\langle i, j\rangle$. Furthermore, we will only consider cubic lattices and will set the lattice constant to one, $a = 1$. Hence, for the spatial coordinates of the lattice sites we have $\mathbf{x}_i \in \mathbb{N}^3$. In addition, throughout this thesis we will use natural units, i.e., $\hbar = c = 1$.

There are two competing mechanisms in this model. On the one hand, the system can gain energy via the kinetic term by letting its particles move through the system, favoring delocalized particles. On the other hand, the on-site repulsion yields a penalty in energy when two particles occupy the same lattice site. Thus, the system will also try to reduce the overlap of the single-particle states, favoring localized particles. The ratio of U and J determines which of the two mechanisms will be the dominant one. In order to get a first understanding of the interplay of these two mechanisms, it is instructive to consider the two limiting cases of either vanishing interaction or vanishing hopping amplitude.

In the first case, $U = 0$ and $J > 0$, the system becomes non-interacting and, assuming periodic boundary conditions, can be solved by a Fourier transformation to momentum space,

$$\hat{b}_{\mathbf{p}} = \frac{1}{\sqrt{N_i}} \sum_i e^{\mathrm{i}\mathbf{p}\cdot\mathbf{x}_i}\, \hat{b}_i \,, \tag{2.3}$$

where N_i is the total number of lattice sites and the values of the components of $\mathbf{p}$ are restricted to an interval of length 2π. Since there is no Pauli principle limiting the number of particles that can occupy the same state, it is not sensible to consider the system in the grand canonical ensemble, but one should rather use the canonical ensemble with a fixed number of particles. The Hamiltonian then takes the following form,

$$\hat{H}_{BH} = \sum_{\mathbf{p}} (\varepsilon_0 + \varepsilon_{\mathbf{p}}) \hat{b}^\dagger_{\mathbf{p}} \hat{b}_{\mathbf{p}} \,, \tag{2.4}$$

where for the case of a d-dimensional cubic lattice the dispersion relation is given by

$$\varepsilon_{\mathbf{p}} = -2J \sum_{a=1}^{d} \cos p_a \,. \tag{2.5}$$

The multi-particle eigenstates are product states of the extended single-particle Bloch states $|\mathbf{p}\rangle = \hat{b}^\dagger_{\mathbf{p}}|0\rangle$, where $|0\rangle$ is the empty lattice. At zero temperature, $T = 0$, all bosons will occupy the single-particle ground state. The system would then be described by one macroscopically occupied quantum state, i.e., it would form a BEC.

In the second case, $J = 0$ and $U > 0$, which is also referred to as the *atomic limit* , the full Hamiltonian reduces to its local part, $\hat{H}_{BH} \to \hat{H}_{loc}$, and all lattice sites are decoupled. The full eigenstates of the system are then again product states, but now of the local eigenstates on every site. Since the Hamiltonian commutes with the occupation number operators, $[\hat{H}_{loc}, \hat{n}_i] = 0$, the full eigenstates will be product states of local particle number eigenstates. Thus, in contrast to the extended ground state in the non-interacting case, here each boson is localized on a single site.

Due to the translational invariance, in the ground state all sites will be occupied by the same number of particles, which is determined by minimizing the local potential

$$E_n = (\varepsilon_0 - \mu) n + \frac{U}{2} n(n-1) \tag{2.6}$$

for $n \in \mathbb{N}$. As shown later in section 3.1.2, this leads to the condition

$$\frac{\mu - \varepsilon_0}{U} < n_g < \frac{\mu - \varepsilon_0}{U} + 1 \tag{2.7}$$

for the ground state occupation number n_g.

If we consider n_g as a function of μ/U, we see that the ground state particle number is constant within intervals of length one. The transition to a ground state with one additional particle per site, $n_g \to n_g + 1$, happens discontinuously when $(\mu - \varepsilon_0)/U = n_g$. Here, the states with n_g and $n_g + 1$ particles have the same energy, and hence, it does not cost energy to add or remove a particle. Thus, at $T = 0$ the system is only compressible when the ratio $(\mu - \varepsilon_0)/U$ is an integer number, and incompressible otherwise.

These two limiting cases suggest that the properties of the model will be completely different, depending on whether we are in the strongly correlated ($J/U \ll 1$) or the weakly correlated regime ($J/U \gg 1$). In the following, we want to discuss the main characteristics of these two cases.

2.1.2 The Strongly Correlated Regime: Mott Lobes

In the previous section, we have discussed that in the atomic limit, $J = 0$, particles are strictly localized on single lattice sites. For finite hopping amplitude, $J > 0$, this strict localization is lifted. However, in the strongly correlated regime, $J/U \ll 1$, the on-site repulsion can still lead to a suppression of the particle transport, turning the system into an insulator. One of the firsts who suggested the possibility of a metal-insulator transition driven by particle-particle interaction was Mott in 1961 [12]. The underlying mechanism can be understood best by directly considering the Bose-Hubbard model.

In the case of integer filling, $\rho = N/N_i \in \mathbb{N}$, i.e., when the total number of particles N is an integer multiple of the number of lattice sites N_i, the local energy $\hat{H}_{loc}$ will be minimal for a particle configuration with the same number of bosons on each site, $n_i = \rho$ for all i. If now a boson tunnels from one site to another and the particle configuration is changed,

$$|\ldots, \rho, \rho, \ldots\rangle \to |\ldots, \rho - 1, \rho + 1, \ldots\rangle\,, \tag{2.8}$$

the total local energy changes as well,

$$\begin{aligned} &\langle \ldots, \rho - 1, \rho + 1, \ldots | \hat{H}_{loc} | \ldots, \rho - 1, \rho + 1, \ldots\rangle - \langle \ldots, \rho, \rho, \ldots | \hat{H}_{loc} | \ldots, \rho, \rho, \ldots\rangle \\ &= \frac{U}{2}\Big[(\rho - 1)(\rho - 2) + (\rho + 1)\rho \; - \; 2\rho(\rho - 1)\Big] \\ &= U\,. \end{aligned} \tag{2.9}$$

Thus, each tunneling process away from the ideal configuration comes with a penalty in energy of the size of the repulsion strength U. On the other hand, if the ground state is a linear combination of different occupation number configurations, the total energy is reduced due to the kinetic term of the Hamiltonian $\hat{H}_{kin}$. Nevertheless, if the hopping amplitude is small compared to the interaction strength, contributions away from the ideal configuration will be suppressed. Hence, the particles are highly immobile and transport will vanish, i.e., the system will be an insulator.

Now, suppose we want to add or remove a boson to or from a system with integer filling,

$\rho \in \mathbb{N}$. In the grand canonical ensemble, this is triggered by adjusting the chemical potential, such that the ground state with one particle more or less becomes favorable in energy. Following the argumentation in [30] by Freericks and Monien, we assume that the ground state with integer filling is, to first approximation, well described by the atomic limit solution,

$$|\Psi_{\rho N_i}\rangle = \prod_{i=1}^{N_i} \frac{1}{\sqrt{\rho!}} (\hat{b}_i^\dagger)^\rho |0\rangle = |\rho, \rho, \ldots, \rho\rangle \,, \tag{2.10}$$

where $|0\rangle$ is the empty lattice. Furthermore, we assume that the ground states for the particle number sectors $N = \rho N_i \pm 1$ may be approximated by a single particle or hole *on top* of the localized ρN_i particles,

$$|\Psi_{\rho N_i+1}\rangle = \frac{1}{\sqrt{\rho+1}} \sum_{i=1}^{N_i} f_i^+ \, \hat{b}_i^\dagger |\Psi_{\rho N_i}\rangle \tag{2.11}$$

and

$$|\Psi_{\rho N_i-1}\rangle = \frac{1}{\sqrt{\rho}} \sum_{i=1}^{N_i} f_i^- \, \hat{b}_i |\Psi_{\rho N_i}\rangle \,, \tag{2.12}$$

with $f_i^\pm$ being the expansion coefficients. This is again motivated by the fact that the creation of additional particle-hole pairs comes with a penalty in energy, see equation (2.9). With this, the energy differences between the ground states of the particle number sectors can be written as

$$\begin{aligned} \Delta E_+ &= \langle \Psi_{\rho N_i+1} | \hat{H}_{BH} | \Psi_{\rho N_i+1} \rangle - \langle \Psi_{\rho N_i} | \hat{H}_{BH} | \Psi_{\rho N_i} \rangle \\ &= \langle \Psi_{\rho N_i+1} | \hat{H}_{loc} | \Psi_{\rho N_i+1} \rangle + \langle \Psi_{\rho N_i+1} | \hat{H}_{kin} | \Psi_{\rho N_i+1} \rangle - \langle \Psi_{\rho N_i} | \hat{H}_{loc} | \Psi_{\rho N_i} \rangle \\ &= U \left(\rho - \frac{\mu - \varepsilon_0}{U} + \frac{\Delta E_{kin}^+}{U} \right) \end{aligned} \tag{2.13a}$$

and

$$\begin{aligned} \Delta E_- &= \langle \Psi_{\rho N_i} | \hat{H}_{BH} | \Psi_{\rho N_i} \rangle - \langle \Psi_{\rho N_i-1} | \hat{H}_{BH} | \Psi_{\rho N_i-1} \rangle \\ &= U \left(\rho - 1 - \frac{\mu - \varepsilon_0}{U} - \frac{\Delta E_{kin}^-}{U} \right) , \end{aligned} \tag{2.13b}$$

where $\Delta E_{kin}^\pm = \langle \Psi_{\rho N_i \pm 1} | \hat{H}_{kin} | \Psi_{\rho N_i \pm 1} \rangle$ is the kinetic energy of the particle or hole state. The transition from $|\Psi_{\rho N_i-1}\rangle$ to $|\Psi_{\rho N_i}\rangle$ happens when ΔE_- vanishes, and the transition from $|\Psi_{\rho N_i}\rangle$ to $|\Psi_{\rho N_i+1}\rangle$ when ΔE_+ vanishes. For the corresponding chemical potentials μ_+ and μ_-, with $\Delta E_\pm(\mu_\pm) = 0$, we obtain

$$\frac{\mu_+ - \varepsilon_0}{U} = \rho + \frac{\Delta E_{kin}^+}{U} \tag{2.14}$$

and

$$\frac{\mu_- - \varepsilon_0}{U} = \rho - 1 - \frac{\Delta E_{kin}^-}{U} \,. \tag{2.15}$$

From this, it follows that

$$\frac{\mu_+ - \mu_-}{U} = 1 + \frac{\Delta E_{kin}^+ + \Delta E_{kin}^-}{U} \,. \tag{2.16}$$

Thus, if the kinetic energies are small against the repulsion strength, the states with a filling smaller and larger than the integer filling are separated by a finite amount of energy. This gap is known as the Mott-Hubbard gap. Within the gap, the particle number is constant, and thus, the compressibility vanishes, $\kappa = (\mathrm{d}N/\mathrm{d}\mu) = 0$. Such an insulator with an energy spectrum that is gaped due to strong interactions is known as a Mott insulator (MI).

In order to determine $\Delta E^{\pm}_{kin}$, one needs to calculate the expansion coefficients $f^{\pm}_i$. This can be done by representing the full Hamiltonian $\hat{H}_{BH}$ in the subspace of the local particle or hole states,

$$|i^+\rangle = \frac{1}{\sqrt{\rho+1}}\,\hat{b}_i^\dagger|\Psi_{\rho N_i}\rangle \quad \text{and} \quad |i^-\rangle = \frac{1}{\sqrt{\rho}}\,\hat{b}_i|\Psi_{\rho N_i}\rangle\,, \tag{2.17}$$

respectively. In doing so, one obtains

$$\hat{H}^{\pm}_{BH} \equiv \sum_{i,j} |i^\pm\rangle\langle i^\pm|\hat{H}_{BH}|j^\pm\rangle\langle j^\pm| = \sum_i E_0^\pm |i^\pm\rangle\langle i^\pm| - J^\pm \sum_{\langle ij\rangle} |i^\pm\rangle\langle j^\pm|\,, \tag{2.18}$$

with $E_0^\pm = \langle\Psi_{\rho N_i\pm1}|\hat{H}_{loc}|\Psi_{\rho N_i\pm1}\rangle$, $J^+ = (\rho+1)J$ and $J^- = \rho J$. The ground state of $\hat{H}^{\pm}_{BH}$ determines the coefficients $f^{\pm}_i$. Apparently, the particle and hole states are each described by a non-interacting tight-binding Hamiltonian, which, as discussed in the previous section, is diagonalized by performing a Fourier transformation to momentum space. The ground state is given by the Bloch state with zero momentum, $\mathbf{p} = 0$, leading to the following kinetic energies,

$$\Delta E^+_{kin} = -2dJ(\rho+1) \quad \text{and} \quad \Delta E^-_{kin} = -2dJ\rho\,, \tag{2.19}$$

see also equation (2.5). With this, the size of the gap can be written as

$$\frac{\mu_+ - \mu_-}{U} = 1 - \frac{dJ}{U}(4\rho+2)\,. \tag{2.20}$$

Thus, from this first approximation we can estimate that the gap closes when $dJ/U > 1/(4\rho+2)$. Of course, the disappearance of the gap implies that the system is not in the strongly correlated regime anymore, and thus, the approximations made might not necessarily be valid anymore.

This result allows us to draw a first phase diagram for the Bose-Hubbard model, where the phase space is parametrized by μ/U and dJ/U, see figure (2.1a). For fixed chemical potential $\mu/U \notin \mathbb{N}$, the transition from the compressible to the incompressible phase takes place at a finite value J/U. For $\mu/U \in \mathbb{N}$, the system is compressible even in the atomic limit, $J/U \to 0$. The incompressible regions with constant particle numbers are referred to as the *Mott lobes*. As the first available states below and above the Mott-Hubbard gap are hole- and particle-like, respectively, the shape of the Mott lobes is asymmetric. Furthermore, within this approximation, the qualitative shape of the Mott lobes does not depend on the dimension of the system, which only enters via the quantity dJ/U.

In [30], this *strong coupling expansion* was performed by taking into account terms up to third order in J/U, yielding a modified form of the Mott lobes, see figure (2.1b). The higher order terms introduce a direct dependence of the Mott lobes on the dimension d, leading to slightly larger lobes in one dimension, $d = 1$, and smaller lobes in higher dimensions, $d \geq 2$. A comparison with previous results from quantum Monte Carlo (QMC) calculations for finite systems [31, 32] showed very good agreement for $d = 1$. More recent QMC simulations (for the first Mott lobe) [33] also find very good agreement for $d = 3$, except for the tip of the lobe, where the strong-coupling expansion seems to overestimate the extent of the MI regions.

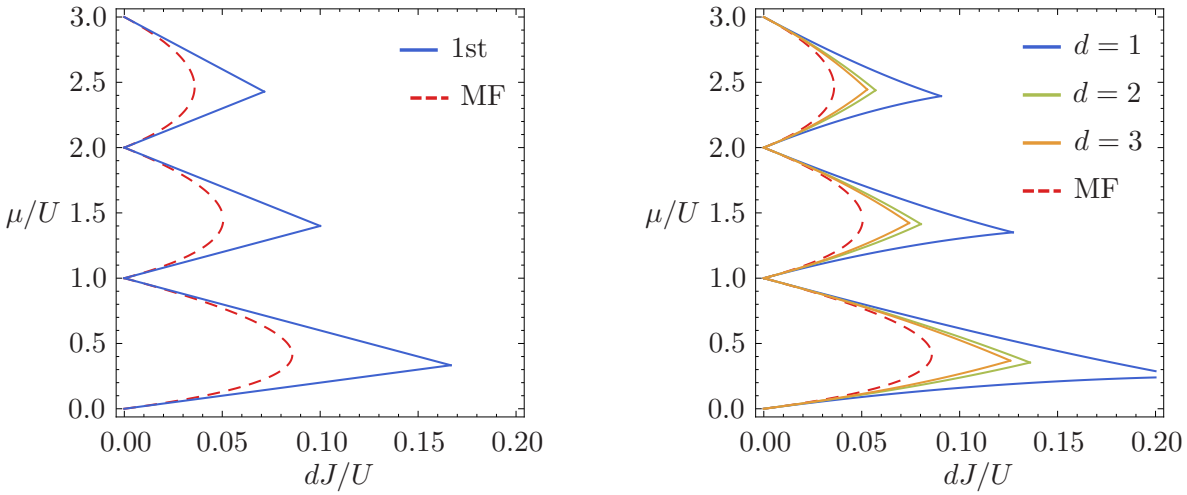

(a) 1st order approximation

(b) 3rd order expansion

Figure 2.1: **(a)** The boundary between the Mott insulating and the non-gaped phase. In each Mott lobe, the compressibility vanishes and the particle number is constant. The solid blue curve shows the phase boundary according to the simple expansion (first order in J/U) starting from the atomic limit. The dashed red curve shows the phase boundary obtained from the MF/decoupling approximation [27]. **(b)** The phase boundary obtained from the strong-coupling expansion [30] for $d = 1, 2, 3$ (solid lines) including terms up to third order in J/U. Again, the dashed red curve shows the MF phase boundary. For both diagrams, the on-site energy was explicitly set to zero, $\varepsilon_0 = 0$.

The strong-coupling expansion was later extended further [34], taking into account higher order terms in J/U and yielding perfect agreement with direct numerical calculations, see for example [35].

While the strong-coupling expansion proves to be a very good method to resolve the shape of the Mott lobes, by design it cannot be used to investigate the regions in between the Mott lobes. Another rather simple approach that can be applied also away from the MI regions comes in the form of the *decoupling approximation*, which is a mean-field (MF) approximation for the kinetic part of the Hamiltonian. As we will discuss this approach in full detail in chapter 3, here we only want to mention its basic ideas.

In essence, the process of a boson tunneling between sites i and j is replaced by a hopping from site i (and j) into and out of a particle bath, characterized by the mean-field parameter ψ,

$$\hat{b}_i^\dagger \hat{b}_j \quad \rightarrow \quad \hat{b}_i^\dagger \langle \hat{b}_j \rangle + \langle \hat{b}_i^\dagger \rangle \hat{b}_j - \langle \hat{b}_i^\dagger \rangle \langle \hat{b}_j \rangle \equiv \psi\, \hat{b}_i^\dagger + \psi^* \hat{b}_j - |\psi|^2 \,. \tag{2.21}$$

The above replacement defines the MF parameter as the ground state expectation value of the bosonic operators $\hat{b}_i$, $\psi = \langle \hat{b}_i \rangle$, which is equal for all lattice sites due to the translational invariance of the model. Applying this transformation to the Hamiltonian $\hat{H}_{BH}$ yields

$$\hat{H}_{BH} \quad \rightarrow \quad \hat{H}^{MF} = \sum_i \hat{h}_i - \sum_{\langle ij \rangle} |\psi|^2 \tag{2.22}$$

with the local MF Hamiltonian

$$\hat{h}_i = (\varepsilon_0 - \mu)\hat{n}_i + \frac{U}{2}\hat{n}_i(\hat{n}_i - 1) - zJ\left(\psi^*\hat{b}_i + \psi\,\hat{b}_i^\dagger\right), \tag{2.23}$$

where $z = 2d$ is the number of nearest neighbors. Apparently, this approximation decouples the lattice sites with respect to the bosonic operators. Thus, the eigenstates of $\hat{H}^{MF}$ will be product states of the local eigenstates of the $\hat{h}_i$. Due to the translational invariance, it is sufficient to solve the problem for one arbitrary site i, which reduces the full lattice problem to a much simpler local one.

The local ground state $|G_i\rangle$ of $\hat{h}_i$ will depend on the MF parameter ψ, $|G_i\rangle = |G_i(\psi)\rangle$. In turn, ψ is determined by the local ground state, $\psi = \langle\hat{b}_i\rangle = \langle G_i(\psi)|\hat{b}_i|G_i(\psi)\rangle$. This implies that the problem has to be solved self-consistently.

The MF parameter is also referred to as the *superfluid order parameter*, as for the pure model it determines the boundary between the gapless (and, as we will see in the next section, SF) phase and the MI phase. It is easy to see that for $\psi = 0$, the MF Hamiltonian corresponds to the atomic limit ($J/U = 0$) Hamiltonian with strictly localized particles. Thus, a vanishing order parameter can be identified with the MI phase, while a finite ψ corresponds to the gapless phase. The resulting phase boundary is plotted in figure 2.1a and 2.1b in comparison to the results from the strong-coupling expansion. Again, the dimension only enters via the quantity dJ/U and not directly. As it can be seen, the MF approach underestimates the extent of the Mott lobes drastically in one dimension and a little less drastically in two and three dimensions. Still, the basic characteristics of the phase diagram are captured qualitatively for larger hopping amplitudes and also quantitatively for small hopping amplitudes.

In the context of the Bose-Hubbard model, the idea of decoupling the kinetic term by introducing a complex field was first employed by Fisher et al. [1] for the case of infinite range hopping, $J_{ij} = J/N_i$, where this led to the definition of an effective action, from which a phase diagram could be constructed. Motivated by this approach, in [36, 37] the idea of decoupling the lattice sites was implemented for the tight-binding Bose-Hubbard model by treating the problem using the Gutzwiller ansatz, i.e., assuming the full lattice states to factorize into local states. The decoupling approximation was then further formalized by Sheshadri et al. [27], resulting in the form of the theory as presented above.

The theory can also be applied to the case of on-site energies with a spatial dependence, $\varepsilon_0 \to \varepsilon_i$, i.e., to a system without translational invariance. There, the model has to be treated as a system of N_i local sites coupled via the order parameter, which is still much easier than the full lattice problem. For example, in [38] this method was used to resolve the density distribution of a cold bosonic atoms in a two-dimensional optical lattice superimposed with a harmonic trap. Moreover, it can also be applied to the disordered Bose-Hubbard model, either by treating the model on a decoupled lattice [39], or by accounting for the randomness by introducing a probability distribution for the order parameter [28]. This will be discussed in detail in chapter 3.

An improvement over this static MF approximation comes in the form of the bosonic dynamical mean-field theory (B-DMFT) [40], which applies the self-consistency condition to the local Green's function and, thereby, introduces a modified coupling of the local site to the particle bath. The phase diagram obtained within the B-DMFT yields very good agreement with QMC simulations, which, however, comes at the cost of being numerically much more demanding than the static MF approach.

2.1.3 The Weakly Correlated Regime: Bogoliubov Excitations

In the previous section, we have discussed the Bose-Hubbard model near the MI phase, where it is reasonable to expand the system in terms of local states. Far away from the Mott lobes, however, this approach will not be justified anymore. In order to find a suitable description of the problem, we will again introduce the MF parameter. However, this time we will, in addition, consider the fluctuations from this mean field. Here, we will loosely follow the presentation in [41] and [42], modified to the case of a discrete lattice.

We start by rewriting the bosonic operators as follows,

$$\hat{b}_i = \langle \hat{b}_i \rangle + \big(\hat{b}_i - \langle b_i \rangle\big) \equiv \psi_i + \hat{\delta}_i \,, \tag{2.24}$$

where $\hat{\delta}_i$ is the fluctuation operator and ψ_i the ground state expectation value of the bosonic operator. The full Hamiltonian can then be expressed in terms of the ψ_i and $\hat{\delta}_i$,

$$\hat{H}_{BH} = E_0 + \hat{H}_1 + \hat{H}_2 + \hat{H}_3 + \hat{H}_4 \,, \tag{2.25a}$$

with

$$E_0 = \sum_i \Big[\varepsilon_0 - \mu + \frac{U}{2}|\psi_i|^2\Big]|\psi_i|^2 - J\sum_{\langle ij\rangle} \psi_i^* \psi_j \tag{2.25b}$$

and

$$\hat{H}_1 = \sum_i \Big[\varepsilon_0 - \mu + U|\psi_i|^2\Big]\big(\psi_i^* \hat{\delta}_i + \psi_i \hat{\delta}_i^\dagger\big) - J\sum_{\langle ij\rangle} \big(\psi_i^* \hat{\delta}_j + \psi_j \hat{\delta}_i^\dagger\big) \tag{2.25c}$$

and

$$\hat{H}_2 = \sum_i \Big[\varepsilon_0 - \mu + 2U|\psi_i|^2\Big]\hat{\delta}_i^\dagger \hat{\delta}_i + \sum_i \frac{U}{2}\big(\psi_i^* \psi_i^* \hat{\delta}_i \hat{\delta}_i + \psi_i \psi_i \hat{\delta}_i^\dagger \hat{\delta}_i^\dagger\big) - J\sum_{\langle ij\rangle} \hat{\delta}_i^\dagger \hat{\delta}_j \,. \tag{2.25d}$$

The remaining terms $\hat{H}_3$ and $\hat{H}_4$ contain fluctuation operators in third and forth order, respectively, and can be neglected, assuming the fluctuations are small. This turns the model into a non-interacting one for the fluctuation operators.

Let us first investigate the term of zeroth order in the fluctuations, E_0, which depends solely on the mean field ψ_i. For small fluctuations, it will account for the major contribution to the total energy, thus we assume that the mean field will adjust itself to minimize E_0, leading to

$$\frac{\partial E_0}{\partial \psi_i^*} = \Big[\varepsilon_0 - \mu + U|\psi_i|^2\Big]\psi_i - J\sum_j^{\langle ij\rangle} \psi_j \stackrel{!}{=} 0 \,. \tag{2.26}$$

The above equation is known as the (time-independent) Gross-Pitaevskii equation (GPE), here in its discrete form. We have already established in the previous section that for the pure system we have $\psi_i \equiv \psi$. Choosing $\psi \in \mathbb{R}$ yields the two following solutions,

$$\psi_0 = 0 \quad \text{and} \quad \psi_1 = \sqrt{(\mu - \varepsilon_0 + zJ)/U} \,, \tag{2.27}$$

where the non-trivial solution ψ_1 only exists for $\mu - \varepsilon_0 + zJ > 0$. From

$$E_0(\psi_1) = -\frac{(\mu - \varepsilon_0 + zJ)^2}{2U} < 0 = E_0(\psi_0) \tag{2.28}$$

we see that ψ_1 is always the global minimum, i.e., the mean field is always finite for $\mu - \varepsilon_0 + zJ > 0$. In particular, the Mott lobes will not be resolved within this approach, implying that its validity is restricted to the weakly correlated regime. In order to obtain the correct behavior in the strongly correlated regime, the particle-particle interaction has to be treated exactly.

Next, we turn to the term linear in the fluctuations, $\hat{H}_1$. It is easy to see that

$$\hat{H}_1 = \sum_i \left[\frac{\partial E_0}{\partial \psi_i^*} \hat{\delta}_i^\dagger + \frac{\partial E_0}{\partial \psi_i} \hat{\delta}_i \right]. \tag{2.29}$$

Thus, if the mean field is determined by the Gross-Pitaevskii equation (2.26), the contributions linear in the fluctuations vanish, i.e., $\hat{H}_1 = 0$.

This leaves us with only one remaining term, namely $\hat{H}_2$. The difficulty of solving $\hat{H}_2$ lies in its *anomalous* terms containing either only two creation or two annihilation operators, which break the particle number conservation. In order to solve this problem, one introduces a new set of bosonic operators, which are defined via the relation

$$\hat{\delta}_i = \sum_j \left[u_{ij} \hat{\alpha}_j - v_{ij}^* \hat{\alpha}_j^\dagger \right]. \tag{2.30}$$

This transformation is known as the *Bogoliubov transformation* and the α-bosons as the *Bogoliubov quasi-particles*. One can show that this transformation diagonalizes the Hamiltonian $\hat{H}_2$, if the coefficients u_{ij} and v_{ij} are the solutions to the so-called *Bogoliubov - de Gennes* equations (see [42] for the details).

Here, we want to restrict ourselves to a simpler version of this problem, i.e., the weakly correlated regime for N particles in the canonical ensemble. We know that for the non-interacting case, $U = 0$, all bosons will occupy the Bloch state with zero momentum, $\mathbf{p} = 0$. Now, we want to investigate how this changes when we turn on the interaction. Therefore, we first perform a Fourier transformation to momentum space,

$$\hat{H}_{BH} = \sum_{\mathbf{p}} \varepsilon_{\mathbf{p}} \hat{b}_{\mathbf{p}}^\dagger \hat{b}_{\mathbf{p}} + \frac{U}{2N_i} \sum_{\mathbf{p}\mathbf{p}'\mathbf{q}} \hat{b}_{\mathbf{p}+\mathbf{q}}^\dagger \hat{b}_{\mathbf{p}'-\mathbf{q}}^\dagger \hat{b}_{\mathbf{p}} \hat{b}_{\mathbf{p}'}, \tag{2.31}$$

where we have set $\varepsilon_0 = 0$. For small U/J, it is still reasonable to assume that most particles occupy the single-particle ground state, and thus, $|\mathbf{p} = 0\rangle$ is still macroscopically occupied. We therefore replace the corresponding operator by an amplitude, $\hat{b}_0 \to b_0 = \sqrt{N_0}$, where N_0 is the number of bosons in the single-particle ground state. Note, that this replacement it slightly different from the introduction of the mean field amplitude and $\psi = \langle \hat{b}_i \rangle \neq \langle \mathbf{p} = 0 | \hat{b}_i | \mathbf{p} = 0 \rangle$.

Applying this approximation to the Hamiltonian and neglecting direct interactions between the non-condensed particles $\hat{b}_{\mathbf{p}}$ with $\mathbf{p} \neq 0$ yields

$$\hat{H}_{BH} = \varepsilon_{\mathbf{p}=0} N_0 + \frac{U}{2N_i} N_0^2 + \sum_{\mathbf{p}\neq 0} \varepsilon_{\mathbf{p}} \hat{b}_{\mathbf{p}}^\dagger \hat{b}_{\mathbf{p}} + \frac{U}{2N_i} N_0 \sum_{\mathbf{p}\neq 0} \left(4 \hat{b}_{\mathbf{p}}^\dagger \hat{b}_{\mathbf{p}} + \hat{b}_{\mathbf{p}} \hat{b}_{-\mathbf{p}} + \hat{b}_{\mathbf{p}}^\dagger \hat{b}_{-\mathbf{p}}^\dagger \right), \tag{2.32}$$

which again introduces anomalous terms with only two creation or annihilation operators. Since N_0 is an unknown quantity, it has to be eliminated from the Hamiltonian using the identity

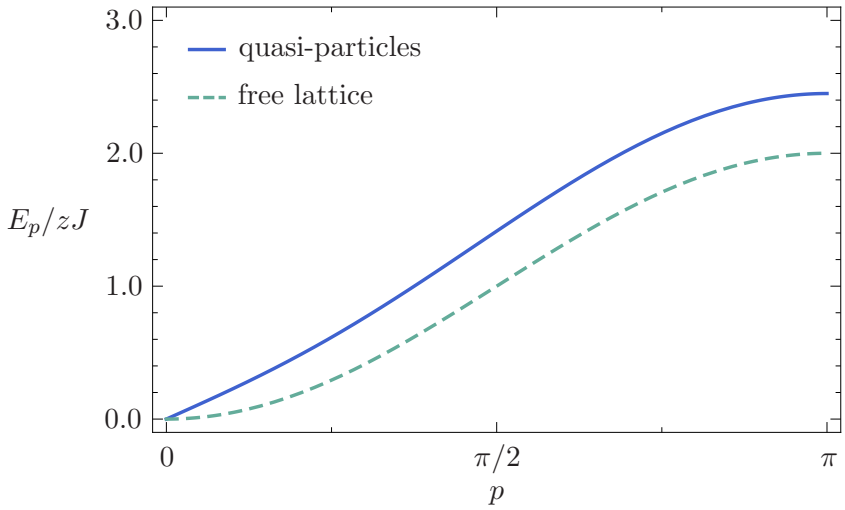

Figure 2.2: The solid blue curve shows the dispersion $E_{\mathbf{p}}$ of the Bogoliubov quasi-particles for $U\rho/zJ = 0.5$, the dashed green curve the excitation energies $E_{\mathbf{p}} = \varepsilon_{\mathbf{p}} - \varepsilon_{\mathbf{p}=0}$ of the non-interacting system.

$N = N_0 + \sum_{\mathbf{p}\neq 0} \hat{b}^\dagger_{\mathbf{p}} \hat{b}_{\mathbf{p}}$ for the total number of particles N. This yields

$$\hat{H}_{BH} = N\left[\varepsilon_{\mathbf{p}=0} + \frac{U\rho}{2}\right] + \sum_{\mathbf{p}\neq 0} (\varepsilon_{\mathbf{p}} - \varepsilon_{\mathbf{p}=0} + U\rho)\hat{b}^\dagger_{\mathbf{p}}\hat{b}_{\mathbf{p}} + \frac{U\rho}{2}\sum_{\mathbf{p}\neq 0}\left(\hat{b}_{\mathbf{p}}\hat{b}_{-\mathbf{p}} + \hat{b}^\dagger_{\mathbf{p}}\hat{b}^\dagger_{-\mathbf{p}}\right), \tag{2.33}$$

where we have again neglected all interaction terms between the non-condensed particles. In order to diagonalize the Hamiltonian, we now perform the Bogoliubov transformation,

$$\hat{b}_{\mathbf{p}} = u_{\mathbf{p}}\hat{\alpha}_{\mathbf{p}} - v^*_{-\mathbf{p}}\hat{\alpha}^\dagger_{-\mathbf{p}} \quad \text{and} \quad \hat{b}^\dagger_{\mathbf{p}} = u^*_{\mathbf{p}}\hat{\alpha}^\dagger_{\mathbf{p}} - v_{-\mathbf{p}}\hat{\alpha}_{-\mathbf{p}}\,, \tag{2.34}$$

where one has to choose $|u_{\mathbf{p}}|^2 - |v_{-\mathbf{p}}|^2 = 1$ in order to fulfill the permutation relations of the initial boson operators. Plugging these definitions back into $\hat{H}_{BH}$, one obtains

$$\hat{H}_{BH} = N\left[\varepsilon_{\mathbf{p}=0} + \frac{U\rho}{2}\right] + \sum_{\mathbf{p}}\left[E_{\mathbf{p}}\hat{\alpha}^\dagger_{\mathbf{p}}\hat{\alpha}_{\mathbf{p}} + \frac{U_{\mathbf{p}}}{2}\,\hat{\alpha}_{\mathbf{p}}\hat{\alpha}_{-\mathbf{p}} + \frac{U^*_{\mathbf{p}}}{2}\,\hat{\alpha}^\dagger_{\mathbf{p}}\hat{\alpha}^\dagger_{-\mathbf{p}} + |v_{\mathbf{p}}|^2 - u_{\mathbf{p}}v^*_{\mathbf{p}}\right], \tag{2.35a}$$

where

$$E_{\mathbf{p}} = \left[\varepsilon_{\mathbf{p}} - \varepsilon_{\mathbf{p}=0} + U\rho\right]\left(|u_{\mathbf{p}}|^2 + |v_{\mathbf{p}}|^2\right) - U\rho\left(u_{\mathbf{p}}v^*_{\mathbf{p}} + u^*_{\mathbf{p}}v_{\mathbf{p}}\right) \tag{2.35b}$$

and

$$U_{\mathbf{p}} = U\rho\left(u_{\mathbf{p}}u_{-\mathbf{p}} + v_{\mathbf{p}}v_{-\mathbf{p}}\right) - \left[\varepsilon_{\mathbf{p}} - \varepsilon_{\mathbf{p}=0} + U\rho\right]\left(u_{\mathbf{p}}v_{-\mathbf{p}} + u_{-\mathbf{p}}v_{\mathbf{p}}\right). \tag{2.35c}$$

Apparently, the Hamiltonian is diagonal with respect to the quasi-particles if we demand $U_{\mathbf{p}} = 0$ for all $\mathbf{p}$. Making the ansatz $u_{\mathbf{p}} = u_{-\mathbf{p}} \in \mathbb{R}$ and $v_{\mathbf{p}} = v_{-\mathbf{p}} \in \mathbb{R}$ and using the condition $U_{\mathbf{p}} = 0$, the quasi-particle energies can be written as

$$E_{\mathbf{p}} = \left[\varepsilon_{\mathbf{p}} - \varepsilon_{\mathbf{p}=0}\right]\left(u_{\mathbf{p}} + v_{\mathbf{p}}\right)^2, \tag{2.36}$$

The coefficients $u_{\mathbf{p}}$ and $v_{\mathbf{p}}$ can be expressed using the hyperbolic functions (see [42]), leading to

$$\left(u_{\mathbf{p}} + v_{\mathbf{p}}\right)^2 = \sqrt{\frac{\varepsilon_{\mathbf{p}} - \varepsilon_{\mathbf{p}=0} + 2U\rho}{\varepsilon_{\mathbf{p}} - \varepsilon_{\mathbf{p}=0}}}\,, \tag{2.37}$$

and thus

$$E_{\mathbf{p}} = \sqrt{\varepsilon_{\mathbf{p}} - \varepsilon_{\mathbf{p}=0}}\sqrt{\varepsilon_{\mathbf{p}} - \varepsilon_{\mathbf{p}=0} + 2U\rho}\,. \tag{2.38}$$

Figure 2.2 shows a plot of the above dispersion of the Bogoliubov quasi-particles in comparison with the free lattice dispersion. For small momenta, the dispersion becomes linear,

$$E_{\mathbf{p}} \approx \sqrt{2zJU\rho}\,|\mathbf{p}|\,, \tag{2.39}$$

whereas for larger momenta it attains (very) roughly the form of the free lattice dispersion shifted by an effective mass term due to the interaction with the condensate,

$$E_{\mathbf{p}} \approx \varepsilon_{\mathbf{p}} - \varepsilon_{\mathbf{p}=0} + U\rho\,. \tag{2.40}$$

2.1.4 Landau Criterion for Superfluidity

In section 2.1.2, we have established that the Bose-Hubbard model undergoes a phase transition from a gaped to a gapless phase as a function of the ratio J/U, where the gaped phase was identified as the MI phase. We want to conclude the brief introduction to the pure Bose-Hubbard model by discussing the nature of the gapless phase, i.e., its SF nature.

Let us start by revisiting the Landau criterion for superfluidity [10], where we will again follow the presentation in [42]. Suppose, our system is confined by walls in all but one spatial dimension and the walls are movable along the axis of this free dimension. The system is supposed to be in its equilibrium state in a rest frame R and the walls are moving with velocity $-\mathbf{v}$ along the free axis. In its rest frame, the energy of the system is $E = E_0$ and the total momentum vanishes by definition, $\mathbf{P} = 0$. If we perform a Galilean transformation into the rest frame R' of the walls, the system now moves with the velocity $\mathbf{v}$. Accordingly, in this frame its energy is given by $E' = E_0 + \frac{1}{2}M\mathbf{v}^2$ and its momentum by $\mathbf{P}' = M\mathbf{v}$, where M is the total mass of the system.

Now, suppose the walls can interact with our system via friction and can reduce the total momentum $\mathbf{P}'$ by inducing excitations in the system. These excitation, however, will only take place, if they are energetically *profitable*, i.e., lower the total energy. Let us assume that one excitation with momentum $\mathbf{p}$ was induced. This changes the energy and the momentum of the system to $E = E_0 + E_{\mathbf{p}}$ and $\mathbf{P} = \mathbf{p}$, respectively. In the moving frame R', the new momentum is $\mathbf{P}' = \mathbf{p} + M\mathbf{v}$, and therefore, the new energy is given by

$$E' = E_0 + \mathbf{P}'/2M \approx E_0 + E_{\mathbf{p}} + \frac{1}{2}M\mathbf{v}^2 + \mathbf{v}\cdot\mathbf{p}\,, \tag{2.41}$$

where we have assumed that $M \gg \mathbf{p}^2$. By changing the total momentum of the system, its kinetic energy in the moving frame can be reduced. This, however, comes with the cost of increasing the system's internal energy by $E_{\mathbf{p}}$. Thus, for this process to be profitable the following inequality must be fulfilled,

$$E_{\mathbf{p}} + \mathbf{v}\cdot\mathbf{p} < 0\,. \tag{2.42}$$

The total momentum is reduced the most if $\mathbf{v}$ and $\mathbf{p}$ are antiparallel, which yields $|\mathbf{v}| > E_\mathbf{p}/|\mathbf{p}|$. If $E_\mathbf{p}$ was just the normal lattice dispersion $\varepsilon_\mathbf{p}$, we would have $|\mathbf{v}| > E_\mathbf{p}/|\mathbf{p}| \propto |\mathbf{p}|$ for $|\mathbf{p}| \ll 1$. Thus, for any given $\mathbf{v}$ the condition would be fulfilled for small enough momenta $\mathbf{p}$. However, as we have found in the previous section the energy of the lowest excitations of the weakly correlated Bose-Hubbard model goes linearly with the momentum, see (2.39). Therefore, we have

$$|\mathbf{v}| > E_\mathbf{p}/|\mathbf{p}| = \sqrt{2zJU\rho} > 0\,, \tag{2.43}$$

which implies that there exists a minimal velocity below which the system is insensitive to friction with the walls. In other words, it can move without friction along the walls, making it a superfluid.

The dispersion relation giving rise to this behavior was derived based on the assumption that almost all particles are condensed into the single-particle ground state. The system can only reduce its kinetic energy by inducing elementary excitations, which for small momenta are always more costly than the energy that can be gained from reducing the kinetic energy while conserving the total momentum.

This argument, however, can only be made when it is possible to calculate the spectrum of the elementary excitations. In the strongly correlated regime this will not be the case anymore. Thus, if we want to continue to work with the picture of a mean field and quantum fluctuations, we need to investigate how a Galilean transformation into a moving frame affects these quantities, which will be the topic of the next section.

2.1.5 Mean Field Amplitude and Superfluid Velocity

In order to investigate how the order parameter behaves under a Galilean transformation, we need to revisit the GPE in its time-dependent form. For simplicity, here we will use the description in terms of field operators,

$$\hat{\Psi}(\mathbf{x}) = \sum_i \langle \mathbf{x}|i\rangle \hat{b}_i\,, \tag{2.44}$$

where $|i\rangle$ is the local single-particle state corresponding to the operator $\hat{b}_i$. This allows us to write the Hamiltonian (within the canonical ensemble) as

$$\hat{H}_{BH} = \int \mathrm{d}^3x\, \hat{\Psi}^\dagger(\mathbf{x}) \left(\frac{-\nabla^2}{2m} + V(\mathbf{x}) \right) \hat{\Psi}(\mathbf{x}) + \frac{1}{2} \int \mathrm{d}^3x\, \mathrm{d}^3x'\, \hat{\Psi}^\dagger(\mathbf{x}) \hat{\Psi}^\dagger(\mathbf{x}') U(\mathbf{x}-\mathbf{x}') \hat{\Psi}(\mathbf{x}') \hat{\Psi}(\mathbf{x})\,, \tag{2.45}$$

where m is the particle mass, $V(\mathbf{x})$ the lattice potential, and $U(\mathbf{x}-\mathbf{x}')$ the two-particle interaction term. The parameters of the Bose-Hubbard model are related to these quantities as follows,

$$\int \mathrm{d}^3x\, \langle i|\mathbf{x}\rangle \left(\frac{-\nabla^2}{2m} + V(\mathbf{x}) \right) \langle \mathbf{x}|j\rangle = \begin{cases} \varepsilon_0 & \text{for } i = j, \\ -J_{ij} & \text{for } i \neq j, \end{cases} \tag{2.46a}$$

and

$$\int \mathrm{d}^3x \int \mathrm{d}^3x' \langle i|\mathbf{x}\rangle \langle j|\mathbf{x}'\rangle U(\mathbf{x}-\mathbf{x}') \langle \mathbf{x}'|k\rangle \langle \mathbf{x}|l\rangle = \begin{cases} U & \text{for } i=j=k=l, \\ 0 & \text{otherwise.} \end{cases} \tag{2.46b}$$

The equation of motion for the field operator can be calculated using the Heisenberg equation of motion, yielding

$$\mathrm{i}\frac{\mathrm{d}}{\mathrm{d}t}\hat{\Psi}(\mathbf{x},t) = \left(\frac{-\nabla^2}{2m} + V(\mathbf{x}) + \int \mathrm{d}^3x'\, \hat{\Psi}^\dagger(\mathbf{x}',t)U(\mathbf{x}-\mathbf{x}')\hat{\Psi}(\mathbf{x}',t)\right)\hat{\Psi}(\mathbf{x},t)\,. \tag{2.47}$$

Writing $\hat{\Psi}(\mathbf{x},t) = \psi(\mathbf{x},t) + \delta\hat{\Psi}(\mathbf{x},t)$, with $\psi(\mathbf{x},t) = \langle\hat{\Psi}(\mathbf{x},t)\rangle$ being the mean field amplitude (or the order parameter) and $\delta\hat{\Psi}(\mathbf{x},t)$ the fluctuations operator, one can derive the time-dependent GPE for the mean field by omitting all fluctuation terms,

$$\mathrm{i}\frac{\mathrm{d}}{\mathrm{d}t}\psi(\mathbf{x},t) = \left(\frac{-\nabla^2}{2m} + V(\mathbf{x}) + \int \mathrm{d}^3x'\, U(\mathbf{x}-\mathbf{x}')|\psi(\mathbf{x}',t)|^2\right)\psi(\mathbf{x},t)\,. \tag{2.48}$$

Comparing this with the time-independent GPE (2.26) (which was derived in the grand canonical ensemble), it follows that $\psi(\mathbf{x},t) = \psi(\mathbf{x})e^{-\mathrm{i}\mu t}$.

If we now, for simplicity, consider the free case, $V(\mathbf{x}) = 0$, and perform a Galilean transformation into a moving frame, $\hat{\Psi}(\mathbf{x},t) \to \hat{\Psi}'(\mathbf{x}',t)$ with $\mathbf{x}' = \mathbf{x} + \mathbf{v}t$, it is a straightforward calculation to show that the relation

$$\hat{\Psi}'(\mathbf{x}',t) = \hat{\Psi}(\mathbf{x}'-\mathbf{v}t,t)e^{\mathrm{i}\left(m\mathbf{v}\cdot\mathbf{x}' - \frac{1}{2}m\mathbf{v}^2t\right)} \tag{2.49}$$

must be fulfilled in order for $\hat{\Psi}'(\mathbf{x}',t)$ to be a solution of the equation of motion (2.47). For the order parameter this implies

$$\psi'(\mathbf{x}',t) = \psi\, e^{\mathrm{i}S(\mathbf{x}',t)}\,, \tag{2.50}$$

with the complex phase

$$S(\mathbf{x},t) = m\mathbf{v}\cdot\mathbf{x} - \left(\frac{m}{2}\mathbf{v}^2 - \mu\right)t\,, \tag{2.51}$$

where we have assumed a uniform order parameter in the rest frame of the bosonic system, $\psi(\mathbf{x}) = \psi$. This means that the order parameter in the moving frame acquires a complex phase that depends on the spatial coordinate and oscillates in time. On the other hand, if we consider the moving frame to be at rest and the bosonic system to be in motion, it follows that the order parameter of a uniformly moving bosonic system acquires a complex phase varying in space and time. The velocity of the bosonic system is given by the gradient of the phase $S(\mathbf{x},t)$,

$$\mathbf{v} = \frac{1}{m}\nabla S(\mathbf{x},t)\,. \tag{2.52}$$

In turn, this implies that a constant movement of the whole bosonic system can be induced by imposing a phase gradient upon the order parameter. This can be done, for example, by fixing the complex phase of $\psi(\mathbf{x},t)$ on two opposite boundaries of the system to different values.

If the lattice potential is turned on, $V(\mathbf{x}) \neq 0$, the situation immediately becomes more complicated. The question one could ask then is whether the system as a whole or only a fraction of it is transported by the current. According to the theory of the two-fluid hydrodynamics, see, for example, [42], one can divide the total particle density ρ into a normal and a SF part, $\rho = \rho_n + \rho_s$. At finite temperature, $T > 0$, both ρ_n and ρ_s will contribute to the total density ρ. According to an argument by Leggett [14, 43], in the limit $T \to 0$ the SF fraction of the density will tend to unity for pure bosonic systems, $\rho_s/\rho \to 1$. Thus, it is generally accepted that the conducting phase of the pure Bose-Hubbard model is the SF phase [1].

This concludes this brief introduction to the pure Bose-Hubbard model. Before we move on to discuss the disordered case, it is useful to first consider the characteristics of the non-interacting disordered lattice model, i.e., the Anderson Hamiltonian and the phenomenon of Anderson localization.

2.2 Anderson Localization

In the following section, we will review few of the most important cornerstones of the theory of Anderson localization. As the theory was developed with the intention of describing conductance in impure solids, it focuses on fermionic rather than bosonic particles.

2.2.1 Absence of Diffusion

In his seminal work *Absence of Diffusion in Certain Random Lattices* [18], Anderson investigated the problem of a particle *jumping* through a random lattice. In order to start with the simplest model possible, he considered the following discrete Schrödinger equation,

$$\mathrm{i}\,\frac{\mathrm{d}}{\mathrm{d}t}a_i = \varepsilon_i a_i + \sum_{k}^{k\neq i} J_{ik} a_k\,, \tag{2.53}$$

where a_i is the probability amplitude for finding the particle on site i. The above equation of motion corresponds to the well known Anderson Hamiltonian,

$$\hat{H}_A = \sum_i \varepsilon_i\, \hat{b}_i^\dagger \hat{b}_i + \sum_{ij}^{i\neq j} J_{ij}\, \hat{b}_i^\dagger \hat{b}_j\,, \tag{2.54}$$

where now, in contrast to the Bose-Hubbard model, the on-site energies are not equal for all lattice sites, but randomly distributed according to a probability distribution function $P_\varepsilon(\varepsilon)$. which can be characterized by a width W. This could be, for example, a simple box distribution,

$$P_\varepsilon(\varepsilon) = \begin{cases} 1/W & \text{if } -W/2 < \varepsilon < +W/2\,, \\ 0 & \text{otherwise.} \end{cases} \tag{2.55}$$

The question he posed was whether a particle initially located at some point in space would diffuse away into the infinite system or not. If the particle diffuses into the infinite system, all amplitudes will vanish for large times, $\lim_{t\to\infty} a_i(t) = 0$ for all i. If the particle is localized within a finite region in space, the amplitude will remain finite in that region, $\lim_{t\to\infty} a_i(t) \neq 0$ for some i.

In order to study this behavior, it us useful to take a look at the eigenstates of the system. Let $\{|\psi_\alpha\rangle\}$ be the complete set of eigenstates with corresponding eigenenergies E_α. Then, the local state $|i\rangle$ of site i can be expressed as follows,

$$|i\rangle = \sum_\alpha \langle\psi_\alpha|i\rangle\, |\psi_\alpha\rangle\,. \tag{2.56}$$

If an eigenstate is extended, its overlap with site i scales with the system size, $\langle i|\psi_\alpha\rangle \sim 1/\sqrt{N_i}$, and vanishes in the thermodynamic limit, $N_i \to \infty$. Only if a state is localized (or bound) in

a region containing site i, the overlap remains finite for $N_i \to \infty$. Now, we place a particle on site i at $t = 0$ and study its evolution in time,

$$a_i(t) = \langle i|i(t)\rangle = \sum_\alpha \langle\psi_\alpha|i\rangle\langle i|\psi_\alpha(t)\rangle = \sum_\alpha |\langle\psi_\alpha|i\rangle|^2 \, e^{-\mathrm{i}E_\alpha t} \,. \tag{2.57}$$

Due to the oscillating terms, $a_i(t)$ will fluctuate and at times may become zero even in the localized regime. Therefore, it is more advisable to look at the temporal average of $a_i(t)$. We can test whether state $|i\rangle$ on site i has a finite overlap with a localized state at energy E by considering the following quantity,

$$\lim_{t\to\infty} \frac{1}{t} \int_0^t \mathrm{d}t' e^{\mathrm{i}Et'} a_i(t') = \sum_\alpha |\langle\psi_\alpha|i\rangle|^2 \lim_{t\to\infty} \frac{1}{t} \int_0^t \mathrm{d}t' e^{\mathrm{i}(E-E_\alpha)t'} = \sum_\alpha |\langle\psi_\alpha|i\rangle|^2 \, \delta_{E,E_\alpha} \,. \tag{2.58}$$

The above expression is only finite if there is a localized state with energy $E_\alpha = E$, that has a finite overlap with site i. However, the complete set of eigenstates of $\hat{H}_A$ is, in general, hard to obtain. Therefore, we will expand the above expression perturbatively using the Green's function formalism, see also appendices B.1 and B.2. The probability amplitudes are related to the retarded single-particle Green's functions as follows,

$$a_k(t) = \mathrm{i}G^R_{ki}(t) \quad \text{for} \quad a_k(0) = \delta_{k,i} \text{ and } t > 0 \,. \tag{2.59}$$

The long-time average (2.58) can be expressed in terms of the Fourier transformed of the full local Green's function,

$$\lim_{t\to\infty} \frac{1}{t} \int_0^t \mathrm{d}t' e^{\mathrm{i}Et'} a_i(t') \sim \lim_{\eta\to 0} \mathrm{i}\eta \, G_{ii}(E + \mathrm{i}\eta) \,. \tag{2.60}$$

with $E \in \mathbb{R}$. In appendix B.2, it is shown that the full Green's functions can be expanded in terms of the locator functions,

$$G_{ij}(E) = G^0_i(E)\delta_{ij} + G^0_i(E) \sum_l^{l\neq i} J_{il} G_{lj}(E) \,. \tag{2.61}$$

with the locators

$$G^0_i(E) = \frac{1}{E - \varepsilon_i} \,. \tag{2.62}$$

By introducing the local self-energy $\Sigma_{ii}(E)$, the locator expansion can be written as

$$G_{ii}(E) \equiv G^0_i(E) + G^0_i(E)\Sigma_{ii}(E)G_{ii}(E) = \frac{1}{E - \varepsilon_i - \Sigma_{ii}(E)} \,. \tag{2.63}$$

The self-energy consists of all hopping sequences (or paths) starting and ending at site i without hopping onto the site in between (see [44], for example),

$$\Sigma_{ii}(E) = \sum_k J_{ik} G^0_k(E) J_{ki} + \sum_{kl}^{l\neq i} J_{ik} G^0_k(E) J_{kl} G^0_l(E) J_{li} + \ldots \tag{2.64}$$

Anderson then investigated the convergence of the self-energy for a tight-binding version of the

model, $J_{ik} = -J$ for i, k nearest neighbors and $J_{ik} = 0$ otherwise, and $E = 0$, i.e., the center of the band. Since the on-site energies are random numbers, the self-energy has to be treated as a random quantity as well. After a long derivation including certain approximations, it is found that if the ratio of the width W and the hopping amplitude J is larger than some critical ratio, $(W/J) > (W/J)_c$, the expansion series of the self-energy will converge *almost always* (again, see [44] for a more pedagogic presentation of Anderson's original work [18]). From this result, it was then concluded that the system is completely localized and no diffusion will take place. The transition from a phase with both localized and extended states to a phase with a completely localized spectrum is called the *Anderson transition*.

A rigorous proof for the existence of a critical disorder strength $(W/J)_c$ was later presented in [45, 46], where it was shown that either for strong disorder or low energies the particles will localize. Furthermore, in [47] it was shown that for one-dimensional systems ($d = 1$), the DOS is discrete (or point-like) for any finite disorder width, and thus, all states are localized. In other words, the critical disorder strength is zero, $(W/J)_c = 0$ for $d = 1$.

2.2.2 The Localization Length

In the previous section, we have discussed that above a certain critical disorder strength $(W/J)_c$, no diffusion is taking place anymore and particles become localized in finite regions in space. We have already concluded that this implies that the eigenstates of the system become localized as well, see equation (2.58). In the following we want to discuss the character of these eigenstates. Of course, since the random potential is always finite, the states cannot be bound in a strict sense. Rather, they are *exponentially localized*,

$$|\langle i|\psi_\alpha\rangle| \sim e^{-|\mathbf{x}_i - \mathbf{x}_\alpha|/\xi_\alpha} \quad \text{for } |\mathbf{x}_i - \mathbf{x}_\alpha| \to \infty\,, \tag{2.65}$$

that is, the envelope of the wave function decreases exponentially when moving away from a certain point in space $\mathbf{x}_\alpha$ (see [48], for example). The decay is governed by the *localization length* ξ_α. The larger ξ_α, the further the wave function spreads into the system. For an extended state that scales with the system size, the localization length is infinitely large. The exact form of each eigenstate depends on the realization of disorder (i.e., the actual values of the ε_i) and is highly non-trivial.

This also means that in order to determine an average localization length, the eigenstates would have to be calculated all over again for each new disorder realization. This appears to be highly impractical and, as we will see later, it is possible to define the localization length in terms of already disorder averaged quantities using the *self-consistent theory of localization*.

2.2.3 Lifshitz Tails

From [45], we already know that states far enough away from the center of the band ($E = 0$) are localized, even if the disorder is below the critical value. This can be understood in a very intuitive way using an argument made by Lifshitz [49].

Let us assume that the probability distribution P_ε is only finite in the interval $[-W/2, +W/2]$. For a tight-binding hopping term and a d-dimensional cubic lattice, the density of states (DOS) then stretches from $E_{min} = -W/2 - 2Jd$ to $E_{max} = +W/2 + 2Jd$. The theoretical upper and lower bounds correspond to a lattice with all on-site energies equal to $+W/2$ or $-W/2$, respectively. In these cases, the eigenstates are given by Bloch states $|\mathbf{p}\rangle \sim \sum_i e^{-\mathrm{i}\mathbf{p}\cdot\mathbf{x}_i}|i\rangle$, with

corresponding eigenenergies

$$\varepsilon_{\mathbf{p}} = \pm W/2 - 2J \sum_{a=1}^{d} \cos p_a \quad \text{with } p_a \in (-\pi, +\pi]\,. \tag{2.66}$$

The two wave vectors yielding the highest and lowest energy are given by $\mathbf{p}_+ = (\pi, \ldots, \pi)$ and $\mathbf{p}_- = (0, \ldots, 0)$, respectively. Of course, in the thermodynamic limit, $N_i \to \infty$, the probability for such a realization would vanish. Nevertheless, the probability for finding a large but finite region with on-site energies $\varepsilon_i \approx \pm W/2$ will still be finite. Eigenstates that have energies close to the upper or lower boundary of the DOS must then be localized within such a region. If the region is large enough, we can assume that the eigenstates are more or less identical to those of the tight-binding model, with the condition that they must vanish on the boundaries since they should be localized. Assuming the region to extend from 0 to L in each direction, the eigenstates are given by $|\mathbf{p}\rangle \sim \sum_i \prod_{a=1}^{d} \sin(p_a x_{i,a}) |i\rangle$, where

$$p_a = \frac{\pi}{L}\, n \quad \text{with } n = 1, 2, 3, \ldots, L-1\,. \tag{2.67}$$

The eigenenergies are the same as for the Bloch states, see expression (2.66). However, due to the boundary conditions the wave vectors $\mathbf{p}_+$ and $\mathbf{p}_-$ are forbidden. Thus, for a large but finite region of length L with $\varepsilon_i = -W/2$ for all i, the lowest possible energy is given by

$$E_{min}(L) = -W/2 - 2J \sum_{a=1}^{d} \cos(\pi/L) \approx -W/2 - 2Jd + \frac{\pi^2 d}{L^2}\,, \tag{2.68a}$$

whereas for a region with $\varepsilon_i = +W/2$ for all i, the highest possible energy is given by

$$E_{max}(L) = +W/2 - 2J \sum_{a=1}^{d} \cos(\pi(L-1)/L) \approx +W/2 + 2Jd - \frac{\pi^2 d}{L^2}\,. \tag{2.68b}$$

This result can now be used to express the DOS. The probability for finding a state with energy $E_{min}(L)$ or $E_{max}(L)$ is given by the probability of finding a corresponding region of length L. This probability should be proportional to $(1/W)^{L^d}$, with L^d being the number of sites in that region. From the above equations we know that

$$E_{min}(L) - E_{min} = E_{max} - E_{max}(L) = \pi^2 d/L^2 \sim 1/L^2. \tag{2.69}$$

Thus, the DOS at the edges of the band falls off exponentially,

$$N(E_{min/max} \pm E) \sim e^{-C\,|E_{min/max} \pm E|^{-d/2}}\,, \tag{2.70}$$

where C is some positive constant. These exponential tails of the DOS are called *Lifshitz tails*. They are very hard to resolve in a direct numerical approach, as one needs very large system sizes and many disorder realizations in order to reproduce them. As we will see later, this is also the main reason the stochastic mean-field theory does not yield the correct phase boundary between compressible and incompressible phase, see section 3.2.4. In the following, we will refer to the states contributing to the Lifshitz tails as the *Lifshitz states*.

2.2.4 Mobility Edges

In the previous section, we have established that states at the upper and lower edges of the DOS are localized in large potential fluctuations. This implies that extended states, if present, have to be located in the middle of the band. According to an argument by Mott [50], this goes even further, in that localized and extended states are strictly separated in energy.

Suppose, there are two eigenstates of $\hat{H}_A$ with the same energy E, one localized ($|\psi_l\rangle$) and one extended ($|\psi_e\rangle$). If we change the on-site energy for a certain i infinitesimally, $\varepsilon_i \to \varepsilon_i + \delta$ with $\delta \ll 1$, this will induce a coupling between the two states. The Hamiltonian in the subspace spanned by the two states is given by

$$\hat{H} = \begin{pmatrix} E + \delta|\langle i|\psi_l\rangle|^2 & \delta\langle\psi_l|i\rangle\langle i|\psi_e\rangle \\ \delta\langle\psi_e|i\rangle\langle i|\psi_l\rangle & E + \delta|\langle i|\psi_e\rangle|^2 \end{pmatrix} \tag{2.71}$$

As the extended state $|\psi_e\rangle$ has a finite amplitude $\langle i|\psi_e\rangle$ on every site i, we can choose i such that $\langle i|\psi_l\rangle$ is finite as well. The new eigenstates are then given by

$$|\psi_+\rangle \sim |\psi_l\rangle + \frac{\langle\psi_e|i\rangle}{\langle\psi_l|i\rangle}|\psi_e\rangle \quad \text{and} \quad |\psi_-\rangle \sim |\psi_l\rangle - \frac{\langle i|\psi_l\rangle}{\langle i|\psi_e\rangle}|\psi_e\rangle\,. \tag{2.72}$$

Apparently, they do not depend on the perturbation parameter δ, which is due to the initial degeneracy. Furthermore, since both new states contain admixtures of the extended state $|\psi_e\rangle$, none of them is localized.

Mott argued that the density of states should not depend on such an infinitesimal perturbation. Thus, the assumption that there was a localized and an extended state at the same energy must have been wrong in the first place. From that, one can conclude that there is no coexistence of extended and localized states at the same energy. The commonly accepted picture derived from this argument is that for $(W/J) < (W/J)_c$, the energy regime of the localized states extends from the Lifshitz tails to two certain points in energy, the so-called *mobility edges*, see figure 2.3. In between the two mobility edges lies the regime of the extended states. If the disorder strength W/J is increased, the mobility edges shift further towards the center of the band, until both coincide and all states are localized. This should happen exactly at the critical disorder strength, i.e., the Anderson transition.

2.2.5 Coherent Backscattering

The locator expansion used in the original article by Anderson [18] is a perturbation series in powers of the hopping amplitude J. Thus, it is only applicable when J is small compared to the other parameters of the system, i.e., in the case of strong disorder where W/J is large. In fact, the Anderson transition was determined by the breakdown of the locator expansion. We already know that for $d = 1$, systems are localized even for very small disorder. Here, the picture of states bound in large potential fluctuations cannot be valid anymore. As also pointed out by Anderson, the critical disorder strength found in [18] has to be understood as an upper bound for the possibility of extended states.

The mechanism responsible for the localization of states even for small disorder strengths is the coherent superposition of quantum waves. This can be understood quite intuitively by considering the probability $P_{i\to j}$ for a particle to propagate from site i to site j. According to equation (2.61), the probability amplitude can be written as a sum over the amplitudes $A_{\mathcal{C}_{ij}}$

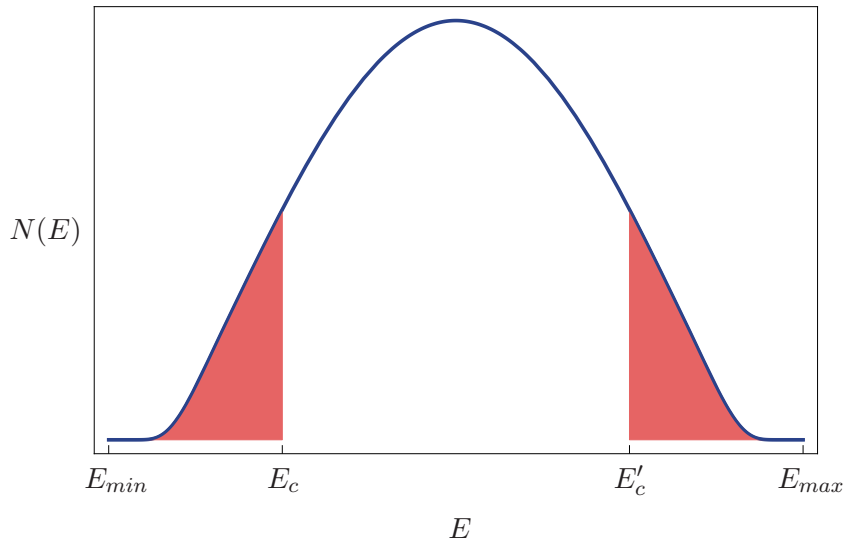

Figure 2.3: A sketch of a typical density of states $N(E)$ for a disordered system for $(W/J) < (W/J)_c$, ranging from E_{min} to E_{max}, with the Lifshitz tails and the two mobility edges E_c and E_c'. The energy regimes of the localized states are indicated by the red filling.

contributed by each path $\mathcal{C}_{ij}$, see also figure 2.4a. Thus, we have

$$P_{i\to j} = \Big|\sum_{\mathcal{C}_{ij}} A_{\mathcal{C}_{ij}}\Big|^2 = \sum_{\mathcal{C}_{ij}} \big|A_{\mathcal{C}_{ij}}\big|^2 + \sum_{\mathcal{C}_{ij}\neq\mathcal{C}'_{ij}} A_{\mathcal{C}_{ij}} A^*_{\mathcal{C}'_{ij}}\,. \tag{2.73}$$

The first term corresponds to the classical contribution and the second term to the corrections due to quantum interferences between different paths. Because of the randomness of the on-site energies, the complex phase accumulated along different paths will be a random quantity as well. Thus, in general quantum corrections to the classical probability will be suppressed and would vanish in a disorder average.

Now, if we specifically consider the probability for a particle returning to its initial site, $P_{i\to i}$, then for each path $i \to j_1 \to j_2 \to \ldots \to j_{n-1} \to j_n \to i$, there exists a time-reversed path $i \to j_n \to j_{n-1} \to \ldots \to j_2 \to j_1 \to i$, see figure 2.4b. If the system is invariant under time-reversal, which is the case for the Anderson Hamiltonian, then both paths yield the same amplitude. In particular, they will have the same complex phase, i.e., they are phase coherent. Thus, for the probability $P_{i\to i}$ we can write

$$P_{i\to i} = 2\sum_{\mathcal{C}_{ii}} \big|A_{\mathcal{C}_{ii}}\big|^2 + \textit{incoherent contributions}\,, \tag{2.74}$$

i.e., the probability for a quantum mechanical particle to return to its initial site is twice as large as it would be for a classical particle. This effect is called *coherent backscattering*. Furthermore, as the total probability is a conserved quantity and is normalized to one, $\sum_j P_{i\to j} = 1$, the probability for the particle diffusing away into the infinite system must be reduced compared to the classical case.

This intuitive picture carries on into the actual calculations of physical quantities, such as the

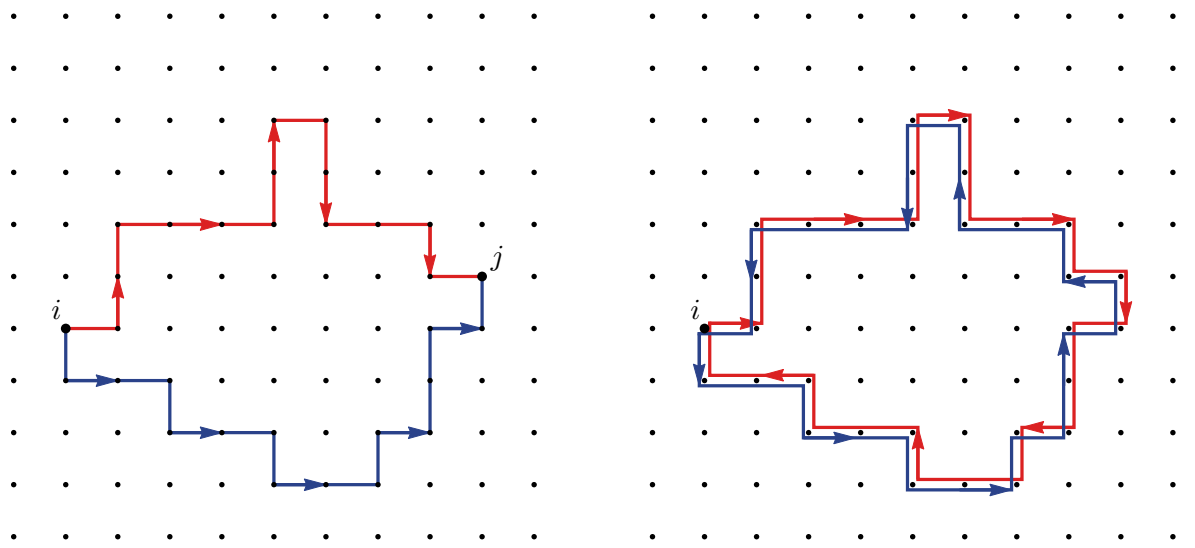

(a) $i \to j$ (b) $i \to i$

Figure 2.4: **(a)** Two arbitrary paths from site i to site j. **(b)** Two paths starting and ending at the same site i that are related by time-reversal symmetry.

conductivity. Within linear response theory (see [51], for example), one obtains the following expression for the conductivity tensor in energy-momentum representation for $T \to 0$,

$$\sigma_{\alpha\beta}(\mathbf{q},\omega) = \frac{e^2}{\pi}\frac{1}{N_i}\sum_{\mathbf{p}\mathbf{p}'} p_\alpha \langle G^R_{\mathbf{p}_+\mathbf{p}'_+}(\varepsilon_F+\omega) G^A_{\mathbf{p}'_-\mathbf{p}_-}(\varepsilon_F)\rangle p'_\beta \,, \tag{2.75}$$

with $\mathbf{q}$ and ω being the wave vector and the frequency of the external field coupling to the system, respectively, ε_F the Fermi energy, and $\mathbf{p}_\pm = \mathbf{p} \pm \mathbf{q}/2$. The integration kernel is actually the disorder-averaged particle-hole propagator that is also at the core of the self-consistent theory of localization, see appendix B.4.1. As explained there, the particle-hole propagator can be expanded in terms of the disorder-averaged single-particle Green's functions,

$$\langle G^{R/A}_{\mathbf{p}}(E)\rangle = \frac{1}{E - \varepsilon_{\mathbf{p}} - \Sigma^{R/A}_{\mathbf{p}}(E) \pm \mathrm{i}\eta} \,, \tag{2.76}$$

i.e., an expansion in terms of an extended state basis. Similar to the locator expansion, which is reasonable in the strong disorder case where the true eigenstates are localized and J/W is a small parameter, the extended state expansion is suitable for the opposite case, i.e., weak disorder with W/J being the small parameter.

The largest contribution arises from the so called *ladder diagrams*, see figure 2.5a. They correspond to the classical contribution in expression (2.73) and yield the Drude result for conductivity in the static limit (see [51] for the derivation),

$$\sigma^0 = \lim_{\mathbf{q},\omega\to 0} \sigma_{\alpha\alpha}(\mathbf{q},\omega) = \frac{ne^2\tau}{m} \,, \tag{2.77}$$

where n is the particle density, m the particle mass, e the elementary charge, and τ the transport

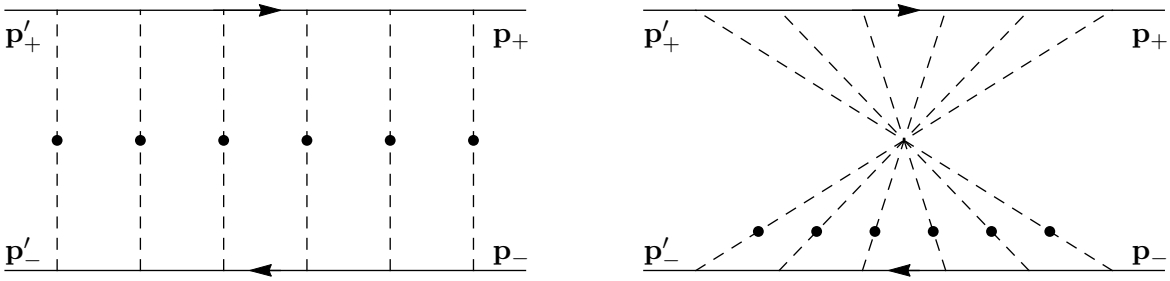

(a) Ladder Diagram (b) Maximally Crossed Diagram

Figure 2.5: The two types of diagrams that lead to the largest contribution to the disorder-averaged particle-hole propagator. The solid lines indicate the disorder-averaged particle (moving rightwards/forward in time) or hole propagator (moving leftwards/backward in time). The dashed lines indicate scattering processes at the same impurity. The ladder diagrams correspond to the classical contribution, the maximally crossed diagrams to the contribution arising from coherent backscattering, see also figure 2.4b.

relaxation time.

The next-to-leading order contributions come from the class of the *maximally-crossed diagrams*, see figure 2.5b. They are connected to the ladder diagrams by time-reversal of either the particle or the hole propagator line, i.e., the diagrams that arise from coherent backscattering. They yield a finite correction to the classical conductivity,

$$\delta\sigma(\mathbf{q}=0,\omega) = -\frac{2e^2}{\pi}\int_{1/L}^{1/l}\frac{\mathrm{d}^d Q}{(2\pi)^d}\frac{1}{-\mathrm{i}\omega/D_0+\mathbf{Q}^2}\,, \tag{2.78}$$

where the integration is taken over $\mathbf{Q}=\mathbf{p}+\mathbf{p}'$ and has to be cut off at the inverse of the mean free path l due to certain approximations made in the derivation of $\delta\sigma$. Furthermore, a finite system size L sets a lower boundary on the possible momenta (again, see [51] for the derivation).

As one would expect from the considerations made at the beginning of this section, the contributions from coherent backscattering are negative and lead to a decreased conductivity. This result will be of importance in the next section. In the static limit, the above integral yields

$$\delta\sigma = \lim_{\omega\to 0}\delta\sigma(\mathbf{q}=0,\omega) = -\frac{2e^2}{\pi}\frac{\Omega_d}{(2\pi)^d}\int_{1/L}^{1/l}\mathrm{d}Q\,Q^{d-3}\,, \tag{2.79}$$

where Ω_d is the surface element in d dimensions. In one and two dimensions, the integral is divergent in the thermodynamic limit, $L\to\infty$, for any value of l, i.e., for any disorder strength. This implies a breakdown of the expansion series in terms of extended states, suggesting that in the thermodynamic limit any small disorder leads to a complete localization not only for $d=1$, but for $d=2$ as well.

In three dimensions, $\delta\sigma$ is proportional to $1/l$ and, thus, gets larger the larger the disorder strength becomes. This suggests, that in three dimensions the Anderson transition might be triggered by the effect of coherent backscattering.

2.2.6 Scaling Theory of Localization

We already mentioned that in one dimension any small amount of disorder immediately causes all states to localize [47]. Although there exists no rigorous proof, it is generally agreed upon that in three dimensions there is a coexistence of localized and extended states below a certain critical disorder strength. This already implies that the localizing effect of disorder strongly depends on the dimension of the system.

In 1979, Abrahams, Anderson, Licciardello, and Ramakrishnan introduced the *scaling theory of localization* [19], which is fundamental to the modern picture of localization. Motivated by previous works of Landauer [52], Thouless and co-workers [53–55], and Wegner [56], they investigated the dependence of the (dimensionless) conductance $g = \sigma/(e^2)L^{d-2}$ on the system size. They made the assumption that for already large systems the scaling behavior is determined by the conductance itself and does not depend on microscopic properties, such as, the realization of disorder. For simplicity, let us consider a d-dimensional hypercube with Volume L^d. If the length L is now scaled by a factor n, $L \to nL$, the new conductance $g(nL)$ should only depend on $g(L)$ and n,

$$g(nL) = f\big(n, g(L)\big)\,, \tag{2.80}$$

where f is the function that determines the scaling behavior. For the logarithmic derivative of $g(nL)$, one obtains

$$\beta \equiv \frac{\mathrm{d}\ln g(nL)}{\mathrm{d}\ln nL} = \frac{nL}{g(nL)}\frac{\mathrm{d}g(nL)}{\mathrm{d}nL} = \frac{n}{g(nL)}\frac{\mathrm{d}}{\mathrm{d}n}f\big(n, g(L)\big)\,. \tag{2.81}$$

If we set $n = 1$, we get

$$\beta = \frac{\mathrm{d}\ln g(L)}{\mathrm{d}\ln L} = \frac{1}{g(L)}\frac{\mathrm{d}}{\mathrm{d}n}f\big(n, g(L)\big)\Big|_{n=1} = \beta\big(g(L)\big)\,. \tag{2.82}$$

Apparently, the scaling function β depends only implicitly on the length L. In the limit of very large conductance, Ohm's law should be valid, i.e., $g(L) \sim L^{d-2}$ for $g \gg 1$. In the localized regime where $g \ll 1$, the scaling behavior should be determined by exponential decay of the wave functions, and thus, $g \sim e^{-L/\xi}$, where ξ is the characteristic localization length of the system. For the β-function we then obtain

$$\beta(g) = \begin{cases} d-2 & \text{for } g \gg 1, \\ \ln g & \text{for } g \ll 1. \end{cases} \tag{2.83}$$

According to the results by Wegner [56], the Anderson transition is a second order phase transition, i.e., the conductivity vanishes continuously at the transition from the conducting to the insulating phase (which is in contrast to previous predictions of a *minimal conductivity* [57]),

$$\sigma \sim (E - E_c)^s\,. \tag{2.84}$$

Therefore, it is assumed that β is a smooth and monotonous function of g. With this, one can interpolate between the two limits, yielding a function as plotted in figure 2.6. From this we can now obtain the scaling behavior for $L \to \infty$ of any system, if we only know its conductance for a given size.

Let us start with the simplest case, $d = 1$. Here, the scaling function is always negative, $\beta(g) < 0$ for any g. From this it follows that the conductance always decreases if the system

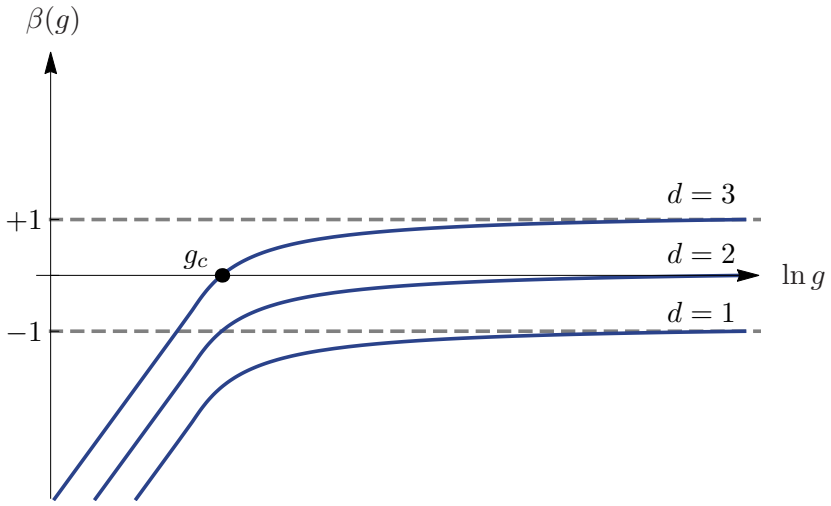

Figure 2.6: A qualitative plot of the scaling function $\beta(g)$ for $d = 1, 2, 3$. The horizontal dashed lines indicate the asymptotic behavior for $g \to \infty$. The black dot indicates the critical conductance g_c at which the scaling function vanishes for $d = 3$.

size is increased,

$$\frac{\mathrm{d}g}{\mathrm{d}L} = \frac{g}{L}\,\beta(g) < 0\,. \tag{2.85}$$

In accordance to the previous findings, a one-dimensional system always scales towards the insulating phase in the thermodynamic limit, i.e., it is always completely localized.

For three dimensions, there exists a critical conductance g_c where the scaling function becomes zero. For all $g < g_c$, $\beta(g)$ is negative and thus scales to the insulating limit for $L \to \infty$. On the other hand, for $g > g_c$ the scaling function is always positive and the system would flow towards the metallic solution. Thus, in three dimensions the scaling theory predicts the existence of both insulating or localized and conducting or non-localized systems.

For a given system size L, the conductance can be tuned by changing the disorder strength. For example, if $g(L, W/J) < g_c$, one could decrease the disorder strength until $g(L, W/J) > g_c$, thus turning a (in the thermodynamic limit) completely localized system into a system with extended states, i.e., triggering the Anderson transition. The divergence of the localization length when approaching the critical point from the localized regime is described by

$$\xi \sim (E_c - E)^{-\nu}\,. \tag{2.86}$$

The critical exponent ν is related to the one describing the behavior of the conductivity (see equation (2.84)) as follows, $s = \nu$.

For two dimensions, the situation is a little more complicated, as $\beta(g) \to 0$ for $g \to \infty$. Without making further assumptions, it is not necessarily clear whether the limit is approached from above or below. The former would imply that there is a critical conductance and, therefore, also a transition from the localized to the extended phase in two dimensions. The latter implies, that two-dimensional systems always scale towards zero conductance, i.e., there is no extended phase in two dimensions. At this point we have to recall the results from perturbation theory presented in the previous section. There, we found that the first quantum corrections to the classical result were negative, see equation (2.78). This suggests that, in fact, the limit is

approached from below and there is an *absence of quantum diffusion in two dimensions.*

The results of the scaling theory have been supported by further theoretical as well as numerical analysis, see [48] for a review, [58], or [59] for a more recent numerical study. However, there were doubts raised about the validity of the assumption of one single parameter determining the scaling behavior. In [60], for example, it was suggested that instead of only looking at the disorder-averaged conductance g, one rather has to observe the behavior of the probability distribution of the conductance, especially in the region near the critical conductance g_c in $d = 3$, where the distribution becomes very broad. Apart from that, the main results of the scaling theory are widely accepted and it is viewed as a milestone in the theory of Anderson localization.

Lastly, it should be noted again that this main result of the scaling theory relies on the time-invariance of the system. Hence, any mechanism that breaks this invariance, such as, magnetic couplings, can alter the asymptotic behavior for $g \to \infty$. Furthermore, no particle-particle interactions were considered when deriving the expressions for the conductivity. Thus, the result of the scaling theory is only valid for the non-interacting case and could change, once interactions are taken into account.

2.2.7 Self-Consistent Theory of Localization

We want to conclude this brief introduction to the topic of Anderson localization by presenting the method we will use to calculate transport properties later in this work, which is the *self-consistent theory of localization*, introduced in 1980 by Vollhardt and Wölfle [29]. This section will present the motivation that led to the formulation of the theory, as well as the most important steps of its derivation. In appendix B.4, a more detailed introduction to the theory can be found.

In section 2.2.5, we discussed that the most important quantum corrections to the classical conductivity arise from the class of maximally crossed diagrams. We also found that these corrections diverge in the thermodynamic limit for $d = 1, 2$ and can become very large for $d = 3$, see equation (2.78). Since, of course, the conductivity cannot become negative, this implies that the simple perturbation theory is invalid for these cases and additional contributions canceling the divergent behavior need to be taken into account to obtain a valid result for the conductivity.

To circumvent this problem, one would like to find a quantity that actually diverges at the phase transition. This quantity could then be calculated by taking into account only the most divergent terms. Using the continuity equation, the conductivity (2.75) can be written in terms of the density-response function $\chi(\mathbf{q}, \omega)$,

$$\sigma(\mathbf{q}, \omega) = -\frac{e^2}{\pi} \frac{\mathrm{i}\omega}{q^2} \chi(\mathbf{q}, \omega) \,. \tag{2.87}$$

In [29, 61], the density response is then expressed in terms of the density of states $N(E)$ and the density-density correlation function $\Phi_{\rho\rho}$,

$$\chi(\mathbf{q}, \omega) = 2N(\varepsilon_F) + \frac{\mathrm{i}\omega}{\pi} \Phi_{\rho\rho}(\varepsilon_F, \mathbf{q}, \omega) \,, \tag{2.88}$$

where $\Phi_{\rho\rho}$ is the momentum-integrated particle-hole propagator. It can be shown to have the following form,

$$\phi_{\rho\rho}(E, \mathbf{q}, \omega) = \frac{2\pi \mathrm{i} N(E)}{\omega + \mathrm{i} q^2 D(E, \omega)} \,, \tag{2.89}$$

with $D(E,\omega)$ being the *generalized diffusion coefficient*, see appendix B.4.1 for the definitions and the derivation. Using expressions (2.88) and (2.89) and taking the limit $q \to 0$, the conductivity can be expressed in terms of the diffusion,

$$\sigma(\omega) = 2e^2 N(\varepsilon_F) D(\varepsilon_F, \omega). \tag{2.90}$$

Apparently, if the diffusion coefficient vanishes, the conductivity becomes zero as well, which would mark the Anderson transition. The diffusion coefficient itself can be expressed in terms of the so-called *current relaxation kernel* $M(E,\omega)$,

$$D(E,\omega) \sim \frac{1}{2\,\mathrm{Im}\,\Sigma^A(E) - \mathrm{i}\omega + M(E,\omega)}\,. \tag{2.91}$$

In the static limit, $\omega \to 0$, the relaxation kernel has to diverge for the diffusion coefficient to vanish. Hence, $M(E,\omega)$ is the quantity that can be approximated by taking into account only the most divergent contributions.

In [29, 61], all diagrams are then classified with respect to their contributions from maximally crossed diagrams, leading to a relation between $M(E,\omega)$ and the density-density correlation function $\Phi_{\rho\rho}$. As $\Phi_{\rho\rho}$ in turn depends on the diffusion coefficient $D(E,\omega)$, this allows for a self-consistent treatment of the problem, which leads to the following conditional equation,

$$D(E,\omega) = D_0(E) + \frac{2\,\mathrm{Im}\,\Sigma^A(E)}{[\pi N(E)]^2 D_0(E)} \frac{1}{(N_i)^2} \sum_{\mathbf{p}\mathbf{p}'} (\mathbf{v}_p \cdot \hat{\mathbf{q}}) \, \frac{\mathrm{Im}\left\{\langle G^A_{\mathbf{p}}(E)\rangle \langle G^A_{\mathbf{p}'}(E)\rangle^2\right\}}{(\mathbf{p}+\mathbf{p}')^2 - \mathrm{i}\omega/D(E,\omega)} \, (\mathbf{v}_{p'} \cdot \hat{\mathbf{q}})\,. \tag{2.92}$$

Again, see appendix B.4.1 for the derivation. In accordance to the results of the scaling theory, the self-consistent theory finds complete localization for any small amount of disorder in $d = 1, 2$, whereas in three dimensions it predicts a transition from the localized to the diffusive phase. Moreover, in [62] it is shown that the self-consistent theory yields the same critical behavior as predicted by the scaling approach. However, for the critical exponents it predicts $\nu = s = 1$, which deviates from the actual value, which is obtained numerical using finite-size scaling to be rather $\nu = s \approx 1.6$ [58]. Thus, it is expected that the critical regime is not reproduced quantitatively, but only qualitatively by the self-consistent theory.

Initially developed for weak disorder and a model of random impurities, the theory was later generalized to the case of strong disorder modeled by the Anderson Hamiltonian [64–67]. Surprisingly, both approaches lead to the same final equation for the diffusion coefficient. A numerical evaluation of the theory presented in [67] finds good quantitative agreement of both the localization length in $d = 1, 2, 3$ as well as the position of the phase boundary in $d = 3$ when compared to results obtained from exact diagonalization and finite size scaling (see [68], for example). This suggests that the regime where the self-consistent theory fails to describe the correct behavior is rather small. Therefore, it represents a solid method to numerically resolve the Anderson transition, especially when one wants to cover a wide range of parameters as it will be the case in this work.

To conclude this section, in figure 2.7 we show the phase diagram for the Anderson Hamiltonian with a box shaped disorder distribution as obtained numerically from the self-consistent theory. As explained in appendices B.3 and B.4, the theory is evaluated within the coherent potential approximation (CPA). For fixed disorder width W/J, the mobility edge separates regions with finite and vanishing diffusion, $D(E,\omega=0) > 0$ and $D(E,\omega=0) = 0$, respectively.

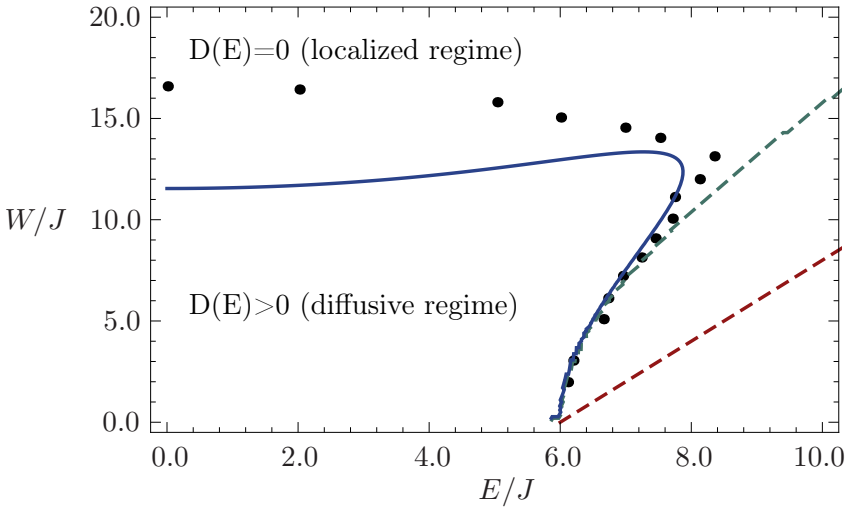

Figure 2.7: The solid blue curve shows the mobility edge for the upper half of the spectrum as obtained from the self-consistent theory of localization for a 3D cubic lattice and a box-shaped disorder distribution with different ratios W/J (the spectrum is mirror symmetric around $E = 0$). The mobility edge separates regions with finite and zero diffusion in the static limit, $D(E) = \lim_{\omega\to 0} D(E, \omega)$. The dashed red curve shows the upper band edge $E_{max} = W/2 + 2dJ$, the green dashed curve the band edge obtained within the CPA, see appendix B.3. The dots show numerical results taken from [63], which were calculated using exact diagonalization and finite size scaling. Apparently, in the critical region of the Anderson transition the results produced by the self-consistent theory differ from the numerical ones, as we would expect.

The full Anderson transition is then determined by the ratio $(W/J)_c$, above which the complete spectrum is localized.

Comparing our results with those obtained by exact diagonalization in [63], we see that, indeed, the self-consistent theory does not resolve the Anderson transition quantitatively, but only qualitatively. The predicted critical disorder is $(W/J)_c \approx 11.7$, which is smaller than the correct value $(W/J)_c \simeq 16.5$ (see [59]). Moreover, the transition to the localized regime at $E = 0$, i.e., in the center of the band, happens before all of the remaining spectrum is localized, which contradicts the picture of the two mobility edges established in section 2.2.4. The evaluation of the theory in [67] matches the numerical predictions much better, which must be a consequence of certain approximations used there to perform the momentum integrations in expression (2.92). However, our result for the mobility edge is in very good agreement with the one presented in [69], which was also obtained from the self-consistent theory, but where a different method of evaluation was used. Nevertheless, we need to keep in mind that this theory only allows us to describe the Anderson transition on a qualitative level.

2.3 The Disordered Bose-Hubbard Model

In this final section of the introductory chapter, we want discuss the effect of disorder on a bosonic lattice system. Therefore, we consider the disordered Bose-Hubbard model, which is

defined by the following Hamiltonian,

$$\hat{H} = \sum_i \Big((\varepsilon_i - \mu)\hat{n}_i + \frac{U}{2}\hat{n}_i(\hat{n}_i - 1) \Big) - J \sum_{\langle ij \rangle} \hat{b}_i^\dagger \hat{b}_j \,. \tag{2.93}$$

The parameters are the same as for the pure Bose-Hubbard model (2.1), except for the on-site energies, which are now randomly distributed like in the Anderson Hamiltonian (2.54), $\varepsilon_0 \to \varepsilon_i$, again with a probability distribution P_ε that is only finite in the interval $[-W/2, +W/2]$. The above Hamiltonian can be viewed either as the pure Bose-Hubbard model extended by an on-site disorder term, or the Anderson Hamiltonian with an additional on-site repulsion term.

Introducing disorder to the system will have a series of consequences, first of which is the shrinking of the Mott lobes as a function of the disorder width W/U up to a point where the MI regions completely vanish. Furthermore, for small hopping amplitudes one expects the emergence of an additional phase separating the MI from the SF phase. Unlike the MI phase, it is not gaped, but still insulating due to the localizing effect of the disorder. This third phase is called the Bose glass (BG) phase and was first conjectured by Fisher et al. [1]. Finally, a more subtle effect of the disorder is the reduction of the SF fraction in the conducting phase. Unlike to the pure model, where at $T = 0$ the system as a whole is SF, here a finite fraction of the system will not contribute to the SF motion.

In the following subsections, we want to address these topics in more detail, starting with the effect of disorder on the shape of the Mott lobes.

2.3.1 Mott Lobes: Shifted Phase Boundaries

A good starting point to understand how the disorder affects the shape of the Mott lobes is again the atomic limit, $J/U = 0$, where the full ground state factorizes into a product of local particle number eigenstates.

For the pure case, see section 2.1, we found that for certain values of the chemical potential, $(\mu - \varepsilon_0)/U = n_g \in \mathbb{N}$, the local particle numbers n_g and $n_g + 1$ are degenerate in energy, $E_{n_g} = E_{n_g+1}$. Hence, it does not cost any energy to add or remove a particle and the system becomes compressible, $\kappa \sim \partial N/\partial\mu > 0$. For intermediate values of μ, i.e., $n_g < (\mu - \varepsilon_0)/U < n_g + 1$, this degeneracy is lifted and the local occupation number is fixed to n_g particles. Thus, here the system is incompressible, $\kappa = 0$.

In the disordered case, the on-site energies are distributed within an interval of finite width W. Thus, there may be a fraction of sites i with on-site energies ε_i such that $(\mu - \varepsilon_i)/U = n_g \in \mathbb{N}$, while for other sites this ratio is not an integer. Hence, there can be a coexistence of compressible and incompressible sites for one value of μ. The whole system, of course, is only incompressible if all sites are incompressible. This implies that a system is compressible if

$$\frac{\mu - \varepsilon}{U} = n_g \in \mathbb{N} \quad \text{for at least one } \varepsilon \in [-W/2, +W/2] \,, \tag{2.94}$$

which yields the following parameter ranges in which systems will be compressible,

$$n_g - \frac{W}{2U} \leq \mu/U \leq n_g + \frac{W}{2U} \quad \text{with } n_g = 0, 1, 2, 3 \ldots \tag{2.95}$$

Thus, in contrast to the pure case, where the system was compressible only for certain points of μ/U, here the compressible phases extend over finite intervals on the μ/U-axis. Consequently,

the incompressible regions with fixed local occupation numbers n_g are now restricted to smaller intervals,

$$n_g - 1 + \frac{W}{2U} \leq \mu/U \leq n_g - \frac{W}{2U}\,. \tag{2.96}$$

Increasing the disorder strength W/U will further shrink the MI regions, until at some point they vanish completely. This takes place when the lower and the upper boundaries of the regions coincide,

$$n_g - 1 + \frac{W}{2U} = n_g - \frac{W}{2U} \quad \Leftrightarrow \quad W/U = 1\,. \tag{2.97}$$

Thus, for large disorder, $W/U \geq 1$, there will no longer be any Mott lobes.

Now, let us investigate what happens if we leave the atomic limit and consider finite hopping amplitudes, $J/U > 0$, where we again follow the argumentation of [23]. In the pure case the boundary to the Mott lobes was determined by the point where it became energetically favorable to add a particle (or a hole) to the system, see section 2.1.2. On the one hand, adding a particle increases the energy due to the interaction term, on the other hand the system can reduce the total energy via the kinetic term. At some point, the gain from the kinetic term outweighs the costs due to the interactions and the system becomes compressible. The kinetic energy was estimated using the assumption that the added particle (or hole) could be treated like a single boson moving on top of a localized particle background. It would then occupy the lowest lying single-particle state available.

This argument can also be applied to the disordered case, with the only difference being that the added particle will now move through a system with random on-site energies. The problem of finding the lowest lying states of a disordered system was already discussed in section 2.2.3. There, we found that the eigenstates of the Anderson Hamiltonian with very low or very high energies are localized within rare regions with constant on-site energies $\varepsilon_i \simeq \pm W/2$. They contribute to the Lifshitz tails of the single-particle spectrum, which is exponentially decaying towards its upper and lower boundaries $E_{max} = 2dJ + W/2$ and $E_{min} = -(2dJ + W/2)$, respectively. In the thermodynamic limit, $N_i \to \infty$, one will be able to find such regions of arbitrary large size, and thus, can approach the boundaries E_{min} and E_{max} to arbitrary precision.

This will also apply to the particle/hole added on top of the Mott insulator, i.e., it will be localized within a rare potential fluctuation and its energy will be shifted by $-W/2$ compared to the pure case (see equation (2.19)). Consequently, the lower half of each Mott lobe will be shifted upwards by $W/2$, whereas the upper half will be shifted downwards by $-W/2$. The resulting phase diagram is plotted in figure 2.8a for two finite disorder strengths $W/U = 0.5, 0.8$ as well as for the pure case for comparison. Indeed, the Mott lobes shrink when the width of the on-site energy distribution is increased.

The argument of the rare potential fluctuations can also be applied to the decoupling approximation, which will be discussed later in detail in section 3.2.3. Also here, the disorder results in a shift of the upper and lower parts of the Mott lobes by $\mp W/2$, see figure 2.8b.

2.3.2 Depletion of the Condensate and the Superfluid

In sections 2.1.4 and 2.1.5, we have discussed that for the pure Bose-Hubbard model at $T = 0$, the whole density contributes to the SF motion, and thus, the SF density ρ_s equals the total density ρ, i.e., $\rho = \rho_s$. We also saw in section 2.1.3, that due to the interaction not all particles will be part of the condensate. This led to the introduction of the Bogoliubov quasi-particles.

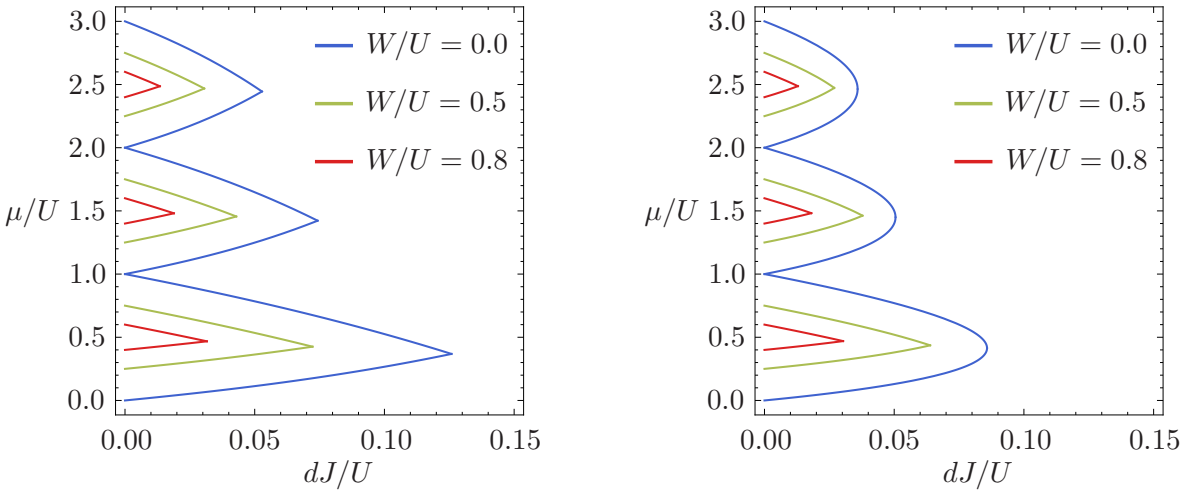

(a) Strong-coupling expansion

(b) Decoupling approximation

Figure 2.8: The first three Mott lobes calculated within **(a)** the strong-coupling expansion [23] and **(b)** the decoupling approximation [27], in each case for three different disorder strengths W/U.

From our review of the phenomenon of Anderson localization in section 2.2, we know that as soon as disorder is introduced to a non-interacting system, states at the upper and lower boundaries of the density of states will be localized in space. The extended states are found in the middle of the band and are separated from the localized states by the mobility edges. Therefore, it is reasonable to assume that due to the localization of the low lying part of the single-particle spectrum, also in the interacting case a fraction of the total density will be localized in space, and thus, cannot contribute to the SF motion, i.e., $\rho \neq \rho_s$ for $W > 0$.

In the following we want to present some previous studies of this depletion of the condensate and the SF fraction due to the disorder, starting with [70]. In this rather direct approach, the Bose-Hubbard model is studied assuming a binary (or Bernoulli) distribution for the on-site energies,

$$P_\varepsilon(\varepsilon) = p\delta(\varepsilon) + (1-p)\delta(\varepsilon - W)\,. \tag{2.98}$$

They consider the time-independent GPE (2.26) and solve it for different disorder realizations on a two-dimensional lattice of $N_i = 32 \times 32$ sites, a particle number $N = 10^4$, and two different disorder strength $W/J = 5, 50$ (note that the notation was adjusted to the one used in this work). The SF fraction is extracted by applying complex boundary conditions to the mean field amplitude in x-direction, $\psi_{i+L,j} = e^{\mathrm{i}\Phi}\psi_{i,j}$. The energy shift (normalized by N) due to the phase gradient is attributed to the kinetic energy of the SF fraction (see also [71]),

$$E(\Phi) - E(0) = \rho_s \frac{\mathbf{p}^2}{2m}\,. \tag{2.99}$$

Remembering equation (2.52), which provided a relation between the SF velocity and the phase

gradient of ψ_i, one can write

$$\mathbf{p} = \nabla S(\mathbf{x}, t) = \frac{\Phi}{L}\hat{\mathbf{e}}_x \quad \Rightarrow \quad \rho_s = 2mL^2 \frac{E(\Phi) - E(0)}{\Phi^2} \,. \tag{2.100}$$

In doing so, they find that for strong interactions, $U/J \gtrsim 1$, the SF fraction reaches one, $\rho_s \to 1$, i.e., the SF density approaches the total density. Reducing the interaction strength, the condensate fraction decreases and finally vanishes for $U/J \to 0$. For the larger disorder strength, the fraction falls off more rapidly.

The reason for this is the localized nature of the low lying single-particle spectrum. The mechanism preventing all bosons from occupying the single-particle ground state is the repulsive interaction, serving as a substitute for the Pauli principle. Bosons occupying the same localized single-particle state feel a greater repulsion than bosons in different states with a small overlap in space. Therefore, the larger the interaction strength, the more the bosons will try to distribute themselves on different states, eventually leading to the occupancy of extended states. On the other hand, the smaller the repulsion, the more the particles will condense into the lowest-lying states, i.e., those in the Lifshitz tails, leading to a localization of the total density. Therefore, this regime is also referred to as the *Lifshitz glass* .

As the approach described above only solves the GPE, it neglects the fluctuations from the mean field. In [72–74], the Bogoliubov theory as described in section 2.1.3 is generalized to the disordered case using a perturbative approach to treat the disorder potential, which limits this theory to small disorder strengths, but allows for an analytic treatment. In very good agreement with previous numerical approaches to the problem [71], they find that the stronger the disorder strength, the more the condensate is depleted, and provide the following intuitive picture. In the pure case, the reason for the depletion of the condensate is the repulsive on-site interaction between the particles. In the disordered case, the condensate will not be uniformly distributed in space, but will be deformed with regions of higher as well as lower densities. In the high-density regions, the effect of the interaction is enlarged, leading to an overall enhanced depletion of the condensate.

Another way to approach the problem are QMC simulations, see, for example, [75] for $d = 1$, [76, 77] for $d = 2$, and [24] for $d = 3$. Here, the SF fraction is calculated from the *winding number* [78], which is again a measure for the response of the system to boundary conditions. It should be noted, that these QMC approaches treat systems with *small* total number of lattice sites, $N_i < 1000$, in order to be numerically feasible. The results for different finite sizes are then extrapolated to the thermodynamic limit using finite size scaling. In all cases, it is found that the smaller the hopping amplitude J and the larger the disorder strength W/J, the smaller the SF fraction. Eventually, the SF fraction vanishes. However, this transition from (partial) SF to non-SF takes place before the incompressible MI region is reached, i.e., there is a phase separating the SF from the MI regime for disordered systems. This intermediate phase is identified with the BG phase, which will be the topic of the next section.

2.3.3 The Bose Glass Phase and the Theorem of Inclusions

Inspired by the results of the renormalization group approach for one-dimensional interacting systems with disorder by Giamarchi and Schulz [22], which implied the existence of two different localized phases, one with spatially homogenous and one with spatially inhomogeneous particle density, the existence of the BG phase was first conjectured by Fisher et al. in their fundamental work [1] on the problem of interacting bosons in a disordered environment.

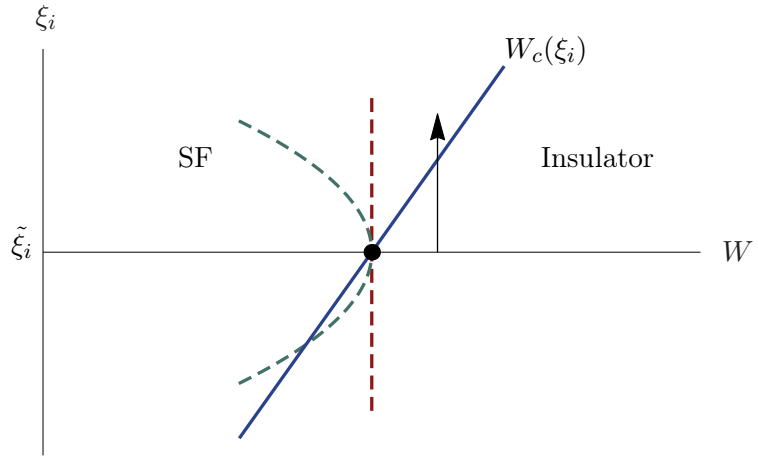

Figure 2.9: A sketch of the critical disorder width W_C against one microscopic parameter ξ_i characterizing the disorder distribution. The blue line shows a phase boundary that is monotonous as a function of ξ_i, the dashed green curve a boundary with an extremum at $\tilde{\xi}_i$. The dashed red line shows a phase boundary which is independent of ξ_i. The black dot marks the critical disorder width $W_c(\tilde{\xi}_i)$ at $\tilde{\xi}_i$ (picture is reproduced from [79]).

A intuitive way of understanding the origin of this second phase can be obtained by again starting from the MI regime and considering the nature of the particle density that is added or removed when leaving the Mott lobes by increasing or decreasing the chemical potential, respectively, for fixed hopping J/U (i.e., in vertical direction in figure 2.8). For the pure case, see section 2.1.2, the wave function of the extra particle or hole is an extended Bloch state, i.e., particle density is added to or removed from all lattice sites. Hence, the system becomes globally compressible and is, therefore, not an insulator.

For the disordered case, see section 2.3.1, the first state available is a Lifshitz state, i.e., a state exponentially localized in a rare potential fluctuation. Thus, the change in particle density is limited to a finite region in space as well, leaving the residual lattice incompressible (in an exponential sense). Moreover, the lowest lying Lifshitz states are localized on separate islands and will have no spatial overlap, making the residual system insensitive to the added particle density. Therefore, one can assume that this picture is not only valid for the very first added particle/hole, but until a finite fraction of these lowest lying Lifshitz states are occupied. Thus, in the vicinity of the Mott lobes, the system becomes only locally compressible, and therefore, has to be an insulator globally.

When moving away from the Mott lobes, one has to leave this simple single-particle picture and, in principle, needs to treat the full multi-particle localization problem. Due to the complexity of this problem, this is something one usually tries to avoid, and one either has to rely on approximations, see, for example, [28] (which we will discuss in detail in the next chapter), or one needs to restrict the calculations to small system sizes, see previous section. Thus, instead of investigating the BG phase itself, it is useful to consider the problem from the opposite direction, i.e., coming from the SF phase.

This brings us to the so-called *theorem of inclusions*, which states that there is no direct transition from the SF to the MI phase. Following the argument of Pollet et al. [24] and Gurarie et al. [79], we consider the SF to insulator transition (or, more general, a transition from a gapless phase to a second phase, which may or may not be gaped). The probability

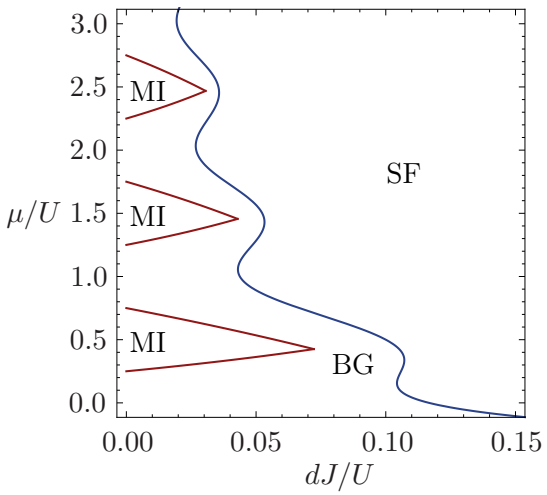

Figure 2.10: Qualitative phase diagram for the disordered Bose-Hubbard model. The red curves separate the MI regions from the compressible BG phase, the blue curve indicates the transition from the insulating BG to the SF phase.

distribution P_ε shall be characterized by its finite width W as well as a set of parameters $\{\xi_i\}$ that determine the shape of the distribution, i.e., the distribution function is not limited to box distributions. This is a crucial point for the proof of the theorem. An example for such a parameter would be one of the moments of the distribution function.

Now, for a given set of $\{\xi_i\}$, there will be a critical disorder width at which the transition from SF to insulator takes place, $W_c(\{\xi_i\})$. Let us concentrate on one of the many parameters ξ_i and observe $W_c(\xi_i)$ while keeping the remaining parameters fixed, see figure 2.9 for an illustration. If $W > W_c(\tilde{\xi}_i)$, the system is an insulator for $\xi_i = \tilde{\xi}_i$. Now, if we assume that W_c is a monotonous function of ξ_i (blue line), then we can trigger the transition to the SF phase by changing the parameter ξ_i while keeping W fixed as indicated by the arrow, i.e., $\tilde{\xi}_i \to \tilde{\xi}_i + \delta$. If W is very close to $W_c(\tilde{\xi})$, only a very small δ is needed to trigger the transition. The argument now is the following: suppose the disorder potential was modeled according to the distribution with $\xi_i = \tilde{\xi}_i$. In the thermodynamic limit, $N_i \to \infty$, and if δ is small enough, one will always be able to find arbitrary large regions in space that could also correspond to the distribution with $\xi_i = \tilde{\xi}_i + \delta$. This implies that the insulating phase *includes* arbitrarily large regions that are locally SF, and therefore, compressible. Thus, the insulating phase itself has to be compressible and cannot be the gaped MI phase. Consequently, there will always be a compressible, insulating phase in between the SF and the MI phases and no direct transitions are possible.

Of course, this argument does not work if W_c is non-monotonous as a function of ξ_i (green dashed curve in figure 2.9) for *all* parameters. However, this would mean that, for example, one could trigger a transition from SF to BG by decreasing the second moment of the distribution (i.e., its standard deviation from $\varepsilon = 0$), which does not appear to be reasonable.

Finally, one could ask the question of how a transition from a gapless to a gaped phase would be possible at all according to this theorem. As we have discussed, the MI to gapless transition is caused by the formation of locally gapless regions, which are (for fixed μ/U and J/U) induced by increasing the width W/U. Thus, this transition is independent from the specifics of the disorder distribution and would correspond to a horizontal line in the phase diagram, see dashed red line

in figure 2.9. In this case, one cannot reach the other phase by changing the parameter ξ, and thus, the argument does not hold.

With this result, we can now draw a qualitative phase diagram for the disordered Bose-Hubbard model, see figure 2.10. The Mott lobes are separated from the SF phase by the compressible, but insulating BG phase. For small filling, $\mu/U \to E_{min}/U$ (i.e., the lower band edge of the single-particle Anderson Hamiltonian), one expects the BG phase (or the Lifshitz Glass, see section 2.3.2) to extend to larger values of J/U as the bosons will occupy the localized Lifshitz states first.

This concludes this brief introduction to the disordered Bose-Hubbard model. In the next chapter, we will discuss the MF theory [27] (or decoupling approximation) for both the pure and the disordered model, which will be used later as the foundation for the effective single-particle approach we developed in order to resolve the SF to BG transition.

CHAPTER 3

Mean-Field Theory for the Disordered Bose-Hubbard Model

In section 2.1.2 we have already mentioned the MF or decoupling approximation, which was introduced by Sheshadri et al. [27] in 1993. In the following, we will discuss its application to both the pure and the disordered Bose-Hubbard model in detail.

3.1 Mean-Field Theory for the Bose-Hubbard Model

In the strongly correlated regime, the interaction energy will dominate over the kinetic energy. Thus, if we want to describe the model in this regime using an approximative method, it appears to be reasonable to apply the approximation to the kinetic term while treating the interaction term exactly. This is the motivation for the decoupling approximation, which uses a MF approach to reduce the full lattice problem to a local one.

The starting point is to define the MF parameter as $\psi_i = \langle GS|\hat{b}_i|GS\rangle$, with $|GS\rangle$ being the ground state of the system. Note, that the Bose-Hubbard Hamiltonian conserves the total number of particles. Thus, the expectation value of a single annihilation (or creation) operator would always yield zero. Therefore, the above definition of the MF parameter has to be understood as an expectation value with respect to the ground state of the MF Hamiltonian we will define below.

With this definition, the kinetic term $\hat{H}_{kin}$ is rewritten as follows,

$$\begin{aligned}\hat{H}_{kin} &= -J\sum_{\langle ij\rangle}\big(\underbrace{\hat{b}_i^\dagger - \psi_i^*}_{\equiv\hat{\delta}_i^\dagger} + \psi_i^*\big)\big(\underbrace{\hat{b}_j - \psi_j}_{\equiv\hat{\delta}_j} + \psi_j\big) \\ &= -J\sum_{\langle ij\rangle}\left(\hat{\delta}_i^\dagger\hat{\delta}_j + \psi_i^*\hat{b}_j + \psi_j\hat{b}_i^\dagger - \psi_i^*\psi_j\right). \end{aligned} \tag{3.1}$$

Assuming the particle fluctuations to be small compared to the total particle number, we omit terms quadratic in the $\hat{\delta}_i$. This approximation will, of course, be good especially near the transition, where fluctuations are suppressed due to the formation of the Mott-Hubbard gap. Moving away from the phase transition, the fluctuations will become more important. Applying

this approximation yields

$$\hat{H}_{kin} \approx \hat{H}_{kin}^{MF} = -J \sum_{\langle ij \rangle} \left(\psi_i^* \hat{b}_j + \psi_j \hat{b}_i^\dagger - \psi_i^* \psi_j \right) . \tag{3.2}$$

Defining the bath amplitude for site i as $\Psi_i = \sum_j' \psi_j$, where the summation is taken over all neighboring sites of i, the MF Hamiltonian can be written as

$$\hat{H}^{MF} = \hat{H}_{loc} + \hat{H}_{kin}^{MF} = \sum_i \left((\varepsilon_0 - \mu)\hat{n}_i + \frac{U}{2}\hat{n}_i(\hat{n}_i - 1) - J(\Psi_i \hat{b}_i^\dagger + \Psi_i^* \, \hat{b}_i) \right) + J \sum_{\langle ij \rangle} \psi_i^* \psi_j \, . \tag{3.3}$$

The hopping term of the above MF Hamiltonian now explicitly breaks particle conservation, as the hopping from one site to a nearest neighbor site has been replaced by a hopping into and out of a bath for each lattice site. Hence, the eigenstates of $\hat{H}^{MF}$ will not be particle number eigenstates. In particular, this is true for its ground state $|GS\rangle$, and thus, $\psi_i = \langle GS|\hat{b}_i|GS\rangle$ can yield a finite number.

From the translation invariance of the Hamiltonian, it follows that all MF parameters have to be the same,

$$\psi_i \equiv \psi \quad \text{for all sites } i \, , \tag{3.4}$$

and one can write

$$\hat{H}^{MF} = \sum_i \hat{h}_i \, , \tag{3.5}$$

with

$$\hat{h}_i \equiv (\varepsilon_0 - \mu)\hat{n}_i + \frac{U}{2}\hat{n}_i(\hat{n}_i - 1) - zJ \left(\psi^* \hat{b}_i + \psi \, \hat{b}_i^\dagger \right) + zJ|\psi|^2 \, , \tag{3.6}$$

where z is the number of nearest neighbors. The MF approximation has decoupled the full lattice Hamiltonian into a sum of independent, local Hamiltonians $\hat{h}_i$. As a consequence, the ground state of $\hat{H}^{MF}$ will be a product state of the local ground states $|G_i\rangle$ of the different $\hat{h}_i$,

$$|GS\rangle = |G_1\rangle \otimes |G_2\rangle \otimes \cdots \otimes |G_{N_i}\rangle \, , \tag{3.7}$$

and it directly follows that

$$\psi = \langle GS|\hat{b}_i|GS\rangle = \langle G_i|\hat{b}_i|G_i\rangle \, . \tag{3.8}$$

In other words, the MF parameter is also only a purely local quantity. Hence, it is sufficient to solve the problem for each $\hat{h}_i$ separately. Since they are all identical, we can restrict ourselves to treating $\hat{h}_i$ for one arbitrary lattice site and will drop the lattice index i in the following.

Moreover, by applying the global gauge transformation $\hat{b} \to \hat{b}e^{-\mathrm{i}\varphi}$, where φ is the complex phase of the order parameter, $\psi = |\psi|e^{\mathrm{i}\varphi}$, the order parameter is rotated onto the real axis, $\psi \to |\psi|$. Hence, we can always assume the order parameter to be real and non-negative, $\psi \geq 0$.

3.1.1 Direct Diagonalization

The ground state of $\hat{h}$ depends on the MF parameter, $|G\rangle = |G(\psi)\rangle$. The MF parameter, in turn, is determined by the ground state $|G\rangle$. Thus, the problem has to be solved self-consistently. For a given ψ, the ground state can be calculated by diagonalizing $\hat{h}$. From this, a new MF parameter can be calculated via equation (3.8). Starting with an initial guess for ψ and then iterating these two steps, the solution is obtained when the new ψ equals the one used as the

input parameter, $\psi = \langle G(\psi)|\hat{b}|G(\psi)\rangle$.

In order to actually perform the diagonalization, the local Hamiltonian is expressed in terms of the local particle number eigenstates $|n\rangle$. With $\mathbb{1} = \sum_{n=0}^{\infty} |n\rangle\langle n|$, $\hat{b}|n\rangle = \sqrt{n}|n-1\rangle$, and $\hat{b}^\dagger|n\rangle = \sqrt{n+1}|n+1\rangle$, one obtains

$$\begin{aligned}
\hat{h} &= \sum_{mn} |m\rangle\langle m|\hat{h}|n\rangle\langle n| \\
&= \sum_{n=0}^{\infty} \Big(E_n|n\rangle\langle n| - zJ\psi\sqrt{n+1}\big(|n\rangle\langle n+1| + |n+1\rangle\langle n|\big)\Big) + zJ\psi^2\mathbb{1} \\
&= \begin{pmatrix}
E_0 & -zJ\psi & 0 & & & \\
-zJ\psi & E_1 & -\sqrt{2}zJ\psi & 0 & & \\
0 & -\sqrt{2}zJ\psi & E_2 & -\sqrt{3}zJ\psi & 0 & \\
 & 0 & -\sqrt{3}zJ\psi & E_3 & -\sqrt{4}zJ\psi & 0 \\
 & & \ddots & \ddots & \ddots & \ddots & \ddots
\end{pmatrix} + zJ\psi^2\mathbb{1}\,,
\end{aligned} \tag{3.9}$$

where

$$E_n = (\varepsilon_0 - \mu)n - \frac{U}{2}n(n-1)\,. \tag{3.10}$$

Figure 3.1 shows a sketch of the local potential E_n plotted against the particle number n. The minimum of the potential is located at $n_0 = (\mu - \varepsilon_0)/U + \frac{1}{2}$, which, of course, does not need to be an integer number. Moving away from this minimum, the potential increases quadratically.

Consecutive particle numbers, for example, n and $n+1$, are coupled by a term proportional to $-\sqrt{n+1}zJ\psi$. Thus, the larger the particle numbers, the stronger the coupling.

Finally, the term quadratic in ψ only adds a diagonal shift of the energies and does not affect the eigenstates. As ψ is determined solely by the ground state $|G\rangle$, this quadratic term can be neglected in the following.

As mentioned before, the on-site energy is set to zero, $\varepsilon_0 = 0$. In the following, we will omit it in our notation. Furthermore, we will measure the energy in units of the interaction strength,

$$\hat{h} \quad \rightarrow \quad \frac{\hat{h}}{U} = -\frac{\mu}{U}\hat{n} + \frac{1}{2}\hat{n}(\hat{n}-1) - \frac{zJ}{U}\psi(\hat{b} + \hat{b}^\dagger) \tag{3.11}$$

Hence, there are only two independent parameters, μ/U and zJ/U. Moreover, this implies that the results will only quantitatively depend on the spatial dimension of the system, $d = z/2$. We restrict ourselves to treating the three dimensional case, $z = 6$. Results for one and two dimension can be obtained by simply rescaling the hopping amplitude.

Diagonalizing the real matrix (3.9) will yield a ground state of the following form,

$$|G\rangle = \sum_n g_n|n\rangle \quad \text{with} \quad g_n \in \mathbb{R}\,, \tag{3.12}$$

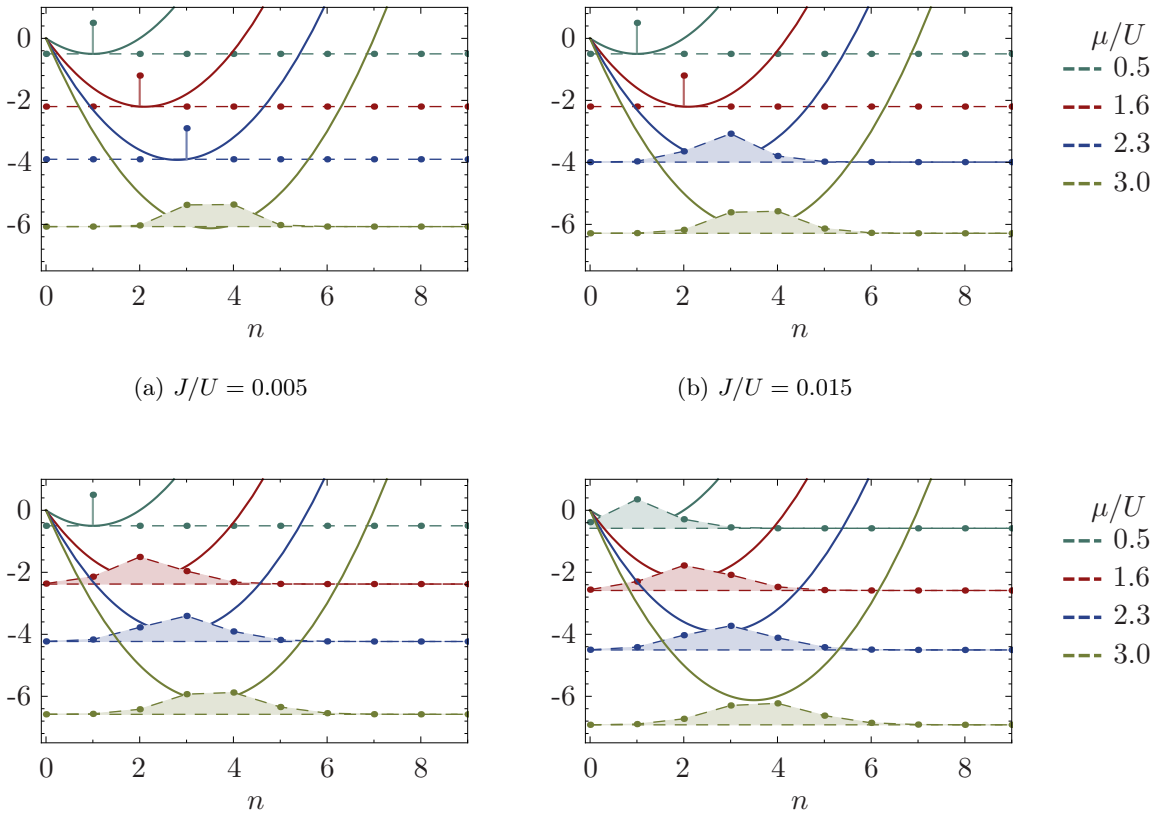

(a) $J/U = 0.005$ (b) $J/U = 0.015$

(c) $J/U = 0.025$ (d) $J/U = 0.035$

Figure 3.1: The solid curves show the local potential E_n as a function of the particle number n for different μ and with $\varepsilon_0 = 0$ and $U = 1$. In addition, the dot-dashed curves show the ground state for each μ and different hopping amplitudes J/U, where the ground state energy was used as an offset in y-direction. The filling indicates that the ground state is an extended state in Fock space. If there is no filling, but only one single dot, it means that the ground state is a particle number eigenstate.

which leads to the order parameter

$$\begin{aligned}\psi &= \sum_{nm} g_n g_m \langle n|\hat{b}|m\rangle \\ &= \sum_{n} g_n g_{n+1} \sqrt{n+1}\,. \end{aligned} \tag{3.13}$$

In order to actually find $|G\rangle$ numerically, the infinite Fock space has to be truncated at some finite particle number. For small hopping amplitudes and not too large μ, one finds that the ground states are centered at the minimum n_0 of the local potential E_n and decrease rather rapidly when moving away from n_0. We found that for our purposes it is more than sufficient to choose the cutoff particle number to be $n_c = 30$.

Moving on, from the above expression for ψ one can conclude that ψ gets larger if the particle numbers n, which contribute the most to the ground state, get larger. Furthermore, since the

coefficients g_n of consecutive n are multiplied, ψ also gets larger if the ground state gets more broadly distributed in Fock space. To see this, consider the simplified case of only three possible particle numbers n, $n+1$ and $n+2$, which is a good approximation for small J. Using that the eigenstates are normalized to one, we have

$$\begin{aligned}\psi &= g_n g_{n+1}\sqrt{n+1} + g_{n+1}g_{n+2}\sqrt{n+2} \\ &= \left(g_n\sqrt{n+1} + g_{n+2}\sqrt{n+2}\right)\sqrt{1-g_n^2-g_{n+2}^2}\end{aligned} \tag{3.14}$$

In order to find the maximal ψ, we have to differentiate with respect to g_n and g_{n+2}. This yields

$$\sqrt{n+1}\sqrt{1-g_n^2-g_{n+2}^2} - g_n\frac{g_n\sqrt{n+1}+g_{n+2}\sqrt{n+2}}{\sqrt{1-g_n^2-g_{n+2}^2}} = 0 \tag{3.15a}$$

and

$$\sqrt{n+2}\sqrt{1-g_n^2-g_{n+2}^2} - g_{n+2}\frac{g_n\sqrt{n+1}+g_{n+2}\sqrt{n+2}}{\sqrt{1-g_n^2-g_{n+2}^2}} = 0\,, \tag{3.15b}$$

which leads to

$$(n+1)\left(g_n^2-g_{n+2}^2\right) + 1 - g_n^2 - 2g_{n+2}^2 = 0\,. \tag{3.16}$$

This equation is solved by $g_n = g_{n+1} = g_{n+2} = \sqrt{1/3}$. Hence, ψ is maximal if the ground state wave function is equally distributed in Fock space. Of course, the general case of an infinite number of possible n is more complex, but in general it holds that the broader the ground state wave function, the larger the order parameter.

Figure 3.1 shows the ground states for different chemical potentials and hopping amplitudes. Figure 3.2a shows the corresponding MF parameters for the same μ as a function of J.

First, we note that the larger the hopping amplitude, the broader the ground state wave function is distributed in Fock space. This is also reflected in a growth of the order parameter ψ, which is to be expected as we argued above. Furthermore, particle numbers larger than n_0 tend to get more populated than those smaller than n_0. This can be seen best when n_0 is integer or half integer, that is, when $E_{n_0+1} = E_{n_0-1}$ or $E_{n_0+1/2} = E_{n_0-1/2}$, respectively. There, we find that $g_{n_0+1} > g_{n_0-1}$ and $g_{n_0+1/2} > g_{n_0-1/2}$, respectively, which is a result of the fact that the coupling between particle number sectors gets stronger for larger n.

Going into the opposite direction and decreasing the hopping amplitude, we find that for small enough J the MF parameter vanishes for all μ, except for the special case of $\mu \in \mathbb{N}$, here $\mu = 3$. For integer μ, the minimum n_0 of the potential E_n is exactly in the middle of two integer particle numbers $n_\pm = n_0 \pm 1/2$. Hence, n_+ and n_- have the same potential energy, $E_{n_+} = E_{n_-}$, leading to a degenerate ground state for $J = 0$. Because of the degeneracy, the order parameter is not well defined in this case. For finite $J > 0$, this degeneracy is lifted. Using the approximation

$$|G\rangle \approx g_{n_-}|n_-\rangle + g_{n_+}|n_+\rangle \quad \text{for} \quad J \ll 1, \tag{3.17}$$

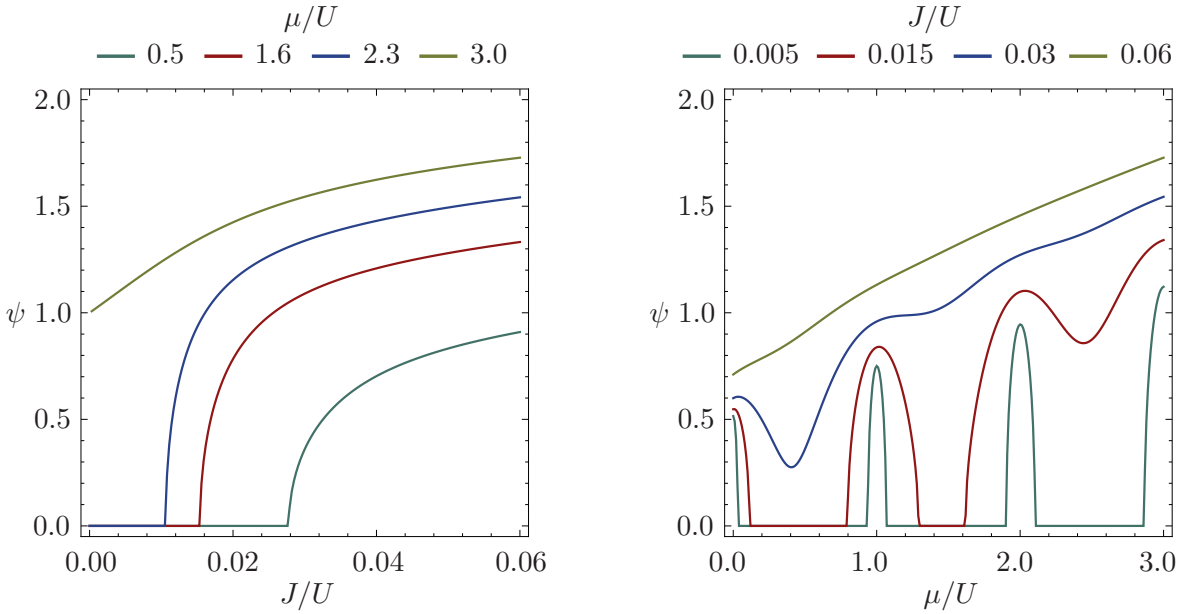

(a) Fixed chemical potentials

(b) Fixed hopping amplitudes

Figure 3.2: The MF order parameter ψ plotted **(a)** as a function of J/U for different fixed chemical potentials μ/U and **(b)** as a function of μ/U for different fixed hopping amplitudes J/U.

one easily finds that $g_{n_-} = g_{n_+} = \sqrt{1/2}$, which leads to the order parameter

$$\lim_{J\to 0} \psi = \frac{\sqrt{n_+}}{2} = \frac{\sqrt{\mu/U + 1}}{2} \quad \text{for } \mu \in \mathbb{N}. \tag{3.18}$$

Hence, for $\mu \in \mathbb{N}$ and $J > 0$, one will always obtain a finite MF parameter $\psi > 0$.

In all other cases, that is, when $\mu \notin \mathbb{N}$, there is always a finite $J_0 > 0$ with $\psi = 0$ for all $J < J_0$. This can be understood as follows. One particle number will always yield a minimal energy E_n. Populating the particle number sectors away from this n therefore costs energy. Hence, this can only happen if the kinetic term is able to compensate for these additional costs. At a certain point, however, the hopping amplitude becomes too small for this, and the ground state turns into a Fock state. Consequently, ψ is exactly zero in these cases.

Instead of looking at ψ as a function of the hopping amplitude, we can also consider the order parameter as a function of μ/U for fixed J/U, which is shown in figure 3.2b. Here, the behavior is a little more complex. It can be understood best by starting from the atomic limit, $J/U = 0$. In that case, all eigenstates are also particle number eigenstates, and the ground state is given by the particle number n_g with the lowest E_n, $|G\rangle = |n_g\rangle$. As we discussed above, for $\mu/U \in \mathbb{N}$ the ground state is degenerated and as a consequence, $\lim_{J\to 0} \psi(J/U) > 0$, see equation (3.18). For any other $\mu/U \notin \mathbb{N}$, $\psi = 0$ for $J/U = 0$.

From this, one would expect that for small but finite hopping amplitudes, $J/U \ll 1$, there are islands around $\mu/U = 0, 1, 2\ldots$ with finite ψ. For μ/U close enough to the degenerated case, the energies of n_g and $n_g + 1$ (or n_g and $n_g - 1$) are so close that already a small hopping amplitude can compensate for the cost of occupying states away from the particle number n_g. Still, these regions will be separated by gaps in which $\psi = 0$.

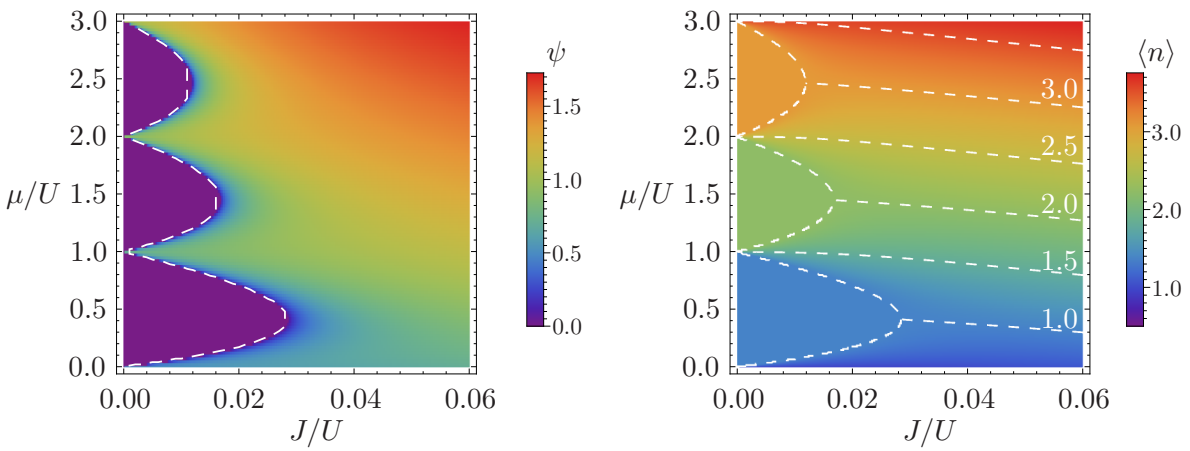

(a) MF order parameter ψ

(b) Average particle number $\langle n \rangle$

Figure 3.3: **(a)** The MF order parameter ψ as a function of J/U and μ/U. The white dashed curve indicates the boundary between regions with finite and vanishing compressibility κ. **(b)** The average particle number per site $\langle n \rangle$ as a function of J/U and μ/U. The white dashed curves indicate the trajectories of constant lattice filling.

Upon increasing the hopping amplitude further, the regions with finite ψ should grow in size as the kinetic energy gets larger. At some point, neighboring regions will overlap and the gaps will be closed.

Furthermore, we already found that, in general, the order parameter gets larger for larger particle numbers, which is also reflected in equation (3.18). As for larger ψ the coupling between the Fock states gets larger as well, one would expect the islands of finite ψ around $\mu/U \in \mathbb{N}$ to become larger for larger μ/U.

This is exactly the behavior one finds when numerically evaluating the MF formalism and which is depicted in figure 3.2b. A density plot of ψ as a function of both J/U and μ/U is shown in figure 3.3a, which gives a more complete overview on the behavior of ψ. In accordance with the above considerations, the regions with vanishing order parameter reach up only to a finite hopping amplitude J/U and get smaller for larger μ/U. Nevertheless, in the limit $J/U \to 0$ they all extend from one integer $\mu/U \in \mathbb{N}$ to the next higher one, $\mu/U + 1$.

Now, let us discuss the implications of a vanishing order parameter. First of all, when $\psi = 0$ there is no hopping into and out of the bath. Thus, each boson is strictly localized on a single, fixed site. From this it directly follows that the system is an insulator, as no transport can take place when all particles are localized.

Furthermore, as shown in appendix A.1 the zero-temperature compressibility vanishes if the order parameter is zero,

$$\lim_{T \to 0} \kappa = 0 \text{ for } \psi = 0. \tag{3.19}$$

This means, that in the regions where the order parameter vanishes, the system is gaped. This is consistent with the numerical results, see figure 3.4. For the smaller hopping amplitude, $J/U = 0.015$, we see the system entering the first and also the second region where $\psi = 0$. Within both regions, the particle number is constant, first at $n_g = 1$ and then at $n_g = 2$.

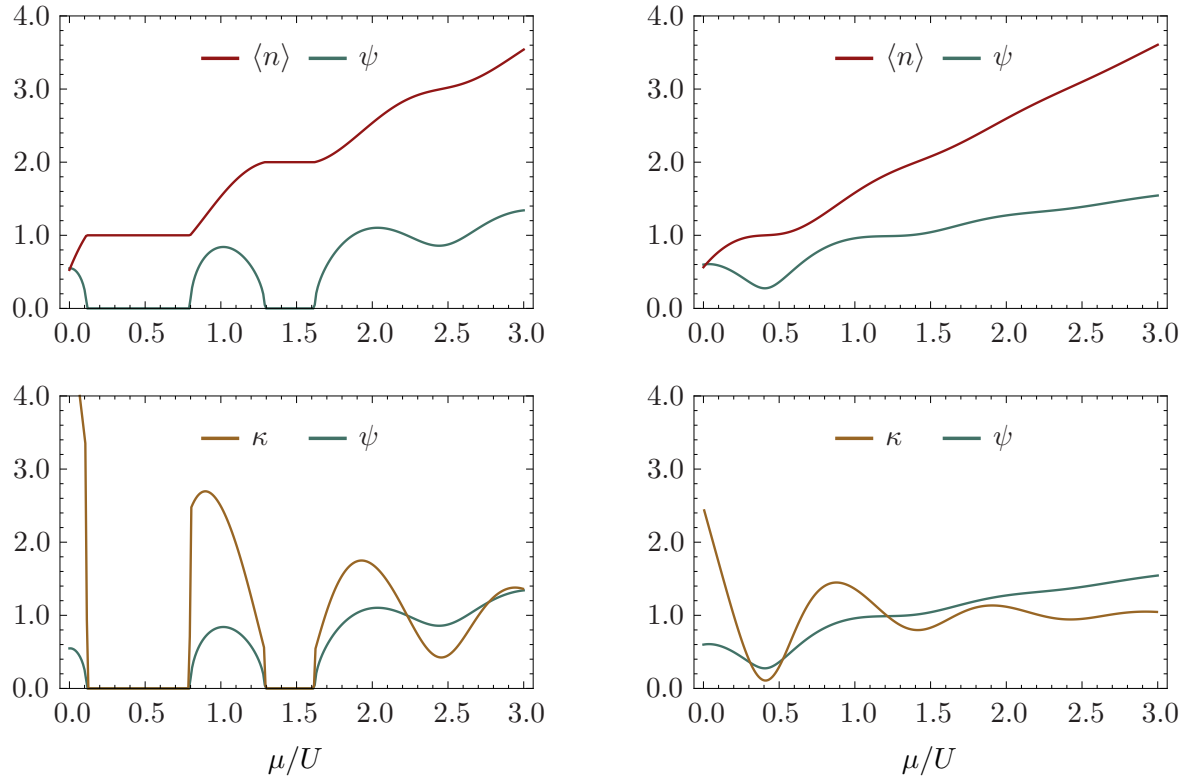

(a) $J/U = 0.015$ (b) $J/U = 0.03$

Figure 3.4: The upper plots show the average local particle number and the lower plots the compressibility, each as a function of the chemical potential μ/U for two fixed hopping amplitudes $J/U = 0.015$ and $J/U = 0.03$. For comparison, also the order parameter ψ is plotted.

Consequently, in these regions the compressibility vanishes, $\kappa = 0$.

For the larger hopping amplitude, $J/U = 0.03$, the system never enters the regions where $\psi = 0$. Consequently, the compressibility is always finite and the system is never gaped.

In figure 3.3b, a complete parameter scan of the average particle number as a function of both J/U and μ/U is shown. Again, we see that within the regions where $\psi = 0$, the average particle number is an integer and the compressibility vanishes. Outside these regions, the particle number varies continuously and the compressibility is finite.

These results imply that we can identify a system with a vanishing order parameter with a Mott insulator. The regions where $\psi = 0$ correspond to the Mott lobes.

3.1.2 Perturbation Theory

In the following, we will discuss an alterative way to obtain the boundary between MI and SF phase, which was introduced in [80] and can also be found in the textbook [81]. Here, the phase boundary is calculated in perturbation theory, where one employs that the MF order parameter vanishes at the phase transition. Hence, we can interpret the terms containing ψ as

small perturbations to the local energies,

$$\hat{h} = \hat{h}^0 - zJ\psi\,\hat{h}^1 + zJ\psi^2 \tag{3.20a}$$

with

$$\hat{h}^0 = (\varepsilon_0 - \mu)\hat{n} + \frac{U}{2}\hat{n}(\hat{n}-1) \tag{3.20b}$$

and

$$\hat{h}^1 = \hat{b}^\dagger + \hat{b}\,. \tag{3.20c}$$

The unperturbed ground state is given by $|G^{(0)}\rangle = |n_g\rangle$, where $n_g \in \mathbb{N}$ is the particle number with the smallest energy, $E_{n_g} < E_n$ for all $n \neq n_g$. For $n_g = 0$, we find

$$E_0 < E_1 \quad \Leftrightarrow \quad (\mu - \varepsilon_0) < 0 = n_g\,, \tag{3.21}$$

and similar, for $n_g > 0$ we have

$$\begin{aligned} & E_{n_g} < E_{n_g\pm1} \\ \Leftrightarrow \quad & 0 < E_{n_g\pm1} - E_{n_g} \\ \Leftrightarrow \quad & 0 < \pm(\varepsilon_0 - \mu) \pm \frac{U}{2}(2n_g - 1 \pm 1)\,. \end{aligned} \tag{3.22}$$

Both results lead to

$$\frac{\mu - \varepsilon_0}{U} < n_g < \frac{\mu - \varepsilon_0}{U} + 1\,. \tag{3.23}$$

In other words, n_g is the smallest integer larger than $(\mu - \varepsilon_0)/U$. Again, we note that for $(\mu-\varepsilon_0)/U \in \mathbb{N}$ the ground state for $J = 0$ and, hence, also the ground state of $\hat{h}^0$ is degenerated, and the MF theory as well as this perturbation theory are not well defined.

As shown in appendix A.2 the following expression for the ground state energy can be derived in perturbation theory,

$$E_G = E_{n_g} + \Big(zJ\Delta_G^{(2)} + 1\Big)zJ\psi^2 + \Delta_G^{(4)}(zJ\psi)^4 + \mathcal{O}\big((zJ\psi)^6\big)\,. \tag{3.24}$$

The coefficients $\Delta_G^{(2)} < 0$ and $\Delta_G^{(4)} > 0$ are given in the appendix A.2. A plot of E_G is shown in figure 3.5a. The correct value for the order parameter is found by minimizing E_g as a function of ψ. If the coefficient for the second order term is positive, i.e., $zJ\Delta_G^{(2)} + 1 > 0$, the minimum is located at $\psi = 0$. When the coefficient is negative, i.e., $zJ\Delta_G^{(2)} + 1 < 0$, the energy E_g has a Mexican hat shape with its minimum at a finite value of ψ. As we argued in the previous section, the first case would correspond to a MI, the second case to a SF. Hence, the phase boundary is given by the point where the coefficient vanishes,

$$\begin{aligned} & 0 = zJ\Delta_G^{(2)} + 1 \\ \Leftrightarrow \quad & 0 = zJn_g(E_{n_g+1} - E_{n_g}) + zJ(n_g+1)(E_{n_g-1} - E_{n_g}) - (E_{n_g-1} - E_{n_g})(E_{n_g+1} - E_{n_g}) \\ & \quad = zJn_g(\varepsilon_0 - \mu + Un_g) + zJ(n_g+1)\big(\mu - \varepsilon_0 - U(n_g-1)\big) \\ & \qquad - \big(\mu - \varepsilon_0 - U(n_g-1)\big)(\varepsilon_0 - \mu + Un_g) \\ & \quad = (\mu - \varepsilon_0)^2 - \big(U(2n_g - 1) - zJ\big)(\mu - \varepsilon_0) + U^2 n_g(n_g - 1) + UzJ\,. \end{aligned} \tag{3.25}$$

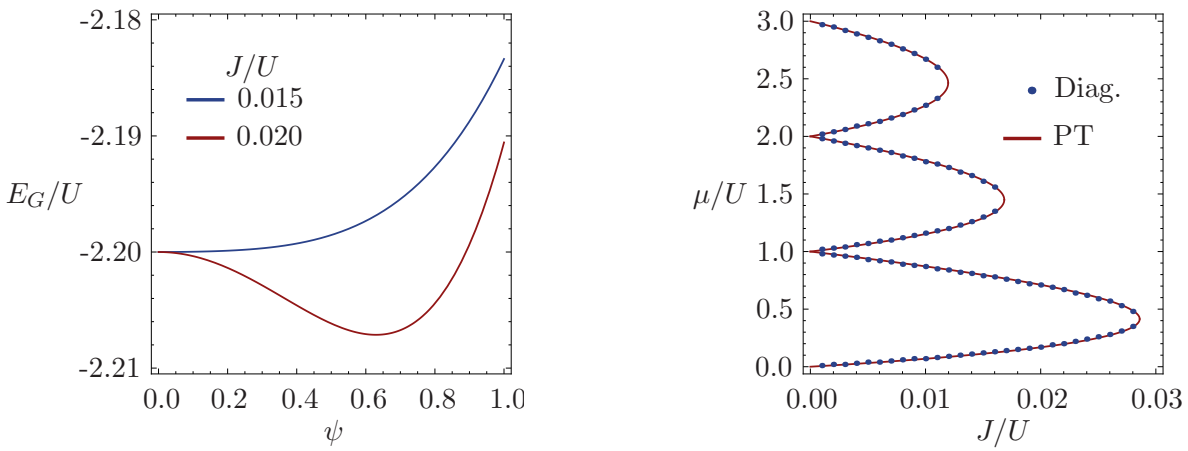

(a) $\mu/U = 1.6$

(b) Phase boundary

Figure 3.5: **(a)** The ground state energy as derived in perturbation theory for $\mu/U = 1.6$ and two values for J. The first, $J = 0.015$, shows the characteristic form of E_G for a system in the MI phase, with the minimal energy at $\psi = 0$. The second curve for $J = 0.020$ shows the Mexican hat shape, resulting in a finite ψ and putting the system into the SF phase. **(b)** Comparison of the phase boundary obtained by diagonalization (blue dots) and perturbation theory (red curve).

which is solved by

$$\frac{\mu - \varepsilon_0}{U} = \frac{2n_g - 1 - zJ/U}{2} \pm \sqrt{\frac{(2n_g - 1 - zJ/U)^2}{4} - n_g(n_g - 1) - zJ/U} \,. \tag{3.26}$$

Figure 3.5b shows a plot of the above phase boundary in comparison with the one obtained by diagonalization as described in the previous section. Apparently, the result from perturbation theory matches the numerically exact result quite well.

3.2 Stochastic Mean-Field Theory for the Disordered Bose-Hubbard Model

In the following sections, we want to translate the MF theory, as it was described in the previous section for the pure case, to the disordered Bose-Hubbard model. There exists a work by Bissbort and Hofstetter [28], in which such a theory was already developed. Although the approach presented here was started independently from this previous work, its implementation is more or less the same and we arrive at the same results. The conclusion we draw from these results, however, differ significantly from those made in [28].

3.2.1 Decoupling Approximation

Since the only terms that include the disorder are the on-site energies, the decoupling approximation for the hopping term can be conducted analogously to the pure case, yielding

$$\hat{H}^{MF} = \sum_i \hat{h}_i + J \sum_{\langle ij \rangle} \psi_i^* \psi_j \,, \tag{3.27}$$

and

$$\hat{h}_i = (\varepsilon_i - \mu)\hat{n}_i + \frac{U}{2}\hat{n}_i(\hat{n}_i - 1) - J(\Psi_i \hat{b}_i^\dagger + \Psi_i^* \, \hat{b}_i) \,. \tag{3.28}$$

with the MF parameters $\psi_i = \langle GS|\hat{b}_i|GS\rangle$, $|GS\rangle$ being the ground state of $\hat{H}^{MF}$, and the bath amplitude $\Psi_i = \sum_j' \psi_j$. Hence, the full ground state will again be a product state of the local ground states $|G_i\rangle$, that is, $|GS\rangle = |G_1\rangle \otimes |G_2\rangle \otimes \cdots \otimes |G_{N_i}\rangle$, with N_i being the number of lattice sites. For the MF parameter, it again follows that $\psi_i = \langle GS|\hat{b}_i|GS\rangle = \langle G_i|\hat{b}_i|G_i\rangle$.

Now, the first consequence of introducing disorder to the system is that the translational invariance is broken. Since the local ground states $|G_i\rangle$ depend on the local on-site energies ε_i, they will, in general, be different from site to site. Hence, we can also no longer assume all MF parameters to have the same value, and in general, we have $\psi_i \neq \psi_j$ for $i \neq j$. This means that unlike to the ordered case, we cannot replace the bath amplitude Ψ_i, which is the sum of the MF parameters on the neighboring sites of i, by the MF parameter of the site itself, $\Psi_i \neq z \cdot \psi_i$.

Furthermore, we cannot assign the energy correction terms $\psi_i^* \psi_j$ to specific $\hat{h}_i$. Fortunately, these terms do not need to be taken into account in the following, since we will determine the ground state of the local Hamiltonians by diagonalization in Fock space.

First, however, we want to place one further constraint on the ψ_i. Therefore, we consider the total ground state energy. With

$$\hat{h}_i^0 = (\varepsilon_i - \mu)\hat{n}_i + \frac{U}{2}\hat{n}_i(\hat{n}_i - 1) \,, \tag{3.29}$$

we can write

$$E_{GS} = \langle GS|\hat{H}^{MF}|GS\rangle = \sum_i \langle G_i|\hat{h}_i^0|G_i\rangle - J \sum_{\langle ij \rangle} \psi_i^* \psi_j \,, \tag{3.30}$$

Now, we want to focus on site k and collect all terms that directly depend on the ground state

of this site,

$$E_{GS} = \langle G_k|\hat{h}_k|G_k\rangle + \sum_{i\neq k}\langle G_i|\hat{h}_i^0|G_i\rangle - J\sum_{\langle ij\rangle}^{i,j\neq k}\psi_i^*\psi_j\,, \tag{3.31}$$

Expressing the local ground states in terms of the local Fock states, $|G_k\rangle = \sum_{n_k} g_{k,n_k}|n_k\rangle$, yields

$$\begin{aligned}\langle G_k|\hat{h}_k|G_k\rangle &= \sum_{n_k}|g_{k,n_k}|^2\langle n_k|\hat{h}_i^0|n_k\rangle - 2J\sum_{n_k}\mathrm{Re}\left\{\Psi_k g_{k,n_k}g_{k,n_k+1}^*\right\}\sqrt{n_k+1}\\ &= \sum_{n_k}|g_{k,n_k}|^2\langle n_k|\hat{h}_i^0|n_k\rangle\\ &\quad - 2J|\Psi_k|\sum_{n_k}|g_{k,n_k}||g_{k,n_k+1}|\sqrt{n_k+1}\cos\left(\phi_k - \varphi_{k,n_k+1} + \varphi_{k,n_k}\right),\end{aligned} \tag{3.32}$$

where ϕ_k and the φ_{k,n_k} are the complex phases of the bath amplitude $\Psi_k = |\Psi_k|e^{\mathrm{i}\phi_k}$ and the coefficients $g_{k,n_k} = |g_{k,n_k}|e^{\mathrm{i}\varphi_{k,n_k}}$, respectively. Apparently, the above matrix element and, thus, also E_{GS} are minimal when all cosines evaluate to one, which yields the condition

$$\varphi_{k,n_k+1} - \varphi_{k,n_k} = \phi_k \quad \text{for all } k, n_k. \tag{3.33}$$

Plugging this into the expression for the MF parameter ψ_k, one obtains

$$\begin{aligned}\psi_k &= \sum_{n_k} g_{k,n_k}^* g_{k,n_k+1}\sqrt{n_k+1}\\ &= \sum_{n_k}|g_{k,n_k}||g_{k,n_k+1}|e^{\mathrm{i}(\varphi_{k,n_k+1}-\varphi_{k,n_k})}\sqrt{n_k+1}\\ &= e^{\mathrm{i}\phi_k}\sum_{n_k}|g_{k,n_k}||g_{k,n_k+1}|\sqrt{n_k+1}\,.\end{aligned} \tag{3.34}$$

In order to minimize E_{GS}, the local MF parameter has to have the same complex phase as the bath amplitude.

With this result, we now turn to the local Hamiltonians $\hat{h}_i$, which we want to solve for a given Ψ_i. As from now on we will consider only a single-site, we again drop the index i. Analogously to the non-disordered case, we expand $\hat{h}$ in terms of the local Fock states $|n\rangle$,

$$\begin{aligned}\hat{h} &= \sum_{mn}|m\rangle\langle m|\hat{h}|n\rangle\langle n|\\ &= \sum_{n=0}^{\infty}\Big(E_n|n\rangle\langle n| - J\sqrt{n+1}\big(\Psi^*|n\rangle\langle n+1| + \Psi|n+1\rangle\langle n|\big)\Big)\,.\end{aligned} \tag{3.35}$$

Redefining the Fock states as $|\widetilde{n}\rangle = e^{\mathrm{i}n\phi}|n\rangle$, we can transform the above complex matrix into a real one,

$$\hat{h} = \sum_{n=0}^{\infty}\Big(E_n|\widetilde{n}\rangle\langle\widetilde{n}| - J|\Psi|\sqrt{n+1}\big(|\widetilde{n}\rangle\langle\widetilde{n}+1| + |\widetilde{n}+1\rangle\langle\widetilde{n}|\big)\Big)\,, \tag{3.36}$$

where $E_n = \langle n|\hat{h}^0|n\rangle$. The ground state then takes the following form,

$$|G\rangle = \sum_n \widetilde{g}_n|\widetilde{n}\rangle = \sum_n \widetilde{g}_n e^{\mathrm{i}n\phi}|n\rangle \stackrel{!}{=} \sum_n |g_n|e^{\mathrm{i}\varphi_n}|n\rangle\,. \tag{3.37}$$

First, this reproduces equation (3.33), that is, $\varphi_n = n\phi$ with the gauge $\varphi_0 = 0$. Second, we see that $|g_n| = \widetilde{g}_n$. As $\widetilde{g}_n$ does only depend on $|\Psi|$, we can conclude that the absolute values of the expansion coefficients of the ground state in Fock space only depend on the absolute value of the bath amplitude, and not on its complex phase. Consequently, the absolute value of ψ only depends on $|\Psi|$ and, as shown before, the complex phase of ψ is determined solely by the complex phase ϕ of Ψ. Hence, both can be tuned independently.

With this result, we can make one further assumption. From equation (3.32) one can see that the larger the absolute value of the bath amplitude, the smaller the total energy E_{GS}. Therefore,

$$|\Psi| = \Big|\sum_{j=1}^{z}\psi_j\Big| = \Big|\sum_{j=1}^{z}|\psi_j|e^{\mathrm{i}\phi_j}\Big| \tag{3.38}$$

has to be maximized in order to minimize the energy. Here, the summation is taken over all z nearest neighbors of the considered site. Apparently, $|\Psi|$ is the largest if all complex phases ϕ_j are set to the same value, which is then, of course, also the complex phase of Ψ. Consequently, the complex phase of ψ is the same as the one of the neighboring MF parameters ψ_j, and hence all MF parameters have the same complex phase ϕ.

Knowing this, we can rotate all ψ_i onto the real, non-negative axis by the same global gauge transformation as in the previous section, that is, $\hat{b}_i \to \hat{b}_i e^{-\mathrm{i}\phi}$. With this, the local Hamiltonian can finally be written as

$$\hat{h} = \sum_{n=0}^{\infty}\Big(E_n|n\rangle\langle n| - J\Psi\sqrt{n+1}\big(|n\rangle\langle n+1| + |n+1\rangle\langle n|\big)\Big)\,. \tag{3.39}$$

with $\Psi = \sum_{j=1}^{z}\psi_j \geq 0$.

3.2.2 Self-Consistent Integral Equation

In the previous section, we showed how to arrive at the local Hamiltonian (3.39). As a consequence of the decoupling approximation, the eigenstates of the full MF Hamiltonian factorize into product states of the local eigenstates. This drastically simplifies the problem of finding the ground state, as one now has to solve N_i local systems of dimension $n_c + 1$, n_c being the cutoff particle number and N_i the number of lattice sites, instead of one non-local system of dimension $(n_c+1)^{N_i}$. However, in contrast to the case of the pure Bose-Hubbard model, here the local Hamiltonians still contain parameters depending on their neighboring sites in form of the bath amplitude. Thus, the problem still is a lattice problem and each local ground state depends on all on-site energies,

$$|G_i\rangle = |G_i(\varepsilon_i, \Psi_i)\rangle = \big|G_i\big(\varepsilon_i, \Sigma_j'\psi_j(\varepsilon_j, \Psi_j)\big)\big\rangle = \cdots = |G_i(\varepsilon_1, \varepsilon_2, \ldots, \varepsilon_{N_i})\rangle\,. \tag{3.40}$$

In principle, it can be solved for finite systems the same way it is done for the non-disordered case in section 3.1.1, that is, by starting with an initial guess for each MF parameter ψ_i, finding the ground states $|G_i\rangle$, calculating new MF parameters from these ground states, and then

iterating these steps until convergence is achieved. The criterion for convergence now reads

$$\psi_i \stackrel{!}{=} \langle G_i(\Psi_i)|\hat{b}_i|G_i(\Psi_i)\rangle = \langle G_i(\Sigma_j'\psi_j)|\hat{b}_i|G_i(\Sigma_j'\psi_j)\rangle \quad \text{for all } i. \tag{3.41}$$

In practice, this way of solving the problem still is limited to rather small systems. In a work by Niederle and Rieger [39], this has actually been done for two dimensions and systems with up to 100×100 lattice sites. This would equate to only $33 \times 33 \times 33$ sites in three dimension, i.e., very small system sizes.

Note that on top of this, one has to take into account that the onsite energies are randomly distributed. For a given realization of energies $\{\varepsilon_1, \varepsilon_2, \ldots, \varepsilon_{N_i}\}$ one will obtain a certain set of MF parameters $\{\psi_1, \psi_2, \ldots, \psi_{N_i}\}$. In order to find the probability $P_{\{\psi_i\}}$ for such a set $\{\psi_i\}$, one has to integrate over all possible combinations of onsite energies and add up the contributions corresponding to this specific set,

$$\begin{aligned}
&P_{\{\psi_i\}}(\psi_1, \psi_2, \ldots, \psi_{N_i}) \\
&= \int \mathrm{d}\varepsilon_1 P_\varepsilon(\varepsilon_1) \int \mathrm{d}\varepsilon_2 P_\varepsilon(\varepsilon_2) \ldots \int \mathrm{d}\varepsilon_{N_i} P_\varepsilon(\varepsilon_{N_i})\, \delta\Big(\psi_1 - \big\langle G_1(\{\varepsilon_j\})\big|\, \hat{b}_1 \,\big|G_1(\{\varepsilon_j\})\big\rangle\Big) \\
&\qquad \times \delta\Big(\psi_2 - \big\langle G_2(\{\varepsilon_j\})\big|\, \hat{b}_2 \,\big|G_2(\{\varepsilon_j\})\big\rangle\Big) \ldots \delta\Big(\psi_{N_i} - \big\langle G_{N_i}(\{\varepsilon_j\})\big|\, \hat{b}_{N_i} \,\big|G_{N_i}(\{\varepsilon_j\})\big\rangle\Big)\,.
\end{aligned} \tag{3.42}$$

As it is not feasible to actually calculate the probability distribution for the full set of MF parameters, we will try to derive a distribution for the local parameters. The probability distribution for one local MF parameter is obtained as follows,

$$\begin{aligned}
P_\psi(\psi) &= \int \mathrm{d}\psi_1 \int \mathrm{d}\psi_2 \ldots \int \mathrm{d}\psi_{N_i} P_{\{\psi_i\}}(\{\psi_i\}) \delta(\psi - \psi_1) \\
&= \int \mathrm{d}\varepsilon_1 P_\varepsilon(\varepsilon_1) \int \mathrm{d}\varepsilon_2 P_\varepsilon(\varepsilon_2) \ldots \int \mathrm{d}\varepsilon_{N_i} P_\varepsilon(\varepsilon_{N_i})\, \delta\Big(\psi - \big\langle G_1(\{\varepsilon_j\})\big|\, \hat{b}_1 \,\big|G_1(\{\varepsilon_j\})\big\rangle\Big)\,,
\end{aligned} \tag{3.43}$$

where instead of $i = 1$, equally any other site could have been chosen. Since $|G_1\rangle$ only implicitly depends on the on-site energies ε_j for $j \neq 1$, we can write

$$\begin{aligned}
P_\psi(\psi) &= \int \mathrm{d}\varepsilon_1 P_\varepsilon(\varepsilon_1) \int \mathrm{d}\varepsilon_2 P_\varepsilon(\varepsilon_2) \ldots \int \mathrm{d}\varepsilon_{N_i} P_\varepsilon(\varepsilon_{N_i})\, \delta\Big(\psi - \big\langle G_1(\varepsilon_1, \Psi_1)\big|\, \hat{b}_1 \,\big|G_1(\varepsilon_1, \Psi_1)\big\rangle\Big) \\
&= \int \mathrm{d}\varepsilon P_\varepsilon(\varepsilon) \int \mathrm{d}\Psi \underbrace{\int \mathrm{d}\varepsilon_1 \int \mathrm{d}\varepsilon_2 P_\varepsilon(\varepsilon_2) \ldots \int \mathrm{d}\varepsilon_{N_i} P_\varepsilon(\varepsilon_{N_i})\, \delta\Big(\Psi - \Psi_1(\{\varepsilon_i\})\Big)\delta(\varepsilon - \varepsilon_1)}_{\equiv P_\Psi(\Psi|\,\varepsilon)} \\
&\qquad \times \delta\Big(\psi - \big\langle G_1(\varepsilon, \Psi)\big|\, \hat{b}_1 \,\big|G_1(\varepsilon, \Psi)\big\rangle\Big) \\
&= \int \mathrm{d}\varepsilon P_\varepsilon(\varepsilon) \int \mathrm{d}\Psi P_\Psi(\Psi|\,\varepsilon)\, \delta\Big(\psi - \big\langle G(\varepsilon, \Psi)\big|\, \hat{b} \,\big|G(\varepsilon, \Psi)\big\rangle\Big)\,.
\end{aligned} \tag{3.44}$$

In the last step the index for the lattice site was dropped, reflecting that the matrix element does depend only on the values for the onsite energy and the bath amplitude. Also, the conditional probability $P_\Psi(\Psi|\,\varepsilon)$ for the bath amplitude Ψ and a given onsite energy ε for the central site was introduced. Writing the distribution function this way, the full lattice problem is now condensed into one single probability function for the bath amplitude Ψ.

Unfortunately, it is not possible to obtain this function, so at this point, we need to make one further approximation: We will assume that the probability distribution for the full set of MF parameters factorizes into the product of the probabilities of the local parameters,

$$P_{\{\psi_i\}}\big(\{\psi_i\}\big) \to \prod_i P_\psi(\psi_i)\,. \tag{3.45}$$

First of all, this implies that the probability for the MF parameter on a certain site does not depend on the values of the onsite energies on the neighboring sites. Consequently, we have

$$P_\Psi(\Psi|\,\varepsilon) \quad \to \quad P_\Psi(\Psi) = \prod_{i=1}^{z} P_\psi(\psi_i)\,, \tag{3.46}$$

and therefore, the integral for the local probability distribution reads

$$P_\psi(\psi) = \int \mathrm{d}\varepsilon P_\varepsilon(\varepsilon) \prod_{i=1}^{z} \int \mathrm{d}\psi_i P_\psi(\psi_i)\, \delta\Big(\psi - \big\langle G\big(\varepsilon, \Sigma_{j=1}^{z}\psi_j\big)\big|\,\hat{b}\,\big|G\big(\varepsilon, \Sigma_{j=1}^{z}\psi_j\big)\big\rangle\Big)\,. \tag{3.47}$$

Second, we note that although the probabilities for the MF parameters are not correlated anymore, the MF parameters themselves still depend on the bath amplitudes, and therefore, on the values for the ψ_i on the neighboring sites.

To conclude this section, we note that the above equation is apparently a transient equation and has to be solved self-consistently. This is done analogously to the non-disordered case by taking an initial guess, however, this time not for the MF parameter ψ, but for its probability distribution P_ψ. Performing the integration, one obtains a new distribution, which is then plugged back into the right site of equation (3.47). The integration has to be repeated until the solution converges, that is, the distribution we use to evaluate the integral equals the one we receive from performing the integration.

3.2.3 The Phase Boundary for the Disordered System

For the pure case, there were two characteristic behaviors when iterating the self-consistent conditional equation for the order parameter,

$$\psi^{(s+1)} = \langle G(\psi^{(s)})|\hat{b}|G(\psi^{(s)})\rangle \quad \longrightarrow \quad \begin{cases} \psi = 0 & \text{MI Phase} \\ \psi > 0 & \text{SF Phase} \end{cases} \quad \text{for } s \to \infty\,, \tag{3.48}$$

where $\psi^{(s)}$ is the order parameter after s iteration steps (which, of course, depends on the choice for the starting value $\psi^{(0)}$). For the disordered case, we have to solve the conditional equation for the probability distribution,

$$P_\psi^{(s+1)} = F\left[P_\psi^{(s)}\right] \quad \longrightarrow \quad P_\psi = ? \quad \text{for } s \to \infty\,, \tag{3.49}$$

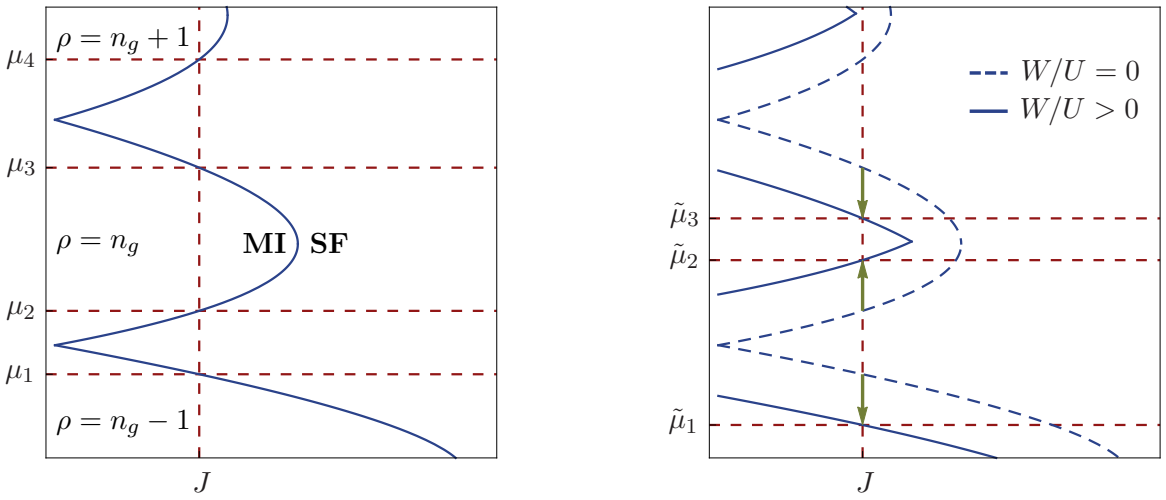

(a) No disorder: $W = 0$ (b) Finite disorder: $0 < W < U$

Figure 3.6: **(a)** A sketch of the phase diagram for zero disorder and fixed interaction U, focused on the Mott lobe with filling $\rho = n_g$. The blue curve shows the boundary between MI and SF phase. The intersection points of the dashed red lines indicate the transition points for a fixed hopping J. **(b)** The same plot, but now with finite disorder, $W/U > 0$, but still smaller than the atomic limit band gap, $W < U$. The dashed blue line shows the phase boundary for $W/U = 0$ for comparison. The green arrows indicate the shift by $W/2$ due to the disorder.

where F is the functional of P_ψ given in equation (3.47) and $P_\psi^{(s)}$ the distribution after s iteration steps. Apparently, $P_\psi(\psi) = \delta(\psi)$ is always a solution to the conditional equation,

$$\begin{aligned} F\left[\delta(\psi)\right] &= \int \mathrm{d}\varepsilon P_\varepsilon(\varepsilon) \prod_{i=1}^{z} \int \mathrm{d}\psi_i \delta(\psi_i)\, \delta\Big(\psi - \big\langle G\big(\varepsilon, \Sigma_{j=1}^{z}\psi_j\big)\big|\, \hat{b}\, \big|G\big(\varepsilon, \Sigma_{j=1}^{z}\psi_j\big)\big\rangle\Big) \\ &= \underbrace{\int \mathrm{d}\varepsilon P_\varepsilon(\varepsilon)}_{=\,1}\; \delta\big(\psi - \underbrace{\big\langle G(\varepsilon,0)\big|\, \hat{b}\, \big|G(\varepsilon,0)\big\rangle}_{=\langle n_0|\hat{b}|n_0\rangle = 0}\big) \\ &= \delta(\psi)\,, \end{aligned} \tag{3.50}$$

where in the last step we have used that for a vanishing bath amplitude, $\Psi = 0$, the ground state is a particle number eigenstate $|n_0\rangle$, and thus, the MF parameter is zero for any ε. This solution implies, that all MF parameters are zero. By the same arguments as for the non-disordered case, this result corresponds to the MI phase, where each particle is localized on a single site.

By a simple consideration, we can already determine a situation which inevitably leads to this solution. Therefore, we again consider the pure case $\varepsilon_i = \varepsilon_0 = 0$ for all i, see figure 3.6a. When we focus on the region around the Mott lobe with the filling factor $\rho = n_g$, then for fixed J and U there are four important values for the chemical potential. First, μ_1 is the upper transition point from the Mott lobe with filling $\rho = n_g - 1$ to the SF phase, then μ_2 and μ_3 are the lower and upper transition points for the Mott lobe with $\rho = n_g$, and finally, μ_4 marks the lower transition to the Mott lobe with $\rho = n_g + 1$. Consequently, for $\mu_1 < \mu < \mu_2$ and $\mu_3 < \mu < \mu_4$ the system is in the SF phase, whereas for $\mu_2 < \mu < \mu_3$ the system is in the MI phase.

Now, if we allow for a finite onsite energy, the system can be pushed from the MI to the SF

phase (and vice versa) for fixed μ. For $\mu_2 < \mu - \varepsilon_0 < \mu_3$, the system is still an insulator. We will call sites with these onsite energies *locally incompressible*. For any positive input value, the conditional equation (3.48) will always lead to a smaller MF parameter,

$$\psi^{(s)} > \psi^{(s+1)} = \langle G(\psi^{(s)})|\hat{b}|G(\psi^{(s)})\rangle \to 0 \text{ for } s \to \infty. \tag{3.51}$$

However, if $\mu_1 < \mu - \varepsilon_0 < \mu_2$ or $\mu_3 < \mu - \varepsilon_0 < \mu_4$, the system is shifted into the SF phase. Sites with such onsite energies will be called *locally compressible*. Depending on the input value, the conditional equation leads to a smaller, equal or larger MF parameter,

$$\begin{aligned} \psi^{(s)} &> \psi^{(s+1)} \quad \text{for} \quad \psi^{(s)} > \psi, \\ \psi^{(s)} &= \psi^{(s+1)} \quad \text{for} \quad \psi^{(s)} = \psi, \\ \psi^{(s)} &< \psi^{(s+1)} \quad \text{for} \quad \psi^{(s)} < \psi. \end{aligned} \tag{3.52}$$

Without disorder, all onsite energies are the same, and thus, all sites are either compressible or not. When the disorder is switched on and the onsite energies are randomly distributed, this is not necessarily the case anymore. In addition to the above two cases, we now have a third case where some sites are compressible and some are incompressible. To link these cases to the non-disordered ones, we can make use of the fact that the only thing that changes for the local Hamiltonians $\hat{h}_i$ when switching on disorder is that the bath amplitude is not a multiple of the local MF parameter anymore,

$$\Psi = z\psi \quad \longrightarrow \quad \Psi_i = {\sum_j}' \psi_j \,. \tag{3.53}$$

Hence, for a fixed realization of disorder we can still use the same conditional equation (3.48), but have to replace the input parameter as follows,

$$\psi_i^{(s+1)} = \langle G\big(\tfrac{1}{z}\Sigma_j'\psi_j^{(s)}\big)|\,\hat{b}\,|G\big(\tfrac{1}{z}\Sigma_j'\psi_j^{(s)}\big)\rangle \,, \tag{3.54}$$

where the summation is taken over all nearest neighbors of site i and s is again indicating the iteration step.

Let us first consider the case of all sites being locally incompressible. Then, for all sites i equation (3.51) holds true, and we have

$$\psi_i^{(s+1)} < \frac{1}{z}{\sum_j}' \psi_j^{(s)} \,, \tag{3.55}$$

In other words, the MF parameter on every site i is smaller than the mean of the MF parameters on its neighboring sites in the previous step. For the total mean value of the MF parameter, we have

$$\overline{\psi^{(s+1)}} = \frac{1}{N_i}\sum_i \psi_i^{(s+1)} < \frac{1}{N_i}\sum_i \frac{1}{z}\sum_j^{\langle ij\rangle} \psi_j^{(s)} = \frac{1}{N_i}\sum_i \psi_i^{(s)} = \overline{\psi^{(s)}} \,. \tag{3.56}$$

No matter how small the $\psi_i^{(s)}$, on average the $\psi_i^{(s+1)}$ are smaller. Thus, the only stable solution is given by $\psi_i = 0$ for all sites i.

For the case of all sites being locally compressible, each onsite energy ε_i would lead to a finite

MF parameter in the non-disordered case with $\varepsilon_0 = \varepsilon_i$. The set of all these parameters has a smallest element $\psi_{min} > 0$. If we choose $\psi_i^{(s)} = \psi_{min}$ for all sites i, then from (3.52) it follows that

$$\psi_i^{(s+1)} \geq \frac{1}{z} \sum_j{}' \psi_k^{(s)} = \psi_{min} \tag{3.57}$$

for all sites i. Thus, ψ_{min} represents a lower boundary for the MF parameters and the converged solutions for the ψ_i will all be finite.

The above findings are not surprising, but exactly what one would expect. More interesting now is the third case, where some fraction of sites is compressible and the other fraction incompressible. Following the argumentation of Freericks and Monien [23], in the thermodynamic limit, $N_i \to \infty$, one will always find arbitrarily large *rare regions* that only consist of compressible sites. If we consider the extreme case where the MF parameter vanishes on all sites surrounding these regions, they can be viewed as isolated systems of finite size. However, since one can find regions like these of any size, there will also be systems large enough to neglect boundary effects. Within these regions, the MF parameter and, therefore, also the compressibility will be finite. Thus, if the probability distribution is such that a fraction of the energies push the sites locally outside of the Mott lobes, the whole system is compressible and, therefore, not a MI anymore.

If we consider a distribution function P_ε that is only finite in the interval $[-W/2, +W/2]$, then for all chemical potentials μ with $\mu_2 < \mu < \mu_2 + W/2$ and $\mu_3 - W/2 < \mu < \mu_3$ one will always find compressible sites. Thus, only for $\tilde{\mu}_2 < \mu < \tilde{\mu}_3$, with $\tilde{\mu}_2 = \mu_2 + W/2$ and $\tilde{\mu}_3 = \mu_3 - W/2$, the system is in the incompressible MI phase. Consequently, the lower boundary of each Mott lobe is shifted upwards by $W/2$ and the upper boundary downwards by $-W/2$, see figure 3.6b. This means that also for the disordered system, the phase boundary only quantitatively depends on the dimensionality of the system within the MF approximation.

The width of the Mott lobe for the fixed hopping amplitude J is then given by $\tilde{\mu}_3 - \tilde{\mu}_2 = \mu_3 - \mu_2 - W$. This value is the largest for $J = 0$, where $\mu_2/U = n_g - 1$ and $\mu_3/U = n_g$ as discussed earlier, and therefore, $\tilde{\mu}_3 - \tilde{\mu}_2 = U - W$. This implies that at $W = U$, the width of the Mott lobes becomes zero. Thus, for strong disorder, $W/U \geq 1$, the Mott lobes will completely vanish for any dimension.

3.2.4 Numerical Results for Three Dimensions

In the previous section, we have made considerations on how the boundary between the gaped and the gapless phase should behave when disorder is introduced to the system. However, apart from the trivial case, $P_\psi(\psi) = \delta(\psi)$, we did not make any predictions for the shape of the actual distribution functions. In this section, we will discuss the numeric results for the distribution functions for the three-dimensional case and try to arrive at an intuitive understanding based on the picture we have established in the previous section. For the distribution P_ε of the onsite energies, we use a simple box shaped function,

$$P_\varepsilon(\varepsilon) = \begin{cases} 1/W & \text{for } \varepsilon \in [-W/2, +W/2], \\ 0 & \text{else.} \end{cases} \tag{3.58}$$

As the integration in the self-consistent equation (3.47) has the dimension $1+z=7$, we use the Monte-Carlo (MC) method to evaluate the integral,

$$\int_{\psi_{min}}^{\psi_{max}} \mathrm{d}\psi f(\psi) \quad \longrightarrow \quad \frac{\psi_{max}-\psi_{min}}{N_i} \sum_{i=1}^{N_i} f(\psi_i) \tag{3.59}$$

with randomly generated $\psi_i \in [\psi_{min}, \psi_{max}]$. Furthermore, the integrand itself contains a δ-distribution whose argument is the result of a matrix diagonalization. Thus, we cannot predict which integration points yield a finite contribution. Therefore, we will proceed as follows. First, we generate a sufficiently large set of data points. Each data point i consists of the actual value $\psi_i = \psi(\varepsilon, \psi_1, \ldots, \psi_z)$ as well as the corresponding probability weight $\mathcal{W}_i = P_\varepsilon(\varepsilon) \cdot P_\psi(\psi_1) \cdot \ldots \cdot P_\psi(\psi_z)$ for randomly generated input parameters ε and $\psi_1, \ldots, \psi_z$. Then, we divide the value range for ψ into intervals $[\psi_s, \psi_{s+1})$ and calculate the average probability for each interval via

$$P_\psi\Big(\frac{\psi_s+\psi_{s+1}}{2}\Big) = \frac{1}{(\psi_{s+1}-\psi_s)\sum_i \mathcal{W}_i} \sum_i \mathcal{W}_i\, \theta(\psi_i-\psi_s)\theta(\psi_{s+1}-\psi_i)\,. \tag{3.60}$$

Note that weighting factors that are the same for each data point can be neglected as they would cancel due to the normalization by the total weight $\sum_i \mathcal{W}_i$. The values ψ_s are chosen such that

$$\Delta\psi_{min} < \psi_{s+1} - \psi_s < \Delta\psi_{max} \tag{3.61}$$

and

$$\left| P_\psi\Big(\frac{\psi_s+\psi_{s+1}}{2}\Big) - P_\psi\Big(\frac{\psi_{s+1}+\psi_{s+2}}{2}\Big) \right| < \Delta P_{max}\,. \tag{3.62}$$

This guarantees that the intervals do not get too small even in regions of large probability weight while at the same time the function P_ψ is well resolved. The parameters $\Delta\psi_{min/max}$ and ΔP_{max} are chosen such that we obtain optimal results. For the MC integration we use linear interpolation to evaluate $P_\psi(\psi)$ for a given ψ. Furthermore, we take special care that single probability weights $\mathcal{W}_i$ do not get too large, as this would introduce fluctuations for P_ψ. To do so, we define an integration grid ψ_t (with roughly the same number of points that are used to resolve P_ψ) such that P_ψ integrated over each of the intervals $[\psi_t, \psi_{t+1})$ leads to the same total probability weight. The integration over ψ is then split into integrations over these intervals,

$$\int \mathrm{d}\psi = \sum_t \int_{\psi_t}^{\psi_{t+1}} \mathrm{d}\psi\,. \tag{3.63}$$

In principle, we now want to perform a MC integration for each interval. As this is not practical, we do the following instead. To generate one ψ for the MC integration, first an interval is chosen randomly, and then one ψ within this interval. This changes the probability of generating a certain ψ as follows,

$$\frac{1}{\psi_{max}-\psi_{min}} \to \frac{1}{N_t}\frac{1}{\psi_{t+1}-\psi_t} \quad \text{for} \quad \psi \in [\psi_{t+1}-\psi_t) \tag{3.64}$$

where N_t is the number of intervals. In order to compensate for this, we have to adjust each weight as follows, $\mathcal{W}_i \to \mathcal{W}_i(\psi_{t+1}-\psi_t)$ for $\psi_i \in [\psi_t, \psi_{t+1})$.

Technically, this has the effect that we choose more points from regions with high probability

density. Each of these points, however, has an effectively reduced probability weight, which eliminates outliers and fluctuations.

For the MC integration, we use the MT19937 (pseudo) random number generator provided by the *GNU Scientific Library* [82]. Furthermore, all matrix diagonalizations are performed using the *LAPACK* package [83].

Let us now start by investigating the dependence of P_ψ on the hopping amplitude J/U. From the findings in the previous section, we can deduce that there are two distinct cases. For $J/U \to 0$, the system can either be gaped or not. In the first case one approaches the atomic limit from above a Mott lobe, in the second case from in between two Mott lobes.

The Dependence of P_ψ on J/U Between the Mott-Lobes

We first consider the non-gaped case, $\mu/U \in [n_g - W/2U, n_g + W/2U]$ with $n_g \in \mathbb{N}$. In figure 3.7, the numeric results for P_ψ for $W/U = 0.6$ and three such μ with $n_g = 1$ are shown. While the distribution functions differ quantitatively for different μ/U, the qualitative behavior is the same in all three instances. For large J/U, the distribution function is non-zero only in a finite region well above $\psi = 0$. To determine the theoretical upper and lower boundaries for ψ, we can again use the argument of the rare large regions with constant on-site energies. There will be one on-site energy that leads to the lowest and one that leads to the highest MF parameter. For $J/U = 0.03$, the MF parameter is finite for any μ/U, see figure (3.2b). The following table compares the theoretically predicted and the numerically obtained upper and lower boundaries for ψ:

μ/U	0.75	1.00	1.25
Theoretical Range for ψ at $J/U = 0.03$	$0.30 \ldots 0.97$	$0.70 \ldots 0.993$	$0.939 \ldots 1.06$
Numerically Obtained Range	$0.53 \ldots 0.96$	$0.76 \ldots 0.987$	$0.944 \ldots 1.05$

Apparently, the numerically obtained range does not equal the predicted one. Still, the numerical range always lies within the predicted range. For $\mu/U = 1.00$ and $\mu/U = 1.25$, the span of possible values for ψ is relatively small. As a consequence, the deviation of the obtained range from the predicted one is also rather small. However, for $\mu/U = 0.75$, the predicted range is quite large and the deviation from that range clearly lies above the numerical precision (which in this case is ~ 0.005 for the lower boundary). This implies that the rare regions are not reproduced by our approach. Moreover, since the deviation is so large it means that the stochastic MF approach underestimates not only the rare regions, but in general regions with MF parameters differing too much from the typical values. This can be understood as follows.

When we went from the pure to the disordered case, the only additional approximation we made was the assumption that the MF parameters on different sites are not correlated, $P_{\{\psi\}}(\{\psi_i\}) \to \prod_i P_\psi(\psi_i)$, see section 3.2.2. Let us consider a simplified case with only two possible onsite energies energies ε_1 and ε_2. They are chosen such that in the pure case ε_1 would lead to a smaller MF parameter than ε_2, $\psi\varepsilon_0 = \varepsilon_1) < \psi(\varepsilon_0 = \varepsilon_2)$. Thus, regions with onsite energies mostly equal to ε_1 also have smaller MF parameters than regions with onsite energies mostly equal to ε_2. Also, the few sites with energies ε_2 within such an ε_1-region will not be able to establish a large MF parameter since they are coupled to a small bath amplitude. The equivalent holds true for the opposite case. Thus, within these regions the MF parameters are strongly correlated and the assumption we have made for the distribution function is not well justified. The occurrence of such regions is underestimated in favor of regions with a more balanced mix of the two energies. As a result, the probability density at the outer boundaries

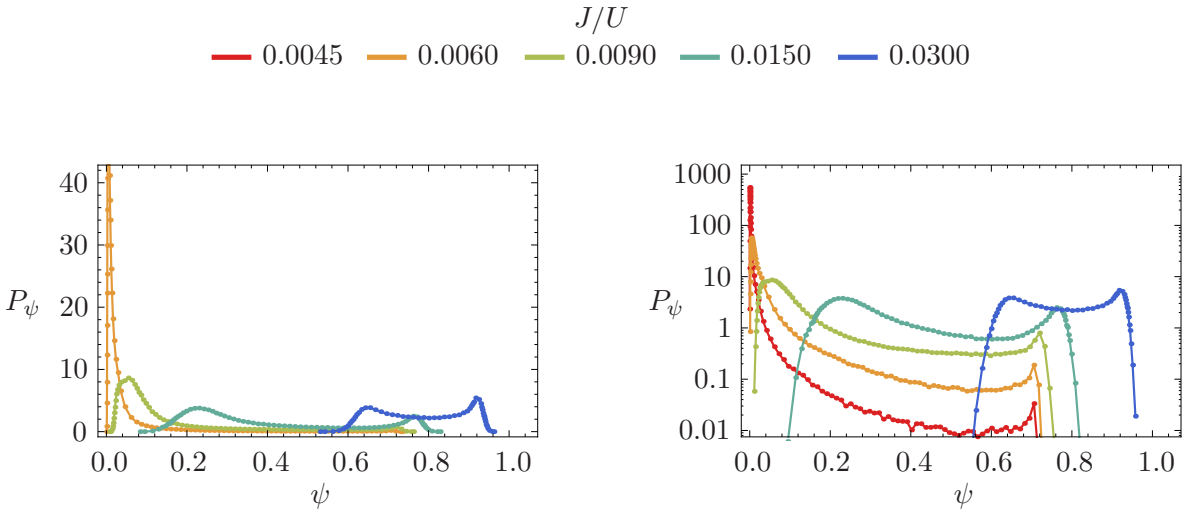

(a) $\mu/U = 0.75$

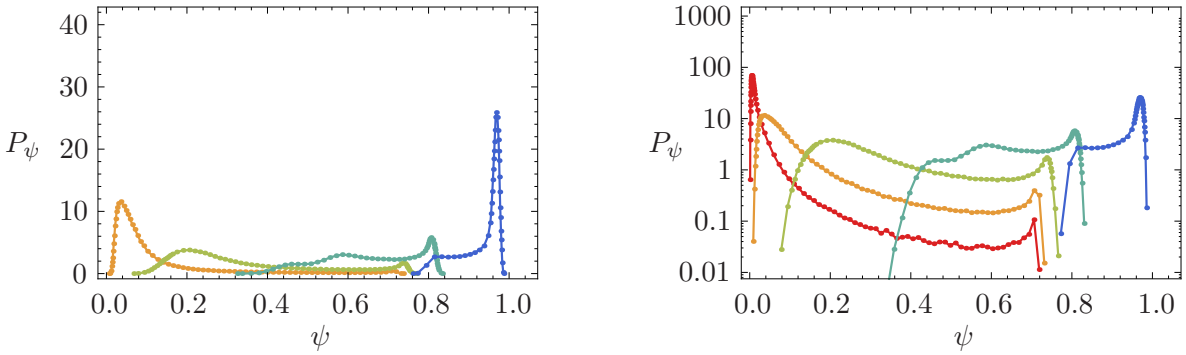

(b) $\mu/U = 1.00$

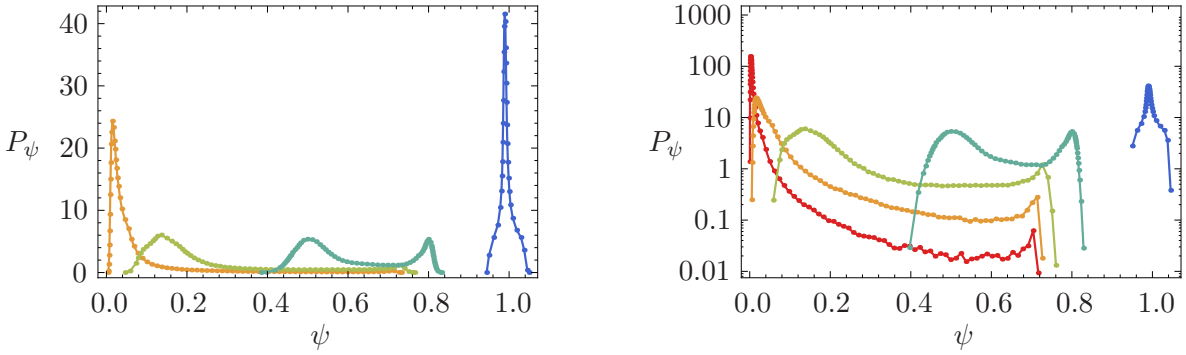

(c) $\mu/U = 1.25$

Figure 3.7: The distribution function $P_\psi(\psi)$ for fixed μ/U and different values of J/U as given in the legend at the top. The disorder width is set to $W/U = 0.6$. The plots on the left use a linear scale and the ones on the right a logarithmic scale. The values for μ/U are chosen such that the system is compressible in the atomic limit.

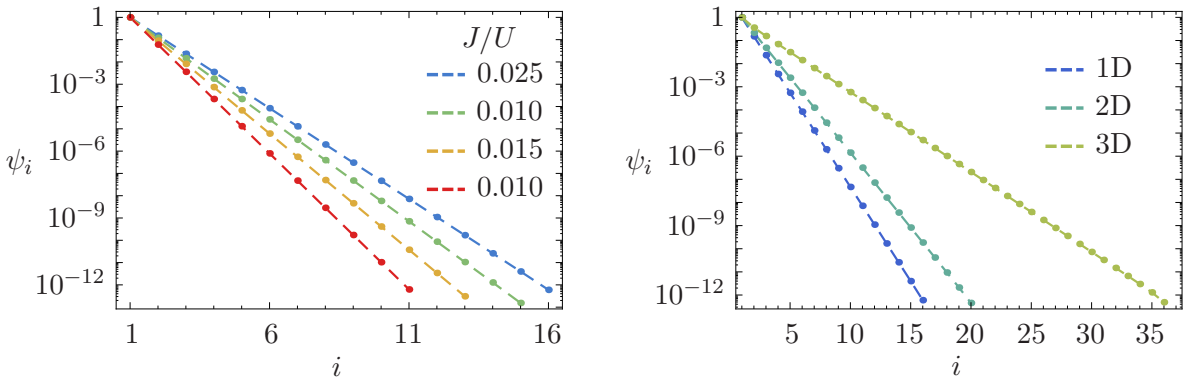

(a) 1D Chain with $\mu/U = 0.5$ and fixed $\psi_1 \equiv 1$

(b) $J/U = 0.025$ and $\mu/U = 0.5$

Figure 3.8: **(a)** The exponential decay of the MF parameter on a 1D chain. Site $i = 1$ has a fixed MF parameter, $\psi_1 \equiv 1$, and is coupled to a chain of incompressible sites ($\mu/U = 0.5$ and $\varepsilon_i = 0$ for $i > 1$). **(b)** Comparison of the decay for different dimensions. For two dimensions, we consider a chain of sites with fixed MF parameter, $\psi_1 \equiv 1$, in one direction. This chain is coupled to layers of incompressible sites in the other direction. The index i enumerates the layers. For three dimensions, we do the same thing, but now for layers of coupled planes. Numerically, this is realized by setting the bath amplitude on layer i to $\Psi_i = \psi_{i-1} + (z-2)\psi_i + \psi_{i+1}$, where $z-2$ is the number of nearest neighbors on the same layer.

for ψ will be reduced. This effect can be quite drastic as we have seen in figure 3.7a and will also be effecting the form of the phase boundary, which we will see later.

Now, when the hopping amplitude is decreased, the distribution also moves towards smaller ψ. Let us again compare the numerically obtained boundaries of P_ψ with the expected ones for $J/U = 0.009$ (green curves in figure 3.7):

μ/U	0.75	1.00	1.25
Theoretical Range for ψ at $J/U = 0.009$	0.0 . . . 0.79	0.0 . . . 0.79	0.0 . . . 0.79
Numerically Obtained Range	0.009 . . . 0.76	0.068 . . . 0.77	0.047 . . . 0.77

Apparently, in this regime the system consists of both locally compressible and incompressible sites, as the expected lower boundary for ψ is zero and the upper boundary is finite. Again, the calculated distribution functions lie within the predicted boundaries. For all three values of μ/U, one finds the same characteristic shape, which is made out of two peaks, each of which is located at one end of the function. The upper peak arises from sites that are locally compressible, the lower peak from sites that are incompressible. The existence of the compressible sites prevents the incompressible ones from establishing a zero MF parameter. Thus, the lower peak is always located at a small, but finite value of ψ. Towards zero, $\psi \to 0$, the distribution functions fall off very rapidly.

Upon decreasing the hopping amplitude further, the lower peak becomes more and the upper peak less pronounced. The general shape of the function, however, does not change. Here, one might ask the question whether it is possible for the MF parameter to become exactly zero on some sites when there are still compressible sites i with finite $\psi_i > 0$. This is related to the question of how fast the MF parameter decays when going from a compressible to an incompressible region on the lattice.

In figure 3.8a a one-dimensional chain of sites is shown. The MF parameter on the first site to the left is fixed to one, $\psi_1 \equiv 1$. The system parameters are chosen such that the other sites are locally incompressible. Still, as they are coupled to the finite MF parameter ψ_1 they will yield a finite MF parameter as well, $\psi_i > 0$ for all i. The further away in space we move from the first site $i = 1$, the smaller the MF parameter gets. In fact, it decays exponentially with distance. Extending this to two- and three-dimensional chains, see figure 3.8b, we see that the decay is less rapid the larger the dimension, but still exponential.

This implies that, although the MF parameter decays exponentially, it only vanishes in the limit of infinitely large incompressible regions. Thus, when there is a fraction of compressible sites in the system, the MF parameter can become very small, but never exactly zero. Adding disorder to the system will not change this behavior.

In between the Mott lobes, there is always a fraction of sites with energies ε_i such that $(\mu - \varepsilon_i)/U = n_g \in \mathbb{N}$. In the atomic limit, these sites will have a degenerated ground state, compare with section 3.1.1 and equation (3.18). For any small hopping, they will yield a finite MF parameter $\psi_i > 0$ with

$$\lim_{t \to 0} \psi_i = \frac{\sqrt{n_g + 1}}{2} \tag{3.65}$$

Thus, in between the Mott lobes one will always find sites with finite ψ_i.

Summarizing the above, the distribution function moves towards very small but finite values of ψ when the hopping is decreased. The existence of compressible sites leads to the occurrence of a small fraction of large ψ. This prevents the MF parameter from becoming exactly zero on any site. Furthermore, since we are neglecting correlations between MF parameters on different sites, the correct upper and lower boundaries for ψ are not reproduced.

The Dependence of P_ψ on J/U Above the Mott-Lobes

Next, we want to investigate the behavior of the distribution function when we approach the atomic limit from above a Mott lobe, $\mu/U \in [n_g - 1 + W/2U, n_g - W/2U]$ with $n_g \in \mathbb{N}$. In this case, there is a transition to the incompressible phase at finite hopping. Figure 3.9 shows the distribution functions for three such μ/U with $n_g = 2$, i.e., above the second Mott lobe. The disorder width is again chosen to be $W/U = 0.6$.

As one would expect, also here the distribution functions move towards smaller values of ψ when the hopping amplitude is decreased. However, there is one important difference compared to the behavior between the Mott lobes. For larger hopping, for example $J/U = 0.0180$, one can still see the two-peak-structure of the distribution function. When decreasing J/U, at some point the upper peak completely vanishes and the whole distribution moves towards $\psi = 0$. This can be seen best in the logarithmic plots of figure 3.9. For each μ/U, the curve for the smallest plotted hopping amplitude falls off faster than exponentially.

This can be understood as follows. In the above section, we argued that the upper peak was due to the sites that are compressible in the limit $J/U \to 0$. Here, however, all sites are incompressible in the atomic limit. On each site the MF parameter goes to zero if we decrease the hopping amplitude. Thus, the distribution moves to zero as a whole without forming an upper peak.

As we have discussed in section 3.2.3, at some point all sites become incompressible. This point should mark the transition from the compressible to the incompressible MI phase. We already found out that the stochastic MF formalism underestimates the probability for finding rare regions. When approaching the phase boundary, most of the sites will have a small MF

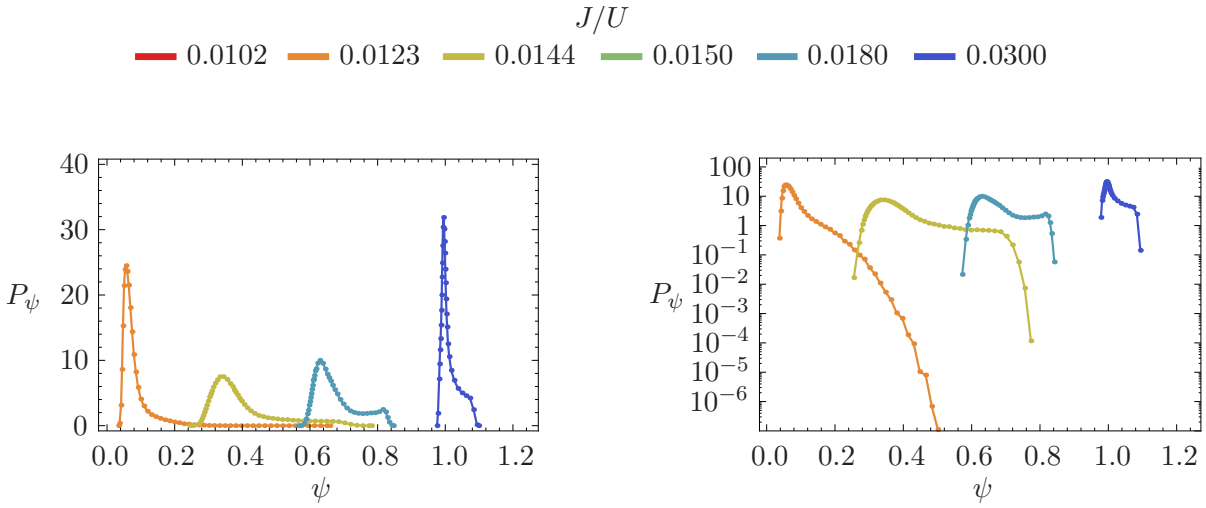

(a) $\mu/U = 1.35$

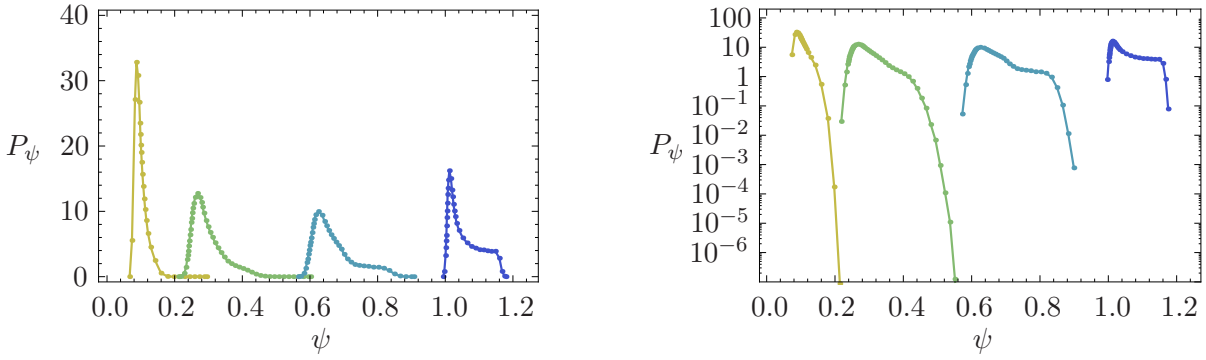

(b) $\mu/U = 1.50$

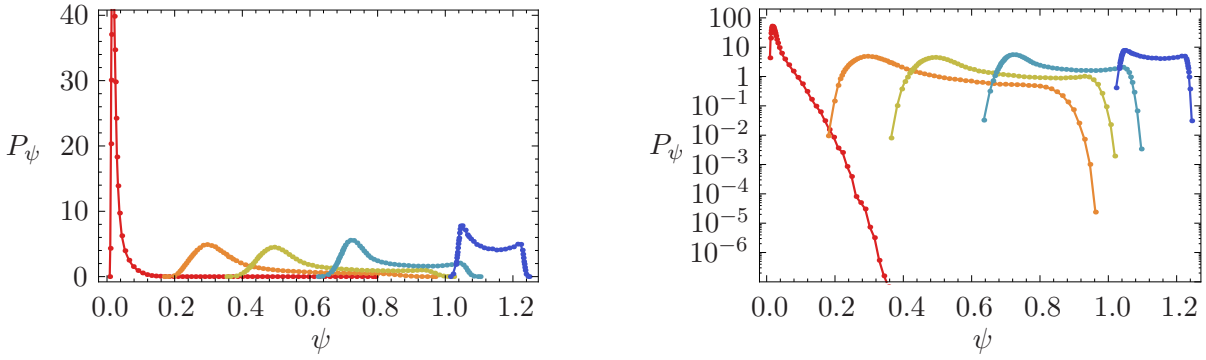

(c) $\mu/U = 1.65$

Figure 3.9: The distribution function $P_\psi(\psi)$ for fixed μ/U and different values of J/U, as given in the legend at the top. The disorder width is set to $W/U = 0.6$. The plots on the left use a linear scale and the ones on the right a logarithmic scale. The values for μ/U are chosen such that the system would be gaped in the atomic limit. The selected values for J/U differ for each μ/U. This is due to the fact that the phase transition takes place at different hopping amplitudes. When approaching the phase boundary, $(J/U) \to (J/U)_c$, we have used a step size of $\Delta(J/U) = \frac{1}{100}(J/U)_{max}$, starting at $(J/U)_{max} = 0.03$. For each μ/U, the smallest plotted value of J/U corresponds to the last point above the transition to the MI phase that is resolved by this step size.

parameter. Fewer and fewer sites will be able to sustain a large ψ_i. These few sites are resoponsible for stabilizing the lower peak of the distribution and preventing a vanishing MF parameter. Since the probability for these sites is underestimated by this formalism, we expect it to yield a phase boundary at hopping amplitudes larger than predicted in section 3.2.3.

Average Quantities and the Phase Boundary

Previously, we have discussed the results for the two typical cases for the probability distribution P_ψ. In order to obtain an overview of the parameter space, we now turn to disorder averaged quantities. Once the probability distribution P_ψ is found, the average $\overline{A}$ of a local observable A is easily obtained as follows,

$$\overline{A} \equiv \langle \hat{A} \rangle_{disorder} = \int \mathrm{d}\varepsilon P_\varepsilon(\varepsilon) \prod_{i=1}^{z} \int \mathrm{d}\psi_i P_\psi(\psi_i) \left\langle G\big(\varepsilon, \Sigma_{j=1}^{z} \psi_j\big) \middle| \hat{A} \middle| G\big(\varepsilon, \Sigma_{j=1}^{z} \psi_j\big) \right\rangle . \tag{3.66}$$

Note that within the stochastic MF approximation, local observables on different sites are uncorrelated,

$$\overline{A_i B_j} = \overline{A_i}\ \overline{B_j} \quad \text{for } i \neq j. \tag{3.67}$$

Let us first consider the behavior of the average MF parameter, $\hat{A} = \hat{b}$. The above integration then simplifies to

$$\overline{\psi} = \int \mathrm{d}\psi P_\psi(\psi)\, \psi \,. \tag{3.68}$$

Figure 3.10 shows the dependence of $\overline{\psi}$ on the hopping amplitude for different fixed chemical potentials. All curves show that the average MF parameter decreases if the hopping amplitude is decreased. However, in accordance to the previous findings, the behavior differs when ap-

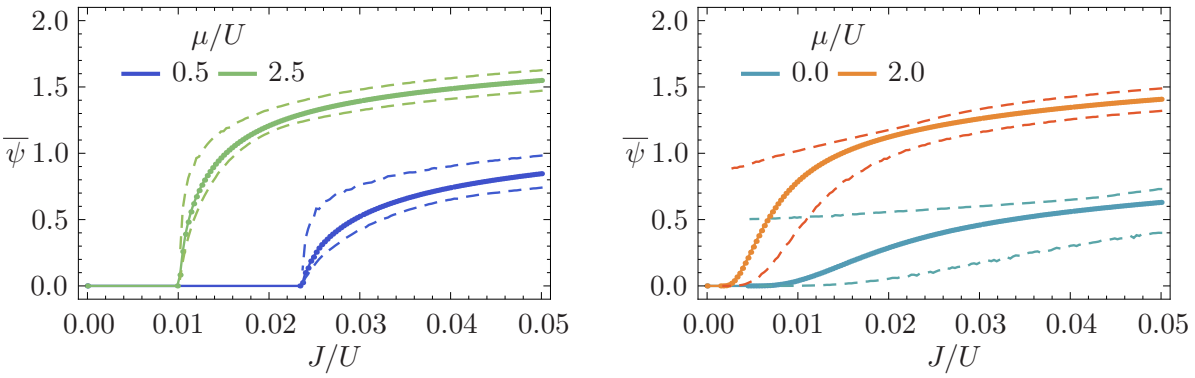

(a) Above Mott lobes

(b) Between Mott lobes

Figure 3.10: The solid lines show the disorder averaged MF parameter $\overline{\psi}$ as a function of J/U for different μ/U and $W/U = 0.6$. The dashed lines show the upper and lower boundaries of the corresponding distribution functions P_ψ. Note, that the dashed curves in **(b)** stop at a finite $J/U > 0$. At these points the numerical evaluation had to be stopped as the lower boundary fell below the numerical precision. However, it is apparent that the upper boundary will approach a finite value in the atomic limit, which is in accordance with our previous considerations.

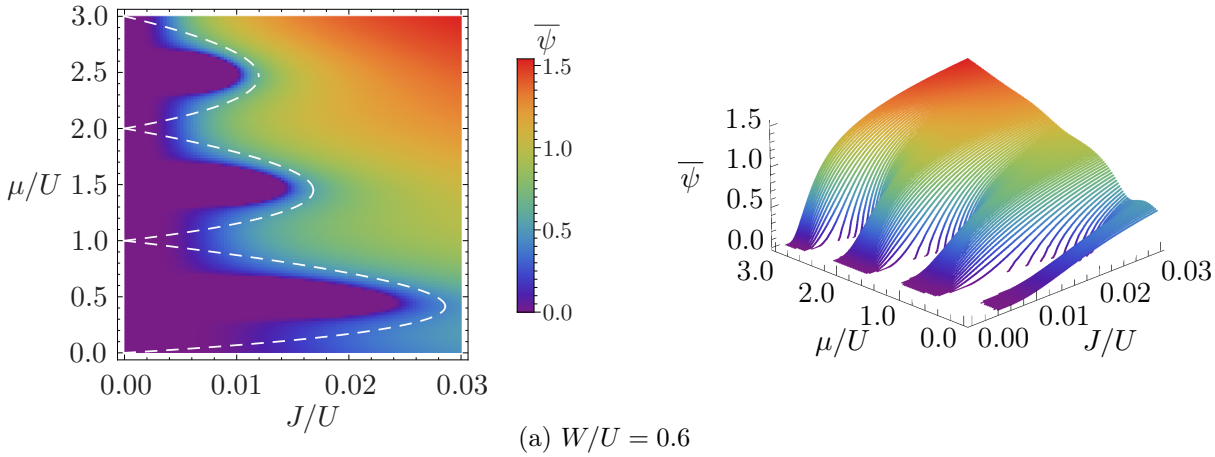

(a) $W/U = 0.6$

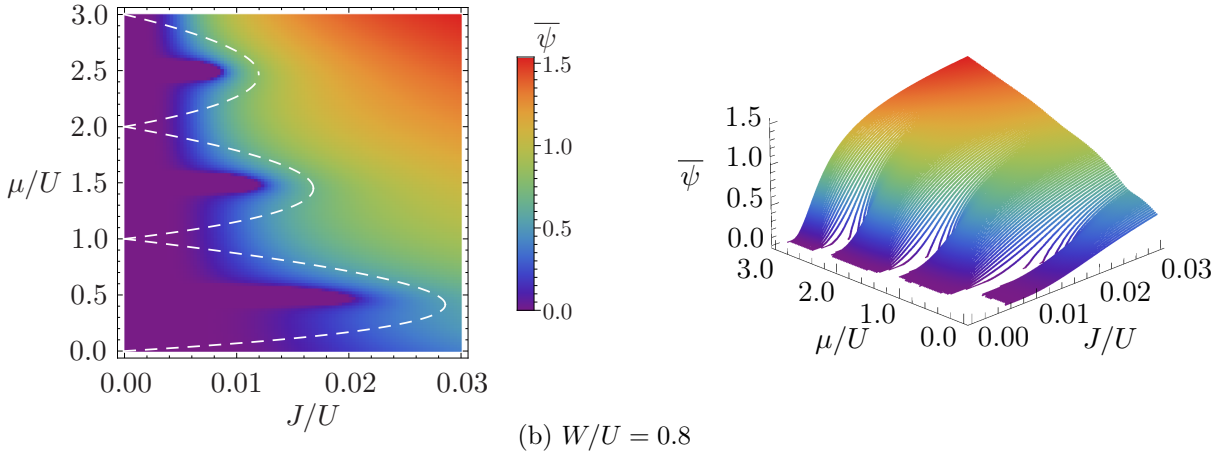

(b) $W/U = 0.8$

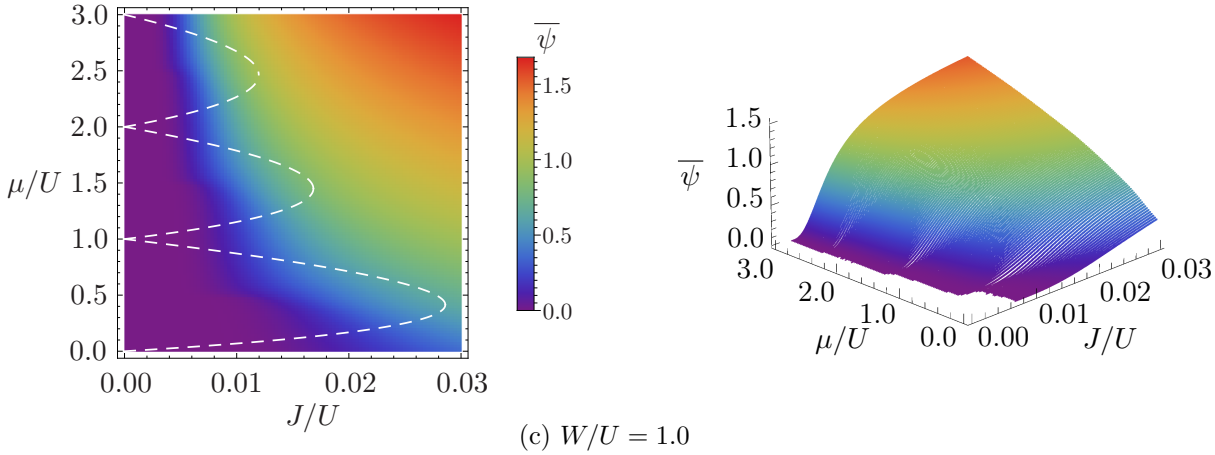

(c) $W/U = 1.0$

Figure 3.11: The disorder averaged MF parameter $\overline{\psi}$ for different disorder widths W/U. For each disorder width, both a density plot and a 3D plot of a set of curves is shown, where each curve corresponds to a fixed chemical potential. All curves stop at finite J/U, indicating a breakdown of the numerical evaluation. For comparison, the pure model's Mott lobes are indicated by the white dashed lines.

proaching the atomic limit either from above a Mott lobe or in between two Mott lobes. In the first case, see figure 3.10a, both the upper and lower boundary of the distribution go to zero at a finite J/U. Consequently, also the average MF parameter will vanish at finite J/U. In the second case, see figure 3.10b, the lower boundary goes to zero while the upper boundary approaches a finite value. Thus, for $J/U > 0$ the average MF parameter will always remain finite.

In figure 3.11, the average MF parameter is shown for different disorder widths W/U, now as a function of both J/U and μ/U. We see that the results are qualitatively in accordance with the predictions made in section 3.2.3. For $W/U < 1$, the phase diagram still consists of the Mott lobes centered around half integer values of μ/U. The sizes of the MI regions are smaller compared to the pure case and decrease when the disorder is increased. When disorder is equal to or larger than the interaction strength, $W/U \geq 1$, the Mott lobes vanish completely.

A problem one runs into when trying to identify the MI regions arises from the fact that we cannot reach the atomic limit numerically. For each μ/U, the MF routine breaks down at some finite hopping amplitude $J/U > 0$. Consequently, close to the atomic limit we cannot distinguish between the MI regions, where $P_\psi(\psi) = \delta(\psi)$, and the regions where $P_\psi(\psi) \approx \delta(\psi)$. Thus, we need to consider another quantity, which is the average particle number $\bar{n}$ ($\hat{A} = \hat{n}$ in equation (3.66)). The compressibility is obtained via $\kappa = \mathrm{d}\bar{n}/\mathrm{d}\mu$.

Figure 3.12 shows both quantities as a function of μ/U for $W/U = 0.6$ and two different hopping amplitudes. For $J/U = 0.015$, the μ-scan crosses the first Mott lobe, where $\bar{n} = 1$ and both $\overline{\psi}$ and κ vanish. For larger μ, the system is well above the MI regions and both $\overline{\psi}$ and κ remain finite.

For $J/U = 0.003$, the system is very close to the atomic limit and all of the three lowest Mott lobes are crossed. As expected, the width of the Mott lobes is roughly $1 - W/U = 0.4$. Furthermore, for $\mu/U \lesssim 0.7$ we encounter the situation described above. Due to the numerical limitations we cannot distinguish between $\overline{\psi} = 0$ (MI) and $0 < \overline{\psi} \ll 1$ (no MI). In order to identify the MI region, we have to use the compressibility κ.

As the actual distribution function is not known for these cases, we use $P_\psi(\psi) \approx \delta(\psi)$ in order to perform the numerical calculations. This, of course, implies that the values obtained for $\bar{n}$ and κ will be the same as in the atomic limit.

Finally, we want to compare the phase boundary obtained via the stochastic MF formalism with the one predicted in section 3.2.3. As a reminder, the argument used there was that if the probability distribution P_ε allows for *locally compressible* sites, one will always find arbitrary large regions of compressible sites in the thermodynamic limit. If these regions are large enough that boundary effects can be neglected, they will be compressible on their own. This immediately makes the whole system compressible. This results in a shift of the upper and the lower boundary of each Mott lobe by $-W/U$ or $+W/U$, respectively, compared to the pure case, see also figure 3.6.

Figure 3.13 shows a comparison of this predicted phase boundary and the one actually obtained with the stochastic MF formalism for two disorder strengths. As can be seen, the deviations are quite large. While in the atomic limit the same phase boundaries are obtained by construction, the larger the hopping amplitude, the more the two boundaries differ. For $W/U = 0.8$, the calculated Mott lobes are nearly twice as large as the ones predicted.

As mentioned before when discussing the results for P_ψ, these deviations originate from the fact that the stochastic MF approach neglects correlations between MF parameters on different sites. Thus, one could not expect a match between the predicted and the calculated boundaries.

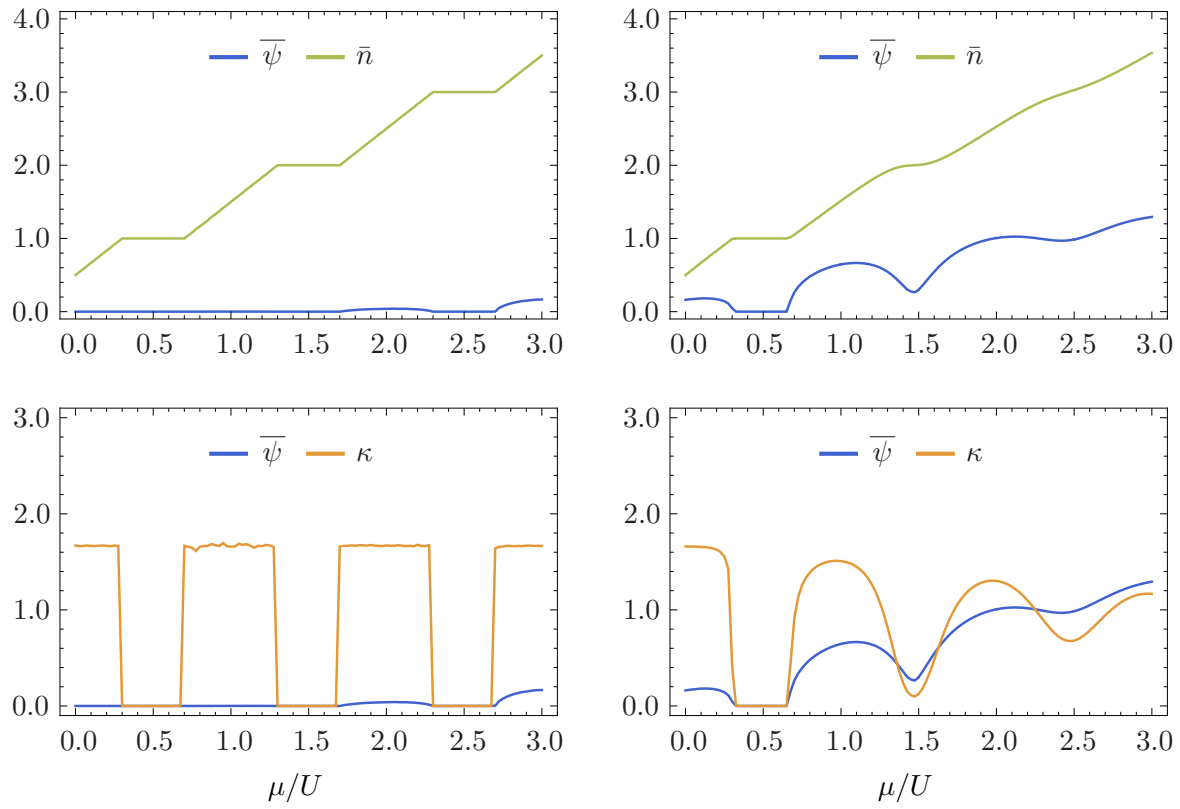

(a) $J/U = 0.003$ (b) $J/U = 0.015$

Figure 3.12: The upper plots show the disorder averaged local particle number and the lower plots the compressibility, each as a function of the chemical potential μ/U for fixed hopping amplitude $J/U = 0.012$ and disorder width $W/U = 0.6$. For comparison, also the average MF parameter $\overline{\psi}$ is plotted.

Still, the deviations are surprisingly large.

3.2.5 Conclusions

In this chapter we have presented a MF formalism (or decoupling approximation) that can be applied to both the pure and the disordered Bose-Hubbard model. It allows us to reduce the full problem of interacting bosons on a lattice to a set of local problems of coupled local particle number eigenstates. For the pure case, one was able to use the translational invariance to further reduce the problem to a single site . Depending on whether the MF parameter ψ was zero or finite, we identified the system to be either in the MI or the SF phase.

Introducing disorder broke the translational invariance and we had to apply one additional approximation, which was neglecting the correlations between MF parameters on different sites. In doing so, the problem again became local. However, instead of one single MF parameter ψ, we now had to determine the probability distribution function $P_\psi(\psi)$. Again, this function determined whether a system was in the MI phase or not. If the only solution we find is given by $P_\psi(\psi) = \delta(\psi)$, the system is incompressible. Only when in addition a non-trivial solution is

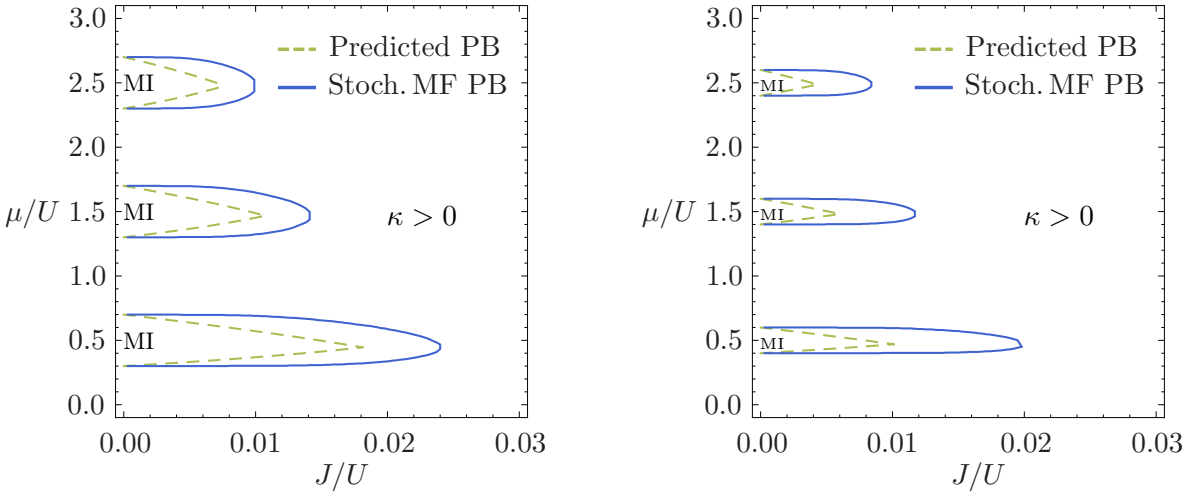

(a) $W/U = 0.6$ (b) $W/U = 0.8$

Figure 3.13: The boundary between compressible and incompressible phase for two disorder strengths. The dashed green curves show the phase boundary (PB) as predicted using the argument of the rare Lifshitz regions. The blue curves show the boundary obtained numerically with the stochastic MF formalism.

found, the system is not in the MI phase.

The interesting question now is how to determine the transition from the BG to the SF phase. In [28] by Bissbort and Hofstetter, it is proposed that one can identify this phase boundary by combining the results for $\overline{\psi}$ and κ obtained from the stochastic MF approach. The three different phases are defined as follows:

	$\overline{\psi} = 0$	$\overline{\psi} > 0$
$\kappa = 0$	MI	-
$\kappa > 0$	BG	SF

According to this definition, the two compressible phases are distinguished using the averaged MF parameter $\overline{\psi}$. This does not concur with our own findings. In appendix A.1, we have shown that a globally vanishing MF parameter implies that the system is incompressible. Thus, the combination $\overline{\psi} = 0$ and $\kappa > 0$ should not be possible.

Also in our numerical evaluation, we found no indication that the MF parameter can vanish within the compressible phase. On the contrary, we argued that while $\overline{\psi}$ can become very small, it will always stay finite due to the existence of what we called *locally compressible* sites.

Moreover, using this definition one finds a direct transition from the MI to the SF phase, which is contradictory to the theorem of inclusions.

Another work we have already mentioned is the one by Niederle and Rieger [39], where the MF formalism was applied to two-dimensional systems. By restricting themselves to finite system sizes and using finite size scaling, they were able to include correlations between the ψ_i on different sites. In order to resolve the MI to SF transition, they define MI and SF sites using

the local expectation value of the particle number,

$$\begin{array}{rcl} \langle \hat{n}_i \rangle \in [I-\gamma, I+\gamma] \text{ for one } I \in \mathbb{N} & \rightarrow & \text{MI site} \\ \text{else} & \rightarrow & \text{SF site} \end{array} \tag{3.69}$$

The parameter γ was chosen to be $\gamma \leq 5 \times 10^{-3}$ for numerical reasons. In other words, if the average particle number of a site is within a sharp interval of width 10^{-2} around an integer value, it is considered to be a MI site. Otherwise, it is a SF site. The system is in the MI or the SF phase, if all sites are either MI or SF sites. If the system consists of both MI and SF sites, it is in the BG phase.

This approach finds the correct shape of the Mott lobes, since it takes into account correlations between different sites. The Mott lobes and the SF region are separated by the BG phase according to their definition. There is no direct transition from MI to SF phase, which is in accordance with the theorem of inclusions.

Now, the problem with this definition is that it is not unambiguous. The parameter γ is chosen freely and does not follow from any physical considerations. Thus, the phase boundary they find depends on a free parameter. For $\gamma \to 0$ the BG phase will become arbitrarily small as the definition for the MI sites will include fewer and fewer sites. Thus, the phase boundary obtained this cannot be the actual phase boundary.

But how should one then determine the transition between the BG and the SF phase? We believe that it is not possible to answer this question within this MF theory. The driving mechanism of this transition should be the localizing effect of the disorder potential, i.e., the phenomenon of Anderson localization. The localizing effect is a consequence of coherent, non-local quantum interference processes. However, by introducing the decoupling approximation we exclude all coherent transport across the lattice. It is replaced by bosons tunneling into and out of a bath. Thus, by construction the effect of Anderson localization cannot be resolved within the local MF theory. Distinguishing between BG and SF phase on the ground of local quantities obtained by an approach that neglects the most important mechanism for this transition does not appear to be very reasonable.

Hence, one might think that the whole approach of treating the disorder Bose-Hubbard model within the stochastic MF theory is to some extent pointless. The effect of the disorder on the shape of the Mott lobes can be determined from the solution to the pure model without making any additional calculations, as we have discussed in section 3.2.3. Thus, no progress in finding either of the two phase boundaries was made.

What one does gain, however, is information about the local physics of the system. In principle, we can calculate the full local spectrum and all corresponding local quantities for any given site. All we need to do now is to find a way to put this information to good use.

What makes the disordered Bose-Hubbard model so difficult to treat is the fact that it combines two problems that are already rather complicated on their own: localization and interaction. This was the reason why we have introduced the MF approximation in the first place. As the transition to the MI phase is driven by the onsite interaction, it was only reasonable to treat the interaction exactly while approximating the kinetic term. In order to describe the transition from BG to SF phase, the transport properties of the system will play the pivotal role. Thus, the approximation we need to apply there should work just the other way around, that is, compromising on the local term in order to treat the kinetic term exactly. In order to find a good approximation for the local properties of the system, we will use the results from the stochastic MF routine.

In the next chapter, we will first introduce an appropriate quantity to determine the transition between BG and SF phase, which will be the superfluid current. Afterward, we will introduce an approximation that maps the full interacting model onto an effective non-interacting one. We will argue that a long-range superfluid current can only be finite when the effective model is not completely localized. Thus, the phase boundary from BG to SF will be determined by the transition of the effective model from the localized to the extended regime. In order to resolve this transition, we will make use of the already developed self-consistent theory of localization by Vollhardt and Woelfle [29, 61, 62] applied to the strongly disordered lattice problem [64–67].

CHAPTER 4

Transport Theory for the Disordered Bose-Hubbard Model

4.1 The Superfluid Current

In the following section, we want to derive a method to calculate the superfluid current, that is, a current not induced by an applied voltage, but a phase gradient, for the disordered Bose-Hubbard model. First, we will define a general expression for a non-local current density operator. Afterward, we will express the expectation value of the current in terms of the retarded and advanced Green's functions. Finally, we will introduce an approximation that reduces the interacting problem to an effective non-interacting one using the local solutions obtained by the stochastic MF theory.

4.1.1 The Current Density Operator

The current density is defined via the continuity equation, which is given by

$$\frac{\mathrm{d}}{\mathrm{d}t}\rho + \nabla \cdot \mathbf{j} = 0\,, \tag{4.1}$$

where ρ is the particle density and $\mathbf{j}$ the current density. The corresponding density operator on the lattice is defined as $\hat{\rho}(x_i) \equiv \hat{\rho}_i = \hat{b}_i^\dagger \hat{b}_i$. Here and in the following, all operators are assumed to be in the Heisenberg representation. Hence, the evolution in time of $\hat{\rho}$ is governed by the Heisenberg equation. Using the explicit form of the disordered Bose-Hubbard Hamiltonian, one obtains

$$\begin{aligned}
\frac{\mathrm{d}}{\mathrm{d}t}\hat{\rho}_k &= \mathrm{i}\big[\hat{H}, \hat{\rho}_k\big] \\
&= -\mathrm{i}J \sum_{\langle ij \rangle} \big[\hat{b}_i^\dagger \hat{b}_j, \hat{b}_k^\dagger \hat{b}_k\big] \\
&= -\mathrm{i}J \sum_{\langle ij \rangle} \Big(\hat{b}_i^\dagger \big[\hat{b}_j, \hat{b}_k^\dagger\big]\hat{b}_k + \hat{b}_k^\dagger \big[\hat{b}_i^\dagger, \hat{b}_k\big]\hat{b}_j\Big) = -\mathrm{i}J \sum_{i}^{\langle ik \rangle} \Big(\hat{b}_i^\dagger \hat{b}_k - \hat{b}_k^\dagger \hat{b}_i\Big)\,.
\end{aligned} \tag{4.2}$$

On the other hand, the divergence on a lattice is defined via the difference quotient,

$$\nabla \cdot \mathbf{j} = \sum_{\alpha=1}^{d} \frac{j_\alpha(\mathbf{x}_i + a\,\hat{\mathbf{e}}_\alpha) - j_\alpha(\mathbf{x}_i)}{\left(\mathbf{x}_i + a\,\hat{\mathbf{e}}_\alpha - \mathbf{x}_i\right)_\alpha}\,, \tag{4.3}$$

where the summation is taken over all spatial dimensions, a is the lattice spacing, and $\hat{\mathbf{e}}_\alpha$ is the unit vector in α-direction. Inserting the expressions (4.2) and (4.3) into equation (4.1) and setting $a = 1$ yields

$$\sum_{\alpha=1}^{d} \left(\mathbf{j}_{i+\alpha} - \mathbf{j}_i\right)_\alpha = \mathrm{i}J \sum_{j}^{\langle ij \rangle} \left(\hat{b}_j^\dagger \hat{b}_i - \hat{b}_i^\dagger \hat{b}_j\right) = \mathrm{i}J \sum_{\alpha=1}^{d} \left(\hat{b}_{i+\alpha}^\dagger \hat{b}_i - \hat{b}_i^\dagger \hat{b}_{i+\alpha} + \hat{b}_{i-\alpha}^\dagger \hat{b}_i - \hat{b}_i^\dagger \hat{b}_{i-\alpha}\right), \tag{4.4}$$

where we have introduced the shorthand notation $j = i \pm \alpha$ corresponding to $\mathbf{x}_j = \mathbf{x}_i \pm \hat{\mathbf{e}}_\alpha$ and in addition used that we only consider cubic lattices. The above equation is solved by

$$\left(\mathbf{j}_i\right)_\alpha = \mathrm{i}J\left(\hat{b}_i^\dagger \hat{b}_{i-\alpha} - \hat{b}_{i-\alpha}^\dagger \hat{b}_i\right) \tag{4.5}$$

Note, that this definition is not unique. Equally, we could have defined the difference quotient as

$$\nabla \cdot \mathbf{j} = \sum_{\alpha=1}^{d} \frac{j_\alpha(\mathbf{x}_i - a\,\hat{\mathbf{e}}_\alpha) - j_\alpha(\mathbf{x}_i)}{\left(\mathbf{x}_i - a\,\hat{\mathbf{e}}_\alpha - \mathbf{x}_i\right)_\alpha}\,, \tag{4.6}$$

which leads to the following expression for the current density operator,

$$\left(\mathbf{j}_i\right)_\alpha = \mathrm{i}J\left(\hat{b}_{i+\alpha}^\dagger \hat{b}_i - \hat{b}_i^\dagger \hat{b}_{i+\alpha}\right). \tag{4.7}$$

The reason for this is, of course, that on the discrete lattice we cannot take the limit $\alpha \to 0$. Hence, the current density operator has to be understood as being attached to the bond connecting two neighboring sites. This is also consistent with the continuity equation in discrete form (4.4), where the change of local particle density on a certain site is linked to the current densities on all bonds connected to the local site.

Whether one uses definition (4.5) or (4.7) is only a matter of convention, that is, how to label the bonds. Alternatively, one could immediately label the current density in terms of the two sites forming the bond,

$$\hat{\mathrm{j}}_{ij} = \mathrm{i}J\left(\hat{b}_i^\dagger \hat{b}_j - \hat{b}_j^\dagger \hat{b}_i\right). \tag{4.8}$$

The above definition has the advantage that it can be generalized from pairs of neighboring sites to sites spatially separated from each other. This is specifically interesting when we want to study the localizing effect of disorder to a system. As localization induced by disorder is a quantum interference effect, it is generically non-local, in contrast to the localization of particles forced by the Mott-Hubbard physics. In order to study the transition to the MI phase, it was justified to reduce the full lattice problem to a single-site problem. Here, however, we have to consider non-local quantities in order to find an appropriate description.

4.1.2 Expectation Value of the Current Density Operator

The expectation value of the non-local current density operator can be rewritten as follows,

$$\begin{aligned} J_{ij}(t) = \frac{1}{Z}\,\mathrm{Tr}\left\{e^{-\beta\hat{H}}\hat{\mathrm{j}}_{ij}(t)\right\} &\equiv \mathrm{i}J\Big[\langle\hat{b}_i^\dagger(t)\hat{b}_j(t)\rangle - \langle\hat{b}_j^\dagger(t)\hat{b}_i(t)\rangle\Big] \\ &= J\Big[G_{ij}^<(t,t) - G_{ji}^<(t,t)\Big] \\ &= J\Big[G_{ij}^<(t,t) + \big(G_{ij}^<(t,t)\big)^*\Big] \\ &= 2J\,\mathrm{Re}\left\{G_{ij}^<(t,t)\right\}, \end{aligned} \tag{4.9}$$

with $\beta = 1/(k_bT)$, k_B being the Boltzmann constant, and $Z = \mathrm{Tr}\left\{e^{-\beta\hat{H}}\right\}$ being the grand canonical partition function. Furthermore, we have introduced the *lesser* Green's function $G^<$. Since in the Heisenberg equation all operators are at equal times, also the operators in the definitions of the local current (4.5) and (4.7) have to be at equal times, as these definitions were derived from the Heisenberg equation. Now, when defining the non-local current density operator (4.8), one is in principle not bound to this restriction. Still, we are interested in exactly this case, that is, an instantaneous current, and thus, all operators are chosen to be at equal times.

In equilibrium, the expectation value of the current density operator is usually vanishing. In order to induce a normal current, the system has to be driven out of equilibrium, for example by switching on a voltage. However, as we will see in the following, it is possible to find an equilibrium state that is carrying a current by introducing a phase gradient.

Now, assuming the system is in equilibrium, the Green's functions only depend on the relative time $t - t'$ and we can perfom a Fourier transformation,

$$G_{ij}^<(E) = \int_{-\infty}^{+\infty} \mathrm{d}t\, e^{\mathrm{i}Et} G_{ij}^<(t,0) \tag{4.10}$$

and

$$G_{ij}^<(t,0) = \int_{-\infty}^{+\infty} \frac{\mathrm{d}E}{2\pi}\, e^{-\mathrm{i}Et} G_{ij}^<(E)\,. \tag{4.11}$$

With this, we can write the current density as an integral over all energies,

$$J_{ij} = 2J \int_{-\infty}^{+\infty} \frac{\mathrm{d}E}{2\pi}\, \mathrm{Re}\left\{G_{ij}^<(E)\right\}. \tag{4.12}$$

As shown in appendix B.1, the lesser function can be expressed in terms of the retarded and advanced Green's functions as follows,

$$G_{ij}^<(E) = b(E)\big(G_{ij}^A(E) - G_{ij}^R(E)\big)\,, \tag{4.13}$$

where $b(E) = 1/(e^{\beta E} - 1)$ is the Bose distribution function. Inserting this into equation (4.12) yields

$$J_{ij} = 2J \int_{-\infty}^{+\infty} \frac{\mathrm{d}E}{2\pi}\, b(E)\, \mathrm{Re}\left\{G_{ij}^A(E) - G_{ij}^R(E)\right\}. \tag{4.14}$$

The Green's functions can be transformed as follows,

$$\begin{aligned}
G_{ij}^{R/A}(E) &= \int_{-\infty}^{+\infty} \mathrm{d}t\, e^{\mathrm{i}(E\pm\mathrm{i}\eta)t} G_{ij}^{R/A}(t) \\
&= -\frac{\mathrm{i}}{Z}\int_0^{\pm\infty} \mathrm{d}t\, e^{\mathrm{i}(E\pm\mathrm{i}\eta)t}\, \mathrm{Tr}\left\{ e^{-\beta\hat{H}}\left[e^{\mathrm{i}\hat{H}t}\hat{b}_i e^{-\mathrm{i}\hat{H}t}, \hat{b}_j^\dagger\right]\right\} \\
&= -\frac{\mathrm{i}}{Z}\int_0^{\pm\infty} \mathrm{d}t\, e^{\mathrm{i}(E\pm\mathrm{i}\eta)t} \sum_{n,m}\Big[\langle\Psi_n|e^{-\beta\hat{H}} e^{\mathrm{i}\hat{H}t}\hat{b}_i e^{-\mathrm{i}\hat{H}t}|\Psi_m\rangle\langle\Psi_m|\hat{b}_j^\dagger|\Psi_n\rangle \\
&\qquad\qquad - \langle\Psi_m|e^{-\beta\hat{H}}\hat{b}_j^\dagger|\Psi_n\rangle\langle\Psi_n|e^{\mathrm{i}\hat{H}t}\hat{b}_i e^{-\mathrm{i}\hat{H}t}|\Psi_m\rangle\Big] \\
&= -\frac{\mathrm{i}}{Z}\int_0^{\pm\infty} \mathrm{d}t\, e^{\mathrm{i}(E\pm\mathrm{i}\eta)t} \sum_{n,m}\left(e^{-\beta E_n} - e^{-\beta E_m}\right) e^{\mathrm{i}(E_n-E_m)t}\langle\Psi_n|\hat{b}_i|\Psi_m\rangle\langle\Psi_m|\hat{b}_j^\dagger|\Psi_n\rangle \\
&= \frac{1}{Z}\sum_{n,m}\left(e^{-\beta E_n} - e^{-\beta E_m}\right)\frac{\langle\Psi_n|\hat{b}_i|\Psi_m\rangle\langle\Psi_m|\hat{b}_j^\dagger|\Psi_n\rangle}{E + E_n - E_m \pm \mathrm{i}\eta}\,, \qquad (4.15)
\end{aligned}$$

where the summation is taken over the eigenstates $|\Psi_n\rangle$ of $\hat{H}$ with corresponding eigenenergies E_n. For the difference between the retarded and the advanced Green's function, one obtains

$$\begin{aligned}
G_{ij}^{A}(E) - G_{ij}^{R}(E) &= \frac{1}{Z}\sum_{n,m}\left(e^{-\beta E_n} - e^{-\beta E_m}\right)\frac{2\mathrm{i}\eta\langle\Psi_n|\hat{b}_i|\Psi_m\rangle\langle\Psi_m|\hat{b}_j^\dagger|\Psi_n\rangle}{(E + E_n - E_m)^2 + \eta^2} \\
&= \frac{2\mathrm{i}\pi}{Z}\sum_{n,m}\left(e^{-\beta E_n} - e^{-\beta E_m}\right)\langle\Psi_n|\hat{b}_i|\Psi_m\rangle\langle\Psi_m|\hat{b}_j^\dagger|\Psi_n\rangle\delta(E + E_n - E_m)\,. \qquad (4.16)
\end{aligned}$$

In order for the real part of the above expression to be finite, the matrix elements

$$\langle\Psi_n|\hat{b}_i|\Psi_m\rangle\langle\Psi_m|\hat{b}_j^\dagger|\Psi_n\rangle \qquad (4.17)$$

have to be complex numbers. However, $\hat{H}$ is real and symmetric and thus, its eigenstates will also be real. Therefore, the matrix elements will be real numbers as well. Consequently, the current density should vanish.

Still, in section 2.1.5 we have found that by applying a gradient to the complex phase of the MF parameter of the boson field, a current can be induced if the system is a superfluid. The phase gradient can be realized by imposing complex boundary conditions to the system and we need to determine how this will affect the eigenstates and, thereby, the single-particle Green's functions $G_{ij}^{R/A}$.

Moreover, we need to find a way to actually calculate $G_{ij}^{R/A}$ in the limit $|\mathbf{x}_i - \mathbf{x}_j| \to \infty$, which is a very difficult task as we have to deal with both disorder and particle-particle interaction at the same time. To do so, inevitably we will have to introduce approximations. Inspired by a previous approach [25, 26] for the fermionic version of this model, we will try to find an effective non-interacting description for the full interacting problem. In the process, we will make use of the results obtained within the MF theory. This will allow us to make a connection to the MF parameter and, thereby, include its phase gradient to the effective non-interacting theory.

In the following, we will restrict ourselves to the limit $T \to 0$, where the Bose distribution

restricts the integration in expression (4.14) to negative energies,

$$J_{ij} = 2J \int_{-\infty}^{0} \frac{\mathrm{d}E}{2\pi} \, \mathrm{Re}\left\{ G_{ij}^{R}(E) - G_{ij}^{A}(E) \right\}, \tag{4.18}$$

4.2 Effective Non-Interacting Model

For the original Anderson Hamiltonian without interactions,

$$\hat{H}_A = \sum_i \varepsilon_i \hat{n}_i - J \sum_{\langle ij \rangle} \hat{b}_i^\dagger \hat{b}_j \,, \tag{4.19}$$

the full single-particle Green's function G_{ij} can be expanded in terms of the local Green's functions G_i as follows,

$$G_{ij}(E) = G_i^0(E)\delta_{ij} - G_i^0(E) J \sum_{l}^{\langle il \rangle} G_{lj}(E) \,, \tag{4.20}$$

with the locator functions

$$G_i^0(E) = \frac{1}{E - \varepsilon_i} \,. \tag{4.21}$$

and $E \in \mathbb{C}$. This expansion is known as the locator expansion, see appendix B.2 for a derivation and also section 2.2.1 for a discussion in the context of Anderson's original work [18]. Interpreting G_{ij} and $G_{ij}^0 = G_i^0 \delta_{ij}$ as the components of matrices G and G^0, respectively, equation (4.20) can also be written as a matrix equation,

$$G(E) = G^0(E) + G^0(E) H_J G(E) \,, \tag{4.22}$$

with $(H_J)_{ij} = -J$ for i, j nearest neighbors and $(H_J)_{ij} = 0$ otherwise. As we will see in the next section, for the Bose-Hubbard model such an expansion only in terms of single-particle Green's functions is not possible and higher Green's functions will appear due to the on-site interaction term. Finally, however, we want to reduce this much more complicated expansion to the *simple* locator expansion of the non-interacting case. Finding a way to do so will be the topic of the next sections.

4.2.1 Locator Expansion of the Interacting Green's Function

Let us start by deriving the equation of motion of the single-particle Green's function for the disordered Bose-Hubbard model,

$$\hat{H} = \sum_i \left((\varepsilon_i - \mu)\hat{n}_i + \frac{U}{2} \hat{n}_i (\hat{n}_i - 1) \right) - J \sum_{\langle ij \rangle} \hat{b}_i^\dagger \hat{b}_j \,. \tag{4.23}$$

This works completely analogously to the non-interacting case, see appendix B.2, and one obtains

$$\mathrm{i} \frac{\mathrm{d}}{\mathrm{d}t} G_{ij}^{R/A}(t) = \delta_{ij}\delta(t) + (\varepsilon_i - \mu)\, G_{ij}^{R/A}(t) - J \sum_{l}^{\langle il \rangle} G_{lj}^{R/A}(t) + U \Gamma_{ij}^{R/A}(t) \,, \tag{4.24}$$

where now $\Gamma_{ij}^{R/A}$ is a higher Green's function,

$$\Gamma_{ij}^{R/A}(t) = \mp\frac{\mathrm{i}}{2}\theta(\pm t)\langle\big[[\hat{n}_i(t)(\hat{n}_i(t)-1),\hat{b}_i(t)],\hat{b}_j^\dagger\big]\rangle = \mp\mathrm{i}\theta(\pm t)\langle[\hat{n}_i(t)\hat{b}_i(t),\hat{b}_j^\dagger]\rangle\,. \tag{4.25}$$

Again, we can perform a Fourier transformation for the equation of motion (4.24),

$$E\,G_{ij}(E) = \delta_{ij} + (\varepsilon_i-\mu)G_{ij}(E) - J\sum_l^{\langle il\rangle} G_{lj}(E) + U\Gamma_{ij}(E)\,, \tag{4.26}$$

with

$$G_{ij}(E\pm\mathrm{i}\eta) = G_{ij}^{R/A}(E) = \int \mathrm{d}t\, e^{\mathrm{i}(E\pm\mathrm{i}\eta)t} G_{ij}^{R/A}(t) \tag{4.27}$$

and

$$\Gamma_{ij}(E\pm\mathrm{i}\eta) = \Gamma_{ij}^{R/A}(E) = \int \mathrm{d}t\, e^{\mathrm{i}(E\pm\mathrm{i}\eta)t} \Gamma_{ij}^{R/A}(t)\,. \tag{4.28}$$

The problem with the equation of motion for the interacting Green's function is that it contains an additional unknown quantity in form of the higher Green's function. In principle, one would have to find Γ_{ij} first before trying to obtain G_{ij}. However, the equation of motion for Γ_{ij} contains even more complicated terms. Hence, this direct approach is not feasible and one has to introduce certain approximations. One way would be to define the self energy, $U\Gamma_{ij} = \sum_l \Sigma_{il}^U G_{lj}$, which can be expanded in a perturbation series. Still, here in addition one has to deal with the on-site disorder, which by itself poses a serious challenge.

In order to overcome this problem, we want to make use of the fact that we already solved the interacting problem locally within the MF approximation. Thus, we again introduce the decoupling approximation. This time, however, we will treat the term including the $\hat{\delta}$-operators as a perturbation to the *unperturbed* or *free* MF Hamiltonian. Let us start by dividing the full Bose-Hubbard Hamiltonian into the MF part and the δ-terms,

$$\hat{H} = \hat{H}^{MF} + \delta\hat{H}\,, \tag{4.29}$$

with

$$\hat{H}^{MF} = \sum_i \hat{h}_i\,, \tag{4.30}$$

where $\hat{h}_i$ is the local MF Hamiltonian for site i as defined in equations (3.27) and (3.28). Furthermore, the fluctuations term is given by

$$\delta\hat{H} = -J\sum_{\langle ij\rangle}\hat{\delta}_i^\dagger\hat{\delta}_j = -J\sum_{\langle ij\rangle}\big(\hat{b}_i^\dagger-\psi_i^*\big)\big(\hat{b}_j-\psi_j\big)\,. \tag{4.31}$$

Analogously to the non-interacting case, we can define the resolvent of $\hat{H}$ as

$$(E-\hat{H})\hat{G}(E) = 1\,. \tag{4.32}$$

and then evaluate the full resolvent in terms of the MF one,

$$\hat{G}(E) = \hat{G}^{MF}(E) + \hat{G}^{MF}(E)\,\delta\hat{H}\,\hat{G}(E)\,, \tag{4.33}$$

where $\hat{G}^{MF}(E) = (E - \hat{H}^{MF})^{-1}$. The above equation has the same structure as the locator expansion (4.22) in the previous section, but instead of matrices in position space, here its constituents are operators acting on the Hilbert space. The question now is how to relate the quantity $\hat{G}$ to the single-particle Green's function G_{ij} we are interested in. Therefore, we return to the spectral representation (4.15) of the Green's function,

$$G_{ij}(E \pm \mathrm{i}\eta) = G_{ij}^{R/A}(E) = \frac{1}{Z} \sum_{n,m} \left(e^{-\beta E_n} - e^{-\beta E_m} \right) \frac{\langle \Psi_n | \hat{b}_i | \Psi_m \rangle \langle \Psi_m | \hat{b}_j^\dagger | \Psi_n \rangle}{E + E_n - E_m \pm \mathrm{i}\eta} \,. \tag{4.34}$$

In the limit $T \to 0$, only the ground state $|\Psi_0\rangle$ contributes to the thermal average,

$$\frac{1}{Z} e^{-\beta E_n} \longrightarrow \delta_{n,0} \,, \tag{4.35}$$

and the expression for the Green's function simplifies as follows,

$$\begin{aligned} G_{ij}(E) &= \sum_n \left[\frac{\langle \Psi_0 | \hat{b}_i | \Psi_n \rangle \langle \Psi_n | \hat{b}_j^\dagger | \Psi_0 \rangle}{E + E_0 - E_n} - \frac{\langle \Psi_n | \hat{b}_i | \Psi_0 \rangle \langle \Psi_0 | \hat{b}_j^\dagger | \Psi_n \rangle}{E + E_n - E_0} \right] \\ &= \sum_n \left[\left\langle \Psi_0 \middle| \hat{b}_i \frac{1}{E + E_0 - \hat{H}} \middle| \Psi_n \right\rangle \langle \Psi_n | \hat{b}_j^\dagger | \Psi_0 \rangle - \left\langle \Psi_0 \middle| \hat{b}_j^\dagger \frac{1}{E + \hat{H} - E_0} \middle| \Psi_n \right\rangle \langle \Psi_n | \hat{b}_i | \Psi_0 \rangle \right] \\ &= \langle \Psi_0 | \hat{b}_i \hat{G}(E_0 + E) \hat{b}_j^\dagger | \Psi_0 \rangle + \langle \Psi_0 | \hat{b}_j^\dagger \hat{G}(E_0 - E) \hat{b}_i | \Psi_0 \rangle \,, \end{aligned} \tag{4.36}$$

where now $E \in \mathbb{C}$. The propagator $\hat{G}$ can then be expanded in terms of the MF locator $\hat{G}^{MF}$ using relation (4.33). In order to make $\hat{G}^{MF}$ an actual free, non-interacting Green's function, we will have to apply certain approximations. Therefore, in the next section we will investigate the structure of $\hat{G}^{MF}$ and $\delta\hat{H}$ within the MF eigenbasis.

4.2.2 The Eigenbasis of the Mean-Field Hamiltonian

In the following we want to derive an approximation for the propagator $\hat{G}$, such that it can be written as a matrix equation in position space analogously to equation (4.22) in the non-interacting case. Therefore, we turn back to equation (4.33), which by iteratively reinserting it into itself can be brought into the following form,

$$\hat{G}(E) = \sum_{l=0}^{\infty} \hat{G}^{(l)}(E) \,, \tag{4.37}$$

with

$$\hat{G}^{(l)}(E) = \underbrace{\hat{G}^{MF}(E)\, \delta\hat{H}\, \hat{G}^{MF}(E) \,\ldots\, \hat{G}^{MF}(E)\, \delta\hat{H}\, \hat{G}^{MF}(E)}_{l\text{-th order in } \delta\hat{H}} = \hat{G}^{MF}(E) \left[\delta\hat{H}\, \hat{G}^{MF}(E) \right]^l . \tag{4.38}$$

As mentioned before, splitting the full Hamiltonian into the MF Hamiltonian and the remaining part containing the δ-operators is motivated by the fact that, in principle, we have already found the solution to $\hat{H}^{MF}$. Since the MF Hamiltonian contains the full particle-particle interaction, this should prevent us from having to introduce higher Green's functions like the one in equation

(4.24). The obvious choice for representing the above operators is the eigenbasis of $\hat{H}^{MF}$. Before evaluating the full expression (4.38), we first want to examine the form of its constituents, $\hat{G}^{MF}$ and $\delta\hat{H}$, within this basis. For the local MF Green's function, we find that it becomes diagonal,

$$\langle\Phi_\alpha|\hat{G}^{MF}(E)|\Phi_\beta\rangle = \left\langle\Phi_\alpha\right| \frac{1}{E-\hat{H}^{MF}} \left|\Phi_\beta\right\rangle = \frac{\delta_{\alpha\beta}}{E-E_\alpha^{MF}}\,, \tag{4.39}$$

where $|\Phi_\alpha\rangle$ and $|\Phi_\beta\rangle$ are eigenstates of $\hat{H}^{MF}$ with corresponding eigenenergies E_α^{MF} and E_β^{MF}, respectively. Hence, it is justified to interpret $\hat{G}^{MF}$ as the analogon to the locator for the non-interacting Anderson Hamiltonian. The perturbation term $\delta\hat{H}$ is, of course, not diagonal in this basis. Still, we can make use of the fact that the MF eigenstates are product states of the local MF eigenstates,

$$\begin{aligned}\langle\Phi_\alpha|\delta\hat{H}|\Phi_\beta\rangle &= -J\sum_{\langle ij\rangle}\langle\Phi_\alpha|\hat{\delta}_i^\dagger\hat{\delta}_j|\Phi_\beta\rangle \\ &= -J\sum_{\langle ij\rangle}\left[\langle\varphi_{i,\alpha_i}|\hat{\delta}_i^\dagger|\varphi_{i,\beta_i}\rangle\langle\varphi_{j,\alpha_j}|\hat{\delta}_j|\varphi_{j,\beta_j}\rangle\prod_{k\neq i,j}\delta_{\alpha_k\beta_k}\right],\end{aligned} \tag{4.40}$$

where $|\Phi_\alpha\rangle = \prod_i|\varphi_{i,\alpha_i}\rangle$ and $|\Phi_\beta\rangle = \prod_i|\varphi_{i,\beta_i}\rangle$, with $|\varphi_{i,\alpha_i}\rangle$ and $|\varphi_{i,\beta_i}\rangle$ being eigenstates of the local MF Hamiltonian $\hat{h}_i$ with eigenenergies ϵ_{i,α_i} and ϵ_{i,β_i}, respectively,

$$\hat{h}_i|\varphi_{i,\alpha_i}\rangle = \epsilon_{i,\alpha_i}|\varphi_{i,\alpha_i}\rangle\,, \tag{4.41}$$

and $E_\alpha^{MF} = \sum_i\epsilon_{i,\alpha_i}$.

Note that we use a different notation for the eigenstates as in the previous chapter, where the MF formalism was introduced. This is due to the fact that now we have to take into account not only the ground states, but the excited states as well. For the total MF ground state, the notation is changed as $|GS\rangle \to |\Phi_0\rangle$, and for for the local ground states, we have $|G_i\rangle \to |\varphi_{i,0}\rangle$.

Moving on, for the matrix elements of the δ-operators one finds that

$$\langle\varphi_{i,\alpha_i}|\hat{\delta}_i|\varphi_{i,\beta_i}\rangle = \langle\varphi_{i,\alpha_i}|\hat{b}_i|\varphi_{i,\beta_i}\rangle - \psi_i\delta_{\alpha_i\beta_i} = \begin{cases} 0 & \text{for } \alpha_i=\beta_i=0, \\ \langle\varphi_{i,\alpha_i}|\hat{b}_i|\varphi_{i,\alpha_i}\rangle - \psi_i & \text{for } \alpha_i=\beta_i\neq 0, \\ \langle\varphi_{i,\alpha_i}|\hat{b}_i|\varphi_{i,\beta_i}\rangle & \text{for } \alpha_i\neq\beta_i. \end{cases} \tag{4.42}$$

First of all, this means that the δ-term cannot induce a transition from ground state to ground state. This is not surprising, as the MF approach was specifically designed this way.

Furthermore, we can conclude that the matrix element (4.40) is only non-vanishing for three distinct cases, the first of which being the one where $|\Phi_\alpha\rangle = |\Phi_\beta\rangle$, with at least two neighboring sites i and j not in their local MF ground states, $\alpha_i \neq 0$ and $\alpha_j \neq 0$. This contribution is an energy correction, which accounts for the fact that the bath amplitude for a certain site is changed when one (or more) of its neighboring sites is not in the MF ground state.

The second case is non-diagonal and takes place when $\alpha_k = \beta_k$ for all $k \neq i$ and at least one nearest neighbor j of i is not in the MF ground state, $\alpha_j \neq 0$. Then, $\delta\hat{H}$ can induce transitions between all local MF eigenstates $|\varphi_{i,\alpha_i}\rangle$ of site i. Again, the intuitive picture here is that the particle bath surrounding site i is in an *excited* state, thus perturbing the states that were obtained with respect to the ground state bath amplitude.

Finally, $\delta\hat{H}$ can induce a simultaneous transition on two neighboring sites i and j, $\alpha_i \neq \beta_i$ and $\alpha_j \neq \beta_j$, with the rest of the lattice remaining in the initial state, $\alpha_k = \beta_k$ for $k \neq i, j$. Combining all cases, we can write

$$\langle\Phi_\alpha|\delta\hat{H}|\Phi_\beta\rangle = \begin{cases} -J\sum_{\langle ij\rangle}\langle\varphi_{i,\alpha_i}|\hat{\delta}_i^\dagger|\varphi_{i,\alpha_i}\rangle\langle\varphi_{j,\alpha_j}|\hat{\delta}_j|\varphi_{j,\alpha_j}\rangle & \text{if } \alpha_i = \beta_i \text{ for all } i, \\ -J\Big[\langle\varphi_{i,\alpha_i}|\hat{b}_i^\dagger|\varphi_{i,\beta_i}\rangle\sum_j^{\langle ij\rangle}\langle\varphi_{j,\alpha_j}|\hat{\delta}_j|\varphi_{j,\alpha_j}\rangle & \text{if } \alpha_i \neq \beta_i \\ \quad + \langle\varphi_{i,\alpha_i}|\hat{b}_i|\varphi_{i,\beta_i}\rangle\sum_j^{\langle ij\rangle}\langle\varphi_{j,\alpha_j}|\hat{\delta}_j^\dagger|\varphi_{j,\alpha_j}\rangle\Big] & \text{and } \alpha_k = \beta_k \text{ for } k \neq i, j \\ -J\Big[\langle\varphi_{i,\alpha_i}|\hat{b}_i^\dagger|\varphi_{i,\beta_i}\rangle\langle\varphi_{j,\alpha_j}|\hat{b}_j|\varphi_{j,\beta_j}\rangle & \text{if } \alpha_i \neq \beta_i,\ \alpha_j \neq \beta_j, \\ \quad + \langle\varphi_{i,\alpha_i}|\hat{b}_i|\varphi_{i,\beta_i}\rangle\langle\varphi_{j,\alpha_j}|\hat{b}_j^\dagger|\varphi_{j,\beta_j}\rangle\Big] & \text{and } \alpha_k = \beta_k \text{ for } k \neq i, j, \\ 0 & \text{else.} \end{cases} \tag{4.43}$$

In order to get a better overview of all the possible transitions, it is useful to consider $\delta\hat{H}$ for a two-site cluster. For simplicity, we will use the following notation for the MF eigenstates, $|\Phi_\alpha\rangle = |\varphi_{1,\alpha_1}\varphi_{2,\alpha_2}\rangle \equiv |\alpha_1\alpha_2\rangle$. Doing so, we obtain

$$\delta\hat{H} = \sum_{\alpha_1,\alpha_2,\beta_1,\beta_2=0}^{\infty} |\alpha_1\alpha_2\rangle\langle\alpha_1\alpha_2|\delta\hat{H}|\beta_1\beta_2\rangle\langle\beta_1\beta_2|$$

$$= \begin{array}{c} \\ |00\rangle \\ |10\rangle \\ |01\rangle \\ |11\rangle \\ |20\rangle \\ |02\rangle \\ |12\rangle \\ |21\rangle \\ |22\rangle \\ \vdots \end{array} \begin{array}{c} \begin{array}{cccccccccc} \langle 00| & \langle 10| & \langle 01| & \langle 11| & \langle 20| & \langle 02| & \langle 12| & \langle 21| & \langle 22| & \dots \end{array} \\ \begin{pmatrix} 0 & 0 & 0 & T_{00;11} & 0 & 0 & T_{00;12} & T_{00;21} & T_{00;22} & \dots \\ 0 & 0 & T_{10;01} & T_{10;11} & 0 & T_{10;02} & T_{10;12} & T_{10;21} & T_{10;22} & \\ 0 & T_{01;10} & 0 & T_{01;11} & T_{01;20} & 0 & T_{01;12} & T_{01;21} & T_{01;22} & \\ T_{11;00} & T_{11;10} & T_{11;01} & \delta E_{11} & T_{11;20} & T_{11;02} & T_{11;12} & T_{11;21} & T_{11;22} & \\ 0 & 0 & T_{20;01} & T_{20;11} & 0 & T_{20;02} & T_{20;12} & T_{20;21} & T_{20;22} & \\ 0 & T_{02;10} & 0 & T_{02;11} & T_{02;20} & 0 & T_{02;12} & T_{02;21} & T_{02;22} & \\ T_{12;00} & T_{12;10} & T_{12;01} & T_{12;11} & T_{12;20} & T_{12;02} & \delta E_{12} & T_{12;21} & T_{12;22} & \\ T_{21;00} & T_{21;10} & T_{21;01} & T_{21;11} & T_{21;20} & T_{21;02} & T_{21;12} & \delta E_{21} & T_{21;22} & \\ T_{22;00} & T_{22;10} & T_{22;01} & T_{22;11} & T_{22;20} & T_{22;02} & T_{22;12} & T_{22;21} & \delta E_{22} & \\ \vdots & & & & & & & & & \ddots \end{pmatrix} \end{array} \tag{4.44}$$

In order to avoid the long expressions of (4.43), we have used the shorthand notation $\delta E_{\alpha_1\alpha_2} = \langle\alpha_1\alpha_2|\delta\hat{H}|\alpha_1\alpha_2\rangle$ and $T_{\alpha_1\alpha_2;\beta_1\beta_2} = \langle\alpha_1\alpha_2|\delta\hat{H}|\beta_1\beta_2\rangle$. The ket- and bra-vectors to the left of and above the matrix are shown to help identifying the rows and columns.

First of all, since all transitions due to the perturbation $\delta\hat{H}$ have at most two neighboring sites involved, the above matrix includes all possible types of processes induced by $\delta\hat{H}$. Second, we see that there are no direct transitions from the MF ground state $|00\rangle$ to the sector with only one excited state, for example, $T_{00;01} = 0$ and $T_{00;20} = 0$. Such a transition can only happen as a second (or higher) order process, where the system goes, for example, first from $|00\rangle$ to $|11\rangle$ and then to $|01\rangle$. If exciting two states is energetically unfavorable, the *single-excitation sector* can be considered to be relatively stable.

Third, within the single-excitation sector the only process that can take place is the *tunneling* of the excitation from its current to a neighboring site, corresponding to the transition amplitude $T_{\alpha_1 0;0\beta_2} \neq 0$. On-site transitions to different excited states are not possible, $T_{\alpha_1 0;\beta_1 0} = 0$.

Finally, once two or more neighboring sites are in excited states, transitions to all other states can take place. From this we can take that the case of one single excitation is a special one, as it is protected from directly decaying to the ground state, which can be interpreted as a kind of *conservation* of the excitations. Furthermore, the perturbation term can induce nearest neighbor hopping processes, much like in the case of the original bosons, also conserving the number of excitations. Exciting more than one site comes with additional costs in energy, which, depending on the actual situation, might suppress these kinds of events, and thus, again force the number of excitations to be conserved

With the above findings and considerations, one might be intrigued to treat the single excitation as an effective particle. In order to do so, we have to make a couple of approximations, which will be discussed in the next section, where we investigate the structure of the expansion series of $\hat{G}$ in terms of the MF locator within the MF eigenbasis.

4.2.3 Representing the Propagator Using the Mean-Field Eigenbasis

With the results of the previous section, we can now turn to the expansion of $\hat{G}$, where we have to evaluate expressions of the form

$$\begin{aligned}\langle\Phi_\alpha|\hat{G}^{(l)}|\Phi_\beta\rangle = \sum_{\mu\ldots\nu} &\langle\Phi_\alpha|\hat{G}^{MF}|\Phi_\alpha\rangle\langle\Phi_\alpha|\delta\hat{H}|\Phi_\mu\rangle\langle\Phi_\mu|\hat{G}^{MF}|\Phi_\mu\rangle\ldots \\ &\ldots\langle\Phi_\nu|\hat{G}^{MF}|\Phi_\nu\rangle\langle\Phi_\nu|\delta\hat{H}|\Phi_\beta\rangle\langle\Phi_\beta|\hat{G}^{MF}|\Phi_\beta\rangle \\ \equiv \sum_{\mu\ldots\nu} &G^{MF}_\alpha T_{\alpha\mu} G^{MF}_\mu \ldots G^{MF}_\nu T_{\nu\beta} G^{MF}_\beta \,. \end{aligned} \tag{4.45}$$

Each summation is taken over the complete MF eigenbasis. However, due to the restrictions on the possible transitions induced by $\delta\hat{H}$, only certain states can be connected by the perturbation term. In the above case, for example, the states $|\Phi_\alpha\rangle$ and $|\Phi_\mu\rangle$ (or $|\Phi_\beta\rangle$ and $|\Phi_\nu\rangle$) have to be equal on all but two neighboring sites. Otherwise, the transition amplitude $T_{\alpha\mu}$ (or $T_{\nu\beta}$) would vanish.

Still, the summation is far from the case of the original locator expansion (4.22), where only sequences of neighboring sites are contributing. But we can put further restrictions on it by considering the expression for the single-particle Green's function,

$$G_{ij}(E) = \langle\Psi_0|\hat{b}_i\hat{G}(E_0+E)\hat{b}_j^\dagger|\Psi_0\rangle + \langle\Psi_0|\hat{b}_j^\dagger\hat{G}(E_0-E)\hat{b}_i|\Psi_0\rangle \tag{4.46}$$

Note, that $|\Psi_0\rangle$ is the ground state with respect to the full Hamiltonian $\hat{H}$, which in general is an unknown quantity. Still, in order to evaluate the above expression as planned, we need to know the expansion of $|\Psi_0\rangle$ with one particle added or removed at a certain site i in terms of the MF eigenstates. To overcome this problem, we have to introduce an approximation,

$$G_{ij}(E) \approx \langle\Phi_0|\hat{b}_i\hat{G}(E_0^{MF}+E)\hat{b}_j^\dagger|\Phi_0\rangle + \langle\Phi_0|\hat{b}_j^\dagger\hat{G}\big(E_0^{MF}-E\big)\hat{b}_i|\Phi_0\rangle\,, \tag{4.47}$$

where the unknown exact ground state $|\Psi_0\rangle$ and its energy E_0 have been replaced by the known

MF ground state $|\Phi_0\rangle$ and the MF ground state energy E_0^{MF}.

Note that this approximation is different from the method of adiabatically switching on and off the perturbation term used in standard perturbation theory. As the MF approximation breaks a symmetry of the original Hamiltonian, that is, particle conservation, the ground states of $\hat{H}$ and $\hat{H}^{MF}$ will be fundamentally different. Thus, one cannot expect the Gell-Mann-Low theorem to be valid in this case.

The motivation to still approximate the exact ground state by the MF one is that we believe the MF theory to capture the local physics quite well. In the following, we will show that it is possible to write down the non-local single-particle Green's function in terms of only local quantities. This approximation then assumes that the local physics of the system are well described by the MF ground state and that changes induced by local operators, such as, $\hat{b}_i$ and $\hat{b}_i^\dagger$, are well resolved by transitions of the local MF eigenstates.

The ground state with one particle added or removed can then be expanded as follows,

$$\hat{b}_i|\Psi_0\rangle \approx \hat{b}_i|\Phi_0\rangle = \sum_\alpha \langle\Phi_\alpha|\hat{b}_i|\Phi_0\rangle\,|\Phi_\alpha\rangle \tag{4.48a}$$

and

$$\hat{b}_i^\dagger|\Psi_0\rangle \approx \hat{b}_i^\dagger|\Phi_0\rangle = \sum_\alpha \langle\Phi_\alpha|\hat{b}_i^\dagger|\Phi_0\rangle\,|\Phi_\alpha\rangle\,, \tag{4.48b}$$

where, in principle, each expansion can be evaluated using the results from the previous chapter. The first thing we note is that, apart from the MF ground state $|\Phi_0\rangle$, only states from the single-excitation sector contribute within this approximation, to be specific, states that have a local excitation on site i,

$$\langle\Phi_\alpha|\hat{b}_i^{(\dagger)}|\Phi_0\rangle = \langle\varphi_{i,\alpha_i}|\hat{b}_i^{(\dagger)}|\varphi_{i,0}\rangle \prod_{k\neq i}\delta_{\alpha_k,0} \tag{4.49}$$

Thus, the summation over the complete MF eigenbasis reduces to a summation over all local MF states on site i,

$$\hat{b}_i|\Psi_0\rangle \approx \sum_{\alpha_i}\langle\varphi_{i,\alpha_i}|\hat{b}_i|\varphi_{i,0}\rangle\,|\varphi_{1,0}\varphi_{2,0}\dots\varphi_{i,\alpha_i}\dots\varphi_{N_i,0}\rangle \equiv \sum_{\alpha_i}\langle\alpha_i|\hat{b}_i|0\rangle\,|\alpha_i\rangle \tag{4.50a}$$

and

$$\hat{b}_i^\dagger|\Psi_0\rangle \approx \sum_{\alpha_i}\langle\varphi_{i,\alpha_i}|\hat{b}_i^\dagger|\varphi_{i,0}\rangle\,|\varphi_{1,0}\varphi_{2,0}\dots\varphi_{i,\alpha_i}\dots\varphi_{N_i,0}\rangle \equiv \sum_{\alpha_i}\langle\alpha_i|\hat{b}_i^\dagger|0\rangle\,|\alpha_i\rangle\,. \tag{4.50b}$$

Here, we have introduced a shortened notation for the states of the single-excitation sector, where it is implied that all sites but site i are in the ground state. Furthermore, since for the exact ground state we have $\langle\Psi_0|\hat{b}_i|\Psi_0\rangle = 0$ due to particle conservation, we assume the MF ground state not to contribute in this expansion, although $\langle\Phi_0|\hat{b}_i|\Phi_0\rangle = \psi_i \neq 0$ outside the MI phase. Thus, in the following all summations taken over the local eigenstates exclude the ground state, $\alpha_i = 0$.

With this, the two terms in (4.47) can be written as

$$\langle\Phi_0|\hat{b}_i\hat{G}(E_0+E)\hat{b}_j^\dagger|\Phi_0\rangle \approx \sum_{\alpha_i\beta_j}\langle 0|\hat{b}_i|\alpha_i\rangle\langle\alpha_i|\hat{G}\big(E_0^{MF}+E\big)|\beta_j\rangle\langle\beta_j|\hat{b}_j^\dagger|0\rangle \tag{4.51a}$$

and

$$\langle\Phi_0|\hat{b}_j^\dagger \hat{G}(E_0 - E)\hat{b}_i|\Phi_0\rangle \approx \sum_{\alpha_j\beta_i}\langle 0|\hat{b}_j^\dagger|\alpha_j\rangle\langle\alpha_j|\hat{G}\big(E_0^{MF} - E\big)|\beta_i\rangle\langle\beta_i|\hat{b}_i|0\rangle\,. \tag{4.51b}$$

Going back to the expansion of $\hat{G}$ given in equation (4.45), we can simplify the expression as follows using the above results,

$$\langle\alpha_i|\hat{G}^{(l)}|\beta_j\rangle = \sum_{\mu\ldots\nu} G^{MF}_{\alpha_i} T_{\alpha_i\mu}\, G^{MF}_{\mu} \ldots G^{MF}_{\nu} T_{\nu\beta_j}\, G^{MF}_{\beta_j}\,, \tag{4.52}$$

where now the outer states $|\alpha_i\rangle$ and $|\beta_j\rangle$ are from the single-excitation sector, the summations, however, are still taken over the complete MF eigenbasis. In order to put a restriction on these summations, let us take a closer look at the first three terms,

$$\begin{aligned} G^{MF}_{\alpha_i}\big(E_0^{MF} \pm E\big) T_{\alpha_i\mu} G^{MF}_{\mu}\big(E_0^{MF} \pm E\big) &= \frac{1}{E_0^{MF} \pm E - E^{MF}_{\alpha_i}}\, T_{\alpha_i\mu}\, \frac{1}{E_0^{MF} \pm E - E^{MF}_{\mu}} \\ &= \frac{1}{\pm E - \Delta E^{MF}_{\alpha_i}} \langle\alpha_i|\delta\hat{H}|\Phi_\mu\rangle \frac{1}{\pm E - \Delta E^{MF}_{\mu}}\,, \end{aligned} \tag{4.53}$$

where we have defined the excitation energy

$$\Delta E^{MF}_{\mu} = E^{MF}_{\mu} - E^{MF}_{0} = \sum_i \big(\epsilon_{i,\mu_i} - \epsilon_{i,0}\big)\,, \tag{4.54}$$

with ϵ_{i,μ_i} being the eigenenergy of the eigenstate $|\varphi_{i,\mu_i}\rangle$ of the local Hamiltonian $\hat{h}_i$. For a state with only one single excitation on site i, this is a local quantity,

$$\Delta E^{MF}_{\mu} = \epsilon_{i,\mu_i} - \epsilon_{i,0} \equiv \Delta\epsilon_{\mu_i} \quad \text{if} \quad \mu_k = 0 \text{ for } k \neq i. \tag{4.55}$$

Again, we use a shortened notation where it is implied that $\Delta\epsilon_{\mu_i}$ is the excitation energy of state $|\mu_i\rangle$. With this, equation (4.53) can be written as

$$G^{MF}_{\alpha_i}\big(E_0^{MF} \pm E\big)\, T_{\alpha_i\mu}\, G^{MF}_{\mu}\big(E_0^{MF} \pm E\big) = \frac{1}{\pm E - \Delta\epsilon_{\alpha_i}} \langle\alpha_i|\delta\hat{H}|\Phi_\mu\rangle \frac{1}{\pm E - \Delta E^{MF}_{\mu}}\,. \tag{4.56}$$

The perturbation $\delta\hat{H}$ can now couple the state $|\alpha_i\rangle$ to several states $|\Phi_\mu\rangle$. With the considerations made in the previous section, we can conclude that $|\Phi_\mu\rangle$ is either a single-, two-, or three-excitations state,

$$|\Phi_\mu\rangle = \begin{cases} |\mu_j\rangle & \text{with } j \text{ being a nearest neighbor of } i, \\ |\mu_i\mu_j\rangle & \text{with } j \text{ being a nearest neighbor of } i, \\ |\alpha_i\mu_j\mu_k\rangle & \text{with } j \text{ and } k \text{ being nearest neighbors and } \mu_i \overset{!}{=} \alpha_i, \end{cases} \tag{4.57}$$

where for $|\mu_i\mu_j\rangle$ and $|\alpha_i\mu_j\mu_k\rangle$ all sites but i, j and i, j, k are in the ground state, analogously to the definition of the single-excitation states $|\alpha_i\rangle$. Since the single-excitation sector does not couple directly to the ground state, $|\Phi_\mu\rangle = |\Phi_0\rangle$ is not possible.

In order to reduce the number of possible states $|\Phi_\mu\rangle$, we will now make some drastic approximations, where we will only consider those states that lead to the highest contribution to the total sum in (4.52). That means that we will choose states based on their excitation

energy, which needs to be close to $\pm E$, and their coupling amplitude, which should be as large as possible.

Now, let us assume that the state $|\alpha_i\rangle$ was chosen because it met these criteria. Then, we can assume that $\Delta\epsilon_{\alpha_i}$ is close to $\pm E$. In order to go from the single- to the three-excitations sector, we need to add two more excitations, which comes at the cost of two additional local excitation energies, $\Delta E_\mu^{MF} = \Delta\epsilon_{\alpha_i} + \Delta\epsilon_{\mu_j} + \Delta\epsilon_{\mu_k}$. Thus, transitions to states with three excitations will be suppressed.

The same argument can be made for transitions to states with two excitations, but only if site i remains in its initial state, $\mu_i = \alpha_i$. Otherwise, it would be possible for site i to go into a state with lower energy, which would then make up for the cost of exciting the neighboring site j, $\Delta\epsilon_{\alpha_i} \approx \Delta\epsilon_{\mu_i} + \Delta\epsilon_{\mu_j}$. However, as we will see later the important energy regime will be the one where $|\alpha_i\rangle$ is a low-lying excitation. Thus, we will also neglect transitions to the two-excitations sector.

Finally, we are left with only one type of transition, namely that of an excitation *hopping* from one site to a neighboring site. With $|\Phi_\mu\rangle = |\mu_j\rangle$, expression (4.56) takes the following form,

$$G_{\alpha_i}^{MF}\big(E_0^{MF} \pm E\big)\, T_{\alpha_i\mu_j}\, G_{\mu_j}^{MF}\big(E_0^{MF} \pm E\big) = \frac{1}{\pm E - \Delta\epsilon_{\alpha_i}} \langle\alpha_i|\delta\hat{H}|\mu_j\rangle \frac{1}{\pm E - \Delta\epsilon_{\mu_j}}\,. \tag{4.58}$$

Of course, the same arguments can be applied to all subsequent transitions, and we can write the l-th order of the propagator, given in equation (4.52), as a sum over all possible sequences of hopping processes from site j to site i,

$$\langle\alpha_i|\hat{G}^{(l)}|\beta_j\rangle = G_{\alpha_i}^{MF} \sum_{\mu_m}^{\langle im\rangle} T_{\alpha_i\mu_m}\, G_{\mu_m}^{MF} \sum_{\nu_n}^{\langle mn\rangle} T_{\mu_m\nu_n}\, G_{\nu_n}^{MF} \ldots G_{\rho_r}^{MF} \sum_{\sigma_s}^{\langle rsj\rangle} T_{\rho_r\sigma_s}\, G_{\sigma_s}^{MF} T_{\sigma_s\beta_j}\, G_{\beta_j}^{MF}\,, \tag{4.59}$$

where we have introduced the shortened notation for a sequence of three nearest neighbors, $\langle rsj\rangle \hat{=} \langle rs\rangle \& \langle sj\rangle$. The summation is taken over all sets of $l-1$ sites $(m, n, \ldots, r, s)$ connecting initial and final site j and i, and for each site m over all local MF excitations μ_m.

This already looks very much like the locator expansion. However, there are still different excited states available on every site. In some instances, the first and the second excited state will be close in energy. In order to choose one state over the other in these cases, we have to take into account an additional factor, which is the coupling strength. The problem now is that the transition amplitude $T_{\mu_i\nu_j}$ depends on two sites, which implies that we cannot choose the right state for site i without taking into account all its neighboring sites. Thus, before selecting the state for site i, we would need to know which states to select on its neighboring sites. This, however, will again depend on the state we would select on site i as well as on all other neighboring sites. Hence, finding the optimal states that lead to the largest coupling immediately becomes a lattice problem.

Fortunately, the nature of the local MF eigenstates will point to one obvious truncation scheme for the state space, which will make these considerations unnecessary. Therefore, in the next section we will examine the local spectrum of the MF model.

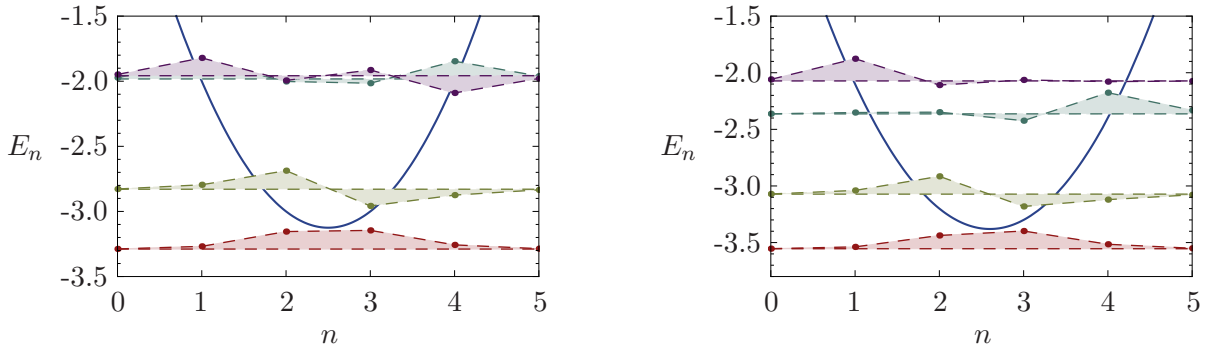

(a) $\mu/U = 2.0$

(b) $\mu/U = 2.1$

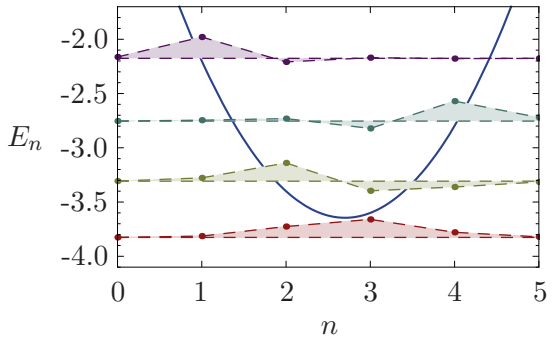

(c) $\mu/U = 2.2$

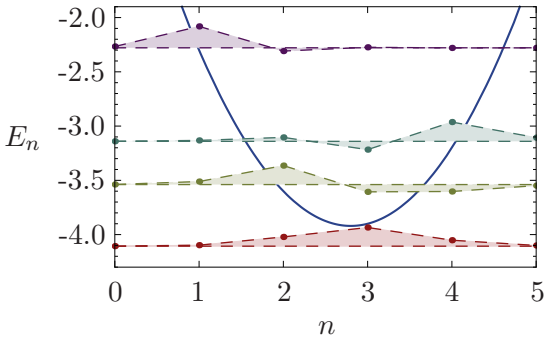

(d) $\mu/U = 2.3$

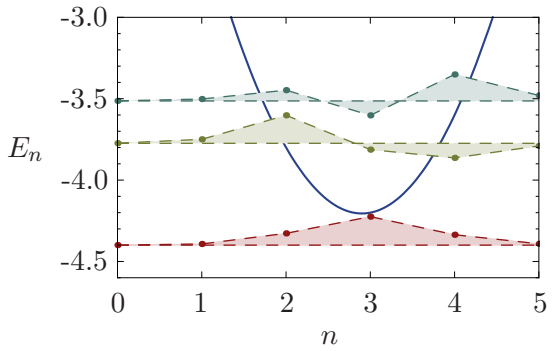

(e) $\mu/U = 2.4$

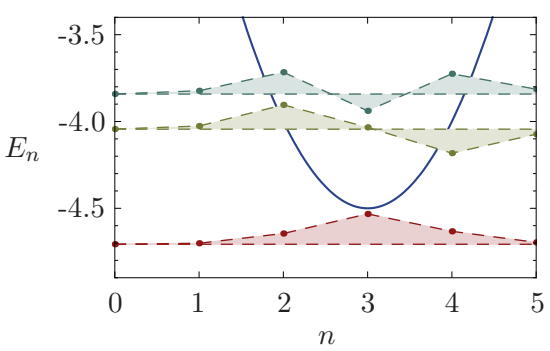

(f) $\mu/U = 2.5$

Figure 4.1: The solid blue curves show the local potential E_n as a function of the local particle number n for different values of μ and $W/U = 0$. The dashed curves show the four lowest MF eigenstates for $J/U = 0.02$, scaled by a factor of 0.2. For each state, its eigenenergy is used as an offset in y-direction (in figure 4.1e and 4.1f, the third excited state is not shown).

4.2.4 Local Spectrum and Transition Amplitudes

In order to investigate the local spectrum, we expand the eigenstates $|\nu_i\rangle$ of the Hamiltonian $\hat{h}_i$ in terms of the local particle number eigenstates $|n_i\rangle$,

$$|\nu_i\rangle = \sum_{n_i=0}^{\infty} \langle n_i|\nu_i\rangle\, |n_i\rangle\,, \tag{4.60}$$

just like it was done for the ground state in chapter 3. In figure 4.1, the low-lying spectrum of $\hat{h}_i$ is plotted for different values of μ. For simplicity, the disorder is set to zero, $W/U = 0$, and the hopping amplitude is fixed to $J/U = 0.02$, such that the system is not in the MI phase. Also, the index i for the specific site has been dropped for readability.

As a reminder, the local potential is given by $E_n = -\mu n + U/2\,(n-1)n$ (with ε_0 set to zero) and its minimum is located at $n_0 = \mu/U + 1/2$. The properties of the ground state were already discussed in section 3.1.1.

Figure 4.1a shows the special case where the minimum of E_n is located at a half integer, $n_0 = 2.5$, just in between two integer particle numbers. Therefore, certain Fock states are degenerated in energy, $E_{n_+} = E_{n_-}$ for $n_\pm = n_0 \pm (n + 1/2)$. As a consequence, the lowest two eigenstates are both centered around $n_0 - 1/2 = 3$ and $n_0 + 1/2 = 4$, and the next two at $n_0 - 3/2 = 2$ and $n_0 + 3/2 = 5$.

A similar situation is found for $\mu/U = 2.5$, see figure 4.1f, where the minimum is located at an integer, n_0, and we have $E_{n_+} = E_{n_-}$ for $n_\pm = n_0 \pm n$. While the ground state is peaked at $n_0 = 3$, the largest contributions to the first and the second excited state stem from the particle numbers $n_0 - 1 = 2$ and $n_0 + 1 = 4$.

For the intermediate cases, see figure 4.1b - 4.1e, this degeneracy is broken, $E_n \neq E_{n'}$ for $n \neq n'$, and the excited states are all more or less strongly peaked at a certain particle number.

Now, let us turn to the corresponding transition amplitudes coupling the excitations on neighboring sites, for which some general properties were already discussed in section 4.2.2. In accordance to equation (4.42), for a transition of the excitation $|\mu_j\rangle$ on site j to $|\nu_i\rangle$ on site i, we have

$$\begin{aligned} T_{\nu_i\mu_j} &= \langle\nu_i|\delta\hat{H}|\mu_j\rangle \\ &= -J\langle\nu_i|\big(\hat{b}_i^\dagger\hat{b}_j + \hat{b}_j^\dagger\hat{b}_i\big)|\mu_j\rangle \\ &= -J\Big(\langle\nu_i|\hat{b}_i^\dagger|0\rangle\langle 0|\hat{b}_j|\mu_j\rangle + \langle\nu_i|\hat{b}_i|0\rangle\langle 0|\hat{b}_j^\dagger|\mu_j\rangle\Big) \\ &\equiv -J\big(\psi_{\nu_i 0}\psi^*_{\mu_j 0} + \psi^*_{0\nu_i}\psi_{0\mu_j}\big)\,, \end{aligned} \tag{4.61}$$

where in the last step we have defined the *transition parameters* $\psi_{\alpha_i\beta_i} = \langle\alpha_i|\hat{b}_i|\beta_i\rangle$ in analogy to the MF parameter ψ_i, which would correspond to $|\alpha_i\rangle = |\beta_i\rangle = |0\rangle$. They are calculated using the expansion (4.60) for the eigenstates,

$$\begin{aligned} \psi_{\alpha_i\beta_i} &= \sum_{n_i m_i=0}^{\infty} \langle\alpha_i|n_i\rangle\langle n_i|\hat{b}_i|m_i\rangle\langle m_i|\beta_i\rangle \\ &= \sum_{n_i=0}^{\infty} \sqrt{n_i+1}\;\langle\alpha_i|n_i\rangle\;\langle n_i+1|\beta_i\rangle\,. \end{aligned} \tag{4.62}$$

$\mu/U = 2.0$

ν_i	1	2	3	4	5	6	7
$\psi_{0\nu_i}$	-0.973	0.812	-0.754	0.105	-0.105	0.00648	0.000140
$\psi_{\nu_i 0}$	0.836	0.519	0.477	0.0300	0.0300	7×10^{-13}	-3×10^{-19}

$\mu/U = 2.1$

ν_i	1	2	3	4	5	6	7
$\psi_{0\nu_i}$	-0.854	1.24	-0.0255	0.197	-2×10^{-6}	0.00956	0.000223
$\psi_{\nu_i 0}$	0.975	0.0736	0.584	6×10^{-6}	0.0305	4×10^{-12}	-2×10^{-18}

$\mu/U = 2.2$

ν_i	1	2	3	4	5	6	7
$\psi_{0\nu_i}$	-0.774	1.33	-0.00737	0.252	-4×10^{-7}	0.0134	0.000332
$\psi_{\nu_i 0}$	1.09	0.0896	0.478	0.0000132	0.0213	2×10^{-11}	-8×10^{-18}

$\mu/U = 2.3$

ν_i	1	2	3	4	5	6	7
$\psi_{0\nu_i}$	-0.770	1.37	-0.00330	0.314	-1×10^{-7}	0.0183	0.000480
$\psi_{\nu_i 0}$	1.18	0.153	0.384	0.0000408	0.0147	1×10^{-10}	-4×10^{-17}

$\mu/U = 2.4$

ν_i	1	2	3	4	5	6	7
$\psi_{0\nu_i}$	-0.918	1.28	-0.00244	0.388	-7×10^{-8}	0.0251	0.000709
$\psi_{\nu_i 0}$	1.20	0.325	0.307	0.000200	0.0103	1×10^{-9}	-2×10^{-16}

$\mu/U = 2.5$

ν_i	1	2	3	4	5	6	7
$\psi_{0\nu_i}$	-1.27	0.903	-0.340	0.338	-0.0251	0.0251	0.00110
$\psi_{\nu_i 0}$	1.05	0.704	0.175	0.174	0.00527	0.00527	-1×10^{-15}

Table 4.1: The transition parameters $\psi_{0\nu_i}$ or $\psi_{\nu_i 0}$ for $W/U = 0$, $J/U = 0.02$ and different values of μ/U.

Similar to the calculation of the MF parameter ψ_i, we have to multiply the expansion coefficients of consecutive Fock states $|n_i\rangle$ and $|n_i + 1\rangle$. Thus, the absolute values of $\psi_{0\nu_i}$ and $\psi_{\nu_i 0}$ should be the largest for the state $|\nu_i\rangle$ that has roughly one particle more or less than the ground state, respectively. This implies that, in general, it is not possible to find one single excited state that maximizes both $\psi_{0\nu_i}$ and $\psi_{\nu_i 0}$.

In table 4.1, the values for the transition parameters for the first seven excited states are listed, again for no disorder, $J/U = 0.02$, and μ/U ranging from 2.0 to 2.5. As one can see, the parameters are the largest for the first two excited states. From there on, the further away one moves from the ground state in energy, the further away one also moves in Fock space. Thus, in general, it holds that the higher the excitation energy, the smaller the transition parameter.

However, for each of the first three or four excited states, $\nu_i \lesssim 4$, at least one of the two amplitudes $\psi_{0\nu_i}$ and $\psi_{\nu_i 0}$ is roughly of the same order of magnitude as the maximal amplitude. Thus, depending on the actual value of E and the energy denominator of the MF locator $G^{MF}_{\nu_i}(E_0 \pm E) = (\pm E - \Delta\epsilon_{\mu_i})^{-1}$, either of these states might be eligible.

An important point, which simplifies the problem of selecting the optimal states, is now given

by the relative sign of $\psi_{0\nu_i}$ and $\psi_{\nu_i 0}$. From table 4.1, it can be seen that for the first excitation, there is a relative minus sign, whereas for the second excited state both parameters have the same algebraic sign. This alternating behavior continues for the higher excitation states. The reason for this is the number of nodes of the eigenstates, i.e., the number of times the expansion coefficients changes its algebraic sign. The ground state has zero nodes, the first excited states one node, the second two nodes, and so on. The reason for this can be seen when applying $\hat{h}_i$ to the eigenstate $|\nu_i\rangle$,

$$\hat{h}_i|\nu_i\rangle = \sum_{n_i}\Big[E_{n_i}\langle n_i|\nu_i\rangle - J\Psi_i\Big(\sqrt{n_i}\langle n_i-1|\nu_i\rangle + \sqrt{n_i+1}\langle n_i+1|\nu_i\rangle\Big)\Big]|n_k\rangle \stackrel{!}{=} E_{\nu_i}|\nu_i\rangle\,, \quad (4.63)$$

leading to

$$\big(E_{\nu_i} - E_{n_i}\big)\langle n_i|\nu_i\rangle + J\Psi_i\Big(\sqrt{n_i}\langle n_i-1|\nu_i\rangle + \sqrt{n_i+1}\langle n_i+1|\nu_i\rangle\Big) \stackrel{!}{=} 0\,, \quad (4.64)$$

for each n_i. Using that the bath amplitude Ψ_i is always positive, for the ground state $|\nu_i = 0\rangle$ it follows that all coefficients $\langle n_i|\nu_i\rangle$ have the same sign since its energy E_{ν_i} is always smaller than the Fock state energies E_{n_i}. We can thus choose the ground state to have only positive coefficients, $\langle n_i|\nu_i\rangle > 0$ for $|\nu_i = 0\rangle$.

For the first excited state $|\nu_i = 1\rangle$ the eigenenergy E_{ν_i} is smaller than all E_{n_i}, except for the lowest lying Fock state. Therefore, the coefficients need to change their sign once in order to fulfill equation (4.64), yielding one node. For the second excited state, there are two Fock states with lower energies, leading to two sign changes of the coefficients and, therefore, two nodes. This scheme continues for higher excitations.

As a result of these nodes, the parameter pairs $\psi_{\nu_i 0}$ and $\psi_{0\nu_i}$ obtain this alternating behavior with respect to their relative algebraic sign. This has now an important consequence for the transition amplitudes,

$$T_{\nu_i\mu_j} = -J\big(\psi_{\nu_i 0}\psi^*_{\mu_j 0} + \psi^*_{0\nu_i}\psi_{0\mu_j}\big)\,. \quad (4.65)$$

If the transition parameter pairs of $|\nu_i\rangle$ and $|\mu_j\rangle$ both have the same relative sign, then the two products in the above expression will have the same algebraic sign, i.e., two either negative or positive quantities are being added. However, if only one parameter pair has a relative minus sign, then also the two products will have a relative minus sign and one would add a positive and a negative quantity, yielding a smaller absolute value. This implies, that the transitions between the first and the second (or the second and the third) exited state are suppressed compared to transitions from first to first and second to second excited state.

Thus, the selection criterion becomes very simple: We either pick always only the first excited states or always only the second excited states. Couplings from the first to the third, for example, are neglected since these states are always well separated in energy. With this restriction to one excitation band, we can always choose the excited states such that both $\psi_{\nu_i 0}\psi^*_{\mu_j 0}$ and $\psi^*_{0\nu_i}\psi_{0\mu_j}$ are positive numbers.

Later, we will compare both cases to each other. Higher excitation bands might also be of interest, but will not be investigated in the present work.

4.2.5 Defining the Effective Model

Having reduced the number of excitations to one per site, we can simplify our notation for the single-excitation states,

$$|\nu_i\rangle \to |i\rangle\,. \tag{4.66}$$

For the MF ground state, we continue to use the notation $|\Phi_0\rangle = |0\rangle$. This will not conflict with the above notation for the single-excitation states, as the enumeration of the lattice sites starts at one, $i = 1, 2, 3, \ldots N_i$.

Accordingly, the notation for the MF locator is changed as follows,

$$G^{MF}_{\nu_i}(E^{MF}_0 \pm E) \quad \longrightarrow \quad G^{MF}_i(\pm E) = \frac{1}{\pm E - \Delta\epsilon_i}\,, \tag{4.67}$$

with $\Delta\epsilon_{\nu_i} \to \Delta\epsilon_i$, where we keep the Δ as a reminder that the energies are excitation energies measured with respect to the ground state energy. Similar, for the transition amplitudes we have

$$T_{\mu_i\nu_j} \quad \longrightarrow \quad T_{ij}\,. \tag{4.68}$$

Expression (4.47) for the single-particle Green's function can then be rewritten as

$$G_{ij}(E) = \langle 0|\hat{b}_i|i\rangle\langle i|\hat{G}(+E)|j\rangle\langle j|\hat{b}^\dagger_j|0\rangle + \langle 0|\hat{b}^\dagger_j|j\rangle\langle j|\hat{G}(-E)|i\rangle\langle i|\hat{b}_i|0\rangle\,, \tag{4.69}$$

where we have dropped the MF ground state energy E^{MF}_0 from the notation in accordance to the new notation for the locator (4.67). If we now go back to the initial definition of the propagator $\hat{G}$, see equation (4.33), its matrix elements can be expressed as

$$\begin{aligned}\langle i|\hat{G}(E)|j\rangle &= \langle i|\hat{G}^{MF}(E)|j\rangle + \langle i|\hat{G}^{MF}(E)\delta\hat{H}\hat{G}(E)|j\rangle \\ &= G^{MF}_i(E)\delta_{ij} + G^{MF}_i(E)\sum_k^{\langle ik\rangle} T_{ik}\langle k|\hat{G}(E)|j\rangle\end{aligned} \tag{4.70}$$

where we have used the completeness of the single-excitation states with respect to the truncated state space,

$$\sum_k |k\rangle\langle k| = 1\,, \tag{4.71}$$

and

$$\langle i|\delta\hat{H}|k\rangle = \begin{cases} T_{ik} & \text{for } i,k \text{ nearest neighbors,} \\ 0 & \text{otherwise.}\end{cases} \tag{4.72}$$

Apparently, equation (4.70) has the same structure as the locator expansion for the non-interacting Anderson Hamiltonian, see equation 4.20. The idea now is that we define a single-particle Hamiltonian that has the same propagator as our truncated single-excitation model.

Comparing the MF locator (4.67) with the original locator (4.21), we find that the excitation energies $\Delta\epsilon_i$ will serve as the onsite energies of the effective model. Furthermore, the bare hopping amplitude J has to be replaced by the transition amplitudes T_{ij}. The resulting effective Hamiltonian for the single-excitation states is then given by

$$\hat{H}_{ex} = \sum_i \Delta\epsilon_i|i\rangle\langle i| + \sum_{ij}^{\langle ij\rangle} T_{ij}|i\rangle\langle j|\,. \tag{4.73}$$

In order to avoid any confusion with the creation and annihilation operators of the initial Bose-Hubbard model, we will not use second quantization to express the effective Hamiltonian. This should also stress the point that the excitations are not completely behaving like actual bosonic particles, but like hard-core bosons. For example, multiple occupation of the same state $|i\rangle$ would be unphysical and is, therefore, not allowed. Furthermore, as we have discussed in section 4.2.2, having more than just one excitation in the system will allow for additional transitions which are not compatible with the idea of the excitation as an effective particle. Therefore, the identification of the local excitations with single particles is only valid when restricting ourselves to the single-particle, or rather single-excitation sector.

4.2.6 Summary

The derivation of the effective model stretched across several sections and might appear a bit unclear at first. Therefore, in this section we want to summarize how we arrived at Hamiltonian (4.73) and repeat the most important steps. The starting point was that we wanted to calculate the single-particle Green's function for the disordered Bose-Hubbard model. In section 4.2.1 we showed that the Fourier transformed Green's function (at zero temperature) can be expressed as

$$G_{ij}(E) = \langle\Psi_0|\hat{b}_i\hat{G}(E_0+E)\hat{b}_j^\dagger|\Psi_0\rangle + \langle\Psi_0|\hat{b}_j^\dagger\hat{G}(E_0-E)\hat{b}_i|\Psi_0\rangle\,, \tag{4.74}$$

where $|\Psi_0\rangle$ is the ground state and E_0 its eigenenergy. Furthermore, this equation introduced the propagator $\hat{G}$,

$$\hat{G}(E) = \left(E-\hat{H}\right)^{-1}. \tag{4.75}$$

The argument of the propagator in equation (4.74) implies that all energies are measured with respect to the ground state energy, $\hat{G}(E_0 \pm E) = \left(\pm E - (\hat{H}-E_0)\right)^{-1}$. By separating the full Hamiltonian into the decoupled MF Hamiltonian $\hat{H}^{MF}$ and the remaining term containing the fluctuations from the mean field,

$$\hat{H} = \hat{H}^{MF} + \delta\hat{H}\,, \tag{4.76}$$

this propagator could be expanded as follows

$$\hat{G}(E) = \hat{G}^{MF}(E) + \hat{G}^{MF}(E)\delta\hat{H}\hat{G}(E)\,, \tag{4.77}$$

where, in analogy to the original locator expansion for the Anderson Hamiltonian, the MF locator was introduced,

$$\hat{G}^{MF}(E) = \left(E-\hat{H}^{MF}\right)^{-1}. \tag{4.78}$$

The next step, see section 4.2.2, was to use the MF eigenbasis in order to represent the locator expansion of the propagator (4.77),

$$\begin{aligned}\langle\Phi_\alpha|\hat{G}|\Phi_\beta\rangle &= \langle\Phi_\alpha|\hat{G}^{MF}|\Phi_\beta\rangle + \langle\Phi_\alpha|\hat{G}^{MF}\delta\hat{H}\hat{G}|\Phi_\beta\rangle \\ &= G_\alpha^{MF}\delta_{\alpha\beta} + G_\alpha^{MF}\sum_\gamma T_{\alpha\gamma}\langle\Phi_\gamma|\hat{G}|\Phi_\beta\rangle\,,\end{aligned} \tag{4.79}$$

where $|\Phi_\alpha\rangle, |\Phi_\beta\rangle$, and $|\Phi_\gamma\rangle$ are eigenstates of $\hat{H}^{MF}$ and $T_{\alpha\gamma} = \langle\Phi_\alpha|\delta\hat{H}|\Phi_\gamma\rangle$. In addition, we have used that the locator is diagonal in this representation, $\langle\Phi_\alpha|\hat{G}^{MF}|\Phi_\beta\rangle = G_\alpha^{MF}\delta_{\alpha\beta}$.

In order to reduce the number of states we have to take into account for the above expansion, in section 4.2.3 we applied a series of approximations. First, we went back to expression (4.74)

for the single-particle Green's function, where we noted that the states $|\Phi_\alpha\rangle$ and $|\Phi_\beta\rangle$ in equation (4.79) need to have a finite overlap with either $\hat{b}_i|\Psi_0\rangle$ or $\hat{b}_i^\dagger|\Psi_0\rangle$ in order to contribute. Since we do not know the exact form of the full ground state, we made the assumption that the local transition induced by the creation or annihilation operators is well resolved by the MF ground state $|\Phi_0\rangle$,

$$\langle\Phi_\alpha|\hat{b}_i|\Psi_0\rangle \approx \langle\Phi_\alpha|\hat{b}_i|\Phi_0\rangle \tag{4.80a}$$

and

$$\langle\Phi_\alpha|\hat{b}_i^\dagger|\Psi_0\rangle \approx \langle\Phi_\alpha|\hat{b}_i^\dagger|\Phi_0\rangle\,. \tag{4.80b}$$

From this, it directly followed that $|\Phi_\alpha\rangle$ (and $|\Phi_\beta\rangle$) is a single-excitation state, see equations (4.50) for the definition. We introduced the short-hand notation $|\Psi_\alpha\rangle \equiv |\alpha_i\rangle$ for these states, where it is understood that all sites are in their local MF ground state, except for site i which is in the excited state α_i.

Furthermore, we argued that transitions from these single-excitation states to MF eigenstates with multiple excitations are suppressed, as for each excitation an additional excitation energy has to be paid. Thus, if we restrict ourselves to the low-energy regime, we can also restrict the state space to the single-excitation sector and the expansion (4.79) can be rewritten as

$$\langle\alpha_i|\hat{G}|\beta_j\rangle = G^{MF}_{\alpha_i}\delta_{\alpha_i\beta_j} + G^{MF}_{\alpha_i}\sum_{\gamma_k}^{\langle ik\rangle} T_{\alpha_i\gamma_k}\langle\gamma_k|\hat{G}|\beta_j\rangle\,. \tag{4.81a}$$

with the transition amplitudes

$$T_{\alpha_i\gamma_k} = \langle\alpha_i|\delta\hat{H}|\gamma_k\rangle = \begin{cases} -J\langle\alpha_i|\big(\hat{b}_i^\dagger\hat{b}_k + \hat{b}_k^\dagger\hat{b}_i\big)|\gamma_k\rangle & \text{for } i,k \text{ nearest neighbors,} \\ 0 & \text{otherwise.} \end{cases} \tag{4.81b}$$

According to equation 4.74, the propagator has to be evaluated for the two arguments $E_0 \pm E$, for which the locator takes the following form,

$$G^{MF}_{\alpha_i}(\pm E) = \frac{1}{\pm E - \Delta\epsilon_{\alpha_i}}\,, \tag{4.82}$$

with $\Delta\epsilon_{\alpha_i}$ being the excitation energy for the local MF eigenstate α_i. This expansion corresponds to a non-interacting tight-binding model with multiple orbitals per site.

In order to map this problem onto Anderson's original locator expansion, we needed to move to a single-orbital model, i.e., restrict the number of excitations to one per site. In section 4.2.4 we therefore investigated the local spectrum of the MF Hamiltonian $\hat{h}_i$. For the transition of an excitation from site j to site i we wrote

$$T_{\nu_i\mu_j} = -J\big(\psi_{\nu_i 0}\psi^*_{\mu_j 0} + \psi^*_{0\nu_i}\psi_{0\mu_j}\big)\,, \tag{4.83}$$

with the transition parameters $\psi_{\alpha_i\beta_i} = \langle\alpha_i|\hat{b}_i|\beta_i\rangle$. We found that due to different relative algebraic signs, the transition from a first to a second excited state was suppressed compared to a transition from first to first or second to second excited state. This led us to the decision to define separate effective models for the first and the second excited states, i.e., for one model all states are either the first or the second excited states.

With this we have reduced the state space to one excitation per site. Thus, each state is

unambiguously determined by the index of excited site. In section 4.2.5 we therefore have introduced a simplified notation, $|\nu_i\rangle \to |i\rangle$, $\Delta\epsilon_{\nu_i} \to \Delta\epsilon_i$, $T_{\nu_i\mu_j} \to T_{ij}$, and $G^{MF}_{\nu_i} \to G^{MF}_i$. The single-particle Green's function can then be written as

$$G_{ij}(E) = \langle 0|\hat{b}_i|i\rangle\langle i|\hat{G}(+E)|j\rangle\langle j|\hat{b}^\dagger_j|0\rangle + \langle 0|\hat{b}^\dagger_j|j\rangle\langle j|\hat{G}(-E)|i\rangle\langle i|\hat{b}_i|0\rangle\,, \tag{4.84}$$

where the propagator is expanded as follows,

$$\langle i|\hat{G}(E)|j\rangle = G^{MF}_i(E)\delta_{ij} + G^{MF}_i(E)\sum_k^{\langle ik\rangle} T_{ik}\langle k|\hat{G}(E)|j\rangle\,. \tag{4.85}$$

with the MF locator

$$G^{MF}_i(E) = \frac{1}{E - \Delta\epsilon_i}\,. \tag{4.86}$$

This expansion of the propagator in terms of the MF locators has the exact same form as the locator expansion for the original Anderson Hamiltonian and we can define the following effective, non-interacting model,

$$\hat{H}_{ex} = \sum_i \Delta\epsilon_i|i\rangle\langle i| + \sum_{\langle ij\rangle} T_{ij}|i\rangle\langle j|\,. \tag{4.87}$$

If we now calculate the single-particle Green's function for this effective Hamiltonian, we will obtain the propagator for the interacting Bose-Hubbard model as a result. Of course, this is only valid within the truncated state space that is restricted to the single-excitation states.

This concludes the derivation of the effective model. In the next section we will see how we can make use of it in order to calculate the current density.

4.3 The Current Density Within the Single-Excitation Approximation

In section 4.1.2, we arrived at the following expression for the current density at zero temperature, $T = 0$,

$$J_{ij} = 2J\int_{-\infty}^{0}\frac{\mathrm{d}E}{2\pi}\,\mathrm{Re}\left\{G^R_{ij}(E) - G^A_{ij}(E)\right\}, \tag{4.88}$$

where the integration is restricted to negative energies, $E \leq 0$. This allows us to simplify expression (4.84) for the single-particle Green's function. The excitation energies in the denominator of the MF locator (4.86) are, by definition, all positive, $\Delta\epsilon_i > 0$ for all i, and will be distributed within some interval $[\Delta\epsilon_{min}, \Delta\epsilon_{max}]$ with $\Delta\epsilon_{min}, \Delta\epsilon_{max} > 0$. Consequently, also all on-site energies of the effective model (4.87) will be distributed within this interval. The first term in (4.84), which corresponds to particle transport, is evaluated at $+E < 0$, i.e., outside of the energy interval of the effective Hamiltonian. As we will see later, in the parameter region of interest the density of states will vanish for negative energies, $N(E) = 0$ for $E < 0$, and thus, the particle contribution to the transport can be neglected.

The second term in (4.84), which corresponds to hole transport, is evaluated at positive energies, $-E > 0$, and will probe the system in regions with finite density of states. Thus, it can yield a finite contribution to the current density and we can reduce the single-particle

Green's function to its hole contribution,

$$G_{ij}(E) \approx \langle 0|\hat{b}_j^\dagger|j\rangle\langle j|\hat{G}(-E)|i\rangle\langle i|\hat{b}_i|0\rangle\,. \tag{4.89}$$

Moving on, in section 4.1.2 we also found that the current density in equilibrium usually vanishes as the integrand is purely imaginary. We concluded that a complex phase must be introduced via the MF parameters. In order to see how this works out, let us again consider the MF locator expansion of the single-particle Green's function, where we concentrate on a certain hopping path C_{ji} from i to j,

$$G_j^{MF} T_{jn} G_n^{MF} T_{nm} G_m^{MF} T_{ml} G_l^{MF} \ldots G_k^{MF} T_{ki} G_i^{MF}\,. \tag{4.90}$$

For the sake of argument, let us now assume that the transition elements have a complex phase,

$$T_{kl} = |T_{kl}| e^{\mathrm{i}\varphi_{kl}}\,. \tag{4.91}$$

Then, expression (4.90) can be rewritten as

$$e^{\mathrm{i}\phi(C_{ji})}\; G_j^{MF}|T_{jn}|G_n^{MF}|T_{nm}|G_m^{MF}|T_{ml}|G_l^{MF}\ldots G_k^{MF}|T_{ki}|G_i^{MF}\,, \tag{4.92}$$

where we have extracted the phase factor accumulated along the path C_{ij},

$$\phi(C_{ji}) \equiv \sum_{(rs)\in C_{ji}} \varphi_{rs} = \varphi_{jn} + \varphi_{nm} + \varphi_{ml} + \ldots + \varphi_{ki}\,. \tag{4.93}$$

If the phase factor does not depend on the specific path C_{ji}, but only on the initial and the final site,

$$\phi(C_{ji}) \to \phi_{ji}\,, \tag{4.94}$$

it will be the same for every path contributing to the Green's functions. Thus, this phase factor can be extracted from the Green's functions themselves,

$$G_{ij}^{R/A} = e^{\mathrm{i}\phi_{ij}}\; \widetilde{G}_{ij}^{R/A}\,, \tag{4.95}$$

where the newly defined Green's functions $\widetilde{G}_{ij}^{R/A}$ correspond to the model with real hopping amplitudes,

$$\hat{H}_{ex} = \sum_i \Delta\epsilon_i |i\rangle\langle i| + \sum_{\langle ij\rangle} |T_{ij}|\; |i\rangle\langle j|\,, \tag{4.96}$$

for which it follows that

$$\mathrm{Re}\,\widetilde{G}_{ij}^{R} = \mathrm{Re}\,\widetilde{G}_{ij}^{A} \tag{4.97a}$$

and

$$\mathrm{Im}\,\widetilde{G}_{ij}^{R} = -\,\mathrm{Im}\,\widetilde{G}_{ij}^{A}\,. \tag{4.97b}$$

With this, the current density can be transformed as follows,

$$\begin{aligned} J_{ij} &= 2J \int_{-\infty}^{0} \frac{\mathrm{d}E}{2\pi} \operatorname{Re}\left\{ e^{\mathrm{i}\phi_{ij}} \left[\widetilde{G}^{R}_{ij}(E) - \widetilde{G}^{A}_{ij}(E) \right] \right\} \\ &= 2J \int_{-\infty}^{0} \frac{\mathrm{d}E}{2\pi} \operatorname{Re}\left\{ \left(\cos\phi_{ij} + \mathrm{i}\sin\phi_{ij} \right) 2\mathrm{i}\, \operatorname{Im} \widetilde{G}^{R}_{ij}(E) \right\} \\ &= 4J \sin\phi_{ij} \int_{-\infty}^{0} \frac{\mathrm{d}E}{2\pi} \operatorname{Im} \widetilde{G}^{A}_{ij}(E)\,. \end{aligned} \tag{4.98}$$

Thus, if there is a finite phase factor $\phi_{ji} \neq 0$, a finite current density between sites i and j is possible, even though no voltage is applied. Still, also the integral itself needs to be finite. If we consider the long range limit, $|\mathbf{x}_i - \mathbf{x}_j| \to \infty$, this will only be the case if the system is in the extended phase. In the Anderson localized phase, the density correlations will fall off exponentially as a function of distance, resulting in a vanishing long range current density. Within the effective single-excitation model (4.96), we can employ already established techniques for the Anderson Hamiltonian to determine whether the system is localized or not. This implies that in order to find the transition from SF to BG, it will not be necessary to actually evaluate the integral in (4.98). In order to check whether the current density can be finite or not, we only need to find the Anderson transition for the effective Anderson Hamiltonian (4.96).

As we will see in the following sections, unfortunately the assumption (4.94) is not fulfilled for the disordered model (or at least, it is not apparent). Thus, in the end we will consider equation (4.98) in the limit $\phi_{ji} \to 0$, where we have $\sin\phi_{ji} \approx \phi_{ji}$ and

$$\lim_{\phi_{ij}\to 0} J_{ij} = 4J \int_{-\infty}^{0} \frac{\mathrm{d}E}{2\pi} \operatorname{Im} G^{A}_{ij}(E)\Big|_{\phi_{ij}=0} \times \lim_{\phi_{ij}\to 0} \phi_{ij}\,. \tag{4.99}$$

In other words, we will assume that for small phases ϕ_{ij} the integral can be evaluated for $\phi_{ij} = 0$. If we recall equation (2.52), which provided a relation between the phase gradient of the mean field $\psi(\mathbf{x},t) = |\psi| e^{\mathrm{i}S(\mathbf{x},t)}$ and the velocity $\mathbf{v}$ of the superfluid for the ordered and continuous case,

$$\mathbf{v} = \frac{1}{m} \nabla S(\mathbf{x},t)\,, \tag{4.100}$$

we can identify $\phi_{ji} \to 0$ with the limit of very small velocities, $|\mathbf{v}| \to 0$. To make the connection between expressions (4.99) and (4.100), we can use that in the localized regime the Green's function will fall off exponentially, whereas in the extended regime it will scale with the system size,

$$G^{A/R}_{ij} \sim \begin{cases} e^{-|\mathbf{x}_i - \mathbf{x}_j|/\xi} & \text{in the localized regime,} \\ \frac{1}{|\mathbf{x}_i - \mathbf{x}_j|} & \text{in the extended regime,} \end{cases} \tag{4.101}$$

and we get

$$J_{ij} \sim \rho_s v \sim \begin{cases} \phi_{ij} e^{-|\mathbf{x}_i - \mathbf{x}_j|/\xi} & \text{in the localized regime,} \\ \frac{\phi_{ij}}{|\mathbf{x}_i - \mathbf{x}_j|} & \text{in the extended regime.} \end{cases} \tag{4.102}$$

Thus, in the localized regime the current density will fall off exponentially and there will be no superfluid density ρ_s in the thermodynamic limit. In the extended regime, we get a term proportional to the phase gradient between sites i and j in accordance to equation (4.100). While it should be clear that this theory cannot describe the system quantitatively (like, for

example, predicting the superfluid density ρ_s), it still is consistent with the general picture of superfluidity on a qualitative level.

In the next sections, we want to investigate how complex boundary conditions will affect the MF parameters and, thereby, the parameters of our effective Hamiltonian, eventually leading to a non-vanishing current density.

4.3.1 Boundary Conditions for the Order Parameter

In this section we want to examine the transition amplitudes in more detail and want to find out how they can obtain a complex phase. We have seen in section 3.2 that in order to minimize the energy, the MF parameters will align their phases. Thus, by a global gauge transformation all MF parameters could be rotated to the positive real axis. Subsequently, also all coefficients of the MF eigenstates turned out to be real numbers which, in the end, would yield real transition amplitudes T_{lm}.

In order to make these amplitudes complex numbers, it is necessary to apply boundary conditions. For simplicity, we consider the case where i and j are separated in x-direction, $\mathbf{x}_i - \mathbf{x}_j = (x_i - x_j)\,\hat{\mathbf{e}}_x$. In the y-z-plane of i and j the complex phase of the MF parameters shall now be fixed to ϕ_i and ϕ_j, respectively. Then, in between the two planes the phase has to change from ϕ_i to ϕ_j, such that the ground state energy is minimized. Furthermore, in the limit of $|x_i - x_j| \to \infty$ it is safe to assume that the phase changes infinitesimally between neighboring sites. Thus, the effect of the boundary conditions on the absolute values of the MF parameters is negligible.

In section 3.2.1 we found that the energy is minimized when for all sites k the quantity

$$\mathrm{Re}\left\{\Psi_k \psi_k^*\right\} \tag{4.103}$$

gets maximized. As a reminder, Ψ_k is the bath amplitude for site k. We already discussed that for a given bath amplitude, the local MF parameter will adjust to the phase of the bath amplitude. In the following, we want to discuss how this relates the complex phases φ_k of $\psi_k = |\psi_k| e^{\mathrm{i}\varphi_k}$ on neighboring sites.

For the pure case, we can make the ansatz that the complex phases are constant within each y-z-plane, which yields

$$\Psi_k \psi_k^* = (\psi_{k-x} + \psi_{k+x})\psi_k^* + \left|\Psi_k^{(y-z)}\right||\psi_k| \tag{4.104}$$

where $\mathbf{x}_{k\pm x} = \mathbf{x} \pm \hat{\mathbf{e}}_x$ and $\Psi_k^{(y-z)}$ are the contributions from the y-z-plane to the bath amplitude. Maximizing this expression as a function of φ_k leads to the condition

$$\begin{aligned} & |\psi_{k+x}| \cos(\varphi_{k+x} - \varphi_k) + |\psi_{k-x}| \cos(\varphi_{k-x} - \varphi_k) \stackrel{!}{=} \max \\ \Leftrightarrow \quad & |\psi_{k+x}| \sin(\varphi_{k+x} - \varphi_k) + |\psi_{k-x}| \sin(\varphi_{k-x} - \varphi_k) = 0\,. \end{aligned} \tag{4.105}$$

With $|\psi_{k+x}| = |\psi_{k-x}|$, it immediately follows that $\varphi_{k+x} - \varphi_k = \varphi_k - \varphi_{k-x}$, and thus,

$$\varphi_k = \tfrac{1}{2}(\varphi_{k+x} + \varphi_{k-x})\,. \tag{4.106}$$

Hence, for a pure system the phase will change linearly from plane i to j,

$$\varphi_l = \frac{\varphi_j - \varphi_i}{x_j - x_i}(x_l - x_i) + \varphi_i \tag{4.107}$$

where x_i, x_j, and x_l are the x-coordinates of the planes i, j, and l, respectively.

For the disordered case, the above ansatz for $\Psi_k^{(y-z)}$ is, of course, not valid anymore. Trying to find the phase field that minimizes the total energy becomes a full lattice problem again, which is something we want to avoid. If we make the reasonable assumption that the phases do not differ significantly on one z-y-plane, then the behavior of the phase field is still mainly governed by equation (4.105). From that, we can at least conclude that the phase field is monotonic,

$$\varphi_{k-x} < \varphi_k \quad \Leftrightarrow \quad \varphi_k < \varphi_{k+x} \tag{4.108a}$$

and

$$\varphi_{k-x} > \varphi_k \quad \Leftrightarrow \quad \varphi_k > \varphi_{k+x}\,. \tag{4.108b}$$

Furthermore, full rotations of the phase by 2π in between i and j can be excluded as they do not minimize the energy.

Now, let us examine the effect of the complex MF parameters on the MF eigenstates. Letting the local Hamiltonian $\hat{h}_k$ (now with a complex $\Psi_k = |\Psi_k| e^{\mathrm{i}\varphi_k}$) act on an eigenstate $|\nu_k\rangle$ yields

$$\hat{h}_k|\nu_k\rangle = \sum_{n_k}\Big[E_{n_k}\langle n_k|\nu_k\rangle - J\Psi_k\sqrt{n_k}\langle n_k-1|\nu_k\rangle - J\Psi_k^*\sqrt{n_k+1}\langle n_k+1|\nu_k\rangle\Big]|n_k\rangle \stackrel{!}{=} E_{\nu_k}|\nu_k\rangle \tag{4.109}$$

leading to

$$\big(E_{n_k} - E_{\nu_k}\big)\langle n_k|\nu_k\rangle - J\Psi_k\sqrt{n_k}\langle n_k-1|\nu_k\rangle - J\Psi_k^*\sqrt{n_k+1}\langle n_k+1|\nu_k\rangle \stackrel{!}{=} 0\,. \tag{4.110}$$

Since the term $E_{n_k} - E_{\nu_k}$ is real and finite, we have the condition

$$\frac{\Psi_k\langle n_k-1|\nu_k\rangle + \Psi_k^*\langle n_k+1|\nu_k\rangle}{\langle n_k|\nu_k\rangle} = E_{n_k} - E_{\nu_k} \stackrel{!}{\in} \mathbb{R}\,, \tag{4.111}$$

which is solved by

$$\langle n_k|\nu_k\rangle = \langle n_k|\widetilde{\nu}_k\rangle e^{\mathrm{i}\varphi_k n_k + \mathrm{i}\varphi_{\nu_k}} \quad \text{for all } n_k\,, \tag{4.112}$$

where $|\widetilde{\nu}_k\rangle$ is the eigenstate for $\varphi_k = 0$, see also equation (4.64). The additional phase φ_{ν_k} is a free parameter and can be absorbed in a redefinition of $|\nu_k\rangle$. Hence, we can set $\varphi_{\nu_k} = 0$. Now, for any transition parameter $\psi_{\mu_i\nu_i}$ it follows that

$$\begin{aligned}
\psi_{\mu_k\nu_k} &= \langle\mu_k|\hat{b}_k|\nu_k\rangle \\
&= \sum_{n_k=0}^{\infty}\sqrt{n_k+1}\,\langle\mu_k|n_k\rangle\langle n_k+1|\nu_k\rangle \\
&= \sum_{n_k=0}^{\infty}\sqrt{n_k+1}\,\langle\widetilde{\mu}_k|n_k\rangle\,\langle n_k+1|\widetilde{\nu}_k\rangle\, e^{\mathrm{i}\varphi_k(n_k+1-n_k)} \\
&\equiv \widetilde{\psi}_{\mu_k\nu_k} e^{\mathrm{i}\varphi_k}\,,
\end{aligned} \tag{4.113}$$

where $\widetilde{\psi}_{\mu_k\nu_k} \in \mathbb{R}$ is the transition parameter of the system without boundary conditions. This means that the transition parameters will have the same complex phase as the MF parameter. Applying a phase gradient to the ψ_i therefore directly induces a phase gradient for the transition parameters. With this result, we can now study the transition amplitudes, which is done in the next section.

4.3.2 Complex Transition Amplitudes

Let us start with the general expression for the transition amplitudes,

$$\begin{aligned} T_{kl} &= -J\big(\psi_{\alpha_k 0}\psi^*_{\alpha_l 0} + \psi^*_{0\alpha_k}\psi_{0\alpha_l}\big)\,, \\ &= -J\Big[\widetilde{\psi}_{\alpha_k 0}\widetilde{\psi}_{\alpha_l 0}\, e^{\mathrm{i}(\varphi_k-\varphi_l)} + \widetilde{\psi}_{0\alpha_k}\widetilde{\psi}_{0\alpha_l}\, e^{-\mathrm{i}(\varphi_k-\varphi_l)}\Big]\,. \end{aligned} \tag{4.114}$$

For very small phase differences, $|\varphi_k - \varphi_l| \ll 1$, we can write

$$\begin{aligned} T_{kl} &= -J\Big[\Big(\widetilde{\psi}_{\alpha_k 0}\widetilde{\psi}_{\alpha_l 0} + \widetilde{\psi}_{0\alpha_k}\widetilde{\psi}_{0\alpha_l}\Big)\cos(\varphi_k-\varphi_l) + \mathrm{i}\Big(\widetilde{\psi}_{\alpha_k 0}\widetilde{\psi}_{\alpha_l 0} - \widetilde{\psi}_{0\alpha_k}\widetilde{\psi}_{0\alpha_l}\Big)\sin(\varphi_k-\varphi_l)\Big] \\ &\approx -J\Big[\Big(\widetilde{\psi}_{\alpha_k 0}\widetilde{\psi}_{\alpha_l 0} + \widetilde{\psi}_{0\alpha_k}\widetilde{\psi}_{0\alpha_l}\Big) + \mathrm{i}\Big(\widetilde{\psi}_{\alpha_k 0}\widetilde{\psi}_{\alpha_l 0} - \widetilde{\psi}_{0\alpha_k}\widetilde{\psi}_{0\alpha_l}\Big)(\varphi_k-\varphi_l)\Big] \\ &\approx -J\Big(\widetilde{\psi}_{\alpha_k 0}\widetilde{\psi}_{\alpha_l 0} + \widetilde{\psi}_{0\alpha_k}\widetilde{\psi}_{0\alpha_l}\Big)e^{\mathrm{i}\Delta_{ij}(\varphi_k-\varphi_l)} \qquad (4.115) \\ &\equiv \widetilde{T}_{kl}e^{\mathrm{i}\Delta_{ij}(\varphi_k-\varphi_l)} \qquad (4.116) \end{aligned}$$

with $\widetilde{T}_{kl}$ being the transition amplitude for zero phase gradient and

$$\Delta_{kl} = \frac{\widetilde{\psi}_{\alpha_k 0}\widetilde{\psi}_{\alpha_l 0} - \widetilde{\psi}_{0\alpha_k}\widetilde{\psi}_{0\alpha_l}}{\widetilde{\psi}_{\alpha_k 0}\widetilde{\psi}_{\alpha_l 0} + \widetilde{\psi}_{0\alpha_k}\widetilde{\psi}_{0\alpha_l}} \leq 1\,, \tag{4.117}$$

where only terms up to first order in $\varphi_k - \varphi_l$ were considered. For the ordered case, $W = 0$, the transition elements are the same on each site and it follows that

$$T_{kl} = \widetilde{T}e^{\mathrm{i}\Delta\cdot(\varphi_k-\varphi_l)}\,, \tag{4.118}$$

where we have omitted the lattice index for all quantities that do not depend on the actual sites. Furthermore, in the previous section we have found that we can choose the boundary conditions such that the phase changes only in one direction, e.g., the x-direction, see equation (4.107). Therefore, the phase $\phi(C_{ij})$ of a certain path C_{ij} from site j to site i, see equation (4.92), only depends on the distance in x-direction The contributions to the phase (not the absolute value) from sections going back and forth in x-direction will cancel each other, while movement in y- and z-direction will not yield any contribution to the complex phase at all. Thus, we get

$$\phi(C_{ji}) = \Delta\cdot\frac{\varphi_j-\varphi_i}{x_j-x_i}(x_j-x_i) = \Delta\cdot(\varphi_j-\varphi_i) \tag{4.119}$$

for each path from i to j. Hence, the phase factor only depends on the phases on the initial and the final site. For the single-particle Green's function we can write

$$\begin{aligned} G_{ij}(E) &= \langle 0|\hat{b}_j^\dagger|j\rangle\langle j|\hat{G}(-E)|i\rangle\langle i|\hat{b}_i|0\rangle \\ &= \langle 0|\hat{b}_j^\dagger|j\rangle\langle j|\hat{G}(-E)|i\rangle\langle i|\hat{b}_i|0\rangle\Big|_{\varphi_i=\varphi_j=0} \times\ e^{\mathrm{i}(1-\Delta)(\varphi_i-\varphi_j)} \\ &= \widetilde{G}_{ij}(E) \times e^{\mathrm{i}(1-\Delta)(\varphi_i-\varphi_j)}\,, \end{aligned} \tag{4.120}$$

i.e., we can extract the phase factor and evaluate the Green's function for $\varphi_i = \varphi_j = 0$ and real transition amplitudes $\widetilde{T}$. Note that compared to our initial considerations at the beginning of section 4.3, which led to expression (4.95), in addition to the phase factor coming from the propagator $\langle j|\hat{G}|i\rangle$ here we now have contributions from the two outer matrix elements. The total phase factor is then

$$\phi_{ij} = (1-\Delta)(\varphi_i - \varphi_j) = \frac{2\left(\widetilde{\psi}_{0\alpha}\right)^2}{\left(\widetilde{\psi}_{\alpha 0}\right)^2 + \left(\widetilde{\psi}_{0\alpha}\right)^2}\,(\varphi_i - \varphi_j)\,, \tag{4.121}$$

where we have again omitted lattice indices for the translational invariant quantities. This expression tells us how the boundary conditions applied to the actual model translate to our effective single-excitation model. Apparently, the effective phase gets larger if $\widetilde{\psi}_{0\alpha} = \langle 0|\hat{b}_i|\alpha_i\rangle$ gets larger as well, i.e., the more *particle-like* the excitations are. On the other hand, it gets smaller for larger $\widetilde{\psi}_{\alpha 0} = \langle \alpha_i|\hat{b}_i|0\rangle$, i.e., the more *hole-like* the excitations are. Moreover, if there was only hole-like transport, $\widetilde{\psi}_{0\alpha} = 0$, the complex phase factor would vanish completely. This implies that, although we are calculating the hole contribution to the Green's function, the particle transport is still important. This stresses the point that the effective model is not a single-particle model, but a single-excitation model, which still contains the multi-particle nature of the underlying Bose-Hubbard model.

Now that we have discussed the pure case, let us turn to the disordered case with $W > 0$. Here, the factor Δ_{kl} in equation (4.116) will depend on the lattice sites k and l and will fluctuate randomly as a function of the on-site energies ε_k and ε_l. Furthermore, the complex phases φ_k and φ_l will fluctuate as well. Still, in the previous section we have argued that one can at least assume the phases to change monotonically from φ_i to φ_j between the boundary planes i and j, see equation (4.108). If we make the assumption that, on average, the phase changes linearly like in the pure case and that, in addition, the fluctuations from this linear behavior are small when we take the limit $|\varphi_i - \varphi_j| \to 0$, we can write

$$\begin{aligned} \phi(C_{ji}) &= \sum_{(k,l)\in C_{ji}} \Delta_{kl}\cdot(\varphi_k - \varphi_l) \\ &\approx \sum_{(k,l)\in C_{ji}} \Delta_{kl}\,\frac{\varphi_j - \varphi_i}{x_j - x_i}(x_k - x_l) \\ &= \left[\frac{1}{x_j - x_i}\sum_{(k,l)\in C_{ji}} \Delta_{kl}\cdot(x_k - x_l)\right]\cdot\ (\varphi_j - \varphi_i) \\ &\approx \Delta_{avg}\cdot(\varphi_j - \varphi_i)\,, \end{aligned} \tag{4.122}$$

where in the last step we have assumed that the summation over all Δ_{kl} can be replaced by the disorder-averaged Δ_{avg}, Since we neglected fluctuations from the linear behavior, again only hopping events in x-direction can contribute to the total phase factor. Furthermore, the contributions to the total phase from going back and forth in x-direction, which can be finite due to the random Δ_{kl}, are also neglected. Within this approximation, the total phase has the same form as in the pure case,

$$\phi_{ij} = (1 - \Delta_{avg})(\varphi_i - \varphi_j)\,, \tag{4.123}$$

with Δ_{avg} now being a disorder-averaged quantity. This, of course, does not represent a thorough derivation, but should only serve as a motivation for approximating the current density according to equation (4.99) in the limit of a small phase difference, $|\varphi_i - \varphi_j| \to 0$.

4.3.3 Summary

The central quantity of interest is the current density,

$$J_{ij} = 2J \int_{-\infty}^{0} \frac{\mathrm{d}E}{2\pi}\, \mathrm{Re}\left\{G^R_{ij}(E) - G^A_{ij}(E)\right\}, \tag{4.124}$$

which we want to evaluate within the single-excitation approximation. We have found that in order for the integrand in the above expression to be finite, we need to apply boundary conditions which fix the complex phase of the MF parameters on two boundary planes i and j of the system to different values φ_i and φ_j. These boundary conditions will result in a finite gradient of the complex phase, which is related to the superfluid velocity, see equation (4.100). In sections 4.3.1 and 4.3.2, we have argued that for a very small phase difference, $|\varphi_i - \varphi_j| \ll 1$, the gradient can be assumed to be constant (or, equivalently, the slope of the phase field is assumed to be linear), which allowed us to extract the phase factor from the single particle Green's functions,

$$G_{ij}(E) = \widetilde{G}_{ij}(E) \times e^{\mathrm{i}(1-\Delta_{avg})(\varphi_i - \varphi_j)}\,, \tag{4.125}$$

where $\widetilde{G}_{ij}$ corresponds to the case without boundary conditions, where $\varphi_i = \varphi_j = 0$. Furthermore, Δ_{avg} is a quantity that depends on the nature of the excitations, see equation (4.117). With this, the expression for the current density can be rewritten as follows,

$$J_{ij} = 4J \sin\phi_{ij} \int_{-\infty}^{0} \frac{\mathrm{d}E}{2\pi}\, \mathrm{Im}\,\tilde{G}^A_{ij}(E)\,, \tag{4.126}$$

with $\phi_{ij} = (1 - \Delta_{avg})(\varphi_i - \varphi_j)$. As we have discussed in the beginning of section 4.3, whether or not the current density is finite is now determined by the mobility edge of the effective single-excitation model. If its spectrum is completely localized, the Green's function will fall off exponentially for all energies E, and the integral will vanish in the limit $|\mathbf{x}_i - \mathbf{x}_j| \to \infty$. If there is, however, an interval with extended states, the integral will be finite and will scale with the system size, see also expressions (4.101) and (4.102). In this case, one finds that the current density is proportional to the gradient of the phase field, as one would expect.

Thus, we now have a recipe to find the boundary between SF and BG phase, which, for a fixed μ/U, is given by the hopping amplitude J/U at which the effective model undergoes the Anderson transition, i.e., when its spectrum becomes completely localized. This concludes this section and we now turn to the numerical evaluation of the theory.

4.4 Numerical Evaluation and Results for Three Dimensions

In this section, we will present all individual steps of the procedure that lets us finally resolve the BG to SF transition. All calculations are performed for three spatial dimensions, $d = 3$. The starting point will be to determine the parameters of the effective Hamiltonian.

4.4.1 Parameters of the Effective Model

The effective single-excitation Hamiltonian was determined to have the following form,

$$\hat{H}_{ex} = \sum_i \Delta\epsilon_i |i\rangle\langle i| + \sum_{\langle ij\rangle} T_{ij} \, |i\rangle\langle j| \tag{4.127}$$

where the parameters are determined by the local excitations $|i\rangle$ and the ground state $|0\rangle$,

$$\Delta\epsilon_i = \langle i|\hat{h}_i|i\rangle - \langle 0|\hat{h}_i|0\rangle \quad \text{and} \quad T_{ij} = \langle i|\delta\hat{H}|j\rangle \, . \tag{4.128}$$

Thus, in order to calculate the parameters of the model, we first need to determine the excited states of the local Hamiltonians $\hat{h}_i$. In section 4.2.4 we have discussed that we will restrict ourselves to the case where we either select only the first excitations or only the second excitations, which we will label by $\alpha = 1$ and $\alpha = 2$, respectively.

Since the on-site energies ε_i of the disordered Bose-Hubbard model are randomly distributed by a distribution function P_ε, the parameters of the effective model will also be randomly distributed. Furthermore, since the excitation energies and the transition elements both depend on the excited state, there will be a correlation between these three quantities. Therefore, in principle one would have to deal with a joint probability distribution $P\big(\Delta\varepsilon, \psi_{0\alpha}, \psi_{\alpha 0}\big)$. However, while it is possible to extend the CPA formalism to models with random hopping amplitudes [84], which is also referred to as off-diagonal disorder (ODD), the self-consistent theory of localization was only derived for the case of random on-site energies, i.e., diagonal disorder without ODD. Without going into detail, as a result of the ODD the self-energy will not be local anymore. This feature, however, was used in the derivation of the self-consistent equation that determines the diffusion coefficient. Hence, in order to include ODD a proper rederivation of the theory is needed. This turns out to be extremely difficult and would eventually require further approximations. Instead, we will introduce an approximation right away that directly allows us to use the self-consistent theory as is. To do so, we will replace the random hopping amplitudes T_{ij} by their disorder-averaged value T_{avg}. This approximation is only justified in the regime of strong disorder where the ratio W/J is large. There, the width of the ODD will be small compared to the width of the diagonal disorder due to the J in expression (4.83) for the effective hopping amplitudes.

Within this approximation, we only need to determine the probability distribution for the excitation energies. Formally we can write

$$P_{\Delta\epsilon}(\Delta\epsilon) = \int \mathrm{d}\varepsilon P_\varepsilon(\varepsilon) \int \mathrm{d}\psi_1 P_\psi(\psi_1) \ldots \int \mathrm{d}\psi_z P_\psi(\psi_z) \delta\big(\Delta\epsilon - \Delta\epsilon(\varepsilon, \psi_1, \ldots, \psi_z)\big) \, , \tag{4.129}$$

where we have used that the local spectrum is determined solely by the local Hamiltonian, which depends on the on-site energy ε and the MF parameters ψ_i on the z nearest neighbor sites. The MF problem was already solved in chapter 3, which provided us with the probability

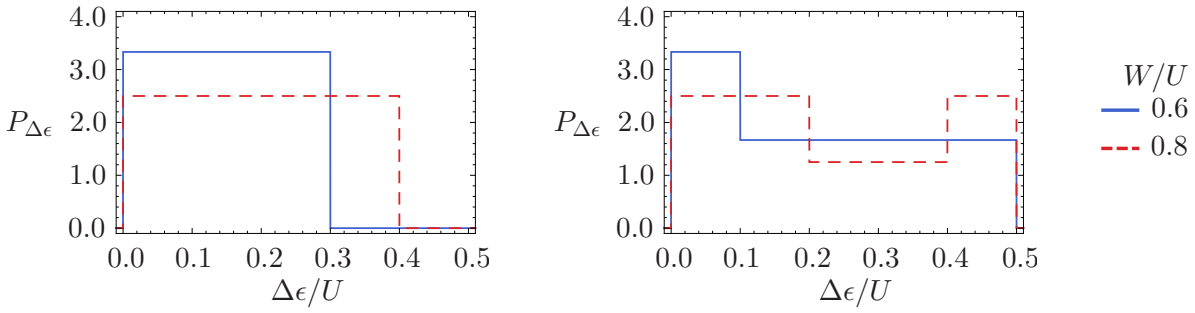

(a) $\mu/U = 1.0$ (b) $\mu/U = 1.2$

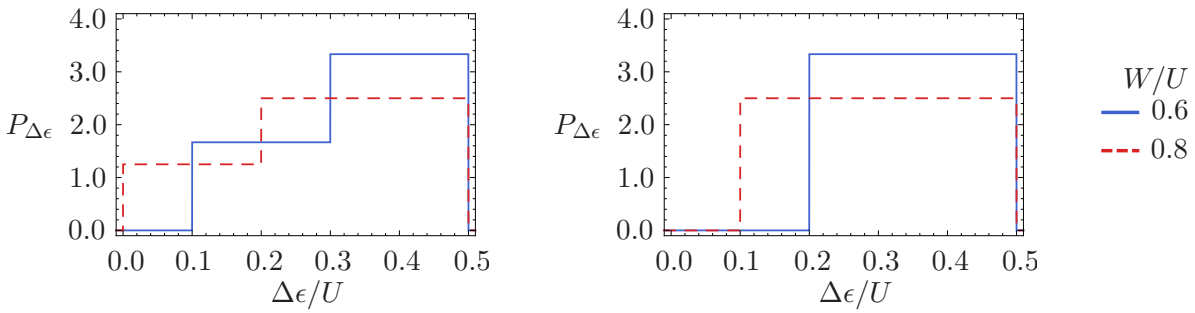

(c) $\mu/U = 1.4$ (d) $\mu/U = 1.5$

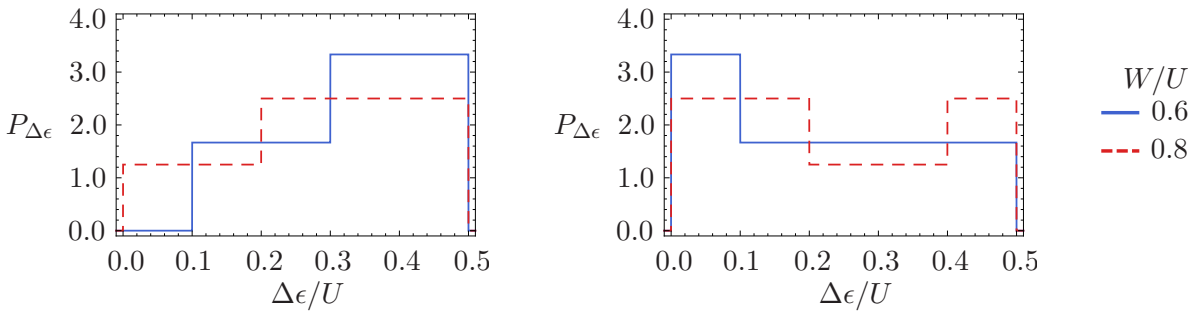

(e) $\mu/U = 1.6$ (f) $\mu/U = 1.8$

Figure 4.2: The excitation energy distribution for $\alpha = 1$ in the atomic limit, $J/U = 0$, for $W/U = 0.6$ (solid blue curve) and $W/U = 0.8$ (dashed red curve).

distribution P_ψ for the MF parameters. Furthermore, the function $\Delta\epsilon(\varepsilon, \psi_1, \ldots, \psi_z)$ gives the excitation energy of the state that was chosen according to the selection criterion for given on-site energy and MF parameters. This, of course, involves diagonalizing the local Hamiltonian, which implies that the probability distribution $P_{\Delta\epsilon}$ has to be determined numerically. Here, we employ the same techniques we already used to determine the MF parameter distribution P_ψ, see also section 3.2.4.

Similar, the disorder-averaged hopping amplitude can be written as

$$\begin{aligned} T_{avg} &= J\big(\overline{\psi^*_{0\alpha_i}\psi_{0\alpha_j}} + \overline{\psi_{\alpha_i 0}\psi^*_{\alpha_j 0}}\big)\,. \\ &= J\big(\overline{\psi^*_{0\alpha_i}}\;\overline{\psi_{0\alpha_j}} + \overline{\psi_{\alpha_i 0}}\;\overline{\psi^*_{\alpha_j 0}}\big)\,. \\ &\equiv J\Big(\big(\overline{\psi_{0\alpha}}\big)^2 + \big(\overline{\psi_{\alpha 0}}\big)^2\Big)\,, \end{aligned} \tag{4.130}$$

with the disorder-averaged transition parameters

$$\overline{\psi_{0\alpha}} = \int \mathrm{d}\varepsilon P_\varepsilon(\varepsilon) \int \mathrm{d}\psi_1 P_\psi(\psi_1) \ldots \int \mathrm{d}\psi_z P_\psi(\psi_z)\; \psi_{0\alpha}(\varepsilon, \psi_1, \ldots, \psi_z) \tag{4.131}$$

and

$$\overline{\psi_{\alpha 0}} = \int \mathrm{d}\varepsilon P_\varepsilon(\varepsilon) \int \mathrm{d}\psi_1 P_\psi(\psi_1) \ldots \int \mathrm{d}\psi_z P_\psi(\psi_z)\; \psi_{\alpha 0}(\varepsilon, \psi_1, \ldots, \psi_z)\,, \tag{4.132}$$

where we have used that expectation values of observables from different lattice sites factorize within the MF theory, see also section 3.2.4. Again, the functions $\psi_{0\alpha}(\varepsilon, \psi_1, \ldots, \psi_z)$ and $\psi_{\alpha 0}(\varepsilon, \psi_1, \ldots, \psi_z)$ give the transition elements for the excited state $|\alpha\rangle$ that was chosen according to the selection criterion (i.e., either always the first or the second excited state) for given input parameters ε and $\psi_1, \ldots, \psi_z$. Also, the excited states are fixed such that the transition parameters all have the same algebraic sign, which is possible as we have discussed in section 4.2.4.

It is useful to first consider the atomic limit, $J/U = 0$. Here, the distribution $P_{\Delta\epsilon}$ can be derived analytically. By comparing the Fock state energies E_n, we already found that the ground state occupation number n_g is determined by

$$n_g < (\mu - \varepsilon)/U < n_g + 1\,, \tag{4.133}$$

see also section 3.1.2. Similar, one finds that for $(\mu - \varepsilon)/U \in (n_g, n_g + 1/2)$ the first excited state is given by $|n_g - 1\rangle$, whereas for $(\mu - \varepsilon)/U \in (n_g + 1/2, n_g + 1)$ it is given by $|n_g + 1\rangle$. Accounting for all possible cases and considering that for $n_g = 0$ only the state $|n_g + 1\rangle$ exists, one finds

$$\begin{aligned} P_{\Delta\epsilon}(\Delta\epsilon) = \frac{1}{W}\Big[&\theta\big(\Delta\epsilon\big)\theta\big(W/2 - \mu - \Delta\epsilon\big) \\ &+ \sum_{n=1}^{\infty}\Big(\theta\big(\Delta\epsilon - \max[0, \mu - W/2 - n]\big)\theta\big(\min[1/2, \mu + W/2 - n] - \Delta\epsilon\big) \\ &\quad + \theta\big(\Delta\epsilon - \max[0, n + 1 - \mu - W/2]\big)\theta\big(\min[1/2, n + 1 - \mu + W/2] - \Delta\epsilon\big)\Big)\Big]\,. \end{aligned} \tag{4.134}$$

Let us concentrate on the case $W/U < 1$ and $\mu/U > 0$. Here, the atomic limit distributions are

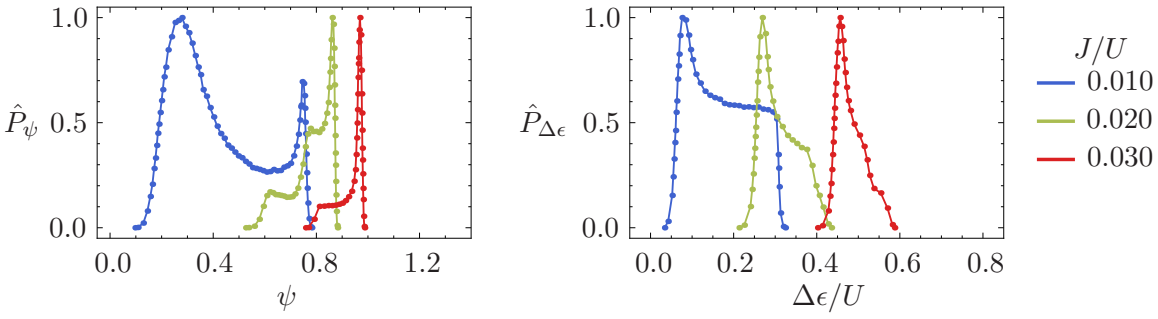

(a) $\mu/U = 1.0$

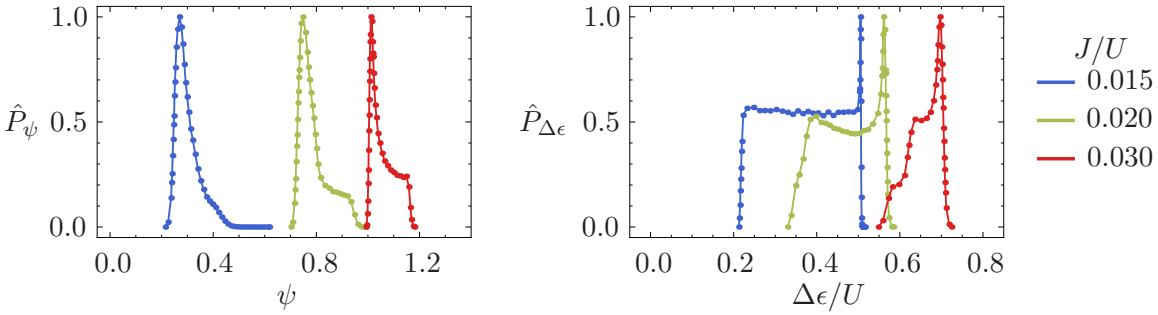

(b) $\mu/U = 1.5$

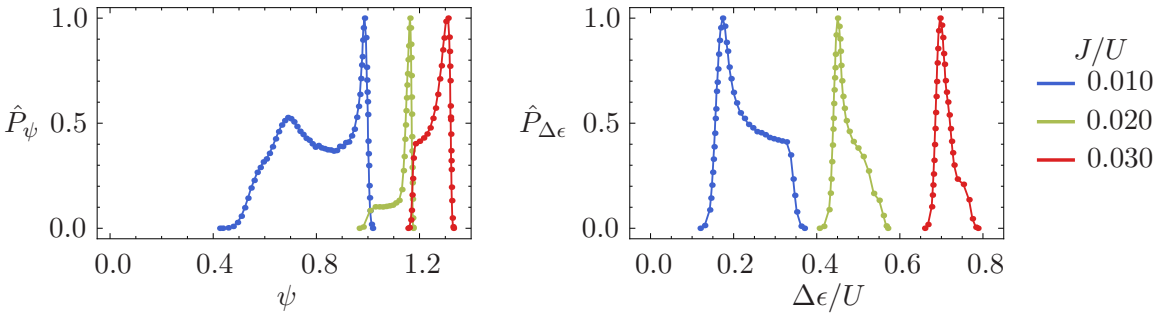

(c) $\mu/U = 2.0$

Figure 4.3: The left column shows the distribution of the MF parameter, the right column the distribution of the excitation energies for the first excited states, for different values of μ/U, J/U and fixed disorder $W/U = 0.6$. All distribution functions are normalized to their maximal value, $\hat{P}_x(x) = P_x(x)/\max\{P_x(x)\}$.

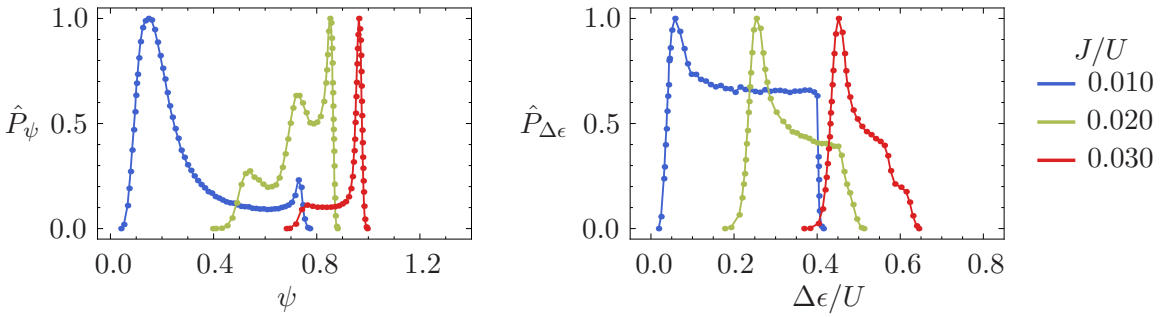

(a) $\mu/U = 1.0$

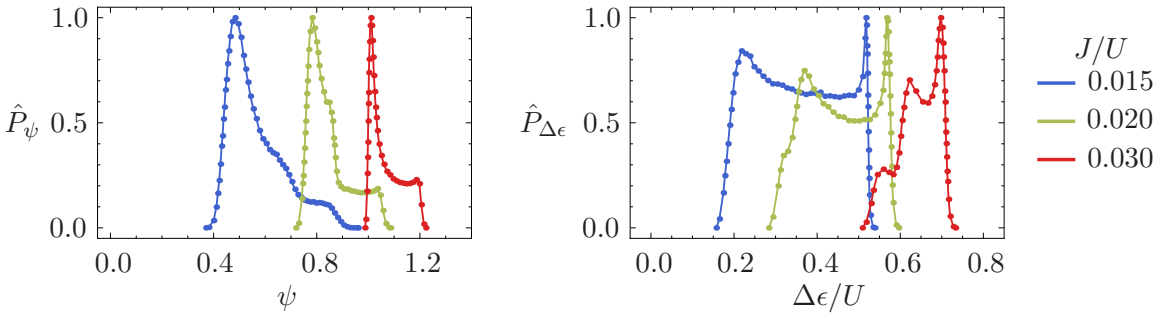

(b) $\mu/U = 1.5$

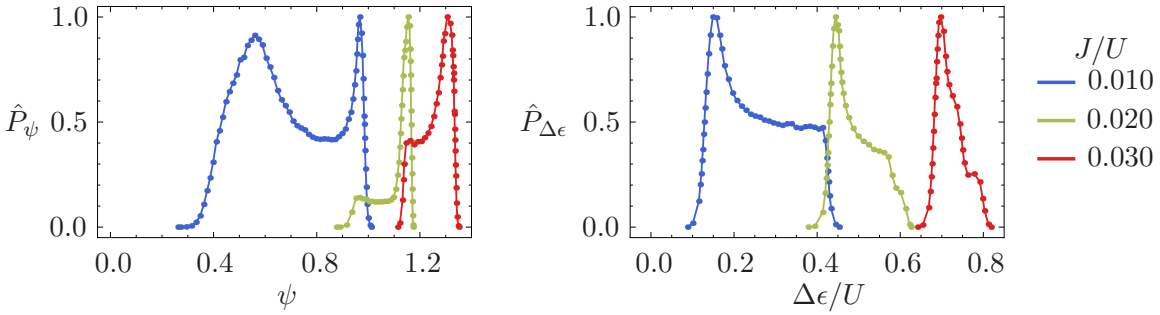

(c) $\mu/U = 2.0$

Figure 4.4: The same plots as in figure 4.3, but now for a different disorder $W/U = 0.8$.

restricted to the energy interval $\Delta\epsilon \in [0, 1/2]$ and are invariant under a shift of the chemical potential by the interaction strength, $\mu/U \to \mu/U + 1.0$. Hence, we can restrict ourselves to considering the distribution for $\mu/U \in [1.0, 2.0]$, see figure 4.2. For $\mu/U = 1.0$ and $\mu/U = 1.5$, $P_{\Delta\epsilon}$ has a width of $W/2$. For the intermediate cases, the width varies between $W/2$ and $1/2$. Furthermore, the effective distribution is always broader for the larger initial disorder width W/U. With this, we can now turn to the general case, $J/U > 0$.

Figures 4.3 and 4.4 show the numeric results for the distribution function $P_{\Delta\epsilon}$ for different values of μ/U, J/U, and W/U for the first excitation band. Also, the corresponding distribution functions P_ψ for the MF parameter are depicted, which were calculated previously and are used to evaluate the integration in (4.129). As always, the on-sites energies ε_i of the initial model are distributed uniformly in the interval $[-W/2, +W/2]$.

The first thing one notices is that the larger the hopping amplitude, the more the excitation energies are shifted towards higher energies. Furthermore, if the average MF parameter $\overline{\psi}$ gets small, $P_{\Delta\epsilon}$ approaches the box-like shape of the atomic limit distributions. For larger J/U and $\overline{\psi}$, this box-like shape gets more and more washed out and at the same time the width of the distribution decreases.

Comparing $\mu/U = 1.0$ and $\mu = 2.0$, we see that the width of the effective distribution is smaller for the larger chemical potential. Furthermore, at $\mu/U = 1.5$, i.e., above the second Mott lobe, the width is increased compared to the two other cases, where the system is in between two Mott lobes. This tells us that the actual shape of the effective distribution depends on the properties of the system in a rather non-trivial way. For example, larger MF parameters can lead to a smaller width of $P_{\Delta\epsilon}$, but do not necessarily need to. Finally, comparing the results for $W/U = 0.6$ and $W/U = 0.8$ in figure 4.3 and 4.4, respectively, we again see that, in general, the larger disorder width leads to a larger width of the effective distribution $P_{\Delta\epsilon}$, as one would expect from the atomic limit results,

Next, in figure 4.5 the distributions for the first and the second excited states are compared for different model parameters. We see that the distribution function for the second excitation band is, in general, more box-like. Again, this can be understood by looking at the eigenstates and the local Fock energies E_n, see figure 4.1. The energies E_n increase quadratically with n when going away from the minimum of the potential. The coupling between the particle numbers, however, increases only with the square root of n, which is therefore suppressed. As a consequence, the higher the excitation, the more it will approach the form of a Fock state. Thus, the effective distributions $P_{\Delta\epsilon}$ for the higher excited states will tend to look more like they would in the atomic limit, i.e., like a composite of boxes.

Furthermore, we see that the energies of the first and the second excitation band are separated. One might think that due to the random on-site energies, there can be second excitations that have a lower excitation energy than first excitations on other sites. However, this is obviously not the case and can be understood best when going again to the atomic limit, $J/U = 0$. Since the on-site energy effectively acts as a local shift of the chemical potential, we can consider the ordered case with $\varepsilon_0 = 0$ for variable μ/U. Again, the ground state particle number n_g is determined by

$$\mu/U < n_g < \mu/U + 1\,. \tag{4.135}$$

For the adjacent particle numbers, we have

$$E_{n_g+1} - E_{n_g} = -\mu + n_g U > 0 \quad \text{and} \quad E_{n_g-1} - E_{n_g} = \mu - (n_g - 1)U > 0\,. \tag{4.136}$$

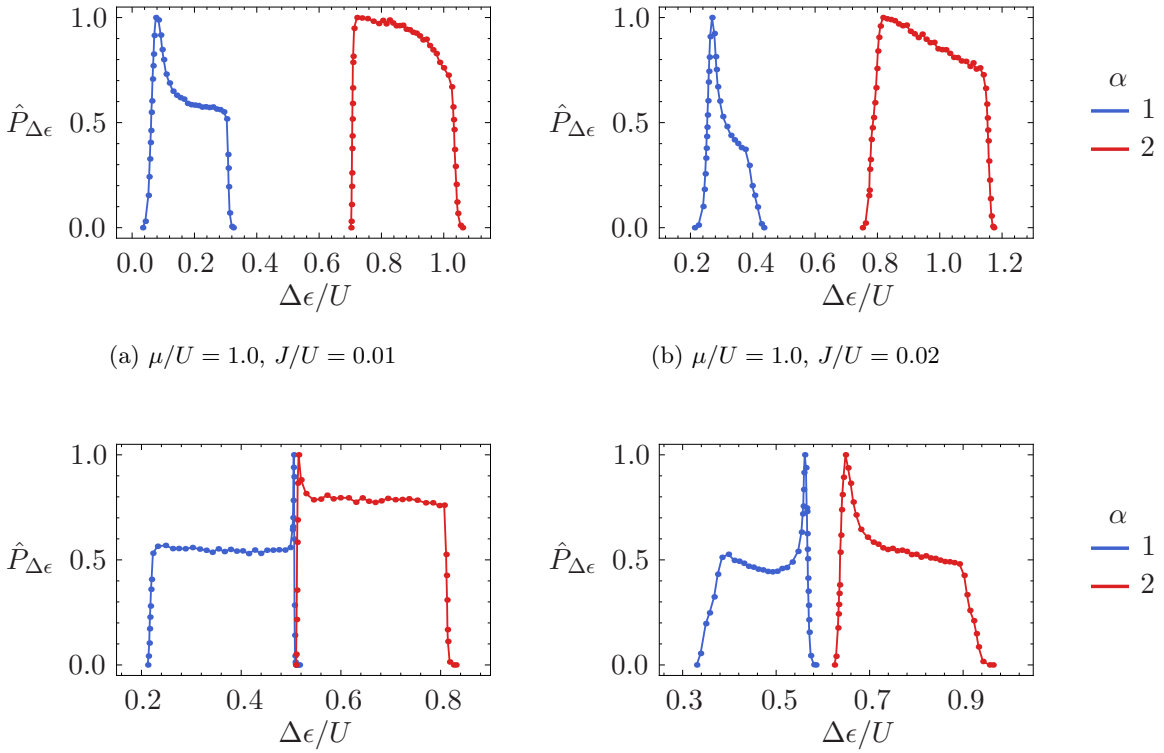

(a) $\mu/U = 1.0$, $J/U = 0.01$

(b) $\mu/U = 1.0$, $J/U = 0.02$

(c) $\mu/U = 1.5$ $J/U = 0.015$

(d) $\mu/U = 1.5$ $J/U = 0.02$

Figure 4.5: Comparison between the effective distributions for the first (blue curve) and the second excitation band (red curve) for $W/U = 0.6$ and different values of μ/U and J/U. Again, the distributions are normalized to their maximal value.

The excitation energies are exactly the same when $\mu/U = n_g - 1/2$, i.e., when the minimum of E_n is located at integer $n = n_g$,

$$E_{n_g+1} - E_{n_g} = E_{n_g-1} - E_{n_g} = U/2\,. \tag{4.137}$$

Going away from this point, one gets

$$E_{n_g\pm1} - E_{n_g} = U/2 \mp (\mu/U - n_g + 1/2)U\,. \tag{4.138}$$

Thus, away from the degenerated point the first excited state always has an excitation energy smaller than $U/2$ and the second excited state an excitation energy larger than $U/2$.

When the hopping is switched on, $J/U > 0$, the coupling between the particle numbers will result in a repulsion of the energy levels, yielding a larger gap between the first and the second excitations. This can be seen best in figure 4.5c and 4.5d. For smaller hopping, when the system is in the vicinity of the second Mott lobe, the two distributions are very close in energy, whereas for the larger hopping they start to separate. Hence, it is justified to categorize the excitations into two bands within the MF theory or, equivalently, the *atomic limit* of our effective model, i.e., $T_{avg} = 0$.

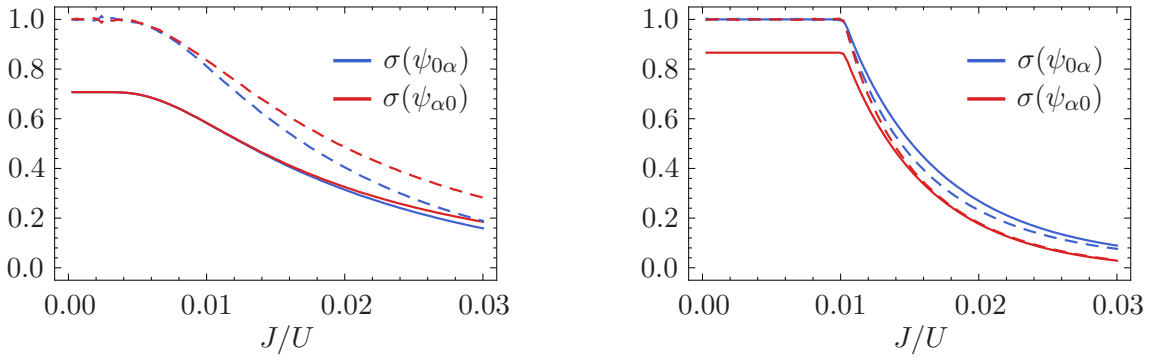

(a) $\mu/U = 1.0$ (b) $\mu/U = 2.5$

Figure 4.6: The standard deviation $\sigma(x)$ of the transition parameters $x = \psi_{0\alpha}, \psi_{\alpha 0}$ for $W/U = 0.6$ and $\alpha = 1$ as a function of the hopping amplitude J/U. The dashed curves show the corresponding relative error, $\sigma(x)/\bar{x}$.

Now, let us investigate the behavior of the average hopping amplitude. In figure 4.6 the standard deviation $\sigma(x) = \left(\overline{x^2} - \bar{x}^2\right)^{1/2}$ for $x = \psi_{0\alpha}, \psi_{\alpha 0}$ is plotted for $\mu/U = 1.0$ and $\mu/U = 2.5$, i.e., once between two Mott lobes and once above one Mott lobe. In principle, both cases show the same behavior, that is, the standard deviation gets larger for smaller J/U. For $\mu/U = 2.5$, the values remain constant once the system enters the Mott lobe at $J/U \simeq 0.01$. Within a Mott lobe, the local Hamiltonian $\hat{h}_i$ is independent of the hopping amplitude and diagonalization will always yield the atomic limit result.

Concerning the validity of our theory, these are actually good news. The error we make by averaging over the hopping amplitudes will be the largest when the hopping is small and the diagonal disorder is the dominating term. For larger hopping, when the kinetic terms becomes more and more important, the error we make by neglecting the ODD gets smaller. Still, the relative error becomes quite large for small J/U and reaches one in the atomic limit. However, this is an approximation we have to make in order to be able to continue with this theory. In figure 4.7 the effective hopping T_{avg} is shown as a function of the initial or *bare* hopping amplitude J/U for various different parameters. For $\alpha = 1$, the effective hopping increases when the bare hopping is increased. Also, in principle T_{avg} is larger for larger μ/U, as a larger chemical potential implies higher filling ρ, see figures 4.7a and 4.7b. However, this is not always the case as can be seen when comparing the curves for $\mu/U = 1.2$ and $\mu/U = 1.4$ in figure 4.7c. Here, the larger chemical potential puts the system above the second Mott lobe, which leads to a reduced effective hopping. Furthermore, in figure 4.7b we can see that the slope of T_{avg} as a function of J/U is slightly increased once the system leaves the MI phase. Within the MI phase, the filling of the lattice is constant, and therefore, T_{avg} increases linearly with J/U. Outside the Mott lobes, the filling (in general) increases with J/U for constant μ/U, see also figure 3.12, leading to a non-trivial dependence of T_{avg} on J/U and an increased slope.

For $\alpha = 2$, shown in figure 4.7d, the behavior is quite different as at some point the growth of the effective hopping T_{avg} is slowed down. Eventually, T_{avg} even decreases slightly when J/U is increased. As we will see later, this will have a rather drastic effect on the behavior of the mobility edges for $\alpha = 2$ as compared to $\alpha = 1$.

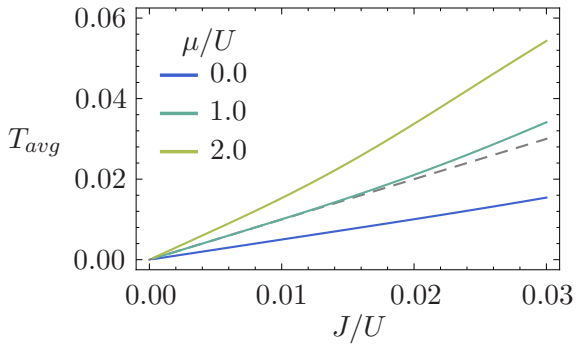

(a) $W/U = 0.6$, $\alpha = 1$

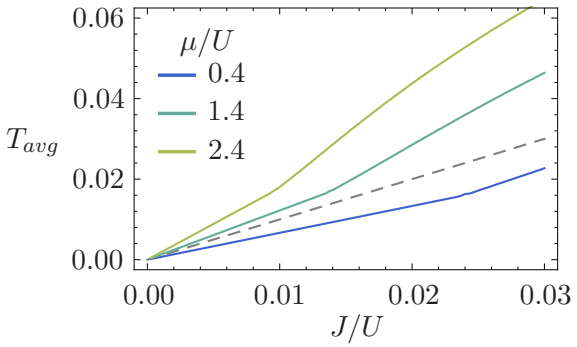

(b) $W/U = 0.6$, $\alpha = 1$

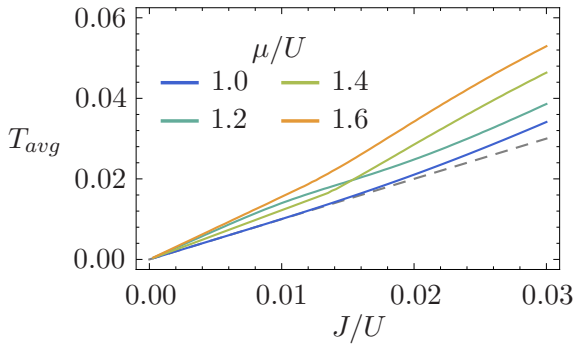

(c) $W/U = 0.6$, $\alpha = 1$

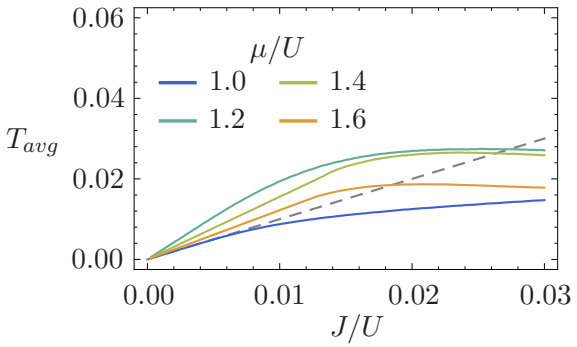

(d) $W/U = 0.6$, $\alpha = 2$

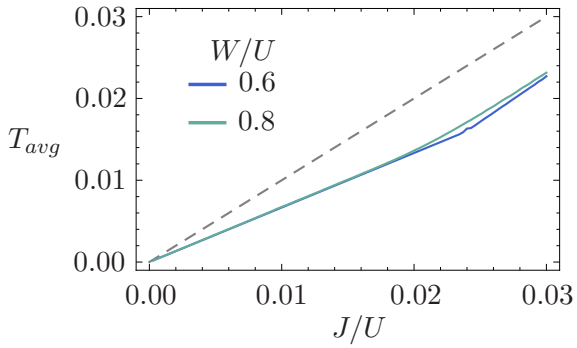

(e) $\mu/U = 0.4$, $\alpha = 1$

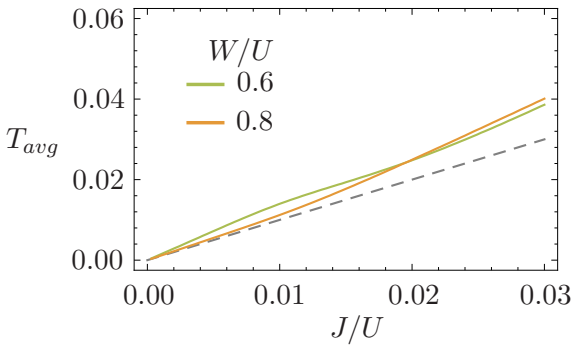

(f) $\mu/U = 1.2$, $\alpha = 1$

Figure 4.7: The disorder-averaged effective hopping amplitude T_{avg} as a function of J/U for different values of W/U, μ/U, and α. T_{avg} is always given in units of the repulsion strength U. The gray dashed line gives the bare hopping, $T_{avg} = J/U$.

Finally, in figures 4.7e and 4.7f we compare T_{avg} for two different disorder strengths, $W/U = 0.6$ and $W/U = 0.8$. For $\mu/U = 0.4$, both systems are in the MI phase for small hopping, and the curves for T_{avg} are practically the same. The system with the larger disorder width leaves the MI phase at smaller hopping, $J/U \simeq 0.020$, see also figure 3.13. At this point, the two curves separate and the effective hopping becomes larger for larger W/U. At $J/U \simeq 0.024$ also the other system leaves the MI phase and the two curves approach each other again.

For $\mu/U = 1.2$, the situation is first reversed with T_{avg} being larger for the smaller W/U. At some point, $J/U \simeq 0.02$, the two curves intersect and T_{avg} is again larger for the larger disorder width.

To sum up the above, the behavior of both $P_{\Delta\epsilon}$ and T_{avg} is rather complex and varies from parameter set to parameter set. The properties of the effective model will depend on the interplay of the two quantities. In order to avoid getting lost in the details, at this point we stop the discussion and will now move on with the numerical evaluation.

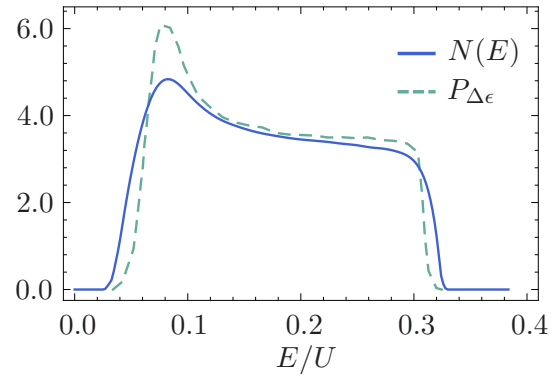

(a) $J/U = 0.010$

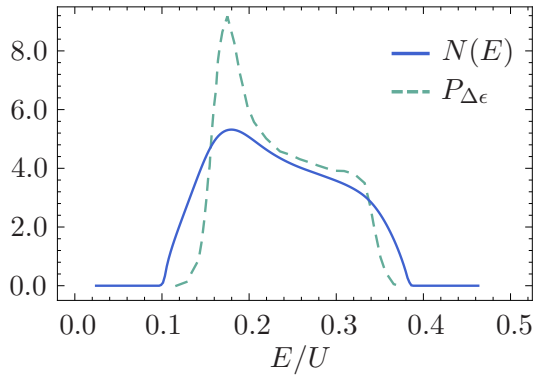

(b) $J/U = 0.015$

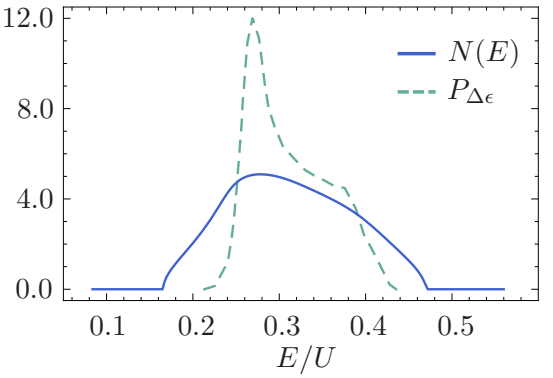

(c) $J/U = 0.02$

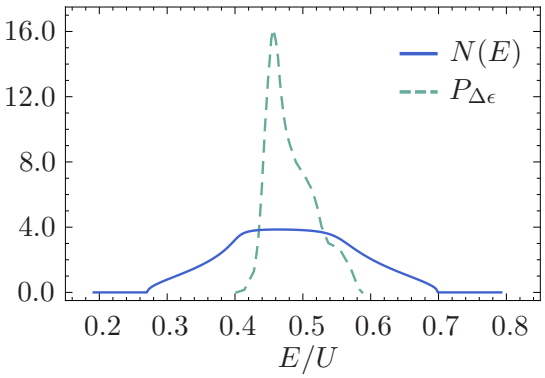

(d) $J/U = 0.030$

Figure 4.8: The CPA DOS $N(E)$ (solid curve) and the underlying energy distribution $P_{\Delta\epsilon}$ (dashed curve) of the first excitation band, for $W/U = 0.6$, $\mu/U = 1.0$, and different hopping amplitudes.

4.4.2 Density of States within the Coherent Potential Approximation

In order to use the self-consistent theory of localization, one first needs to determine the disorder-averaged single-particle Green's function. As already mentioned several times, this will be done employing the coherent potential approximation (CPA). In appendix B.3, starting from the Anderson Hamiltonian the following CPA conditional equation is derived,

$$\int \mathrm{d}\varepsilon P_\varepsilon(\varepsilon) \frac{\varepsilon - \Sigma(E)}{1 - \langle G(E)\rangle\big(\varepsilon - \Sigma(E)\big)} \stackrel{!}{=} 0\,, \tag{4.139}$$

with the disorder-averaged local Green's functions $\langle G(E)\rangle = \langle G_{ii}(E)\rangle$ and the self-energy $\Sigma(E)$. The local Green's function is calculated from the disorder-averaged Green's functions in momentum space,

$$\langle G(E)\rangle = \frac{1}{N_i}\sum_{\mathbf{p}} \langle G_{\mathbf{p}}(E)\rangle\,, \tag{4.140}$$

with

$$\langle G_{\mathbf{p}}(E)\rangle = \frac{1}{E - \varepsilon_{\mathbf{p}} - \Sigma(E)} \tag{4.141}$$

and the free lattice dispersion $\varepsilon_{\mathbf{p}} = -2J\sum_{a=1}^{d}\cos p_a$. To apply the CPA formalism to our effective Hamiltonian, we only need to replace $P_\varepsilon \to P_{\Delta\epsilon}$ and $J \to T_{avg}$. Equation (4.139) is then solved self-consistently as outlined at the end of appendix B.3.

Once the self-energy $\Sigma^{R/A}(E) = \Sigma(E \pm \mathrm{i}\eta)$ is determined for a given energy $E \in \mathbb{R}$, one can calculate the density of states (DOS)

$$N(E) = \mp\frac{1}{\pi}\,\mathrm{Im}\langle G^{R/A}(E)\rangle = \mp\frac{1}{\pi}\,\mathrm{Im}\langle G(E \pm \mathrm{i}\eta)\rangle\,. \tag{4.142}$$

Figure 4.8 shows a comparison of the CPA DOS and the corresponding effective disorder distribution $P_{\Delta\epsilon}$ for fixed $W/U = 0.6$, $\mu/U = 1.0$ and different hopping amplitudes. For small J/U, $N(E)$ has more or less the same shape as $P_{\Delta\epsilon}$. This is to be expected, as a small hopping implies a small effective hopping T_{avg}, and for $T_{avg} = 0$ the density of states equals the disorder distribution. However, due to the finite hopping, the DOS is broadened compared to the disorder distribution.

When J/U is increased, the DOS gets broader and broader and the features of the underlying disorder distribution start to disappear. For $J/U = 0.03$, the DOS has almost completely taken the form of the bare DOS for a pure lattice system. The disorder width is roughly ~ 0.2, whereas the bare DOS would have a width of $\sim 4dJ = 0.36$ (see section 2.1.1), assuming the transition amplitudes being of the order $\mathcal{O}(1)$. This is already the regime where the kinetic term is dominating the disorder term of our effective model and where the approximation $T_{ij} \to T_{avg}$ is not really justified anymore. However, we will see later that the mobility edge is located at smaller hopping, i.e., where the approximation is still applicable.

Figure 4.9 now shows the CPA DOS for both the first and the second excitation band. For $\mu/U = 1.0$, we see that the effect of the hopping is much smaller for the higher band. Furthermore, they remain well separated, unlike for $\mu/U = 1.5$, where the DOS of both *bands* overlap, i.e., one cannot identify two single bands anymore. At this point, one might question the validity of the selection scheme, which strictly separates the first and the second excited states.

Finally, we want to point out one feature of the CPA that is apparent in all plots of the DOS. When performing the calculations, we scan over all energies E within the true upper and lower

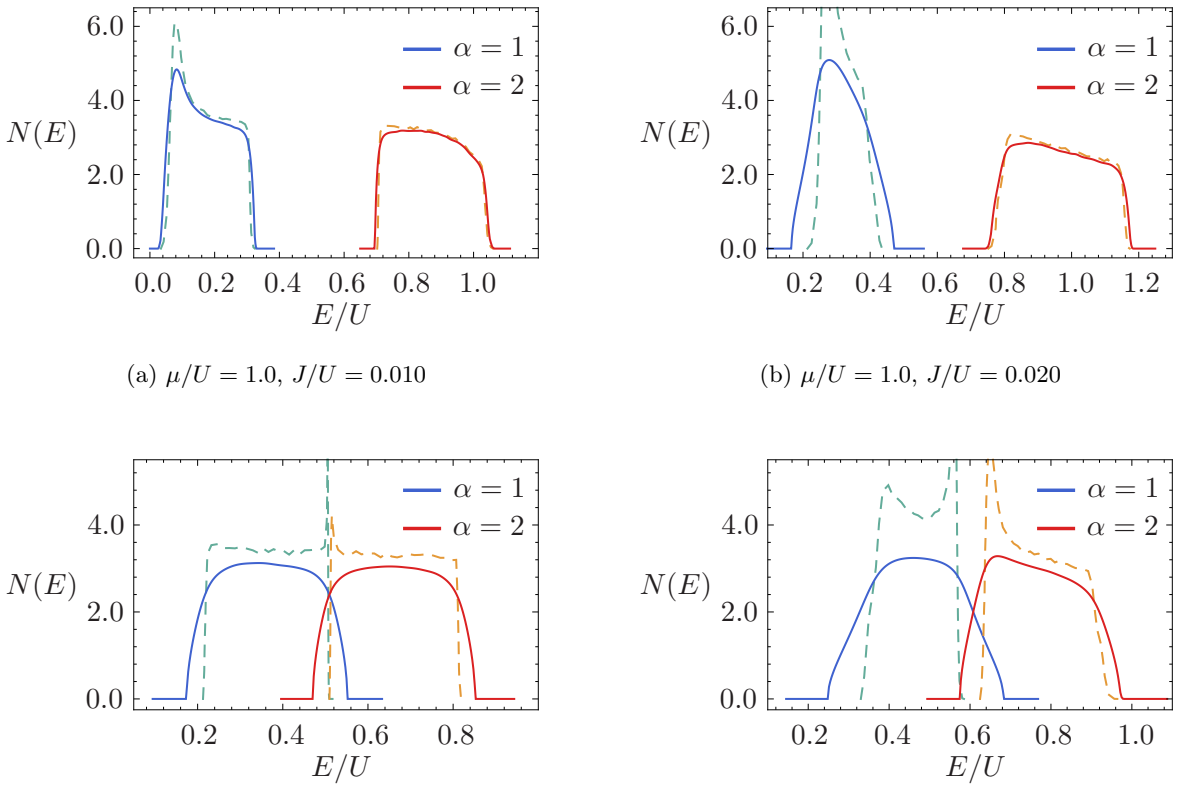

(a) $\mu/U = 1.0$, $J/U = 0.010$

(b) $\mu/U = 1.0$, $J/U = 0.020$

(c) $\mu/U = 1.5$, $J/U = 0.015$

(d) $\mu/U = 1.5$, $J/U = 0.020$

Figure 4.9: The CPA DOS $N(E)$ (solid curves) of the first ($\alpha = 1$) and second ($\alpha = 2$) excitation band, for $W/U = 0.6$, and different values for μ/U and J/U. The dashed curves show the corresponding disorder distributions $P_{\Delta\epsilon}$, see also figure 4.5.

boundaries of the DOS, i.e. $E \in [E_{min}, E_{max}]$ with $E_{min/max} = \Delta\epsilon_{min/max} \mp 2d\,T_{avg}$ (see also section 2.2.3). The CPA DOS, however, is only finite within a smaller interval and vanishes before reaching E_{min} and E_{max}. This is a result of the *single-site approximation* used for the CPA, which basically neglects correlations between different sites, see appendix B.3. Therefore, the CPA is not capable of resolving the highly correlated Lifshitz regions and thus, also not the Lifshitz tails of the true DOS. For the problem of finding the Anderson transition, however, this will not matter as the Lifshitz tails are always localized, see also figure 2.7 in section 2.2.7.

4.4.3 The Diffusion Coefficient and the Localization Length

In section 2.2.7 as well as in appendix B.4, the self-consistent theory of localization was introduced as an approximative method that allows for the calculation of disorder-averaged correlation functions. The theory leads to the definition of a generalized diffusion coefficient $D(E, \omega)$,

which is determined by the self-consistent equation

$$\lim_{\omega\to 0} D(E,\omega) = D_0(E) + \frac{2\,\mathrm{Im}\,\Sigma^A(E)}{[\pi N(E)]^2 D_0(E)} \frac{1}{(N_i)^2} \sum_{\mathbf{p}\mathbf{p}'} (\mathbf{v}_p \cdot \hat{\mathbf{q}}) \frac{\mathrm{Im}\left\{\langle G^A_{\mathbf{p}}(E)\rangle \langle G^A_{\mathbf{p}'}(E)\rangle^2\right\}}{(\mathbf{p}+\mathbf{p}')^2 + 1/\xi(E)^2} (\mathbf{v}_{p'} \cdot \hat{\mathbf{q}}) \,, \tag{4.143}$$

and is related to the localization length $\xi(E)$ via

$$\xi(E) = \lim_{\omega\to 0} \sqrt{-\frac{D(E,\omega)}{\mathrm{i}\omega}} \,. \tag{4.144}$$

In the localized regime, the localization length is finite and the diffusion vanishes, $\xi(E) < \infty$ and $D(E) \equiv \lim_{\omega\to 0} D(E,\omega) = 0$, whereas in the extended regime one has $\xi(E) = \infty$ and $D(E) > 0$. The method we use to evaluate conditional equation (4.143) is presented in appendix B.4.2.

In figure 4.10 both $D(E)$ and $\xi(E)$ are plotted for different J/U, fixed $W/U = 0.6$ and $\mu/U = 1.0$, each time for the first excitation band. The corresponding CPA DOS can be found in figure 4.8.

For $J/U = 0.01$ in figure 4.10a, the diffusion coefficient vanishes across the whole band, and consequently, the localization length stays finite for all energies. Thus, the effective model is in the localized regime. This implies that the disordered Bose-Hubbard model is in the BG phase and no long-range SF current is possible. Moreover, with a maximal localization length of $\xi \simeq 1.5$, the system is deeply localized and the current decays very rapidly. Note that the localization length has two peaks, one at each end of the spectrum, which is plotted in figure 4.8a. The lower peak is more pronounced, which is a consequence of the larger DOS for these energies. This is actually in accordance with results for the original Anderson Hamiltonian with a box distribution [63], which show a similar profile for ξ as a function of the energy.

In figure 4.10b, the same quantities are shown for a larger hopping $J/U = 0.015$. Here, we observe a region in energy with finite diffusion and infinitely large ξ, bound by the two mobility edges. Outside this region, the diffusion vanishes and the localization length is finite, $\xi < \infty$. When approaching the mobility edges from within the localized regions, the localization length diverges, $\xi \to \infty$. Similar, the diffusion vanishes when approaching the mobility edges from within the diffusive (or extended) region. Since the spectrum is not completely localized, long-ranged current is possible and the system is in the SF phase.

Finally, in figure 4.10c the results for even larger hopping is shown, $J/U = 0.02$, where almost the entire spectrum (excluding the Lifshitz tails) is in the diffusive regime, $D(E) > 0$. The upper mobility edge is very close to the upper boundary of the CPA DOS and the divergence of the localization length happens within a very small region in energy. Moreover, the lower mobility edge coincides with the lower boundary of the CPA DOS, i.e., the lower localized region is not resolved.

Now that we have discussed some typical cases for the localization length and the diffusion coefficient for fixed parameters, we will move on to investigate the dependence of these quantities on the parameters of the disorder Bose-Hubbard model. As the Anderson transition can be described either by $D(E)$ or $\xi(E)$ alone, it is sufficient to take only one of them into account. We will restrict ourselves to the diffusion coefficient in the following sections, as it is easier to calculate than the localization length.

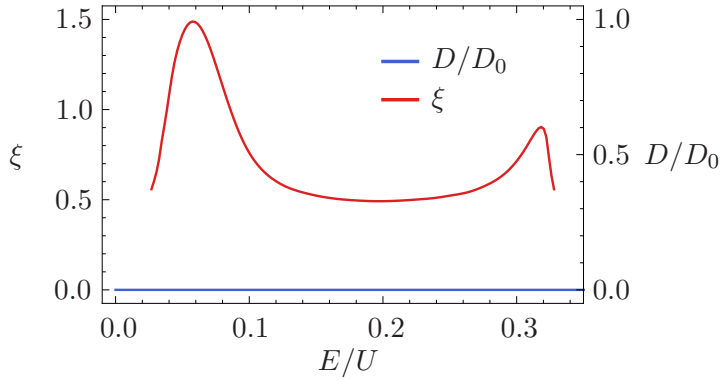

(a) $J/U = 0.010$

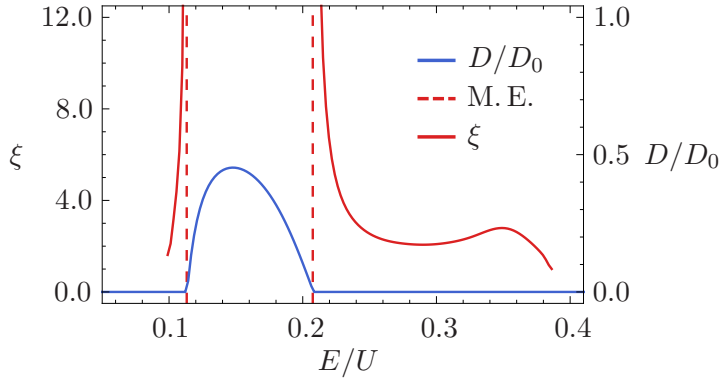

(b) $J/U = 0.015$

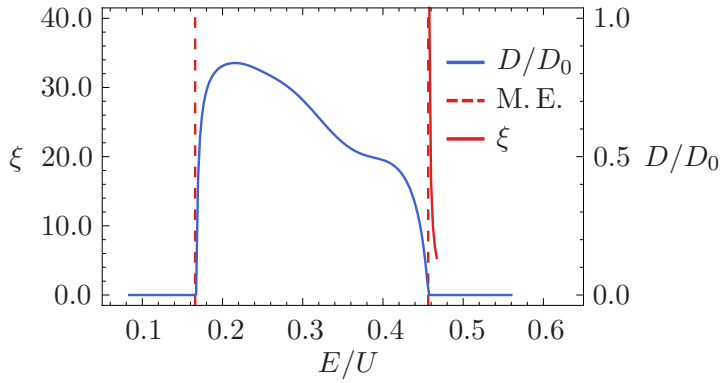

(c) $J/U = 0.020$

Figure 4.10: The localization length $\xi(E)$ and the diffusion coefficient $D(E)$ (normalized by the bare diffusion $D_0(E)$), shown for $W/U = 0.6$, $\mu/U = 1.0$, and different hopping amplitudes J/U. The dashed red lines show the mobility edges (M.E.) of the spectrum. All plots are for the first excitation band, $\alpha = 1$. See figure 4.8 for the corresponding CPA DOS.

4.4.4 Density of States and Diffusion as Functions of the Hopping Amplitude

As discussed in section 2.3.3, the SF to BG transition will be triggered by increasing the strength of the disorder. If the width of the disorder distribution W/U is kept constant, the parameter that has to be varied is the hopping amplitude J/U. For each value of the chemical potential we will then find one critical hopping amplitude at which the effective model undergoes the Anderson transition, i.e., from $D(E) = 0$ for all E to $D(E) > 0$ for some E as shown in figures 4.10a and 4.10b, respectively. This implies that, in principle, for each J/U one has to take into account the full spectrum of the effective model. Before searching for this transition across the whole parameter space of the Bose-Hubbard model, we first will investigate the behavior of the CPA DOS and the diffusion coefficient as functions of J/U for some typical cases of μ/U.

Figure 4.11 shows both quantities for $W/U = 0.6$ and different values of μ/U for the first excitation band, $\alpha = 1$. For $\mu/U = 1.0$ and $\mu/U = 2.0$, i.e., between two Mott lobes, the CPA DOS $N(E)$ first narrows and then broadens again when the hopping amplitude is increased. This is a result of two competing mechanisms. On the one hand, in section 4.4.1 we have seen that the width of the effective energy distribution $P_{\Delta\epsilon}$ gets smaller when J/U is increased. On the other hand, the width of the free lattice DOS increases linearly with J/U. At some point, the broadening due to the kinetic part of the Hamiltonian becomes dominant over the narrowing due to the decreasing width of the disorder distribution.

Furthermore, the lower boundary of $N(E)$ is shifted towards higher energies E when J/U is increased. When J/U is increased, the coupling between the local Fock states in Hamiltonian $\hat{h}_i$ is increased as well, see expression (3.39). As a result, the splitting of the local levels increases, leading to a larger gap between the ground state and the excited states.

For $\mu/U = 1.5$, i.e., above the second Mott lobe, the behavior is a bit different. For $J/U \lesssim 0.014$, the system is in the MI phase (according to the stochastic MF theory, see section 3.2.3). Consequently, all MF parameters vanish, $P_\psi(\psi) = \delta(\psi)$, and the equation (4.129) for $P_{\Delta\epsilon}$ always yields the atomic limit result, independent of the actual J/U. When the hopping is increased, $P_{\Delta\varepsilon}$ remains the same and only T_{avg} is increased. Consequently, the width of $N(E)$ increases monotonically and the lower boundary first shifts towards smaller E. Once the system has left the MI phase, the gap begins to grow due to the same mechanisms as described above.

At this point one might ask why the MI phase is considered at all when determining the BG to SF transition. An integral step for deriving the SF current was applying a gradient to the complex phase of the MF parameters via boundary conditions, see section 4.3.1. In MI phase, where all ψ vanish, this is, of course, not possible, and thus, no finite SF current is possible. Therefore, by construction the transition to the SF phase will take place outside the Mott lobes.

Still, the effective model can also be defined within the MI phase. Of course, here the approximation of averaging over the transition amplitudes, $T_{ij} \to T_{avg}$ is not a very good one anymore. The simple reason for this is that the excitations can be either $|n_g + 1\rangle$ or $|n_g - 1\rangle$, with n_g being the ground state particle number. These states are completely decoupled, $T_{ij} = 0$ for $|i\rangle = |n_g \pm 1\rangle$ and $|j\rangle = |n_g \mp 1\rangle$. The first excitation band (as well as the second) will consist of both types of states. By replacing the hopping amplitudes with the disorder-average, we couple states that are actually decoupled.

However, as we have discussed in section 3.2.3, the stochastic MF theory is not capable of resolving the true shape of the Mott lobes as it cannot reproduce the rare Lifshitz regions. As a result, numerically we obtain $P_\psi(\psi) = \delta(\psi)$ already before the system actually enters the MI phase. In order to take this *Lifshitz regime* also into account, we extend the numerical calculations to these regions, where we approximate the real MF parameter distribution by the

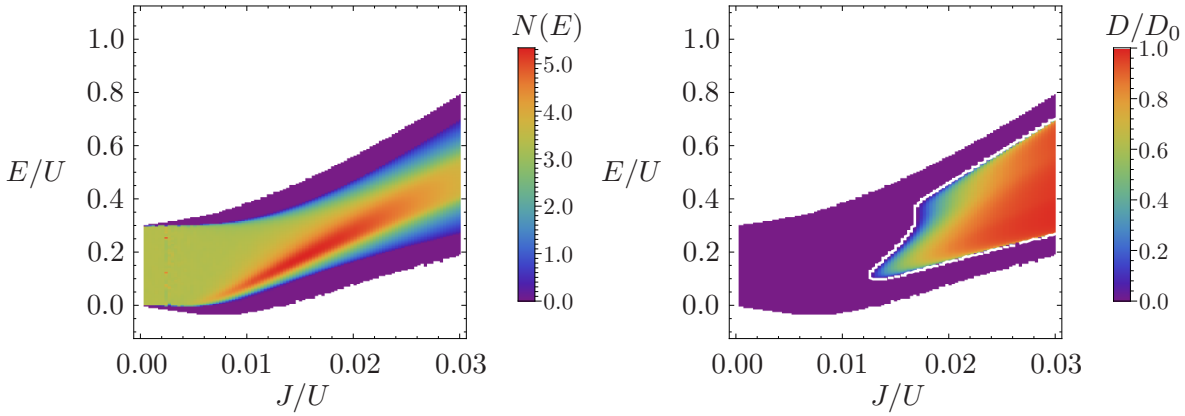

(a) $\mu/U = 1.0$

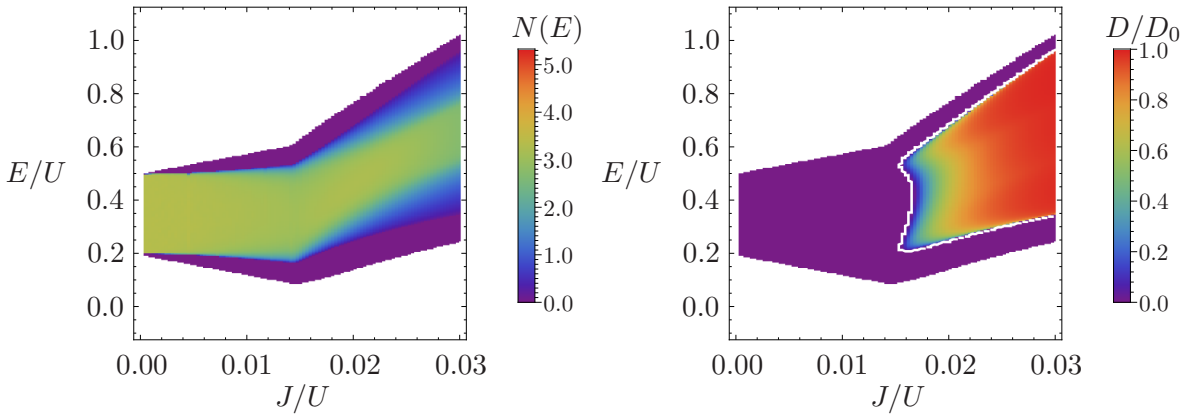

(b) $\mu/U = 1.5$

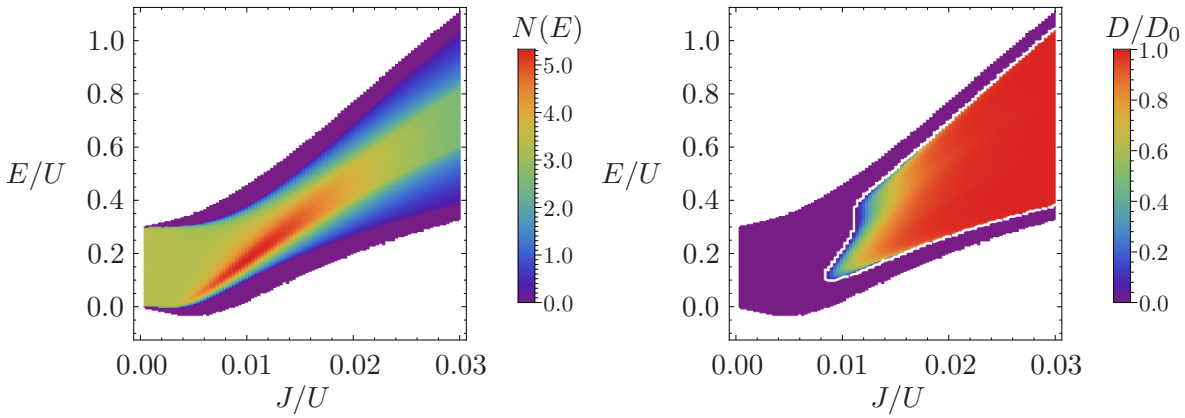

(c) $\mu/U = 2.0$

Figure 4.11: Density plots of the CPA DOS $N(E)$ (left column) and the diffusion coefficient $D(E)$ (right column) for fixed $W/U = 0.6$ and three different values of μ/U. Each plot shows the behavior of the full spectrum as a function of the hopping amplitude J/U. For each value of J/U, the plots of $N(E)$ and $D(E)$ range from the lower to the upper true boundaries of the DOS. The white curves in the diffusion plots show the trajectory of the mobility edges. All plots are for the first excitation band, $\alpha = 1$.

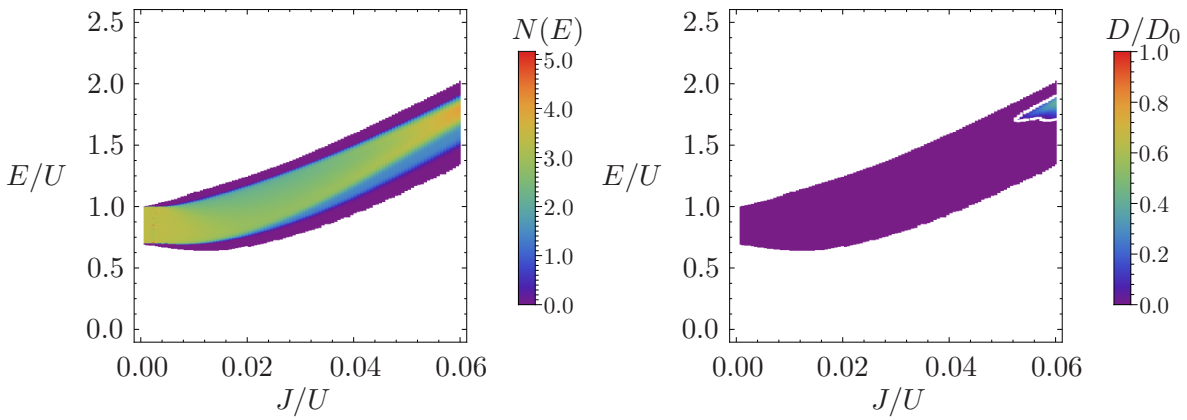

(a) $\mu/U = 1.0$

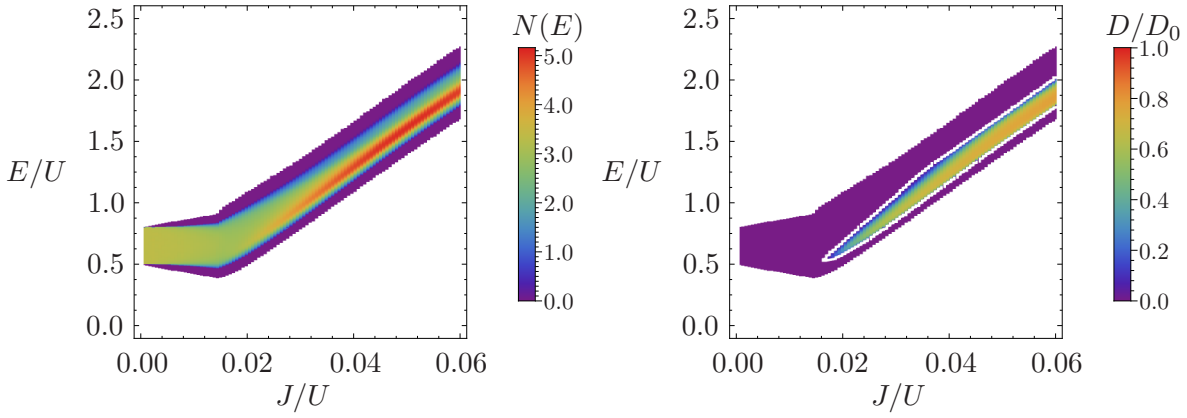

(b) $\mu/U = 1.5$

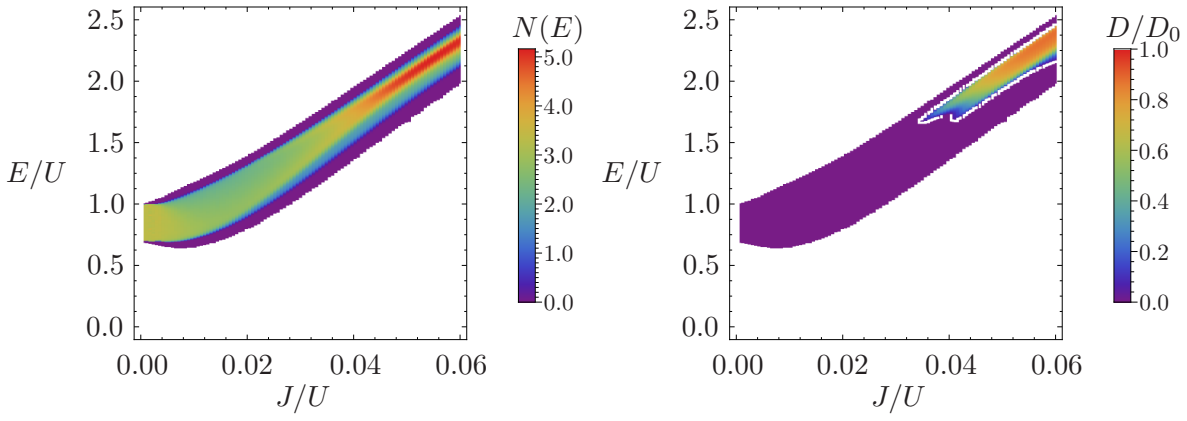

(c) $\mu/U = 2.0$

Figure 4.12: The same plots as in figure 4.11, again for $W/U = 0.6$, but now for the second excitation band, $\alpha = 2$.

numerically obtained δ-distribution. Moreover, in case we find the Anderson transition of the effective model to be located within the actual Mott lobes, it will allow us to draw conclusion about the shortcomings of our theory.

Now, let us turn to the diffusion coefficient $D(E)$. As one would expect, in general the diffusion increases when J/U is increased. As at the same time the band is shifted towards higher E, at the lower boundary of the spectrum the diffusion may also get smaller for fixed E.

Going into the opposite direction, $J/U \to 0$, the regions with vanishing $D(E)$ at the edges of the spectrum start to spread towards the center of the band. Upon further decreasing J/U, at some value of the hopping the diffusion vanishes for all E. This point marks the Anderson transition.

For both $\mu/U = 1.0$ and $\mu/U = 2.0$, the trajectories of the mobility edges exhibit a nose at lower energies E. This is due to the increased DOS at the lower boundary of the spectrum, see also figure 4.8. For $\mu/U = 1.5$, we observe the formation of two noses, i.e., four mobility edges. As the DOS does not show any significant features, see also figures 4.9c and 4.9d, this must be an artifact of the self-consistent theory of localization. In fact, the same unexpected behavior can be observed in the phase diagram of the original Anderson Hamiltonian, see discussion in section 2.2.7.

Between the Mott lobes, $\mu/U = 1.0$ and $\mu/U = 2.0$, the Anderson transition takes place at smaller J/U for the larger chemical potential. This is to be expected since the effective hopping is larger for larger filling. For $\mu/U = 1.5$, the transition is pushed towards larger J/U due to the effect of the Mott lobes on both the excitation spectrum as well as the effective hopping, which we have discussed in section 4.4.1.

In figure 4.12 the same plots are shown, but now for the second excitation band, $\alpha = 2$. It can be seen that the critical J/U, at which the Anderson transition takes place, varies on a much larger scale for different μ/U as compared to the first band.

For $\mu/U = 1.0$ and $\mu/U = 2.0$, the Anderson transition takes place at much higher values of J/U than for $\alpha = 1$. Thus, for finding the BG to SF transition, they can be neglected. For $\mu/U = 1.5$, however, the transition takes place in the same J/U regime as for $\alpha = 1$. Still, here the first excitation band undergoes the transition for smaller J/U than the second band and the BG to SF transition is determined by the first excitations. However, there will be cases where this order is reversed as we will see in the next section.

4.4.5 Trajectory of the Anderson Transition

In the previous section we have seen that for fixed μ/U, the spectrum of the effective model undergoes the Anderson transition at a certain critical hopping amplitude. According to our theory, this point then also corresponds to the SF to BG transition of the disordered Bose-Hubbard model. In order to resolve the boundary between the SF and the BG phase in the $\mu/U - J/U$ parameter space, we need to determine the trajectory of the Anderson transition as a function of μ/U.

In order to find the critical hopping for a given μ/U, we will start by scanning the spectrum for a fixed J/U. Depending on whether we find a completely localized spectrum or not, we will continue to scan the spectrum for a larger or a smaller J/U, respectively. This way, we eventually pinpoint the Anderson transition (with the maximal uncertainty chosen to be 0.03/1000) without having to perform the full scans that were shown in figures 4.11 and 4.12. For each J/U, this involves solving the MF problem and determining the distribution P_ψ, from which we can derive $P_{\Delta\epsilon}$ and T_{avg}. Then, we use the CPA to calculate the disorder-averaged single-particle (or,

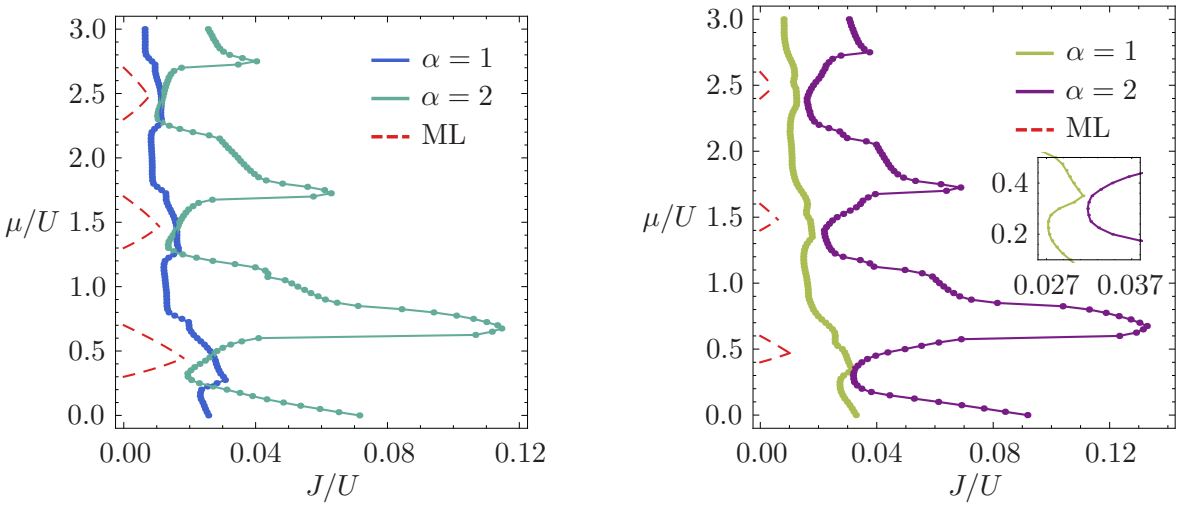

(a) $W/U = 0.6$ (b) $W/U = 0.8$

Figure 4.13: The trajectories of the Anderson transition for $W/U = 0.6$ and $W/U = 0.8$, each time for both the first and second excitations, $\alpha = 1$ and $\alpha = 2$, respectively. The inset in (b) shows a magnification of the region where the curves for the two bands almost touch. The dashed red curves indicate the corresponding first three Mott lobes (ML).

rather, single-excitation) quantities and, finally, calculate the diffusion within the self-consistent theory of localization for all energies E of the excitation spectrum.

The results for $W/U = 0.6$ and $W/U = 0.8$ and $\alpha = 1, 2$ are shown in figure 4.13. First we note that no Anderson transition trajectory crosses the MI phase. Overall, the trajectories move towards smaller J/U for larger μ/U due to the increased filling and the larger T_{avg}. For $\alpha = 1$, the Mott lobes *push* the trajectory towards larger J/U.

As already noted in the previous section, the curve for $\alpha = 2$ varies on a much larger scale than the curve for $\alpha = 1$. At the lower ends of each Mott lobe, $\mu/U \simeq n + W/2$ with $n \in \mathbb{N}$, the two trajectories get very close. As soon as roughly the middle of the Mott lobe is crossed, $\mu/U \gtrsim n + 1/2$, the curve for $\alpha = 2$ rapidly shifts towards larger J/U and reaches its maximum at around $\mu/U \simeq n + 0.75$.

This behavior can be understood best when considering the local MF spectrum for the ordered case. For integer μ/U, there are two particle numbers n and $n + 1$ yielding the lowest energy, $E_n = E_{n+1}$. As a reminder, this leads to the finite compressibility in the atomic limit. Hence, the ground state and the first excited state will be rather close in energy, while the second excited state is at higher energies, see also figures 4.1. For half-integer μ/U, the particle numbers $n_g \pm 1$ yield the same energy, $E_{n_g+1} = E_{n_g-1}$, with n_g being the atomic limit ground state occupation number. Thus, here the first and the second excited state will be close in energy and will also have a similar shape. As a result, in the vicinity of integer μ/U the trajectories for $\alpha = 1$ and $\alpha = 2$ will be separated the most, whereas for half-integer μ/U they approach each other.

For $W/U = 0.8$, the Anderson transition for $\alpha = 1$ always takes place at smaller J/U than for $\alpha = 2$, see also the inset. Thus, here the SF to BG transition is solely determined by the first excitations. However, for $W/U = 0.6$ and certain μ/U, the second excitations delocalize

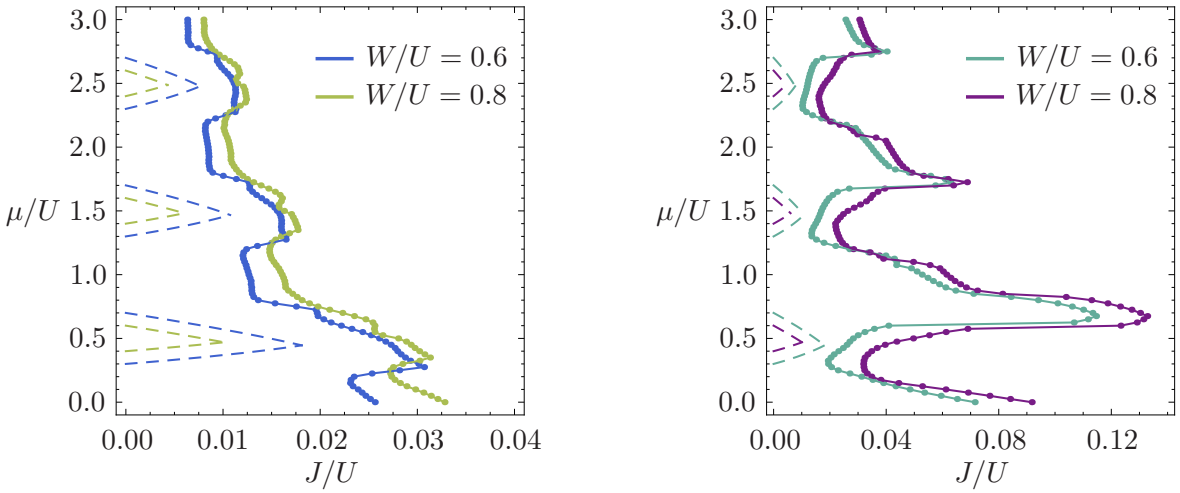

(a) $\alpha = 1$ (b) $\alpha = 2$

Figure 4.14: The trajectories of the Anderson transition for (a) the first and (b) the second excitations, each time for $W/U = 0.6$ and $W/U = 0.8$. The dashed curves indicate the corresponding first three Mott lobes.

at smaller hopping than the first excitations. This happens in the above described regions near the lower ends of the Mott lobes. Therefore, here the second excitations will play a role in determining the BG to SF transition.

Next, let us consider figure 4.14, where for each α the results for $W/U = 0.6$ and $W/U = 0.8$ are compared. As one would expect, in general the increased width of the disorder distribution leads to a shift of the Anderson transition to larger hopping amplitudes. However, this is not the case for all μ/U.

For $\alpha = 1$, see figure 4.14a, near the lower ends of the Mott lobes, $\mu/U \simeq n + W/2$ with $n \in \mathbb{N}$, the Anderson transition takes place at smaller hopping for the larger distribution width W/U. In figure 4.15, the diffusion coefficient for one of these cases, $\mu/U = 1.275$, is plotted for both W/U. As can be seen, there is no unusual behavior directly causing this effect. In fact, the profile of the diffusion appears to be more or less the same for both distribution widths, with the only difference that for $W/U = 0.8$ the transition takes place at $J/U \simeq 0.015$ and for $W/U = 0.6$ at a slightly larger hopping, $J/U \simeq 0.016$.

At first this seems counterintuitive, as a larger W/U will lead to a larger width of the effective distribution $P_{\Delta\epsilon}$. However, in section 4.4.1 we already found that the effective hopping T_{avg} can be larger for the larger disorder width, see figure 4.7e As a reminder, the reason for this was that enlarging the disorder width W/U reduces the size of the Mott lobes. The Anderson transition will depend on the interplay of both quantities, and apparently, in some regions of the parameter space this leads to a transition at smaller J/U for larger W/U.

Note, that also at the upper ends of the Mott lobes, $\mu/U \simeq n + W/2$, the two trajectories get very close, however, here they do not intersect. The mechanism is the same, i.e., the Mott lobe is smaller for the larger W/U, which shifts the trajectory towards smaller J/U.

For the second excitations, see figure 4.14b, the picture is more or less the same, with the larger W/U leading, in general, to an Anderson transition at larger J/U. At the upper and

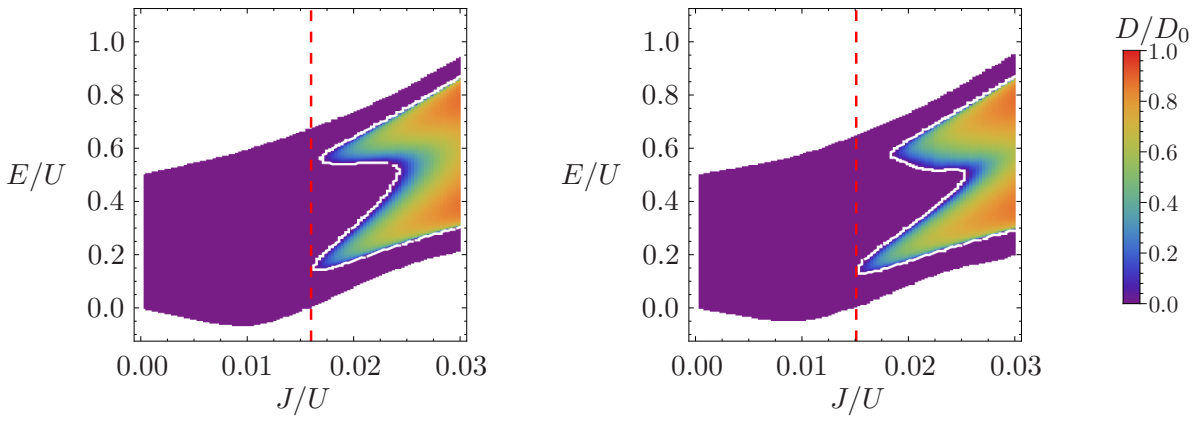

(a) $W/U = 0.6$ (b) $W/U = 0.8$

Figure 4.15: The diffusion coefficient for $\mu/U = 1.275$ and two disorder widths, $W/U = 0.6$ and $W/U = 0.8$, where for fixed J/U the plot ranges from the lower to the upper true boundary of the DOS. The white curves show the trajectories of the mobility edges. The dashed red lines indicate the Anderson transition.

lower ends of the Mott lobes, $\mu/U = n \mp W/2$, the two trajectories approach each other and, in some cases, intersect.

4.4.6 Summary and Complete Phase Diagram

To conclude section 4.4, we want to give a brief summary of all the steps that were necessary to finally obtain the trajectory of the Anderson transition for the effective model. The starting point was the effective single-excitation Hamiltonian

$$\hat{H}_{ex} = \sum_i \Delta\epsilon_i |i\rangle\langle i| + \sum_{\langle ij \rangle} T_{ij} \, |i\rangle\langle j| \tag{4.145}$$

with its parameters being determined by the solutions of the local MF Hamiltonians $\hat{h}_i$ and the MF parameter distribution P_ψ, which we studied for the first two excitation *bands*, $\alpha = 1, 2$. In order to later use the self-consistent theory of localization, it was necessary to eliminate the ODD in $\hat{H}_{ex}$ by replacing the random transition amplitudes with the disorder-averaged effective hopping, $T_{ij} \to T_{avg}$. Judging from the standard deviations of the involved quantities, this approximation is not very good for small hopping amplitudes J/U, but gets better for larger J/U. We justified making this replacement with the argument that for small hopping, the properties of the system should mainly be determined by the diagonal disorder, which is an order of magnitude larger than the ODD if we restrict ourselves to the strong disorder regime, $J \ll W < U$.

With this, the disorder is restricted to the excitation energies $\Delta\epsilon$ and the corresponding probability distribution $P_{\Delta\epsilon}$ can be calculated from the MF parameter distribution P_ψ. We found that, in general, the width of $P_{\Delta\epsilon}$ is large for small average MF parameters $\overline{\psi}$ and decreases when $\overline{\psi}$ is increased. This implies that the distribution width gets smaller for larger J/U and overall also for larger μ/U, where for the latter one has to take into account the

effect of the Mott lobes. Furthermore, the larger the width W/U of the initial on-site energy distribution P_ε, the larger the width of $P_{\Delta\epsilon}$ in the atomic limit. As a result, the width of $P_{\Delta\epsilon}$ is, in general, larger for larger W/U. For the effective hopping amplitude T_{avg}, we found a rather varying behavior. For $\alpha = 1$, T_{avg} is in principle (but not always, due to the Mott lobes) larger for larger J/U and μ/U. For $\alpha = 2$, however, the behavior was quite different, with T_{avg} even getting smaller for larger J/U.

Having determined the parameters of the effective Hamiltonian, in subsections 4.4.2 to 4.4.4 we went on to first calculate the CPA DOS and, from that, the diffusion coefficient $D(E)$ as well as the localization length $\xi(E)$. We found that for fixed μ/U the system undergoes the Anderson transition from $D(E) > 0$ for some E to $D(E) = 0$ for all E at a certain J/U.

In subsection 4.4.5, we then mapped out the trajectory of this transition point as a function of μ/U for $W/U = 0.6$ and $W/U = 0.8$ and $\alpha = 1, 2$. We found that most of the time the first excitation band undergoes the Anderson transition at smaller J/U. However, for $W/U = 0.6$ there were some regions on the μ/U-axis where this order was reversed and the second excitations delocalize at smaller hopping amplitudes.

Furthermore, comparing the results for the two disorder width revealed a non-trivial dependence on W/U, which could be explained as follows. On the one hand, the larger W/U in general leads to a larger width of $P_{\Delta\epsilon}$, which implies that the system with the larger W/U undergoes the transition, in general, at a larger J/U. On the other hand, the Mott lobes are smaller for larger W/U, implying that the system with the larger W/U can leave the atomic limit regime ($\overline{\psi} = 0$) at smaller J/U. We already found that larger MF parameters lead to a smaller width of the effective distribution as well as a larger effective hopping amplitude. In that sense, the system with the larger W/U gets a *head start* for certain μ/U, which can cancel the fact that in the atomic limit it has a broader effective distribution.

As a result, the trajectories for the two different W/U approach each other in the vicinity of the upper and lower ends of the Mott lobes and can even cross, leading to an Anderson transition at smaller J/U for larger W/U. One should again note that this result was obtained while neglecting the ODD. This approximation becomes rather uncontrolled for small hopping, specifically in the vicinity of the Mott lobes.

To conclude this chapter, we can now finally draw the full phase diagram of the disordered Bose-Hubbard model. As argued in section 4.1.2, the BG to SF transition is equivalent to the Anderson transition of the excitation spectrum. Here, we use the transition trajectory of either the first or the second excitations, depending for which type the transition happens at smaller J/U, see also figure 4.13 for comparison. The MI to BG transition can be obtained by shifting the upper and lower halfs of each Mott lobe obtained for the pure system by $\mp W/2$ in μ/U-direction, respectively, as it was explained in section 3.2.3.

Figure 4.16 shows the resulting phase diagram as well as the underlying disorder-averaged MF parameter $\overline{\psi}$, as always for $W/U = 0.6$ and $W/U = 0.8$. Again, we see that the stochastic MF theory overestimates the size of the Mott lobes. Therefore, the regions outside the actual MI phase, for which we still obtain $\overline{\psi} = 0$, can (to some extend) be identified with the Lifshitz regime, where most of the system is locally in the gaped MI phase and only rare isles of gapless regions exist (which are not resolved by the stochastic MF theory).

The BG to SF transition always takes place at some distance from the Mott lobes and also almost always outside the Lifshitz regime. For $W/U = 0.6$, the transition line approaches the Lifshitz regime quite closely and also enters it once at the lower half of the first Mott lobe, where the second excitations determine the phase boundary. Again, this is a region in parameter space where neglecting the ODD is not really justified anymore. For $W/U = 0.8$, the transition line

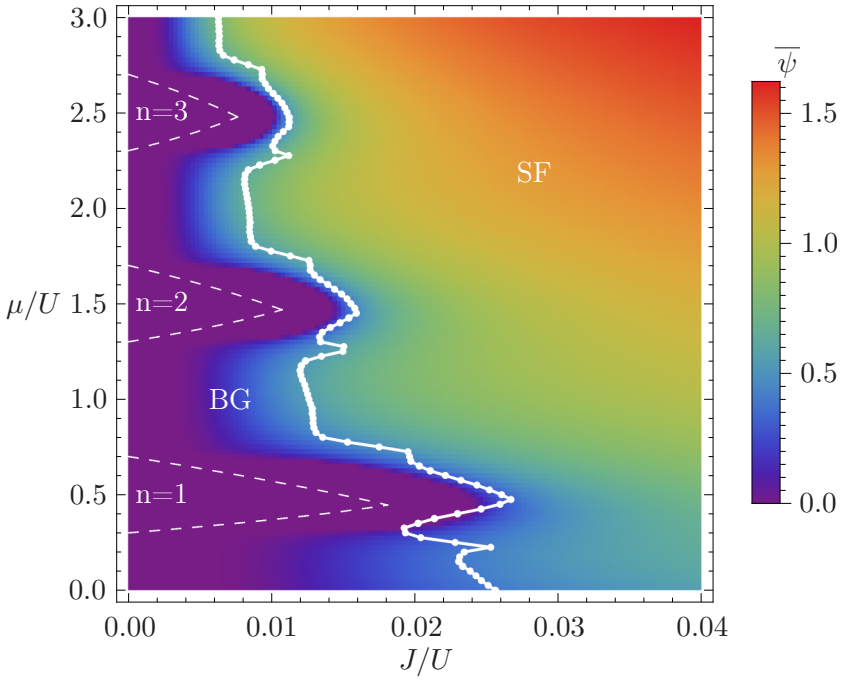

(a) $W/U = 0.6$

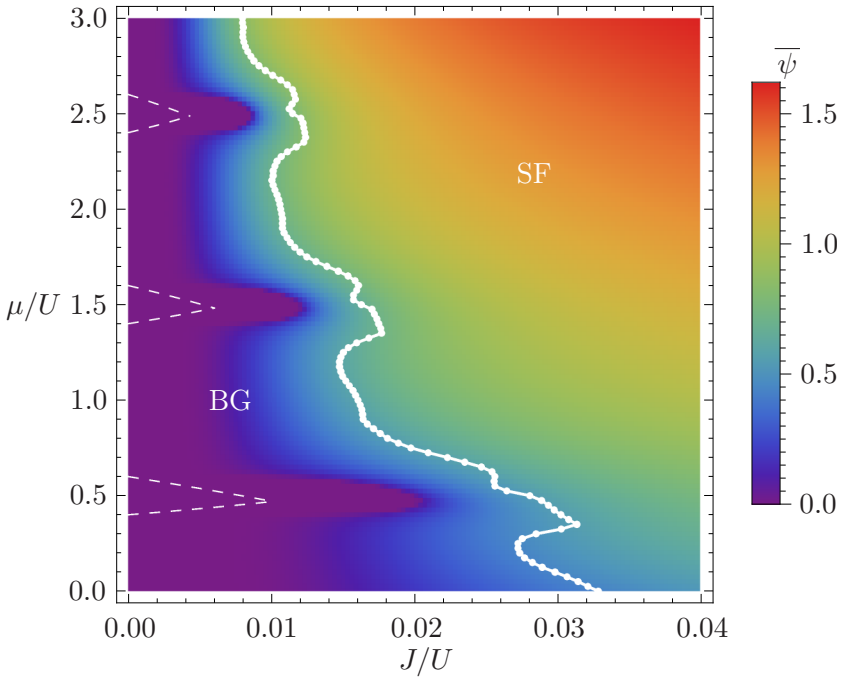

(b) $W/U = 0.8$

Figure 4.16: The complete phase diagram of the Bose-Hubbard model for $W/U = 0.6$ and $W/U = 0.8$. The density plot shows the disorder-averaged MF parameter $\overline{\psi}$. The dashed white curves show the first three Mott lobes with uniform occupation number $n = 1, 2, 3$, respectively. The solid white curve shows the boundary between the localized ($D = 0$) and the diffusive regime ($D > 0$) of the effective model, i.e., between BG and SF phase.

always stays well above the Lifshitz regime and is always determined by the first excitations.

In general, the phase boundary moves to smaller J/U when μ/U is increased. The Mott lobes, however, interrupt this behavior by pushing the phase boundary towards higher J/U again. This is exactly the behavior one would expect and with this final result, we conclude the numerical investigation and discussion of the effective single-excitation approach to the disorder Bose-Hubbard model.

CHAPTER 5

Conclusion

In this work we have studied the disordered Bose-Hubbard model in the regime of both strong interactions and strong disorder. In chapter 3, we discussed a generalization of a MF theory, which was initially developed to describe the MI to SF phase transition in the pure Bose-Hubbard model [27], to the disordered case. Instead of treating the particle-particle interaction in MF, which is suitable in the weakly interacting regime, here the MF approximation is applied to the kinetic term, which replaces the hopping process from one to another lattice site by a tunneling process into and out of a particle bath. Thereby, the lattice sites are decoupled with respect to the bosonic operators, but remain coupled via the bath amplitudes, which can be characterized by the MF parameter. The full lattice problem is reduced to a set of local problems. As the interaction term is treated exactly, this approximation is suitable to describe the transition to the MI phase.

For the pure model, it is possible to employ the translational invariance of the system to further simplify the problem to a single-site one, within which the MF parameter can be determined self-consistently. One finds that a vanishing parameter is equivalent to an incompressible and insulating system, whereas a finite parameter implies finite compressibility. Therefore, the MF parameter functions as an order parameter, which can be used to describe the transition from the gapless SF phase to the gaped MI phase. In doing so, one can derive a qualitatively correct phase diagram of the Bose-Hubbard model with its characteristic Mott lobes.

In the disordered case, the system is not translational invariant anymore and the MF parameter obtains a spatial dependency. In principle, one would have to solve the set of coupled local problems explicitly for a given disorder realization. This was actually done for two dimensions in [39], for the three-dimensional case, however, this is only feasible for rather small system sizes. Therefore, here one introduces one further approximation, which is to neglect spatial correlations between MF parameters. This allows us to decouple the joint probability distribution of all parameters into a product of probability distributions for each single parameter. Thereby, one again arrives at a single-site problem, however, now one has to determine the probability distribution self-consistently. Therefore, this theory is also called the stochastic MF theory [28]. Like in the ordered case, a globally vanishing MF parameter corresponds to the gaped MI phase, whereas finite MF parameters imply a compressible and gapless system. Thus, the theory can describe the transition to the MI phase also for the disordered Bose-Hubbard model.

Evaluating the theory numerically, we found that the disorder leads to a reduction of the size of the MI phase as compared to the pure model. The larger the width W of the disorder

distribution, the more the size of the Mott lobes is reduced, until the MI phase disappears completely when the disorder width becomes dominant over the Coulomb repulsion strength, $W > U$. This result is in accordance with theoretical predictions [1]. However, the actual shape of the Mott lobes of the disordered system can also be obtained by simply shifting the upper and lower halves of the lobes of the pure system [23], which allows us to test the validity of the results. We found that the stochastic MF theory fails to predict the correct shape of the Mott lobes. The reason for this is that the theory does not take into account spatial correlations between the MF parameters. The actual shape of the Mott lobes, however, stems from the existence of the rare Lifshitz regions, which are highly correlated in space. The stochastic MF theory cannot resolve these regions and, as a result, yields Mott lobes that are too large.

Moreover, we argued that it is not possible to make predictions about the phase transition from the insulating BG to the conducting SF phase based on the stochastic MF theory. The MF parameter can only distinguish between gaped and gapless systems. The BG and the SF phase, however, are both gapless, i.e., the MF parameter will be non-vanishing in both phases. The quantity that separates the two phases is, in fact, the SF density and the corresponding SF current, which is finite in the SF and zero in the BG phase. The underlying mechanism that leads to a vanishing SF current is the localizing effect of the disorder. Although Anderson localization means the phenomenon of particles being confined within finite regions in space as a result of a disorder potential, it is still a non-local effect that is driven by coherent particle interference processes. In particular, the Anderson transition from the localized to the diffusive regime cannot be resolved within a purely local theory, such as, the stochastic MF theory.

In chapter 4 we, therefore, introduced a different approach to the disordered Bose-Hubbard model. Because of the complexity of the problem of multi-particle localization, one inevitably has to introduce some kind of approximation in order to obtain any results. One way is to solve the problem only for finite-sized systems using (more or less) exact methods and then scale the results to the thermodynamic limit. This method is numerically very extensive, which puts restrictions on the parameter range one can investigate, and also comes with the risk of neglecting features that would only arise for very large system sizes. Another way would be to treat the Coulomb interaction within a MF approximation. This, however, is not appropriate in this case as the boundary between BG and SF phase is expected to be located in the strongly correlated regime. The approach we took here is therefore a different one, in that we applied an approximation to the Hilbert space by only taking into account those states that are most important for the problem. This eventually allowed us to describe the full interacting problem in terms of a non-interacting effective model.

We first derived an expression for the long-ranged current density in terms of the non-local single-particle Green's function. We then divided the full Hamiltonian into the MF term and the fluctuations from the MF. The fluctuations term was treated as a perturbation to the *unperturbed* MF Hamiltonian, for which the solution was already determined in the previous chapter 3. This led to the expansion of the full single-particle Green's function in terms of an unperturbed Green's function corresponding to the MF Hamiltonian. As the stochastic MF theory treats the Coulomb interaction exactly and approximates only the kinetic part of the Hamiltonian, the perturbation term is also solely kinetic in nature. Therefore, this expansion is structurally similar to the locator expansion of the original Anderson Hamiltonian. The idea now was to subsequently reduce the state space such that, within the truncated state space, this expansion of the single-particle Green's function of the interacting disordered Bose-Hubbard model is identical to the locator expansion of the non-interacting Anderson Hamiltonian.

The natural choice for a representation is given by the complete eigenbasis of the MF Hamil-

tonian, within which the unperturbed Green's function is, by construction, diagonal. The perturbation term then introduces transitions between the MF eigenstates, which can be local transitions as well as nearest neighbor transitions. Furthermore, it can yield an energy correction for certain states, which is a consequence of fluctuations of the particle bath. We found that each term of the expansion series for the Green's function always starts and ends in the single-excitation sector, i.e., the subspace of the Hilbert space in which all sites but one are described by their local MF ground state. With the argument that additional local excitations are suppressed due to the additional costs in energy, we restricted ourselves to this single-excitation sector. This approximation reduces the multi-particle problem effectively to a single-particle one, however, with multiple orbitals. To complete the mapping onto the Anderson Hamiltonian, we needed to restrict the number of local excitations on each site to just one. In order to do so, we had to find a selection criterion.

The two quantities determining the contribution of a certain excitation to the expansion of the Green's function were determined to be the coupling strength of this excitation to the ground state as well as its excitation energy. We found that the higher the excitation, the smaller the coupling strength, from which we concluded that the Anderson transition would take place first at low excitation energies. Therefore, we further restricted our investigations to the regime of small excitation energies and only took into account the first and second excited states in the following. This concluded the derivation of the effective non-interacting Hamiltonian for the single-excitation sector.

We then moved on to investigate the current density within this effective model. We found that in order to obtain a non-vanishing current density, one needs to impose a gradient upon the complex phases of the MF parameters. In the limit of small phase differences, which corresponds to the limit of a small SF velocity, it was possible to condense the effect of the phase gradient on the single-particle Green's function into a single phase factor. This factor could then be extracted from the Green's function, allowing us to identify the vanishing of the SF current density with the Anderson transition of the effective single-excitation model. When the spectrum of the effective model is completely localized, the current density will decay exponentially in space. A finite long-ranged SF current is only possible if the effective model is in the diffusive regime. Therefore, the Anderson transition of the effective model coincides with the BG to SF transition of the disordered Bose-Hubbard model. This essentially restricts the applicability of this theory to the case of three spatial dimensions, as for one and two dimensions the effective non-interacting model would always be localized.

In the final section, we then evaluated the theory numerically in order to resolve this transition in three dimensions. Based upon the results the stochastic MF theory, we derived the parameters of the single-excitation model and determined the excitation spectrum within the CPA as a function of the parameters of the underlying disordered Bose-Hubbard model. Here we had to apply one further approximation in that we neglect the ODD and restrict the disorder to the diagonal part of the effective Hamiltonian. This limits the parameter space we can describe to the strongly disordered regime. In order to describe also the regime of weaker (not weak) disorder, one would have to take into account the ODD. We then used the self-consistent theory of localization to further calculate the localization length and the diffusion coefficient for each excitation spectrum. Monitoring the mobility edges for a fixed chemical potential as a function of the hopping amplitude, we found that the effective model always undergoes the Anderson transition at a certain critical hopping amplitude.

We found that, in general, the effective disorder is stronger for a stronger initial disorder. Furthermore, the effective disorder gets smaller when the MF parameters get larger. As a result,

the Anderson transition, overall, takes place at smaller hopping for either a larger chemical potential or a smaller initial disorder. However, each Mott lobe pushes the transition to larger hopping for the corresponding chemical potentials. As the Mott lobes are smaller for the system with the larger disorder width, this introduced the surprising behavior that at the edges of the Mott lobes the Anderson transition can take place at smaller hopping for a larger initial disorder width.

Resolving this transition as a function of the chemical potential, we obtained the trajectory of the Anderson transition in the parameter space. This transition curve corresponds to the boundary between the localized BG and the conducting SF phase. In accordance to the theorem of inclusions [24], we found that there is always a localized phase separating the MI from the SF phase. This represents our final result and concludes the present work.

APPENDIX A

Mean-Field Theory for the Bose-Hubbard Model

A.1 Compressibility and the Mean-Field Parameter

In this section we want to investigate the relationship between the MF parameter ψ and the compressibility κ. We show that a vanishing parameter is equivalent to a vanishing compressibility. On the other hand, a finite compressibility implies finite MF parameters.

The compressibility κ_T for constant temperature T and particle number N is defined as

$$\kappa_T = -\frac{1}{V}\left(\frac{\partial V}{\partial p}\right)_{T,N} = \frac{V}{N^2}\left(\frac{\partial N}{\partial \mu}\right)_{T,V} . \tag{A.1}$$

In thermodynamics, it describes the relative change of the volume V of a system when the pressure p is varied, thus the name compressibility. Via the Maxwell relations, it can be related to the change of the total particle number when the chemical potential is varied. This is the quantity we are actually interested in, as it tells us whether the system is gaped or not at a certain energy. To keep it simple, we define our compressibility as the change of the total particle number per site when μ is varied,

$$\kappa = \frac{1}{N_i}\left(\frac{\partial N}{\partial \mu}\right)_{T,V} , \tag{A.2}$$

where the system size is kept constant as well as the temperature, since later we want to take the limit $T \to 0$.

The average particle number N is defined via the thermal average with respect to the grand canonical Hamiltonian, in our case the pure and the disordered Bose-Hubbard Hamiltonians,

$$N = \langle \hat{N} \rangle = \frac{1}{Z} \operatorname{Tr}\left\{ e^{-\beta \hat{H}} \hat{N} \right\} = k_B T \frac{\partial}{\partial \mu} \log Z , \tag{A.3}$$

where $Z = \operatorname{Tr}\{e^{-\beta \hat{H}}\}$ is the grand canonical partition function and k_B the Boltzmann constant. For the second step, we have used that $\partial \hat{H}/\partial \mu = -\hat{N}$. Inserting the thermal average into the

definition of κ yields

$$\begin{aligned}\kappa &= \frac{k_B T}{N_i}\frac{\partial^2}{\partial\mu^2}\log Z \\ &= \frac{k_B T}{N_i}\left[\frac{1}{Z}\frac{\partial^2 Z}{\partial\mu^2} - \frac{1}{Z^2}\left(\frac{\partial Z}{\partial\mu}\right)^2\right] \\ &= \frac{1}{k_B T N_i}\left[\langle\hat{N}^2\rangle - \langle\hat{N}\rangle^2\right]. \end{aligned} \tag{A.4}$$

The problem with this expression is that $\langle\hat{N}^2\rangle \to \langle\hat{N}\rangle^2$ for $T \to 0$. Thus, it cannot be directly evaluated at $T = 0$, but we have to take the limit $T \to 0$. In order to do so, in principle we would need to know the eigenstates and eigenenergies of $\hat{H}$. However, as we cannot compute the exact values, we apply the decoupling approximation to the Hamiltonian and calculate the average particle number with respect to the MF Hamiltonian $\hat{H}^{MF} = \sum_i \hat{h}_i + t\sum_{\langle ij\rangle}\psi_i\psi_j$,

$$N \approx \frac{1}{Z^{MF}}\operatorname{Tr}\left\{e^{-\beta\hat{H}^{MF}}\hat{N}\right\} = \sum_i \frac{1}{Z_i}\operatorname{Tr}\left\{e^{-\beta\hat{h}_i}\hat{n}_i\right\} \equiv \sum_i \langle\hat{n}_i\rangle\,, \tag{A.5}$$

with $\hat{N} = \sum_i \hat{n}_i$, $Z^{MF} = \operatorname{Tr}\{e^{-\beta\hat{H}^{MF}}\}$, and $Z_i = \operatorname{Tr}\{e^{-\beta\hat{h}_i}\}$. Thus, the compressibility is given by

$$\kappa = \frac{1}{N_i}\sum_i \frac{\partial\langle\hat{n}_i\rangle}{\partial\mu} = \frac{1}{k_B T N_i}\sum_i \left[\langle\partial\hat{h}_i/\partial\mu\rangle\langle\hat{n}_i\rangle - \langle\hat{n}_i\partial\hat{h}_i/\partial\mu\rangle\right]. \tag{A.6}$$

Now, when evaluating the partial derivative, we have to take into account that the order parameters depend on the chemical potential,

$$\frac{\partial\hat{h}_i}{\partial\mu} = -\hat{n}_i - t(\hat{b}_i + \hat{b}_i^\dagger)\frac{\partial\Psi_i}{\partial\mu}\,. \tag{A.7}$$

Thus, we have

$$\kappa = \frac{1}{k_B T N_i}\sum_i \left[\langle\hat{n}_i^2\rangle - \langle\hat{n}_i\rangle^2 + t\frac{\partial\Psi_i}{\partial\mu}\Big(\langle\hat{n}_i\hat{b}_i\rangle + \langle\hat{n}_i\hat{b}_i^\dagger\rangle - \big(\langle b_i\rangle + \langle\hat{b}_i^\dagger\rangle\big)\langle n_i\rangle\Big)\right] \tag{A.8}$$

First we note that when $\psi_i = 0$ for all i, the terms proportional to t vanish since all eigenstates are particle number eigenstates. For the remaining term we have

$$\begin{aligned}\lim_{T\to 0}\left(\langle\hat{n}_i^2\rangle - \langle\hat{n}_i\rangle^2\right) &= \lim_{T\to 0}\left[\sum_n e^{-\beta\left(E_{i,n}-E_{i,n_g}\right)}n^2 - \left[\sum_n e^{-\beta\left(E_{i,n}-E_{i,n_g}\right)}n\right]^2\right] \\ &= \lim_{T\to 0}\sum_n e^{-\beta\left(E_{i,n}-E_{i,n_g}\right)}n\left[n - \sum_m e^{-\beta\left(E_{i,m}-E_{i,n_g}\right)}m\right] \\ &= \lim_{T\to 0}\sum_n e^{-\beta\left(E_{i,n}-E_{i,n_g}\right)}n(n-n_g)\,, \end{aligned} \tag{A.9}$$

where $E_{i,n}$ is the eigenenergy for particle number n on site i and n_g is the ground state particle number. These terms vanish exponentially and cancel the diverging prefactor in κ. Thus, we

have

$$\lim_{T\to 0} \kappa \to 0 \text{ if all } \psi_i = 0. \tag{A.10}$$

In other words, if the order parameter vanishes globally, the system is gaped.

Furthermore, this means that if the compressibility is finite, $\lim_{T\to 0}\kappa \neq 0$, there have to be finite ψ_i as well. Apart from that, it is difficult to make predictions for the compressibility and we will have to rely on calculating κ numerically.

A.2 Perturbation Theory

In this section, we will derive an expression for the MF ground state energy using standard perturbation theory, as it can be found, for example, in the textbook on quantum mechanics by J.J. Sakurai [85]. However, we will change the notation to fit our problem. This approach was first presented in [80].

Again, the MF Hamiltonian is given by

$$\hat{h} = \hat{h}^0 - tz\psi\,\hat{h}^1 + tz\psi^2\,, \tag{A.11a}$$

with

$$\hat{h}^0 = (\varepsilon_0 - \mu)\hat{n} + \frac{U}{2}\hat{n}(\hat{n}-1) \tag{A.11b}$$

and

$$\hat{h}^1 = \hat{b}^\dagger + \hat{b}\,. \tag{A.11c}$$

As pointed out in section 3.1.2, the eigenstates of $\hat{h}^0$ are given by the particle number eigenstates $|n\rangle$. We will label the unperturbed ground state by $|n_g\rangle$. The full MF ground state can then be written as

$$|\widetilde{G}\rangle = |n_g\rangle + \sum_{n\neq n_g} \tilde{g}_n |n\rangle\,, \tag{A.12}$$

where the normalization is chosen such that $\langle n_g|\widetilde{G}\rangle = 1$. It follows that

$$\begin{aligned}
&(\hat{h} - E_{n_g})|\widetilde{G}\rangle = (\hat{h}^0 - E_{n_g})\sum_{n\neq n_g}\tilde{g}_n|n\rangle + (-tz\psi\,\hat{h}^1 + tz\psi^2)|\widetilde{G}\rangle \\
\Leftrightarrow\quad &\sum_{n\neq n_g}\tilde{g}_n|n\rangle = (\hat{h}^0 - E_{n_g})^{-1}\big(tz\psi\,\hat{h}^1 + \underbrace{(E_G - E_{n_g} - tz\psi^2)}_{\equiv\Delta_G}\big)|\widetilde{G}\rangle \\
\Rightarrow\quad &g_n = \frac{1}{E_n - E_{n_g}}\langle n|(tz\psi\,\hat{h}^1 + \Delta_G)|\widetilde{G}\rangle \qquad \text{for} \qquad n \neq n_g\,,
\end{aligned} \tag{A.13}$$

where E_G is the ground state energy for the full Hamiltonian $\hat{h}$. Plugging this result back into the definition of the ground state yields

$$\begin{aligned}
|\widetilde{G}\rangle &= |n_g\rangle + \sum_{n\neq n_g}|n\rangle\langle n|\frac{1}{E_n - E_{n_g}}(tz\psi\,\hat{h}^1 + \Delta_G)|\widetilde{G}\rangle \\
&= |n_g\rangle + \hat{P}(\hat{h}^0 - E_{n_g})^{-1}(tz\psi\,\hat{h}^1 + \Delta_G)|\widetilde{G}\rangle\,,
\end{aligned} \tag{A.14}$$

with the projection operator $\hat{P} = \mathbb{1} - |n_g\rangle\langle n_g|$. Now, one has to be careful when evaluating Δ_G,

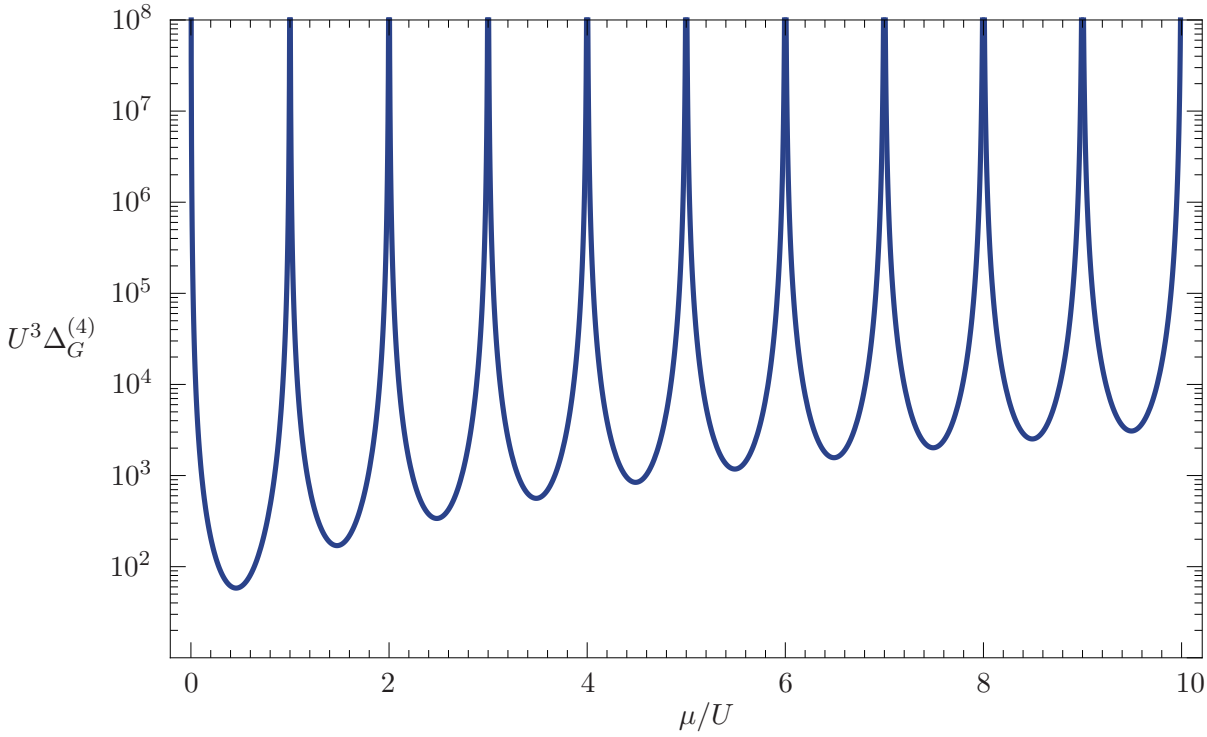

Figure A.1: The fourth order correction $\Delta_G^{(4)}$ to the ground state energy as a function of μ/U for $\varepsilon_0 = 0$.

as it contains the exact ground state energy, which is not known. In order to find a perturbation series for Δ_G, we consider the following matrix element,

$$\begin{aligned}\langle n_g|(tz\psi\,\hat{h}^1 + \Delta_G)|\widetilde{G}\rangle &= \langle n_g|(tz\psi\,\hat{h}^1 + E_G - E_{n_g} - tz\psi^2)|\widetilde{G}\rangle \\ &= \langle n_g|(tz\psi\,\hat{h}^1 + \hat{h} - \hat{h}^0 - tz\psi^2)|\widetilde{G}\rangle \\ &= \langle n_g|(\hat{h} - \hat{h})|\widetilde{G}\rangle = 0\,,\end{aligned} \tag{A.15}$$

and thus,

$$\Delta_G = -tz\psi\langle n_g|\hat{h}^1|\widetilde{G}\rangle\,. \tag{A.16}$$

With this, equation (A.14) can be rewritten as

$$|\widetilde{G}\rangle = |n_g\rangle + tz\psi\,\hat{P}(\hat{h}^0 - E_{n_g})^{-1}\Big(\hat{h}^1 - \langle n_g|\hat{h}^1|\widetilde{G}\rangle\Big)|\widetilde{G}\rangle \equiv \sum_{k=0}^{\infty}(tz\psi)^k|\widetilde{G}^{(k)}\rangle \tag{A.17}$$

and

$$\Delta_G = -\sum_{k=1}^{\infty}(tz\psi)^k\langle n_g|\hat{h}^1|\widetilde{G}^{(k-1)}\rangle \equiv \sum_{k=1}^{\infty}(tz\psi)^k\Delta_G^{(k)}\,, \tag{A.18}$$

which now can be solved iteratively. Evaluating the series up to forth order in ψ yields

$$
\begin{aligned}
|\widetilde{G}^{(0)}\rangle &= |n_g\rangle && \text{(A.19a)}\\
\Delta_G^{(1)} &= -\langle n_g|\hat{h}^1|\widetilde{G}^{(0)}\rangle = 0 && \text{(A.19b)}\\
|\widetilde{G}^{(1)}\rangle &= \hat{P}(\hat{h}^0 - E_{n_g})^{-1}\big(\hat{h}^1 + \Delta_G^{(1)}\big)|\widetilde{G}^{(0)}\rangle\\
&= \frac{\sqrt{n_g}}{E_{n_g-1} - E_{n_g}}|n_g - 1\rangle + \frac{\sqrt{n_g+1}}{E_{n_g+1} - E_{n_g}}|n_g + 1\rangle && \text{(A.19c)}\\
\Delta_G^{(2)} &= -\langle n_g|\hat{h}^1|\widetilde{G}^{(1)}\rangle = -\frac{n_g}{E_{n_g-1} - E_{n_g}} - \frac{n_g+1}{E_{n_g+1} - E_{n_g}} && \text{(A.19d)}\\
|\widetilde{G}^{(2)}\rangle &= \hat{P}(\hat{h}^0 - E_{n_g})^{-1}\Big[\big(\hat{h}^1 + \Delta_G^{(1)}\big)|\widetilde{G}^{(1)}\rangle + \Delta_G^{(2)}|\widetilde{G}^{(0)}\rangle\Big]\\
&= \frac{\sqrt{n_g}}{E_{n_g-1} - E_{n_g}}\frac{\sqrt{n_g-1}}{E_{n_g-2} - E_{n_g}}|n_g - 2\rangle + \frac{\sqrt{n_g+1}}{E_{n_g+1} - E_{n_g}}\frac{\sqrt{n_g+2}}{E_{n_g+2} - E_{n_g}}|n_g + 2\rangle && \text{(A.19e)}\\
\Delta_G^{(3)} &= -\langle n_g|\hat{h}^1|\widetilde{G}^{(2)}\rangle = 0 && \text{(A.19f)}\\
|\widetilde{G}^{(3)}\rangle &= \hat{P}(\hat{h}^0 - E_{n_g})^{-1}\Big[\big(\hat{h}^1 + \Delta_G^{(1)}\big)|\widetilde{G}^{(2)}\rangle + \Delta_G^{(2)}|\widetilde{G}^{(1)}\rangle + \Delta_G^{(3)}|\widetilde{G}^{(0)}\rangle\Big]\\
&= \hat{P}(\hat{h}^0 - E_{n_g})^{-1}\Big[\hat{h}^1|\widetilde{G}^{(2)}\rangle + \Delta_G^{(2)}|\widetilde{G}^{(1)}\rangle\Big]
\end{aligned}
$$

and finally,

$$
\begin{aligned}
\Delta_G^{(4)} &= -\langle n_g|\hat{h}^1|\widetilde{G}^{(3)}\rangle\\
&= -\Big[\frac{\sqrt{n_g}}{E_{n_g-1} - E_{n_g}}\langle n_g - 1| + \frac{\sqrt{n_g+1}}{E_{n_g+1} - E_{n_g}}\langle n_g + 1|\Big]\Big[\hat{h}^1|\widetilde{G}^{(2)}\rangle + \Delta_G^{(2)}|\widetilde{G}^{(1)}\rangle\Big]\\
&= -\frac{\sqrt{n_g}}{E_{n_g-1} - E_{n_g}}\left(\frac{\sqrt{n_g}}{E_{n_g-1} - E_{n_g}}\frac{n_g-1}{E_{n_g-2} - E_{n_g}} + \Delta_G^{(2)}\frac{\sqrt{n_g}}{E_{n_g-1} - E_{n_g}}\right)\\
&\quad - \frac{\sqrt{n_g+1}}{E_{n_g+1} - E_{n_g}}\left(\frac{\sqrt{n_g+1}}{E_{n_g+1} - E_{n_g}}\frac{n_g+2}{E_{n_g+2} - E_{n_g}} + \Delta_G^{(2)}\frac{\sqrt{n_g+1}}{E_{n_g+1} - E_{n_g}}\right)\\
&= \frac{n_g}{(E_{n_g-1} - E_{n_g})^2}\left(\frac{n_g}{E_{n_g-1} - E_{n_g}} + \frac{n_g+1}{E_{n_g+1} - E_{n_g}} - \frac{n_g-1}{E_{n_g-2} - E_{n_g}}\right)\\
&\quad \frac{n_g+1}{(E_{n_g+1} - E_{n_g})^2}\left(\frac{n_g}{E_{n_g-1} - E_{n_g}} + \frac{n_g+1}{E_{n_g+1} - E_{n_g}} - \frac{n_g+2}{E_{n_g+2} - E_{n_g}}\right).
\end{aligned}
$$

With this, the ground state energy can be written as

$$
E_G = E_{n_g} + \Big(\Delta_G^{(2)} + 1/tz\Big)(tz\psi)^2 + \Delta_G^{(4)}(tz\psi)^4 + \mathcal{O}\big((tz\psi)^6\big)\,. \qquad \text{(A.20)}
$$

The expansion parameter $\Delta_G^{(2)}$ is obviously always negative and $\Delta_G^{(4)}$ is always positive, which is not so obvious, but can be seen in figure A.1. Hence, the ground state energy as a function of the order parameter ψ is bound from below and, thus, well defined.

APPENDIX B

Transport Theory for the Disordered Bose-Hubbard Model

B.1 Relations for the Green's Functions

When evaluating the current density (4.9), expectation values of the form $\langle \hat{b}_j^\dagger(t)\hat{b}_i(t)\rangle$ have to be calculated. These expressions can be related to the well known retarded and advanced Green's functions, for which then the already established Green's function formalism can be employed. Following the description in [86], we first define the *greater* Green's function,

$$G_{ij}^{>}(t,t') = -\mathrm{i}\langle \hat{b}_i(t)\hat{b}_j^\dagger(t')\rangle\,, \tag{B.1}$$

and the *lesser* Green's function,

$$G_{ij}^{<}(t,t') = -\mathrm{i}\langle \hat{b}_j^\dagger(t')\hat{b}_i(t)\rangle\,. \tag{B.2}$$

These two quantities appear in the Keldysh formalism for non-equilibrium physics, where the greater and lesser signs refer to the position of the two time arguments on a time-contour. Since we are interested in equilibrium physics, we do not need to go into detail here, but will just use the definitions.

The retarded and advanced Green's functions can be expressed in terms of the greater and lesser functions as follows

$$G_{ij}^{R}(t,t') = -\mathrm{i}\theta(t-t')\langle[\hat{b}_i(t),\hat{b}_j^\dagger(t')]\rangle = +\theta(t-t')\big[G_{ij}^{>}(t,t') - G_{ij}^{<}(t,t')\big] \tag{B.3}$$

and

$$G_{ij}^{A}(t,t') = +\mathrm{i}\theta(t'-t)\langle[\hat{b}_i(t),\hat{b}_j^\dagger(t')]\rangle = -\theta(t'-t)\big[G_{ij}^{>}(t,t') - G_{ij}^{<}(t,t')\big]\,. \tag{B.4}$$

Combining the above two equations yields one further relation,

$$G_{ij}^{R}(t,t') - G_{ij}^{A}(t,t') = G_{ij}^{>}(t,t') - G_{ij}^{<}(t,t')\,. \tag{B.5}$$

With this, we already have established a link between both types of Green's functions. In the expression for the current density, however, only the lesser function appears. Thus, we need to eliminate the greater function from equation (B.5).

The first step is to Fourier transform into frequency space. For the lesser function we obtain

$$\begin{aligned} G_{ij}^{<}(E) &= \int_{-\infty}^{\infty} \mathrm{d}t\, e^{\mathrm{i}Et} G_{ij}^{<}(t,0) \\ &= -\mathrm{i}\int_{-\infty}^{\infty} \mathrm{d}t\, e^{\mathrm{i}Et} \langle \hat{b}_j^\dagger(0)\hat{b}_i(t)\rangle \\ &= -\frac{\mathrm{i}}{Z}\int_{-\infty}^{\infty} \mathrm{d}t\, e^{\mathrm{i}Et} \sum_{n,m} e^{-\beta E_n} \langle n|\hat{b}_j^\dagger|m\rangle\langle m|e^{\mathrm{i}\hat{H}t}\hat{b}_i e^{-\mathrm{i}\hat{H}t}|n\rangle \\ &= -\frac{2\pi\mathrm{i}}{Z}\sum_{n,m} \delta(E - E_n + E_m)\, e^{-\beta E_n}\langle n|\hat{b}_j^\dagger|m\rangle\langle m|\hat{b}_i|n\rangle\,, \end{aligned}$$

where the summations are taken over the eigenbasis of the grand-canonical Hamiltonian $\hat{H}$ and $Z = \mathrm{Tr}\{e^{-\beta\hat{H}}\}$ is the grand-canonical partition function. Similar, for the greater function one can derive

$$\begin{aligned} G_{ij}^{>}(E) &= -\frac{2\pi\mathrm{i}}{Z}\sum_{n,m} \delta(E + E_n - E_m)\, e^{-\beta E_n}\langle n|\hat{b}_i|m\rangle\langle m|\hat{b}_j^\dagger|n\rangle \\ &= -\frac{2\pi\mathrm{i}}{Z}\sum_{n,m} \delta(E - E_n + E_m)\, e^{-\beta E_n} e^{\beta(E_n - E_m)}\langle n|\hat{b}_j^\dagger|m\rangle\langle m|\hat{b}_i|n\rangle \\ &= e^{\beta E} G_{ij}^{<}(E)\,, \end{aligned} \tag{B.6}$$

where in the last step we have used the difference $E_n - E_m$ is fixed by the δ-function. Inserting this result into equation (B.5), we finally have a relation between the lesser function and the advanced and retarded Green's functions,

$$G_{ij}^{<}(E) = b(E)\big[G_{ij}^{A}(E) - G_{ij}^{R}(E)\big]\,, \tag{B.7}$$

where $b(E) = 1/(e^{\beta E} - 1)$ is the Bose distribution.

B.2 Locator Expansion

In this section, we want to derive a perturbative expansion of the single-particle Green's function for the Anderson Hamiltonian

$$\hat{H}_A = \sum_i \varepsilon_i \hat{b}_i^\dagger \hat{b}_i + \sum_{ij}^{i\neq j} J_{ij}\hat{b}_i^\dagger\hat{b}_j\,. \tag{B.8}$$

The evolution in time of the Green's functions is determined by the Heisenberg equation,

$$\begin{aligned} \mathrm{i}\frac{\mathrm{d}}{\mathrm{d}t}G_{ij}^{R/A}(t-t') &= \delta_{ij}\delta(t-t') \mp i\theta\big(\pm(t-t')\big)\langle\big[[\hat{b}_i(t),\hat{H}],\hat{b}_j^\dagger(t')\big]\rangle \\ &= \delta_{ij}\delta(t-t') + \varepsilon_i\, G_{ij}^{R/A}(t-t') + \sum_l^{l\neq i} J_{il} G_{lj}^{R/A}(t-t')\,. \end{aligned} \tag{B.9}$$

Defining the Fourier transformed Green's functions as

$$G_{ij}(E \pm \mathrm{i}\eta) = G_{ij}^{R/A}(E) = \int \mathrm{d}t\, e^{\mathrm{i}(E\pm\mathrm{i}\eta)t} G_{ij}^{R/A}(t)\,, \tag{B.10}$$

where we have chosen $t' = 0$, we can write

$$\int \mathrm{d}t\, e^{\mathrm{i}(E\pm\mathrm{i}\eta)t}\Big[\mathrm{i}\frac{\mathrm{d}}{\mathrm{d}t} G_{ij}^{R/A}(t)\Big] = \int \mathrm{d}t\, e^{\mathrm{i}(E\pm\mathrm{i}\eta)t}\Big[\delta_{ij}\delta(t) + \varepsilon_i\, G_{ij}^{R/A}(t) + \sum_l^{l\neq i} J_{il} G_{lj}^{R/A}(t)\Big]$$

$$\Leftrightarrow \quad -\int \mathrm{d}t\, \Big[\mathrm{i}\frac{\mathrm{d}}{\mathrm{d}t} e^{\mathrm{i}(E\pm\mathrm{i}\eta)t}\Big] G_{ij}^{R/A}(t) = \delta_{ij} + \varepsilon_i\, G_{ij}(E \pm \mathrm{i}\eta) + \sum_l^{l\neq i} J_{il} G_{lj}(E \pm \mathrm{i}\eta)\,,$$

where we have performed a partial integration on the left hand side and used that either the Green's function or the exponential function vanishes at the boundaries. Taking out the remaining integral, we finally obtain

$$E\, G_{ij}(E) = \delta_{ij} + \varepsilon_i\, G_{ij}(E) + \sum_l^{l\neq i} J_{il} G_{lj}(E)\,. \tag{B.11}$$

where now $E \in \mathbb{C}$. Identifying G_{ij} as the components of the Green's function matrix G, the above equation can be rewritten as

$$(E - H_\varepsilon - H_J) G(E) = \mathbb{1}\,, \tag{B.12}$$

with the diagonal matrix H_ε containing the onsite energies, $(H_\varepsilon)_{ij} = \varepsilon_i \delta_{ij}$, and the hopping matrix H_J, with $(H_J)_{ij} = J_{ij}$. The equation is formally solved by matrix inversion,

$$G(E) = (E - H_\varepsilon - H_J)^{-1}\,. \tag{B.13}$$

Interpreting the hopping matrix as a perturbation term, we define the unperturbed Green's function as

$$G^0(E) = (E - H_\varepsilon)^{-1}\,, \tag{B.14}$$

which is diagonal and has the components

$$G_{ij}^0(E) = \frac{\delta_{ij}}{E - \varepsilon_i} \equiv \delta_{ij} G_i^0(E)\,. \tag{B.15}$$

$G_i^0(E)$ is also referred to as the *locator*, in contrast to the full Green's function acting as the propagator. Rearranging the terms in equation (B.12) and inserting the definition of the locator yields

$$G(E) = G^0(E) + G^0(E) H_J G(E)\,, \tag{B.16}$$

or, in terms of the components,

$$G_{ij}(E) = G_i^0(E)\delta_{ij} + G_i^0(E) \sum_l^{l\neq i} J_{il} G_{lj}(E)\,. \tag{B.17}$$

The above equation can be solved iteratively by inserting the expression on the right back into itself. This expansion of the full propagator in terms of the local Green's functions is known as the *locator expansion*.

B.3 Coherent Potential Approximation

For calculating the diffusion integral of the self-consistent theory of localization, one needs the disorder averaged single-particle Green's function,

$$\langle G_{ij}(E)\rangle \equiv \int \mathrm{d}\varepsilon_1 P_\varepsilon(\varepsilon_1) \int \mathrm{d}\varepsilon_2 P_\varepsilon(\varepsilon_2) \ldots \int \mathrm{d}\varepsilon_{N_i} P_\varepsilon(\varepsilon_{N_i}) G_{ij}(E)\,, \tag{B.18}$$

In this section, we will present an approximative method to obtain this quantity, known as the *coherent potential approximation* (CPA), which was introduced by Soven in 1967 [87].

We have already shown in section B.2 that the Green's function can be written as

$$G(E) = \big(E - H_A\big)^{-1}\,, \tag{B.19}$$

where $G(E)$ is a matrix in the discrete lattice space with its elements being the single-particle Green's functions, $(G)_{ij} = G_{ij}$. Furthermore, $H_A = H_\varepsilon - \mu\mathbb{1} + H_J$ is the Anderson Hamiltonian in matrix form, with $(H_\varepsilon)_{ij} = \varepsilon_i \delta_{ij}$ and

$$(H_J)_{ij} = \begin{cases} -J & \text{for } i,j \text{ nearest neighbors,} \\ 0 & \text{otherwise.} \end{cases} \tag{B.20}$$

Now, instead of expanding the full Green's function in terms of the locator functions and treating the kinetic term as a perturbation, one can also approach the problem from the opposite direction. Therefore, we define the free Green's function as

$$G^0(E) = \big(E - H_J\big)^{-1}\,, \tag{B.21}$$

which, unlike the locator, is not diagonal in position space, but can be easily evaluated by transforming to reciprocal space. Equation (B.19) can then be rewritten as

$$G(E) = G^0(E) + G^0(E) H_\varepsilon G(E)\,. \tag{B.22}$$

Performing a disorder average on this equation yields

$$\langle G(E)\rangle = G^0(E) + G^0(E)\langle H_\varepsilon G(E)\rangle\,, \tag{B.23}$$

where it was used that G^0 does only depend on the translational invariant kinetic term and is, therefore, unaffected by the averaging process. By introducing the self-energy $\Sigma(E)$, we can formally solve the above equation,

$$\begin{aligned} \langle G(E)\rangle &= G^0(E) + G^0(E)\Sigma(E)\langle G(E)\rangle \\ &= \Big(E - H_J - \Sigma(E)\Big)^{-1}\,. \end{aligned} \tag{B.24}$$

Note that at this point the self-energy is an unknown matrix and we will only find out later that it is actually a scalar quantity within the CPA. Now, with this definition we go back to

expression (B.19) for the Green's function, which can be transformed as follows,

$$\begin{aligned} G(E) &= \Big(E - H_J - H_\varepsilon\Big)^{-1} \\ &= \Big(E - H_J - \Sigma(E) - \underbrace{\big(H_\varepsilon - \Sigma(E)\big)}_{\equiv V(E)}\Big)^{-1} \\ &= \langle G(E)\rangle + \langle G(E)\rangle V(E) G(E)\,. \end{aligned} \tag{B.25}$$

In other words, we want to expand the full Green's function in terms of the disorder averaged one. The scattering potential $V(E)$ is known as the *effective medium*. If we define the transport matrix T as

$$T = VG\langle G\rangle^{-1}\,, \tag{B.26}$$

we can write

$$G = \langle G\rangle + \langle G\rangle T \langle G\rangle\,, \tag{B.27}$$

where we have dropped the frequency E from our notation for readability. Performing a disorder average on above equation yields

$$\langle G\rangle = \langle G\rangle + \langle G\rangle\langle T\rangle\langle G\rangle\,, \tag{B.28}$$

which leads to the conditional equation

$$\langle T\rangle \stackrel{!}{=} 0\,. \tag{B.29}$$

Combining equations (B.26) and (B.27), we can evaluate the transport matrix in terms of the disorder averaged Green's function,

$$T = V + V\langle G\rangle V + V\langle G\rangle V\langle G\rangle V + V\langle G\rangle V\langle G\rangle V\langle G\rangle V + \dots\,, \tag{B.30}$$

or in terms of its components,

$$T_{ij} = V_{ij} + \sum_{kl} V_{ik}\langle G_{kl}\rangle V_{lj} + \sum_{klmn} V_{ik}\langle G_{kl}\rangle V_{lm}\langle G_{mn}\rangle V_{nj} + \dots\,, \tag{B.31}$$

with $V_{ij} = \varepsilon_i\delta_{ij} - \Sigma_{ij}$. If we now want to impose conditional equation (B.29) on the above expression, we have to take into account that a particle can scatter multiple times off the same potential V_{ij}. This leads to multiple occurrences of the same V_{ij} in one term. When performing the disorder average, they cannot be treated independently. Therefore, we want to collect repeated scattering events off the same potential V_{ij} and merge them into one single quantity. For each scattering potential, we define a new T-matrix,

$$\begin{aligned} t_{ij} &= V_{ij} + V_{ij}\langle G_{ji}\rangle V_{ij} + V_{ij}\langle G_{ji}\rangle V_{ij}\langle G_{ji}\rangle V_{ij} + \dots \\ &= V_{ij}\sum_{\alpha=0}^{\infty}\Big(\langle G_{ji}\rangle V_{ij}\Big)^{\alpha} \\ &= \frac{V_{ij}}{1 - \langle G_{ji}\rangle V_{ij}}\,. \end{aligned} \tag{B.32}$$

With this, we can rewrite equation (B.31) as follows,

$$T_{ij} = t_{ij} + \sum_{kl}^{(i,k)\neq(l,j)} t_{ik}\langle G_{kl}\rangle t_{lj} + \sum_{klmn}^{(i,k)\neq(l,m)\neq(n,j)} t_{ik}\langle G_{kl}\rangle t_{lm}\langle G_{mn}\rangle t_{nj} + \dots \,. \tag{B.33}$$

Now, the disorder average can be performed independently for different t_{ij}. Moreover, only the diagonal t_{ij}, i.e., where $i = j$, contain the on-site energies ε_i. Thus, the t_{ij} with $i \neq j$ are already disorder averaged quantities.

This implies that an arbitrary sequence of T-matrices factorizes under disorder averaging if all diagonal t_{ij} are distinct,

$$\Big\langle t_{ik}\langle G_{kl}\rangle t_{lm}\langle G_{mn}\rangle \dots \langle G_{pq}\rangle t_{qr}\langle G_{rs}\rangle t_{sj}\Big\rangle = \langle t_{ik}\rangle\langle G_{kl}\rangle\langle t_{lm}\rangle\langle G_{mn}\rangle \dots \langle G_{pq}\rangle\langle t_{qr}\rangle\langle G_{rs}\rangle\langle t_{sj}\rangle \tag{B.34}$$

Still, the summations in equation (B.33) will also contain terms where this is not the case. In order to circumvent the difficulties of having to perform disorder averages of correlated t_{ii} we introduce the so-called *single-site approximation*. Within this approximation, it is assumed that a particle never returns to scatter off a certain site a second time if it has scattered off other sites in between. Thus, we can always assume the disorder average to factorize as shown in equation (B.34). Imposing conditional equation (B.29) on equation (B.33) then yields

$$\langle T_{ij}\rangle = \langle t_{ij}\rangle + \sum_{kl}^{(i,k)\neq(l,j)} \langle t_{ik}\rangle\langle G_{kl}\rangle\langle t_{lj}\rangle + \sum_{klmn}^{(i,k)\neq(l,m)\neq(n,j)} \langle t_{ik}\rangle\langle G_{kl}\rangle\langle t_{lm}\rangle\langle G_{mn}\rangle\langle t_{nj}\rangle + \dots \overset{!}{=} 0\,. \tag{B.35}$$

Apparently, this condition is fulfilled if for each t_{ij} we have

$$\langle t_{ij}\rangle \overset{!}{=} 0\,. \tag{B.36}$$

This has two consequences. First of all, for $i \neq j$ we get

$$\langle t_{ij}\rangle = \frac{-\Sigma_{ij}}{1 + \langle G_{ji}\rangle\Sigma_{ij}} \overset{!}{=} 0\,, \tag{B.37}$$

from which it immediately follows that $\Sigma_{ij} = 0$ for $i \neq j$. In other words, the self-energy is diagonal in position space, i.e, it is local.

Second, for the diagonal elements, $i = j$, it follows that

$$\langle t_{ii}\rangle = \int \mathrm{d}\varepsilon_i P_\varepsilon(\varepsilon_i) \frac{\varepsilon_i - \Sigma_{ii}}{1 - \langle G_{ii}\rangle\big(\varepsilon_i - \Sigma_{ii}\big)} \overset{!}{=} 0\,. \tag{B.38}$$

Since the disorder averaged local Green's function is translational invariant, $\langle G_{ii}\rangle = \langle G_{jj}\rangle$ for all i, j, the local self-energy is also translational invariant, $\Sigma_{ii} = \Sigma_{jj}$ for all i, j. Thus we can drop the lattice site index from our notation and write

$$\int \mathrm{d}\varepsilon P_\varepsilon(\varepsilon) \frac{\varepsilon - \Sigma(E)}{1 - \langle G(E)\rangle\big(\varepsilon - \Sigma(E)\big)} \overset{!}{=} 0\,, \tag{B.39}$$

where it should be understood that $\langle G\rangle = \langle G_{ii}\rangle$ is the disorder averaged local Green's function.

Furthermore, since $\langle G \rangle = \langle G(E) \rangle \in \mathbb{C}$, the self-energy will also depend on E and will be a complex number, $\Sigma = \Sigma(E) \in \mathbb{C}$.

To conclude this section, we will briefly sketch how to actually solve the conditional equation in order to obtain $\Sigma(E)$. Therefore, we rearrange the equation as follows,

$$\Sigma = \frac{I_1(\Sigma)}{I_2(\Sigma)} \tag{B.40}$$

with

$$I_1(\Sigma) = \int \mathrm{d}\varepsilon P_\varepsilon(\varepsilon) \frac{\varepsilon}{1 - \langle G \rangle (\varepsilon - \Sigma)} \tag{B.41}$$

and

$$I_2(\Sigma) = \int \mathrm{d}\varepsilon P_\varepsilon(\varepsilon) \frac{1}{1 - \langle G \rangle (\varepsilon - \Sigma)} \,. \tag{B.42}$$

This allows us to solve the equation iteratively. Starting with an initial guess for the self-energy, $\Sigma^{(0)}$, we first calculate the local Green's function $\langle G(E) \rangle$ using equation (B.24) with $\Sigma = \Sigma^{(0)}$. Next, we evaluate the above two integrals I_1 and I_2 and use equation (B.40) to calculate $\Sigma^{(1)}$. This procedure is then iterated, $\Sigma^{(s+1)} = I_1(\Sigma^{(s)})/I_2(\Sigma^{(s)})$, until the desired numerical accuracy is achieved, $|\Sigma^{(s+1)} - \Sigma^{(s)}| < \mathit{threshold}$.

B.4 Self-Consistent Theory of Anderson Localization

In section 2.2.7 we already explained the motivation for developing the self-consistent theory of Anderson localization and stated the most important steps made in its derivation. Here, we want give a brief summary of the derivation, where we will follow the presentation in [67]. A complete and detailed version of the derivation can be found, for example, in the textbook *Quantum Transport Theory* by Rammer [51].

Finally, we will present a method to evaluate the diffusion integral that includes the periodicity of the dispersion relation for lattice models. This method was first introduced by Henseler et al. [26] and we will follow its presentation in [88].

B.4.1 Derivation of the Diffusion

The starting point for deriving the diffusion integral is the disorder averaged particle-hole propagator,

$$\Phi^{RA}_{\mathbf{p}\mathbf{p}'}(E, \omega, \mathbf{q}) = \left\langle G^R_{\mathbf{p}_+\mathbf{p}'_+}(E + \omega) G^A_{\mathbf{p}'_-\mathbf{p}_-}(E) \right\rangle \quad \text{with} \quad \mathbf{p}_\pm = \mathbf{p} \pm \mathbf{q}/2 \,, \tag{B.43}$$

with the Fourier transformed $G^{R/A}_{\mathbf{p}\mathbf{p}'}(E)$ of the single-particle Green's functions in reciprocal lattice (or momentum) space,

$$G^{R/A}_{\mathbf{p}\mathbf{p}'}(t) = \mp \mathrm{i}\theta(\pm t) \langle [\hat{b}_{\mathbf{p}}(t), \hat{b}^\dagger_{\mathbf{p}'}(0)] \rangle \,. \tag{B.44}$$

Here, we are interested in the limits $|\mathbf{q}| \to 0$ and $\omega \to 0$, which correspond to long-range behavior, $|\mathbf{x}_i - \mathbf{x}_j| \to \infty$, in the limit of infinitely large times, $t \to \infty$ (see [69], for example).

We already found out that calculating the disorder averaged Green's function is only possible by applying certain approximations, see section B.3. Here, we now have to evaluate the average of a product of two Green's functions. The idea will be to use the results from the CPA and try

to expand the particle-hole propagator in terms of the averaged single-particle Green's functions. This leads to the formulation of the Bethe-Salpeter equation

$$\begin{aligned}\Phi^{RA}_{\mathbf{pp'}}(E,\omega,\mathbf{q}) =& \langle G^R_{\mathbf{p}_+}(E+\omega)\rangle \langle G^A_{\mathbf{p}_-}(E)\rangle \delta_{\mathbf{pp'}} \\ &+ \langle G^R_{\mathbf{p}_+}(E+\omega)\rangle \langle G^A_{\mathbf{p}_-}(E)\rangle \frac{1}{N_i}\sum_{\mathbf{p''}} U^{RA}_{\mathbf{pp''}}(E,\omega,\mathbf{q})\ \Phi^{RA}_{\mathbf{p''p'}}(E,\omega,\mathbf{q})\,, \end{aligned} \tag{B.45}$$

where $U^{RA}_{\mathbf{pp''}}$ is the irreducible particle-hole vertex. Note that the disorder averaged Green's functions are diagonal in momentum space, $\langle G^{R/A}_{\mathbf{pp'}}\rangle \equiv \langle G^{R/A}_{\mathbf{p}}\rangle \delta_{\mathbf{pp'}}$.

The structure of the Bethe-Salpeter equation can be understood best if we first divide all scattering events of the particle and the hole propagators $G^R_{\mathbf{p}_+\mathbf{p}'_+}$ and $G^A_{\mathbf{p}_-\mathbf{p}'_-}$ into correlated and uncorrelated events, i.e., scattering events at the same and at different impurity potentials V_{ij} (see section B.3 for definition).

If the events are uncorrelated, the disorder average can be performed independently for each Green's function. Only if they scatter off the same impurity one needs to average over both propagators at the same time. The summation of all uncorrelated events taking place in between correlated scatterings leads to the disorder averaged single-particle propagators.

The particle-hole vertex $U^{RA}_{\mathbf{pp''}}$ contains all correlated scattering events that are irreducible with respect to cutting one particle and one hole propagator line (i.e., two lines in total in contrast to just one line for the usual definition of irreducible diagrams). All series of scattering events can then be represented in terms of irreducible vertices connected by the independently averaged particle and hole propagators, yielding the Bethe-Salpeter equation (B.45).

Furthermore, the irreducible particle-hole vertex is connected to the single-particle self-energy $\Sigma^{R/A}_{\mathbf{p}}$ by a Ward identity,

$$\Sigma^R_{\mathbf{p}_+}(E+\omega) - \Sigma^A_{\mathbf{p}_-}(E) = \frac{1}{N_i}\sum_{\mathbf{p'}} U^{RA}_{\mathbf{pp'}}(E,\omega,\mathbf{q})\Big[\langle G^R_{\mathbf{p}'_+}(E+\omega)\rangle - \langle G^A_{\mathbf{p}'_-}(E)\rangle\Big]\,. \tag{B.46}$$

For an intuitive understanding, consider the following. By connecting the particle and the hole line with an additional propagator line at either of the ends of the particle-hole vertex, a new set of diagrams is constructed. The so formed class of diagrams is irreducible with respect to cutting a single propagator line and corresponds to self-energy diagrams. A careful analysis (which can be found chapter 8.8 of [51], for example) leads to the above identity.

Using the Ward identity, we can eliminate the particle-hole vertex from the Bethe-Salpeter equation (B.45). However, we need to make some transformations first (where we drop the function arguments for readability),

$$\begin{aligned} & & \Phi^{RA}_{\mathbf{pp'}} &= \langle G^R_{\mathbf{p}_+}\rangle \langle G^A_{\mathbf{p}_-}\rangle \Big(\delta_{\mathbf{pp'}} + \frac{1}{N_i}\sum_{\mathbf{p''}} U^{RA}_{\mathbf{pp''}}\ \Phi^{RA}_{\mathbf{p''p'}}\Big) \\ \Leftrightarrow \quad & \underbrace{\Big[\big(\langle G^R_{\mathbf{p}_+}\rangle\big)^{-1} - \big(\langle G^A_{\mathbf{p}_-}\rangle\big)^{-1}\Big]}_{=\omega-\varepsilon_{\mathbf{p}_+}+\varepsilon_{\mathbf{p}_-}-\Sigma^R_{\mathbf{p}_+}+\Sigma^A_{\mathbf{p}_-}} \Phi^{RA}_{\mathbf{pp'}} &&= \Big[\langle G^A_{\mathbf{p}_-}\rangle - \langle G^R_{\mathbf{p}_+}\rangle\Big]\Big(\delta_{\mathbf{pp'}} + \frac{1}{N_i}\sum_{\mathbf{p''}} U^{RA}_{\mathbf{pp''}}\ \Phi^{RA}_{\mathbf{p''p'}}\Big) \\ \Rightarrow \quad & \big[\omega - q(\mathbf{v}_p\cdot\hat{\mathbf{q}}) - \Sigma^R_{\mathbf{p}_+} + \Sigma^A_{\mathbf{p}_-}\big]\frac{1}{N_i}\sum_{\mathbf{p'}} \Phi^{RA}_{\mathbf{pp'}} &&= \Big[\langle G^A_{\mathbf{p}_-}\rangle - \langle G^R_{\mathbf{p}_+}\rangle\Big]\Big(1 + \frac{1}{(N_i)^2}\sum_{\mathbf{p'p''}} U^{RA}_{\mathbf{pp''}}\ \Phi^{RA}_{\mathbf{p''p'}}\Big)\,, \end{aligned} \tag{B.47}$$

where $\varepsilon_{\mathbf{p}_+} - \varepsilon_{\mathbf{p}_-} = (\nabla\varepsilon_{\mathbf{p}} \cdot \mathbf{q}) \equiv q(\mathbf{v}_p \cdot \hat{\mathbf{q}})$ with $\hat{\mathbf{q}} = \mathbf{q}/|\mathbf{q}|$ and $q = |\mathbf{q}|$ was used, assuming the limit $q \to 0$.

Replacing the self-energies using the Ward identity and summing over $\mathbf{p}$, the irreducible vertex cancels out and in the limit $\omega, q \to 0$ we have

$$\omega\Phi_{\rho\rho}(E,\omega,\mathbf{q}) - q\Phi_{j\rho}(E,\omega,\mathbf{q}) = 2\pi\mathrm{i}N(E)\,, \tag{B.48}$$

where we have defined the density-density correlation function

$$\Phi_{\rho\rho}(E,\omega,\mathbf{q}) \equiv \frac{1}{(N_i)^2}\sum_{\mathbf{p}\mathbf{p}'}\Phi^{RA}_{\mathbf{p}\mathbf{p}'}(E,\omega,\mathbf{q}) \tag{B.49}$$

and the current-density correlation function

$$\Phi_{j\rho}(E,\omega,\mathbf{q}) \equiv \frac{1}{(N_i)^2}\sum_{\mathbf{p}\mathbf{p}'}(\mathbf{v}_p \cdot \hat{q})\Phi^{RA}_{\mathbf{p}\mathbf{p}'}(E,\omega,\mathbf{q})\,. \tag{B.50}$$

Furthermore, impurity averaged density of states were introduced as

$$N(E) \equiv \frac{1}{\pi}\,\mathrm{Im}\left\{\langle G^A_0(E)\rangle\right\} = \frac{1}{N_i}\sum_p \frac{1}{\pi}\,\mathrm{Im}\left\{\langle G^A_{\mathbf{p}}(E)\rangle\right\}. \tag{B.51}$$

Equation (B.48) can be viewed as a continuity equation for the correlation functions, relating the current and the density correlations with the density of states taking the role of a source term. However, since we do know neither of the two correlation functions, we need a second conditional equation in order to find a solution.

Therefore, we rewrite equation (B.47) as follows,

$$\left[\omega - q(\mathbf{v}_p \cdot \hat{q}) + 2\mathrm{i}\ \mathrm{Im}\left\{\Sigma^A_{\mathbf{p}}\right\}\right]\Phi_{\mathbf{p}} = 2\mathrm{i}\ \mathrm{Im}\left\{\langle G^A_{\mathbf{p}}\rangle\right\}\left(1 + \frac{1}{N_i}\sum_{\mathbf{p}''} U^{RA}_{\mathbf{p}\mathbf{p}''}\ \Phi_{\mathbf{p}''}\right), \tag{B.52}$$

where we have introduced the correlation function integrated over the incoming momentum $\mathbf{p}'$

$$\Phi_{\mathbf{p}} = \frac{1}{N_i}\sum_{\mathbf{p}'}\Phi^{RA}_{\mathbf{p}\mathbf{p}'}\,. \tag{B.53}$$

At this point, we have to introduce the first major assumption of this theory, which is twofold. First, we assume that $\Phi_{\mathbf{p}}$ can be expanded in terms of $\Phi_{\rho\rho}$ and $\Phi_{j\rho}$ for $\omega, q \to 0$,

$$\Phi_{\mathbf{p}} \approx A_{\mathbf{p}}\Phi_{\rho\rho} + B_{\mathbf{p}}\Phi_{j\rho} + \text{"less divergent terms"}\,. \tag{B.54}$$

Second, we assume that all critical behavior is contained in the correlation functions and the coefficients $A_{\mathbf{p}}$ and $B_{\mathbf{p}}$ behave uncritical. Thus, they can be *fitted* by using the simple *ladder approximation* for the Bethe-Salpeter equation (B.45), by which $\Phi_{\mathbf{p}}$, $\Phi_{\rho\rho}$ and $\Phi_{j\rho}$ can be calculated directly.

By inserting approximation (B.54) into equation (B.52), the summation on the right-hand

side can be decoupled from the correlation functions,

$$\frac{1}{N_i}\sum_{\mathbf{p}''} U^{RA}_{\mathbf{p}\mathbf{p}''}\ \Phi_{\mathbf{p}''} \approx \left(\frac{1}{N_i}\sum_{\mathbf{p}''} U^{RA}_{\mathbf{p}\mathbf{p}''}\ A_{\mathbf{p}''}\right)\Phi_{\rho\rho} + \left(\frac{1}{N_i}\sum_{\mathbf{p}''} U^{RA}_{\mathbf{p}\mathbf{p}''}\ B_{\mathbf{p}''}\right)\Phi_{j\rho}\,. \tag{B.55}$$

Using the explicit results for $A_{\mathbf{p}}$ and $B_{\mathbf{p}}$ from the ladder approximation, one obtains a second conditional equation for $\Phi_{\rho\rho}$ and $\Phi_{j\rho}$ (see [67] for the details). Combining the two conditional equations, one obtains the density correlation function (valid in the limit $\omega, q \to 0$),

$$\Phi_{\rho\rho}(E,\omega,q) = \frac{2\pi\mathrm{i}\,N(E) - q^2\frac{R(E)}{\omega+2\mathrm{i}\Sigma^A(E)+\mathrm{i}M(E,\omega)}}{\omega + \mathrm{i}q^2 D(E,\omega)}\,, \tag{B.56a}$$

with

$$R(E) = \frac{1}{2N_i}\sum_{\mathbf{p}}(\mathbf{v}_p\cdot\hat{q})^2\Big[\langle G^A_{\mathbf{p}}(E)\rangle^2 + \langle G^R_{\mathbf{p}}(E)\rangle^2\Big]\,, \tag{B.56b}$$

the *current relaxation kernel*

$$M(E,\omega) = \frac{-2}{\pi N(E) D_0(E)}\frac{1}{(N_i)^2}\sum_{\mathbf{p}\mathbf{p}'}(\mathbf{v}_p\cdot\hat{\mathbf{q}})\,\mathrm{Im}\left\{\langle G^A_{\mathbf{p}}(E)\rangle\right\}U^{RA}_{\mathbf{p}\mathbf{p}'}(E,\omega,q)\left(\mathrm{Im}\left\{\langle G^A_{\mathbf{p}'}(E)\rangle\right\}\right)^2(\mathbf{v}_{p'}\cdot\hat{\mathbf{q}})\,, \tag{B.56c}$$

the *generalized diffusion coefficient*

$$D(E,\omega) = \frac{D_0(E)}{1+\frac{-\mathrm{i}\omega+M(E,\omega)}{2\,\mathrm{Im}\,\Sigma^A(E)}}\,, \tag{B.56d}$$

and the *bare diffusion coefficient*

$$D_0(E) = \frac{1}{\pi N(E)}\frac{1}{N_i}\sum_{\mathbf{p}}(\mathbf{v}_p\cdot\hat{q})^2\Big(\mathrm{Im}\left\{\langle G^A_{\mathbf{p}}(E)\rangle\right\}\Big)^2\,. \tag{B.56e}$$

which originates from the solution in ladder approximation, thus the term *bare* diffusion in contrast to the *generalized* diffusion.

Having derived the general form of the density correlation function, the full particle-hole vertex will now be approximated by its most divergent contributions. In [29, 61] (or also in the textbook [51]) it shown that these are given by the *maximally crossed diagrams*. As they are connected to the ladder diagrams by time-reversal, they be directly obtained from the ladder approximation solution. Classifying all diagrams in terms of the maximally crossed ones and again only keeping the most divergent contributions (see [67], for example), one finds that the full particle-hole vertex is proportional to the density-density correlation function,

$$U^{RA}_{\mathbf{p}\mathbf{p}'}(E,\omega,q) \approx \left(U^{RA}_0(E,\omega)\right)^2\,\Phi_{\rho\rho}(E,\omega,\mathbf{p}+\mathbf{p}')\,, \tag{B.57}$$

where U^{RA}_0 is the *single-site* vertex from ladder approximation (which is the analogon to the T-matrix in single-site approximation used in CPA),

$$U^{RA}_0(E,\omega) = \frac{\Sigma^A(E)-\Sigma^R(E+\omega)}{\langle G^A(E)\rangle - \langle G^R(E+\omega)\rangle}\,. \tag{B.58}$$

Comparing equations (B.56) and (B.57), we see that $\Phi_{\rho\rho}$ is at the core of the current relaxation kernel $M(E,\omega)$, which in turn determines $\Phi_{\rho\rho}$. Thus, these equations have to be solved self-consistently, and hence, the name *self-consistent theory of Anderson localization*.

Furthermore, expression (B.56d) for the diffusion coefficient can be transformed as follows,

$$\begin{aligned} D(\omega)(1-\mathrm{i}\omega/2\,\mathrm{Im}\,\Sigma^A) &= D_0 - \frac{D(\omega)M(\omega)}{2\,\mathrm{Im}\,\Sigma^A} \\ &= D_0 + \frac{D(\omega)}{2\,\mathrm{Im}\,\Sigma^A}\frac{2}{\pi N(E) D_0}\frac{1}{(N_i)^2}\sum_{\mathbf{pp'}}(\mathbf{v}_p\cdot\hat{\mathbf{q}})\,\mathrm{Im}\left\{\langle G^A_{\mathbf{p}}\rangle\right\}U^{RA}_{\mathbf{pp'}}(\omega,q)\left(\mathrm{Im}\left\{\langle G^A_{\mathbf{p'}}\rangle\right\}\right)^2(\mathbf{v}_{p'}\cdot\hat{\mathbf{q}}) \\ &\approx D_0 + \frac{2\,\mathrm{Im}\,\Sigma^A}{[\pi N(E)]^2 D_0}\frac{1}{(N_i)^2}\sum_{\mathbf{pp'}}(\mathbf{v}_p\cdot\hat{\mathbf{q}})\,\frac{\mathrm{Im}\left\{\langle G^A_{\mathbf{p}}\rangle\right\}\left(\mathrm{Im}\left\{\langle G^A_{\mathbf{p'}}\rangle\right\}\right)^2}{(\mathbf{p}+\mathbf{p}')^2 - \mathrm{i}\omega/D(\omega)}\,(\mathbf{v}_{p'}\cdot\hat{\mathbf{q}})\,, \end{aligned} \tag{B.59}$$

where in the last step we have replaced the full vertex by its most divergent contributions, see equation (B.57), and dropped the term proportional to q in the numerator of $\Phi_{\rho\rho}$.

In the localized regime, the diffusion vanishes linearly as a function of the frequency ω,

$$\lim_{\omega\to 0} D(E,\omega) \to -\mathrm{i}\omega\,\xi^2(E) + \mathcal{O}(\omega^2)\,, \tag{B.60}$$

where ξ can be identified as the localization length, see [51] for example. Thus, in the localized regime equation (B.59) becomes

$$I_\xi \equiv D_0 + \frac{2\,\mathrm{Im}\,\Sigma^A}{[\pi N(E)]^2 D_0}\frac{1}{(N_i)^2}\sum_{\mathbf{pp'}}(\mathbf{v}_p\cdot\hat{\mathbf{q}})\,\frac{\mathrm{Im}\left\{\langle G^A_{\mathbf{p}}\rangle\right\}\left(\mathrm{Im}\left\{\langle G^A_{\mathbf{p'}}\rangle\right\}\right)^2}{(\mathbf{p}+\mathbf{p}')^2 - 1/\xi^2}\,(\mathbf{v}_{p'}\cdot\hat{\mathbf{q}}) \stackrel{!}{=} 0\,. \tag{B.61}$$

Finding the root of I_ξ as a function of ξ yields the localization length.

The transition from localized to extended regime is characterized by a diverging localization length, $\xi\to\infty$, and the transition from the opposite direction by a vanishing diffusion coefficient, $D\to 0$. The exact point of the Anderson transition is thus characterized by $D=0$ and $1/\xi^2=0$, yielding the following conditional equation,

$$I_\infty \equiv D_0 + \frac{2\,\mathrm{Im}\,\Sigma^A}{[\pi N(E)]^2 D_0}\frac{1}{(N_i)^2}\sum_{\mathbf{pp'}}(\mathbf{v}_p\cdot\hat{\mathbf{q}})\,\frac{\mathrm{Im}\left\{\langle G^A_{\mathbf{p}}\rangle\right\}\left(\mathrm{Im}\left\{\langle G^A_{\mathbf{p'}}\rangle\right\}\right)^2}{(\mathbf{p}+\mathbf{p}')^2}\,(\mathbf{v}_{p'}\cdot\hat{\mathbf{q}}) \stackrel{!}{=} 0\,. \tag{B.62}$$

Thus, here we have to find the root of I_∞ as a function of the system parameters.

B.4.2 Evaluation of the Diffusion Integral for a Periodic Dispersion Relation

In the previous section we have derived a self-consistent method to calculate the density correlations of a disordered system. An integral part of the derivation was the restriction to small momenta, $q\to 0$. For the free dispersion, $\varepsilon_{\mathbf{p}} = \mathbf{p}^2/2m$, one can use this to rewrite the energy difference as follows,

$$\varepsilon_{\mathbf{p}_+} - \varepsilon_{\mathbf{p}_-} = \sum_{i=1}^{d} q_i\,\frac{\varepsilon_{p_i+q_i/2} - \varepsilon_{p_i-q_i/2}}{q_i} = (\mathbf{q}\cdot\nabla\varepsilon_{\mathbf{p}}) = q(\mathbf{v}_q\cdot\hat{\mathbf{q}}) \quad \text{for } q\to 0\,. \tag{B.63}$$

This made it possible to take the limit $q \to 0$ independently from the momenta $\mathbf{p}$ and $\mathbf{p}'$. However, here we are interested in describing a lattice system, which has a different dispersion relation, $\varepsilon_{\mathbf{p}} = -2J \sum_{i=1}^{d} \cos p_i$. In this case, we have

$$\begin{aligned} \varepsilon_{\mathbf{p}_+} - \varepsilon_{\mathbf{p}_-} &= -2J \sum_{i=1}^{d} \big[\cos(p_i + q_i/2) - \cos(p_i - q_i/2) \big] \\ &= -2J \sum_{i=1}^{d} \big[-2 \sin(p_i) \sin(q_i/2) \big] \\ &= 2 \sin(q/2) (\mathbf{v}_q \cdot \hat{\mathbf{q}}) \,, \end{aligned} \tag{B.64}$$

where for simplicity we have assumed that $\mathbf{q}$ points along one of the coordinate axes, $\hat{\mathbf{q}} = \hat{\mathbf{e}}_i$ with $i = 1, 2,$ or 3. In the limit $q \to 0$, this again yields expression (B.63). We have to be careful, though, when using approximation (B.57) for the particle-hole vertex, where the replacement $\mathbf{q} \to \mathbf{p} + \mathbf{p}'$ is made.

First of all, this tells us that the vertex approximation may only be used for $|\mathbf{p} + \mathbf{p}'| \ll 1$, i.e., $\mathbf{p} \approx -\mathbf{p}'$. These are essentially the contributions arising from coherent backscattering.

Second, we have to take into account that the Bloch states are invariant under a shift of the wave vector by 2π. This restricts the components of the wave vectors to values within an interval of width 2π (i.e., one single *Brillouin zone*), where one usually chooses either $[-\pi, \pi]$ or $[0, 2\pi]$. Thus, the maximal momentum difference is given by 2π. Due to the periodicity, however, this difference is actually zero, and in fact, the sine in (B.64) would take care of this unambiguity.

Here, we are using the theory as it was implemented in [26, 88], where this problem is circumvented by restricting the values of q to the interval $[-\pi, \pi]$. This allows to safely take the limit $\lim_{q \to 0} 2 \sin(q/2) = q$. Nevertheless, it might be interesting to investigate how the results change if one does not make this approximation. This, however, is not within the scope of this work.

Restricting q to $[-\pi, \pi]$ implies that also the components of $\mathbf{p} + \mathbf{p}'$ are confined to this interval. With this information we can now try to evaluate the momentum integration in the self-consistent equation (B.61) for the diffusion,

$$\frac{1}{(N_i)^2} \sum_{\mathbf{p}\mathbf{p}'} (\mathbf{v}_p \cdot \hat{\mathbf{q}}) \, \frac{\operatorname{Im}\big\{\langle G^A_{\mathbf{p}} \rangle\big\} \big(\operatorname{Im}\big\{\langle G^A_{\mathbf{p}'} \rangle\big\}\big)^2}{(\mathbf{p} + \mathbf{p}')^2 + 1/\xi^2} \, (\mathbf{v}_{p'} \cdot \hat{\mathbf{q}}) \,. \tag{B.65}$$

The difficulty of evaluating above integral is that it is $2d$-dimensional, i.e. 6-dimensional for 3 spatial dimensions. The integrations are coupled by the term $(\mathbf{p} + \mathbf{p}')^2$ in the denominator. However, we can make use of the fact that all quantities of the integrand are periodic with respect to the momenta. By performing a Fourier transformation back into real space, we can decouple the two momentum integrals.

Since there is no preferred direction of transport in the Anderson model, without loss of

generality we can choose $\hat{\mathbf{q}} = \hat{\mathbf{e}}_x$. The Fourier transform of the velocity term is then given by

$$\begin{aligned} v(\mathbf{x}) &\equiv \frac{1}{N_i}\sum_{\mathbf{p}} (\mathbf{v}_p \cdot \hat{\mathbf{q}}) e^{-\mathrm{i}\mathbf{p}\cdot\mathbf{x}} \\ &= \frac{1}{N_i}\sum_{\mathbf{p}} (-2J\sin p_x) e^{-\mathrm{i}\mathbf{p}\cdot\mathbf{x}} \\ &= \mathrm{i}J\frac{1}{N_i}\sum_{\mathbf{p}} \left(e^{+\mathrm{i}\mathbf{p}\cdot\mathbf{e}_x} - e^{-\mathrm{i}\mathbf{p}\cdot\mathbf{e}_x}\right) e^{-\mathrm{i}\mathbf{p}\cdot\mathbf{x}} \\ &= \mathrm{i}J\left(\delta^{(d)}_{\mathbf{x},\hat{\mathbf{e}}_x} - \delta^{(d)}_{\mathbf{x},-\hat{\mathbf{e}}_x}\right) \end{aligned} \tag{B.66}$$

where we have used that

$$\frac{1}{N_i}\sum_{\mathbf{p}} e^{-\mathrm{i}\mathbf{p}\cdot(\mathbf{x}-\mathbf{x}')} = \delta^{(d)}_{\mathbf{x},\mathbf{x}'} \tag{B.67}$$

with the Kronecker-δ in d dimensions,

$$\delta^{d}_{\mathbf{x},\mathbf{x}'} = \prod_{i=1}^{d} \delta_{x_i,x_i'}\,. \tag{B.68}$$

For the remaining terms of the integrand we define

$$g(\mathbf{x}) \equiv \frac{1}{N_i}\sum_{\mathbf{p}} \mathrm{Im}\left\{\langle G^A_{\mathbf{p}}\rangle\right\} e^{-\mathrm{i}\mathbf{p}\cdot\mathbf{x}} = \int_{-\pi}^{\pi} \frac{\mathrm{d}^d p}{(2\pi)^d}\, \mathrm{Im}\left\{\langle G^A_{\mathbf{p}}\rangle\right\} \prod_{i=1}^{d} \cos(p_i x_i)\,, \tag{B.69}$$

$$g_2(\mathbf{x}) \equiv \frac{1}{N_i}\sum_{\mathbf{p}} \left(\mathrm{Im}\left\{\langle G^A_{\mathbf{p}}\rangle\right\}\right)^2 e^{-\mathrm{i}\mathbf{p}\cdot\mathbf{x}} = \int_{-\pi}^{\pi} \frac{\mathrm{d}^d p}{(2\pi)^d} \left(\mathrm{Im}\left\{\langle G^A_{\mathbf{p}}\rangle\right\}\right)^2 \prod_{i=1}^{d} \cos(p_i x_i)\,, \tag{B.70}$$

$$C(\mathbf{x}) \equiv \frac{1}{N_i}\sum_{\mathbf{p}} \frac{1}{\mathbf{p}^2 + 1/\xi^2}\, e^{-\mathrm{i}\mathbf{p}\cdot\mathbf{x}} = \int_{-\pi}^{\pi} \frac{\mathrm{d}^d p}{(2\pi)^d} \frac{1}{\mathbf{p}^2 + 1/\xi^2} \prod_{i=1}^{d} \cos(p_i x_i)\,, \tag{B.71}$$

where we have replaced the summation by an integration in the limit $N_i \to \infty$ and have used that $\langle G^A_{\mathbf{p}}\rangle$ and $\mathbf{p}^2$ are invariant under the transformation $\mathbf{p} \to -\mathbf{p}$. From the above form of the Fourier transforms we can also conclude that $g(\mathbf{x}), g_2(\mathbf{x})$, and $C(\mathbf{x})$ are invariant under permutation of the components of $\mathbf{x}$, i.e., $x_i \leftrightarrow x_j$, as well as under the transformation $x_i \to -x_i$.

With these definitions we can rewrite the momentum integral (B.65) as follows,

$$\begin{aligned} &\frac{1}{(N_i)^2}\sum_{\mathbf{p}\mathbf{p}'} (\mathbf{v}_p \cdot \hat{\mathbf{q}})\, \frac{\mathrm{Im}\left\{\langle G^A_{\mathbf{p}}\rangle\right\}\left(\mathrm{Im}\left\{\langle G^A_{\mathbf{p}'}\rangle\right\}\right)^2}{(\mathbf{p}+\mathbf{p}')^2 + 1/\xi^2}\, (\mathbf{v}_{p'} \cdot \hat{\mathbf{q}}) \\ &= \frac{1}{(N_i)^2}\sum_{\mathbf{p}\mathbf{p}'}\sum_{\mathbf{x}_1\ldots\mathbf{x}_5} v(\mathbf{x}_1) g(\mathbf{x}_2) C(\mathbf{x}_3) g_2(\mathbf{x}_4) v(\mathbf{x}_5) e^{\mathrm{i}\mathbf{p}\cdot(\mathbf{x}_1+\mathbf{x}_2+\mathbf{x}_3)} e^{\mathrm{i}\mathbf{p}'\cdot(\mathbf{x}_3+\mathbf{x}_4+\mathbf{x}_5)} \\ &= \sum_{\mathbf{x}_1\ldots\mathbf{x}_5} v(\mathbf{x}_1) g(\mathbf{x}_2) C(\mathbf{x}_3) g_2(\mathbf{x}_4) v(\mathbf{x}_5)\, \delta^{(d)}_{\mathbf{x}_1+\mathbf{x}_2,-\mathbf{x}_3}\, \delta^{(d)}_{\mathbf{x}_4+\mathbf{x}_5,-\mathbf{x}_3} \\ &= \sum_{\mathbf{x}_1\mathbf{x}_2\mathbf{x}_4\mathbf{x}_5} v(\mathbf{x}_1) g(\mathbf{x}_2) C(-\mathbf{x}_1-\mathbf{x}_2) g_2(\mathbf{x}_4) v(\mathbf{x}_5)\, \delta^{(d)}_{\mathbf{x}_1+\mathbf{x}_2,\mathbf{x}_4+\mathbf{x}_5} \end{aligned}$$

$$
\begin{aligned}
&= -J^2 \sum_{\mathbf{x}_1\mathbf{x}_2\mathbf{x}_4\mathbf{x}_5} \left(\delta^{(d)}_{\mathbf{x}_1,\hat{\mathbf{e}}_x} - \delta^{(d)}_{\mathbf{x}_1,-\hat{\mathbf{e}}_x}\right)\left(\delta^{(d)}_{\mathbf{x}_5,\hat{\mathbf{e}}_x} - \delta^{(d)}_{\mathbf{x}_5,-\hat{\mathbf{e}}_x}\right) g(\mathbf{x}_2) C(\mathbf{x}_1+\mathbf{x}_2) g_2(\mathbf{x}_4)\, \delta^{(d)}_{\mathbf{x}_1+\mathbf{x}_2,\mathbf{x}_4+\mathbf{x}_5} \\
&= -J^2 \sum_{\mathbf{x}_2\mathbf{x}_4} g(\mathbf{x}_2) g_2(\mathbf{x}_4) \Big[C(\mathbf{x}_2+\hat{\mathbf{e}}_x)\left(\delta^{(d)}_{\mathbf{x}_2+\hat{\mathbf{e}}_x,\mathbf{x}_4+\hat{\mathbf{e}}_x} - \delta^{(d)}_{\mathbf{x}_2+\hat{\mathbf{e}}_x,\mathbf{x}_4-\hat{\mathbf{e}}_x}\right) \\
&\qquad\qquad - C(\mathbf{x}_2-\hat{\mathbf{e}}_x)\left(\delta^{(d)}_{\mathbf{x}_2-\hat{\mathbf{e}}_x,\mathbf{x}_4+\hat{\mathbf{e}}_x} - \delta^{(d)}_{\mathbf{x}_2-\hat{\mathbf{e}}_x,\mathbf{x}_4-\hat{\mathbf{e}}_x}\right)\Big] \\
&= -J^2 \sum_{\mathbf{x}_2} g(\mathbf{x}_2) \Big[C(\mathbf{x}_2+\hat{\mathbf{e}}_x)\left(g_2(\mathbf{x}_2) - g_2(\mathbf{x}_2+2\hat{\mathbf{e}}_x)\right) - C(\mathbf{x}_2-\hat{\mathbf{e}}_x)\left(g_2(\mathbf{x}_2-2\hat{\mathbf{e}}_x) - g_2(\mathbf{x}_2)\right)\Big] \\
&= -J^2 \sum_{\mathbf{x}} C(\mathbf{x}) \left[g(\mathbf{x}-\hat{\mathbf{e}}_x) - g(\mathbf{x}+\hat{\mathbf{e}}_x)\right]\left[g_2(\mathbf{x}-\hat{\mathbf{e}}_x) - g_2(\mathbf{x}+\hat{\mathbf{e}}_x)\right]. \qquad \text{(B.72)}
\end{aligned}
$$

In this expression, only $C(\mathbf{x})$ depends on ξ. Thus, when iteratively determining the localization length, only this function has to be calculated for each iteration step, $g(\mathbf{x})$ and $g_2(\mathbf{x})$ only need to be evaluated once at the beginning of the procedure.

On the other hand, when calculating I_∞ in order to find the Anderson transition, $C(\mathbf{x})$ is independent of the system parameters and, thus, only needs to be evaluated once.

One can make further use of the invariance of the Fourier transforms under parity transformation, $x_i \leftrightarrow -x_i$, and (for $d = 3$) $x_i \leftrightarrow x_j$, leading to the following expressions,

$\underline{d=1}$:

$$
I_\xi = D_0 - \frac{4J^2 \operatorname{Im}\Sigma^A}{[\pi N(E)]^2 D_0} \sum_{x=1}^{\infty} C(x)\left[g(x+1) - g(x-1)\right]\left[g_2(x+1) - g_2(x-1)\right] \qquad \text{(B.73a)}
$$

$\underline{d=2}$:

$$
\begin{aligned}
I_\xi = D_0 - \frac{8J^2 \operatorname{Im}\Sigma^A}{[\pi N(E)]^2 D_0} \sum_{x=1}^{\infty}\sum_{y=0}^{\infty} & C(\mathbf{x})\left[g(\mathbf{x}-\hat{\mathbf{e}}_x) - g(\mathbf{x}+\hat{\mathbf{e}}_x)\right]\left[g_2(\mathbf{x}-\hat{\mathbf{e}}_x) - g_2(\mathbf{x}+\hat{\mathbf{e}}_x)\right] \\
& \times (1 - \tfrac{1}{2}\delta_{y,0}) \qquad \text{(B.73b)}
\end{aligned}
$$

$\underline{d=3}$:

$$
\begin{aligned}
I_\xi = D_0 - \frac{32J^2 \operatorname{Im}\Sigma^A}{[\pi N(E)]^2 D_0} \sum_{x=1}^{\infty}\sum_{y=0}^{\infty}\sum_{z=0}^{\infty} & C(\mathbf{x})\left[g(\mathbf{x}-\hat{\mathbf{e}}_x) - g(\mathbf{x}+\hat{\mathbf{e}}_x)\right]\left[g_2(\mathbf{x}-\hat{\mathbf{e}}_x) - g_2(\mathbf{x}+\hat{\mathbf{e}}_x)\right] \\
& \times \left(1 - \tfrac{1}{2}\delta_{y,0}\right)\left(1 - \tfrac{1}{2}\delta_{z,0}\right)\left(1 - \tfrac{1}{2}\delta_{y,z}\right) \qquad \text{(B.73c)}
\end{aligned}
$$

For readability, we have changed the notation of the spatial coordinates from $\mathbf{x} = (x_1, x_2, x_3)$ to $\mathbf{x} = (x, y, z)$.

Bibliography

[1] M. P. A. Fisher et al., "Boson localization and the superfluid-insulator transition," *Phys. Rev. B* 40 (1989) 546–570, DOI: 10.1103/PhysRevB.40.546, URL: http://link.aps.org/doi/10.1103/PhysRevB.40.546.

[2] S. N. Bose, "Plancks Gesetz und Lichtquantenhypothese," *Zeitschrift für Physik* 26.1 (1924) 178–181, DOI: 10.1007/BF01327326, URL: http://dx.doi.org/10.1007/BF01327326.

[3] A. Einstein, "Quantentheorie des einatomigen idealen Gases," *Sitzungsberichte der Königlichen Preussischen Akademie der Wissenschaften* 3 (1925).

[4] M. H. Anderson et al., "Observation of Bose-Einstein Condensation in a Dilute Atomic Vapor," *Science* 269.5221 (1995) 198–201, DOI: 10.1126/science.269.5221.198, URL: http://www.sciencemag.org/content/269/5221/198.abstract.

[5] K. Davis et al., "Bose-Einstein Condensation in a Gas of Sodium Atoms," *Phys. Rev. Lett.* 75 (1995) 3969–3973, DOI: 10.1103/PhysRevLett.75.3969, URL: http://link.aps.org/doi/10.1103/PhysRevLett.75.3969.

[6] P. Kapitza, "Viscosity of Liquid Helium below the λ-Point," *Nature* 141.3558 (1938) 74, DOI: 10.1038/141074a0.

[7] J. F. Allen and H. Jones, "New Phenomena Connected with Heat Flow in Helium II," *Nature* 141.3562 (1938) 243–244, DOI: 10.1038/141243a0.

[8] J. G. Daunt and K. Mendelssohn, "Transfer of Helium II on Glass," *Nature* 141 (1938) 911–912, DOI: 10.1038/141911a0.

[9] F. London, "The λ-Phenomenon of Liquid Helium and the Bose-Einstein Degeneracy," *Nature* 141 (1938) 643–644, DOI: 10.1038/141643a0.

[10] L. D. Landau, "The Theory of Superfluidity of Helium II," *J. Phys* 5.1 (1941) 71–90.

[11] N. N. Bogoliubov, *J. Phys USSR* 11.23 (1947).

[12] N. F. Mott, "The transition to the metallic state," *Philosophical Magazine* 6.62 (1961) 287–309, DOI: 10.1080/14786436108243318, URL: http://dx.doi.org/10.1080/14786436108243318.

[13] J. Hubbard, "Electron Correlations in Narrow Energy Bands," *Proceedings of the Royal Society of London. Series A. Mathematical and Physical Sciences* 276.1365 (1963) 238–257, DOI: 10.1098/rspa.1963.0204, URL: http://rspa.royalsocietypublishing.org/content/276/1365/238.abstract.

[14] A. J. Leggett, "Topics in the Theory of Helium," *Physica Fennica* 8 (1973) 125–170.

[15] M. Greiner et al., "Quantum phase transition from a superfluid to a Mott insulator in a gas of ultracold atoms," *Nature* 415.6867 (2002) 39–44.

[16] J. Reppy, "Superfluid helium in porous media," *Journal of Low Temperature Physics* 87.3-4 (1992) 205–245, DOI: 10.1007/BF00114905, URL: http://dx.doi.org/10.1007/BF00114905.

[17] B. C. Crooker et al., "Superfluidity in a Dilute Bose Gas," *Phys. Rev. Lett.* 51 (1983) 666–669, DOI: 10.1103/PhysRevLett.51.666, URL: http://link.aps.org/doi/10.1103/PhysRevLett.51.666.

[18] P. W. Anderson, "Absence of Diffusion in Certain Random Lattices," *Phys. Rev.* 109 (1958) 1492–1505, DOI: 10.1103/PhysRev.109.1492, URL: http://link.aps.org/doi/10.1103/PhysRev.109.1492.

[19] E. Abrahams et al., "Scaling Theory of Localization: Absence of Quantum Diffusion in Two Dimensions," *Phys. Rev. Lett.* 42 (1979) 673–676, DOI: 10.1103/PhysRevLett.42.673, URL: http://link.aps.org/doi/10.1103/PhysRevLett.42.673.

[20] J. Billy et al., "Direct observation of Anderson localization of matter waves in a controlled disorder," *Nature* 453.7197 (2008) 891–894.

[21] S. Kravchenko et al., "Possible metal-insulator transition at B=0 in two dimensions," *Phys. Rev. B* 50 (1994) 8039–8042, DOI: 10.1103/PhysRevB.50.8039, URL: http://link.aps.org/doi/10.1103/PhysRevB.50.8039.

[22] T. Giamarchi and H. J. Schulz, "Localization and Interaction in One-Dimensional Quantum Fluids," *EPL (Europhysics Letters)* 3.12 (1987) 1287, URL: http://stacks.iop.org/0295-5075/3/i=12/a=007.

[23] J. K. Freericks and H. Monien, "Strong-coupling expansions for the pure and disordered Bose-Hubbard model," *Phys. Rev. B* 53 (1996) 2691–2700, DOI: 10.1103/PhysRevB.53.2691, URL: http://link.aps.org/doi/10.1103/PhysRevB.53.2691.

[24] L. Pollet et al., "Absence of a Direct Superfluid to Mott Insulator Transition in Disordered Bose Systems," *Phys. Rev. Lett.* 103 (2009) 140402, DOI: 10.1103/PhysRevLett.103.140402, URL: http://link.aps.org/doi/10.1103/PhysRevLett.103.140402.

[25] P. Henseler, J. Kroha, and B. Shapiro, "Static screening and delocalization effects in the Hubbard-Anderson model," *Phys. Rev. B* 77 (2008) 075101, DOI: 10.1103/PhysRevB.77.075101, URL: http://link.aps.org/doi/10.1103/PhysRevB.77.075101.

[26] P. Henseler, J. Kroha, and B. Shapiro, "Self-consistent study of Anderson localization in the Anderson-Hubbard model in two and three dimensions," *Phys. Rev. B* 78 (2008) 235116, DOI: 10.1103/PhysRevB.78.235116, URL: http://link.aps.org/doi/10.1103/PhysRevB.78.235116.

[27] K. Sheshadri et al., "Superfluid and Insulating Phases in an Interacting-Boson Model: Mean-Field Theory and the RPA," *EPL (Europhysics Letters)* 22.4 (1993) 257, URL: http://stacks.iop.org/0295-5075/22/i=4/a=004.

[28] U. Bissbort and W. Hofstetter, "Stochastic mean-field theory for the disordered Bose-Hubbard model," *EPL (Europhysics Letters)* 86.5 (2009) 50007, URL: http://stacks.iop.org/0295-5075/86/i=5/a=50007.

[29] D. Vollhardt and P. Wölfle, "Anderson Localization in $d \lesssim 2$ Dimensions: A Self-Consistent Diagrammatic Theory," *Phys. Rev. Lett.* 45 (1980) 842–846, DOI: 10.1103/PhysRevLett.45.842, URL: http://link.aps.org/doi/10.1103/PhysRevLett.45.842.

[30] J. K. Freericks and H. Monien, "Phase diagram of the Bose-Hubbard Model," *EPL (Europhysics Letters)* 26.7 (1994) 545, URL: http://stacks.iop.org/0295-5075/26/i=7/a=012.

[31] R. T. Scalettar, G. G. Batrouni, and G. T. Zimanyi, "Localization in interacting, disordered, Bose systems," *Phys. Rev. Lett.* 66 (1991) 3144–3147, DOI: 10.1103/PhysRevLett.66.3144, URL: http://link.aps.org/doi/10.1103/PhysRevLett.66.3144.

[32] G. G. Batrouni and R. T. Scalettar, "World-line quantum Monte Carlo algorithm for a one-dimensional Bose model," *Phys. Rev. B* 46 (1992) 9051–9062, DOI: 10.1103/PhysRevB.46.9051, URL: http://link.aps.org/doi/10.1103/PhysRevB.46.9051.

[33] B. Capogrosso-Sansone, N. V. Prokof'ev, and B. V. Svistunov, "Phase diagram and thermodynamics of the three-dimensional Bose-Hubbard model," *Phys. Rev. B* 75 (2007) 134302, DOI: 10.1103/PhysRevB.75.134302, URL: http://link.aps.org/doi/10.1103/PhysRevB.75.134302.

[34] N. Elstner and H. Monien, "Dynamics and thermodynamics of the Bose-Hubbard model," *Phys. Rev. B* 59 (1999) 12184–12187, DOI: 10.1103/PhysRevB.59.12184, URL: http://link.aps.org/doi/10.1103/PhysRevB.59.12184.

[35] B. Capogrosso-Sansone et al., "Monte Carlo study of the two-dimensional Bose-Hubbard model," *Phys. Rev. A* 77 (2008) 015602, DOI: 10.1103/PhysRevA.77.015602, URL: http://link.aps.org/doi/10.1103/PhysRevA.77.015602.

[36] D. S. Rokhsar and B. G. Kotliar, "Gutzwiller projection for bosons," *Phys. Rev. B* 44 (1991) 10328–10332, DOI: 10.1103/PhysRevB.44.10328, URL: http://link.aps.org/doi/10.1103/PhysRevB.44.10328.

[37] W. Krauth, M. Caffarel, and J.-P. Bouchaud, "Gutzwiller wave function for a model of strongly interacting bosons," *Phys. Rev. B* 45 (1992) 3137–3140, DOI: 10.1103/PhysRevB.45.3137, URL: http://link.aps.org/doi/10.1103/PhysRevB.45.3137.

[38] D. Jaksch et al., "Cold Bosonic Atoms in Optical Lattices," *Phys. Rev. Lett.* 81 (1998) 3108–3111, DOI: 10.1103/PhysRevLett.81.3108, URL: http://link.aps.org/doi/10.1103/PhysRevLett.81.3108.

[39] A. E. Niederle and H. Rieger, "Superfluid clusters, percolation and phase transitions in the disordered, two-dimensional Bose–Hubbard model,"
New Journal of Physics 15.7 (2013) 075029,
URL: http://stacks.iop.org/1367-2630/15/i=7/a=075029.

[40] P. Anders et al., "Dynamical Mean Field Solution of the Bose-Hubbard Model,"
Phys. Rev. Lett. 105 (2010) 096402, DOI: 10.1103/PhysRevLett.105.096402,
URL: http://link.aps.org/doi/10.1103/PhysRevLett.105.096402.

[41] D. A. W. Hutchinson, *Excitations in Bose-Einstein Condensates*, Lecture Notes, 2012.

[42] L. P. Pitaevskii and S. Stringari, *Bose-Einstein condensation*, Internat. Ser. Mono. Phys. Oxford: Clarendon Press, 2003.

[43] A. Leggett, "On the Superfluid Fraction of an Arbitrary Many-Body System at T=0,"
Journal of Statistical Physics 93.3-4 (1998) 927–941,
DOI: 10.1023/B:JOSS.0000033170.38619.6c,
URL: http://dx.doi.org/10.1023/B%3AJOSS.0000033170.38619.6c.

[44] A. Shalgi and Y. Imry, "Localization in Disordered Systems,"
Les Houches 1994: Mesoscopic Quantum Physics, ed. by E. Akkermans et al., Amsterdam: North-Holland, 1995.

[45] J. Fröhlich and T. Spencer, "Absence of diffusion in the Anderson tight binding model for large disorder or low energy,"
Communications in Mathematical Physics 88.2 (1983) 151–184,
DOI: 10.1007/BF01209475, URL: http://dx.doi.org/10.1007/BF01209475.

[46] J. Fröhlich and T. Spencer, "A rigorous approach to Anderson localization,"
Physics Reports 103.1–4 (1984) 9 –25,
DOI: http://dx.doi.org/10.1016/0370-1573(84)90061-9,
URL: http://www.sciencedirect.com/science/article/pii/0370157384900619.

[47] I. Y. Gol'dshtein, S. A. Molchanov, and L. A. Pastur,
"A pure point spectrum of the stochastic one-dimensional schrödinger operator,"
Functional Analysis and Its Applications 11.1 (1977) 1–8, DOI: 10.1007/BF01135526,
URL: http://dx.doi.org/10.1007/BF01135526.

[48] B. Kramer and A. MacKinnon, "Localization: theory and experiment,"
Reports on Progress in Physics 56.12 (1993) 1469,
URL: http://stacks.iop.org/0034-4885/56/i=12/a=001.

[49] I. M. Lifshitz, "The energy spectrum of disordered systems,"
Advances in Physics 13.52 (1964) 483–536, DOI: 10.1080/00018736400101061,
URL: http://dx.doi.org/10.1080/00018736400101061.

[50] N. F. Mott, "Electrons in disordered structures," *Advances in Physics* 16 (1967) 49–144.

[51] J. Rammer, *Quantum Transport Theory*, Frontiers in Physics,
Reading, MA: Westview Press, 2004.

[52] R. Landauer, "Electrical resistance of disordered one-dimensional lattices,"
Philosophical Magazine 21.172 (1970) 863–867, DOI: 10.1080/14786437008238472,
URL: http://dx.doi.org/10.1080/14786437008238472.

[53] J. T. Edwards and D. J. Thouless,
"Numerical studies of localization in disordered systems,"
Journal of Physics C: Solid State Physics 5.8 (1972) 807,
URL: http://stacks.iop.org/0022-3719/5/i=8/a=007.

[54] D. C. Licciardello and D. J. Thouless,
"Constancy of Minimum Metallic Conductivity in Two Dimensions,"
Phys. Rev. Lett. 35 (1975) 1475–1478, DOI: 10.1103/PhysRevLett.35.1475,
URL: http://link.aps.org/doi/10.1103/PhysRevLett.35.1475.

[55] D. C. Licciardello and D. J. Thouless,
"Conductivity and mobility edges for two-dimensional disordered systems,"
Journal of Physics C: Solid State Physics 8.24 (1975) 4157,
URL: http://stacks.iop.org/0022-3719/8/i=24/a=009.

[56] F. Wegner, "Electrons in disordered systems. Scaling near the mobility edge,"
Zeitschrift für Physik B Condensed Matter 25.4 (1976) 327–337,
DOI: 10.1007/BF01315248, URL: http://dx.doi.org/10.1007/BF01315248.

[57] N. F. Mott,
"Conduction in non-crystalline systems IX. the minimum metallic conductivity,"
Philosophical Magazine 26.4 (1972) 1015–1026, DOI: 10.1080/14786437208226973,
URL: http://dx.doi.org/10.1080/14786437208226973.

[58] K. Slevin and T. Ohtsuki,
"Numerical verification of universality for the Anderson transition,"
Phys. Rev. B 63 (2001) 045108, DOI: 10.1103/PhysRevB.63.045108,
URL: http://link.aps.org/doi/10.1103/PhysRevB.63.045108.

[59] A. Eilmes, A. M. Fischer, and R. A. Römer, "Critical parameters for the
disorder-induced metal-insulator transition in fcc and bcc lattices,"
Phys. Rev. B 77 (2008) 245117, DOI: 10.1103/PhysRevB.77.245117,
URL: http://link.aps.org/doi/10.1103/PhysRevB.77.245117.

[60] A. Cohen, Y. Roth, and B. Shapiro,
"Universal distributions and scaling in disordered systems,"
Phys. Rev. B 38 (1988) 12125–12132, DOI: 10.1103/PhysRevB.38.12125,
URL: http://link.aps.org/doi/10.1103/PhysRevB.38.12125.

[61] D. Vollhardt and P. Wölfle, "Diagrammatic, self-consistent treatment of the Anderson
localization problem in $d \lesssim 2$ dimensions," *Phys. Rev. B* 22 (1980) 4666–4679,
DOI: 10.1103/PhysRevB.22.4666,
URL: http://link.aps.org/doi/10.1103/PhysRevB.22.4666.

[62] D. Vollhardt and P. Wölfle,
"Scaling Equations from a Self-Consistent Theory of Anderson Localization,"
Phys. Rev. Lett. 48 (1982) 699–702, DOI: 10.1103/PhysRevLett.48.699,
URL: http://link.aps.org/doi/10.1103/PhysRevLett.48.699.

[63] A. D. Zdetsis et al.,
"Localization in two- and three-dimensional systems away from the band center,"
Phys. Rev. B 32 (1985) 7811–7816, DOI: 10.1103/PhysRevB.32.7811,
URL: http://link.aps.org/doi/10.1103/PhysRevB.32.7811.

[64] T. Kopp, "A diagrammatic two-particle locator theory for disordered systems. I. General formulation," *Journal of Physics C: Solid State Physics* 17.11 (1984) 1897, URL: http://stacks.iop.org/0022-3719/17/i=11/a=011.

[65] T. Kopp, "A diagrammatic two-particle locator theory for disordered systems. II. Self-consistent treatment of the Anderson transition and the role of hopping processes," *Journal of Physics C: Solid State Physics* 17.11 (1984) 1919, URL: http://stacks.iop.org/0022-3719/17/i=11/a=012.

[66] J. Kroha, T. Kopp, and P. Wölfle, "Self-consistent theory of Anderson localization for the tight-binding model with site-diagonal disorder," *Phys. Rev. B* 41 (1990) 888–891, DOI: 10.1103/PhysRevB.41.888, URL: http://link.aps.org/doi/10.1103/PhysRevB.41.888.

[67] J. Kroha, "Diagrammatic self-consistent theory of anderson localization for the tight-binding model," *Physica A: Statistical Mechanics and its Applications* 167.1 (1990) 231 –252, DOI: 10.1016/0378-4371(90)90055-W, URL: http://www.sciencedirect.com/science/article/pii/037843719090055W.

[68] B. Bulka, M. Schreiber, and B. Kramer, "Localization, quantum interference, and the metal-insulator transition," *Zeitschrift für Physik B Condensed Matter* 66.1 (1987) 21–30, DOI: 10.1007/BF01312758, URL: http://dx.doi.org/10.1007/BF01312758.

[69] P. Sheng, *Introduction to Wave Scattering, Localization and Mesoscopic Phenomena; 2nd ed.* Dordrecht: Springer, 2006.

[70] J. Stasińska et al., "The glass to superfluid transition in dirty bosons on a lattice," *New Journal of Physics* 14.4 (2012) 043043, URL: http://stacks.iop.org/1367-2630/14/i=4/a=043043.

[71] K. G. Singh and D. S. Rokhsar, "Disordered bosons: Condensate and excitations," *Phys. Rev. B* 49 (1994) 9013–9023, DOI: 10.1103/PhysRevB.49.9013, URL: http://link.aps.org/doi/10.1103/PhysRevB.49.9013.

[72] C. Gaul and C. A. Müller, "Bogoliubov excitations of disordered Bose-Einstein condensates," *Phys. Rev. A* 83 (2011) 063629, DOI: 10.1103/PhysRevA.83.063629, URL: http://link.aps.org/doi/10.1103/PhysRevA.83.063629.

[73] C. Gaul and C. A. Müller, "Bogoliubov theory on the disordered lattice," *The European Physical Journal Special Topics* 217.1 (2013) 69–78, DOI: 10.1140/epjst/e2013-01755-9, URL: http://dx.doi.org/10.1140/epjst/e2013-01755-9.

[74] C. Gaul and C. A. Müller, "A grand-canonical approach to the disordered Bose gas," *Applied Physics B* 117.3 (2014) 775–784, DOI: 10.1007/s00340-014-5805-2, URL: http://dx.doi.org/10.1007/s00340-014-5805-2.

[75] H. Gimperlein et al., "Ultracold Atoms in Optical Lattices with Random On-Site Interactions," *Phys. Rev. Lett.* 95 (2005) 170401, DOI: 10.1103/PhysRevLett.95.170401, URL: http://link.aps.org/doi/10.1103/PhysRevLett.95.170401.

[76] F. Lin, E. S. Sørensen, and D. M. Ceperley,
"Superfluid-insulator transition in the disordered two-dimensional Bose-Hubbard model,"
Phys. Rev. B 84 (2011) 094507, DOI: 10.1103/PhysRevB.84.094507,
URL: http://link.aps.org/doi/10.1103/PhysRevB.84.094507.

[77] Ş. G. Söyler et al., "Phase Diagram of the Commensurate Two-Dimensional Disordered Bose-Hubbard Model," *Phys. Rev. Lett.* 107 (2011) 185301,
DOI: 10.1103/PhysRevLett.107.185301,
URL: http://link.aps.org/doi/10.1103/PhysRevLett.107.185301.

[78] E. L. Pollock and D. M. Ceperley, "Path-integral computation of superfluid densities,"
Phys. Rev. B 36 (1987) 8343–8352, DOI: 10.1103/PhysRevB.36.8343,
URL: http://link.aps.org/doi/10.1103/PhysRevB.36.8343.

[79] V. Gurarie et al., "Phase diagram of the disordered Bose-Hubbard model,"
Phys. Rev. B 80 (2009) 214519, DOI: 10.1103/PhysRevB.80.214519,
URL: http://link.aps.org/doi/10.1103/PhysRevB.80.214519.

[80] D. van Oosten, P. van der Straten, and H. T. C. Stoof,
"Quantum phases in an optical lattice," *Phys. Rev. A* 63 (2001) 053601,
DOI: 10.1103/PhysRevA.63.053601,
URL: http://link.aps.org/doi/10.1103/PhysRevA.63.053601.

[81] H. T. C. Stoof, D. B. M. Dickerscheid, and K. Gubbels, *Ultracold quantum fields*,
Berlin: Springer, 2009.

[82] B. Gough, *GNU Scientific Library Reference Manual - Third Edition*, 3rd,
Network Theory Ltd., 2009.

[83] E. Anderson et al., *LAPACK Users' Guide*, Third,
Philadelphia, PA: Society for Industrial and Applied Mathematics, 1999.

[84] A. Gonis and J. Garland,
"Rederivation and proof of analyticity of the Blackman-Esterling-Berk approximation,"
Phys. Rev. B 16 (1977) 1495–1502, DOI: 10.1103/PhysRevB.16.1495,
URL: http://link.aps.org/doi/10.1103/PhysRevB.16.1495.

[85] J. J. Sakurai, *Modern Quantum Mechanics (Revised Edition)*, 1st ed.,
Addison Wesley, 1993.

[86] H. Haug and A. Jauho,
Quantum kinetics in transport and optics of semincionductors; 2nd ed.
Berlin: Springer, 2008.

[87] P. Soven, "Coherent-Potential Model of Substitutional Disordered Alloys,"
Phys. Rev. 156 (1967) 809–813, DOI: 10.1103/PhysRev.156.809,
URL: http://link.aps.org/doi/10.1103/PhysRev.156.809.

[88] P. Henseler,
"Interplay of Anderson Localization and Strong Interactions in Disordered Systems,"
PhD thesis: Universität Bonn, 2010,
URL: http://hss.ulb.uni-bonn.de/2010/2040/2040.htm.

Danksagung

Zum Abschluss dieser Arbeit möchte ich mich bei allen bedanken, die mich während der Zeit meiner Promotion unterstützt haben. Zuallererst wäre da mein Doktorvater Hans Kroha, der es mir ermöglicht hat, an diesem interessanten Thema zu arbeiten, und mit mir in vielen und meist auch langen Diskussionen das Projekt vorangetrieben hat. Darüber hinaus hatte ich durch ihn die Gelegenheit zu zwei Forschungsaufenthalten in Singapur, für die ich ihm sehr dankbar bin. Hier muss ich mich natürlich auch bei Cord Müller für die Einladungen nach Singapur bedanken. Während der beiden Aufenthalte hat er mir geholfen, grundlegende Ideen dieser Arbeit zu entwickeln, und war auch anschließend durch eine Vielzahl an Gesprächen direkt am Gelingen der Arbeit beteiligt. Weiterhin bin ich Corinna Kollath dankbar, die sich die Zeit genommen hat, meine Arbeit zu begutachten, und mir einige hilfreiche Hinweise gegeben hat. Danke an alle Mitglieder meiner Arbeitsgruppe für die schöne Zeit und besonderen Dank an Kati, Mauro und Lai, denen die unangenehme Aufgabe zufiel, alle Rechtschreib- und Grammatikfehler der Rohfassung in roter Farbe zu unterstreichen. Danke an (in alphabetischer Reihenfolge) Christa, Dagmar, Patricia und Petra für ihre Geduld mit mir. Danke an Andreas und Hartmut für die abendlichen Unterhaltungen an der Espressomaschine. Danke an Freunde und Familie.
So, und jetzt bin ich schon weg. Ciao... Arrivederci... Goodbye. – Gordon Shumway